N O T I C E

THIS DOCUMENT HAS BEEN REPRODUCED FROM MICROFICHE. ALTHOUGH IT IS RECOGNIZED THAT CERTAIN PORTIONS ARE ILLEGIBLE, IT IS BEING RELEASED IN THE INTEREST OF MAKING AVAILABLE AS MUCH INFORMATION AS POSSIBLE

"Made available under NASA sponsorship in the interest of early and wide dissemination of Earth Resources Survey Program information and without liability for any use made thereof."

Final Report RSC-3753

E82-10343
CR-168960

Orbiting Passive Microwave Sensor Simulation Applied To Soil Moisture Estimation

MAY 1982
RECEIVED
NASA STI FACILITY
ACCESS DEPT.

By

R. W. Newton
B. V. Clark
W. M. Pitchford
Texas A&M University

J. F. Paris
University of Houston

December 1979

MAY 1982
RECEIVED
NASA STI FACILITY
ACCESS DEPT.

Supported by
National Aeronautics and Space Administration
Grant NSG 5266

TEXAS A&M UNIVERSITY
REMOTE SENSING CENTER
COLLEGE STATION, TEXAS

(E82-10343) ORBITING PASSIVE MICROWAVE SENSOR SIMULATION APPLIED TO SOIL MOISTURE ESTIMATION Final Report (Texas A&M Univ.) 219 p HC A10/MF A01 CSCL 08M
N82-25605
Unclas
G3/43 00343

Final Report RSC-3753

ORBITING PASSIVE MICROWAVE SENSOR SIMULATION APPLIED TO SOIL MOISTURE ESTIMATION

by

R. W. Newton
B. V. Clark
J. F. Paris*
W. M. Pitchford

Original photography may be purchased
from EROS Data Center
Sioux Falls, SD 57198

Principal Investigator: R. W. Newton

December 1979

*With University of Houston, Clear Lake City at time of writing, now with NASA Johnson Space Center

Supported by
NATIONAL AERONAUTICS AND SPACE ADMINISTRATION
Grant NSG 5266

TABLE OF CONTENTS

Page

INTRODUCTION. 1

Background 1

Objective. 2

Summary. 3

Model Definition. 3

Model Implementation. 4

Soil Moisture Measurement Feasibility Studies 5

MODEL DEFINITION AND STRUCTURE. 7

Space Platform Coordinate System/Implementation. 8

Antenna Temperature Equations 10

Integral Evaluations. 14

Simulated Ground Scene 18

Scene Construction. 18

Converting Classified Landsat Types to TAMU Percent Class Types. 21

Scene Utilization 28

COMPUTATION 36

Objective and Approach 36

Subroutine BRIGHT. 37

Fortran Code for Subroutine BRIGHT 39

Brightness Temperature as Function of Angle (Subroutine BCORR) 40

Subroutine WATER 45

Subroutine URBAN 47

Subroutine BARE. 48

X-band Algorithm. 49

C-band Algorithm. 51

L-band Algorithm. 51

Fortran Code for Subroutine BARE. 51

PRECEDING PAGE BLANK NOT FILMED

LIST OF FIGURES

Figure		Page
1	Relationship between the scene coordinate system and the satellite platform coordinate system.	9
2	Definition of parameters used in model equations.	11
3	Antenna footprint relative to the nadir position and the scene boundary	16
4	Limitations of the simulation model in terms of field of view requirements and scene size.	19
5	Areas covered by the eight Landsat scenes used to generate the simulated scene.	20
6	Procedure for aggregating and mapping the Texas Parks and Wildlife Landsat classifications into the classes used in the simulation program	24
7	Construction of the 16 bit word that describes the percentages of classes in each 240 x 240 meter simulated scene pixel.	26
8	Relative locations of the Landsat scenes in relation to the entire simulated ground scene.	27
9	Major simulation parameters that must be specified properly in order to maintain consistency between the antenna footprint size and the simulated scene size	29
10	Simulation software initialization with respect to the ground scene coordinate system.	30
11	Calculation of the initial nadir point	31
12	Definition of the parameters describing the limits of the antenna footprint integration.	33
13	Implementation concept of the orbiting microwave radiometer simulation program.	35
14	Plot of the form factor used to estimate brightness temperature as a function of incident angle.	44
15	Plot of the assumed relationship between soil moisture and soil temperature for a temperature parameter of 40°C.	50

Figure Page

16 Example of the roughness parameter effect on brightness temperature 54

17 Example of how the temperature parameter is assumed to effect the water or plant canopy temperature. 55

18 Example of the dependence of brightness temperature on soil moisture for all classes at L-band horizonal polarization 58

19 Example of the dependence of brightness temperature on soil moisture for all classes at L-band vertical polarization. 59

20 Example of the dependence of brightness temperature on soil moisture for all classes at X-band horizonal polarization 60

21 Example of the dependence of brightness temperature on soil moisture for all classes at X-band vertical polarization. 61

22 Example of the dependence of brightness temperature on the soil temperature parameter for both X-band and L-band. 63

23 Percent of water, bare soil and forest classes in each antenna footprint as a function of range for the Waco to Livingston ground track at a resolution of 5 kilometers 67

24 Percent of urban, mixed bare and vegetated and fully vegetated classes in each antenna footprint as a function of range for the Waco to Livingston ground track at a resolution of 5 kilometers 68

25 Percent of water, bare soil and forest classes in each antenna footprint as a function of range for the Kerrville to Houston ground track at a resolution of 5 kilometers 69

26 Percent of urban, mixed bare and vegetated and fully vegetated classes in each antenna footprint as a function of range for the Kerrville to Houston ground track at a 5 kilometer resolution 70

Figure Page

27 Percent of water, bare soil and forest classes in each antenna footprint as a function of range for the Waco to Livingston ground track at a 20 kilometer resolution 71

28 Percent of water, bare soil and forest classes in each antenna footprint as a function of range for the Waco to Livingston ground track at a 60 kilometer resolution. 72

29 Histogram of the percentage of the antenna footprint containing water for the Waco to Livingston ground track at a 5 kilometer resolution 75

30 Histogram of the percentage of the antenna footprint containing bare soil for the Waco to Livingston ground track at a 5 kilometer resolution 76

31 Histogram of the percentage of the antenna footprint containing mixed bare and vegetation for the Waco to Livingston ground track at a 5 kilometer resolution 77

32 Histogram of the percentage of the antenna footprint containing full vegetation for the Waco to Livingston ground track at a 5 kilometer resolution 78

33 Histogram of the percentage of the antenna footprint containing forest for the Waco to Livingston ground track at a 5 kilometer resolution 79

34 Histogram of the percentage of the antenna footprint containing urban for the Waco to Livingston ground track at a 5 kilometer resolution 80

35 Histogram of the percentage of the antenna footprint containing water for the Waco to Livingston ground track at a 5 kilometer resolution 81

36 Histogram of the percentage of the antenna footprint containing bare soil for the Kerrville to Houston ground track at a 5 kilometer resolution 82

Page

37 Histogram of the percentage of the antenna footprint containing mixed bare and vegetation for the Kerrville to Houston ground track at a 5 kilometer resolution 83

38 Histogram of the percentage of the antenna footprint containing full vegetation for the Kerrville to Houston ground track at a 5 kilometer resolution 84

39 Histogram of the percentage of the antenna footprint containing forest for the Kerrville to Houston ground track at a 5 kilometer resolution 85

40 Histogram of the percentage of the antenna footprint containing urban for the Kerrville to Houston ground track at a 5 kilometer resolution 86

41 Computation of brightness temperature as a function of incident angle for L-band in a 20 kilometer resolution for an antenna footprint containing predominantly bare soil and one containing predominantly water. 88

42 Horizontal brightness temperature computed at L-band and a 20 kilometer resolution as a function of range along the Waco to Livingston ground track for a temperature parameter of 10°C and 60°C 89

43 Horizontal brightness temperature computed at L-band and a 5 kilometer resolution for the Waco to Livingston ground track at two soil moistures, 5% and 35%. 91

44 Horizontal brightness temperature computed at C-band and a 5 kilometer resolution for the Waco to Livingston ground track at two soil moistures, 5% and 35%. 92

45 Horizontal brightness temperature computed at X-band and a 5 kilometer resolution for the Waco to Livingston ground track at two soil moistures, 5% and 35%. 93

46 Horizontal brightness temperature computed at L-band and a 20 kilometer resolution for the Waco to Livingston ground track at two soil moistures, 5% and 35% 94

Page

47 Horizontal brightness temperature computed at L-band and a 60 kilometer resolution for the Waco to Livingston ground track at two soil moistures, 5% and 35%. 95

48 Vertical brightness temperature computed at L-band and a 5 kilometer resolution for the Waco to Livingston ground track at two soil moistures, 5% and 35%. 96

49 Horizontal brightness temperature computed at L-band for the Waco to Livingston ground track at a 5 kilometer resolution plotted as a function of percent class of bare soil at two soil moistures, 5% and 35% 100

50 Horizontal brightness temperature computed at L-band for the Waco to Livingston ground track at a 5 kilometer resolution plotted as a function of percent class of mixed bare and vegetation at two soil moistures, 5% and 35% 101

51 Horizontal brightness temperature computed at L-band for the Waco to Livingston ground track at a 5 kilometer resolution plotted as a function of percent class of fully vegetated at two soil moistures, 5% and 35% 102

52 Horizontal brightness temperature computed at L-band for the Waco to Livingston ground track at a 5 kilometer resolution plotted as a function of percent forest class at two soil moistures, 5% and 35%. 103

53 Horizontal brightness temperature computed at C-band for the Waco to Livingston ground track at a 5 kilometer resolution plotted as a function of percent mixed bare and vegetation class at two soil moistures, 5% and 35%. 106

54 Horizontal brightness temperature computed at X-band for the Waco to Livingston ground track at a 5 kilometer resolution plotted as a function of percent mixed bare and vegetation class at two soil moistures, 5% and 35%. 107

55 Horizontal brightness temperature computed at L-band for the Waco to Livingston ground track at a 20 kilometer resolution plotted as a function of percent mixed bare and vegetation class at two soil moistures, 5% and 35%. 109

Page

56 Horizontal brightness temperature computed at L-band for the Waco to Livingston ground track at a 20 kilometer resolution plotted as a function of percent forest class at two soil moistures, 5% and 35%. 110

57 Histogram of the horizontal L-band brightness temperature computed for the Waco to Livingston ground track at 5% and 35% soil moisture and a 5 kilometer resolution 112

58 Histogram of the horizontal L-band brightness temperature computed for the Waco to Livingston ground track at 5% and 35% soil moisture and a 60 kilometer resolution. 113

59 Soil moisture sensitivity of the L-band horizontally polarized brightness temperature for the Waco to Livingston ground track at a 20 kilometer resolution plotted as a function of percent bare soil 114

60 Soil moisture sensitivity of the C-band horizontally polarized brightness temperature for the Waco to Livingston ground track at a 20 kilometer resolution plotted as a function of percent bare soil 115

61 Soil moisture sensitivity of the X-band horizontally polarized brightness temperature for the Waco to Livingston ground track at a 20 kilometer resolution plotted as a function of percent bare soil 116

62 Soil moisture sensitivity of the L-band horizontally polarized brightness temperature for the Waco to Livingston ground track at a 20 kilometer resolution plotted as a function of percent mixed bare and vegetated class. 119

63 Soil moisture sensitivity of the L-band horizontally polarized brightness temperature for the Waco to Livingston ground track at a 20 kilometer resolution plotted as a function of percent fully vegetated class 120

64 Soil moisture sensitivity of the L-band horizontally polarized brightness temperature for the Waco to Livingston ground track at a 20 kilometer resolution plotted as a function of percent forest class. 121

Page

65 Average soil moisture sensitivity plotted as a function of frequency and resolution without regard to class constituency with the antenna footprints 123

66 Soil moisture sensitivity plotted as a function of resolution and frequency for antenna footprints containing less than 40% forest class within the 95% confidence intervals indicated. 125

67 Soil moisture sensitivity plotted as a function of resolution and frequency for antenna footprints containing less than 30% forest class with the 95% confidence intervals indicated. 126

LIST OF TABLES

Table		Page
1	Effects of parameter f on gain pattern shape.	13
2	Class definitions.	22
3	Values for the form factors, FH and FV, as a function of nadir angle.	42
4	Simulation parameters used in Test Runs.	66

INTRODUCTION

Background

NASA has been actively supporting the development of earth resources applications of passive microwave sensors over the last six to eight years. The driving force behind the support of passive microwave sensors is the high potential for estimating soil water interaction. Application areas that are currently receiving much attention and to which soil water is a vital requirement for their success are crop yield production, weather and climate modeling, and watershed management. Prior experimental work supporting the potential of using passive microwave sensors for estimating soil water information has relied heavily on ground and aircraft based sensors [1]-[7]. Although these are natural first phase efforts, the eventual application of such techniques will most likely be their implementation from a space platform.

The ground resolution cells associated with spaceborne passive sensors operating at low microwave frequencies are quite large because of limitations on the antenna size. Thus, acquisition of data from homogeneous, uniform areas as done with low altitude sensors will not be possible with spaceborne systems. At low orbit altitudes, resolutions of spaceborne passive microwave systems on the order of 5 km to 20 km could be achieved with current technology. Resolutions of such dimensions will contain a mixture of the primary scene component, such as agricultural fields, as well as other scene components such as forest, urban areas, lakes, open water and rangeland. Consequently,

results that have been demonstrated quite effectively with low altitude "high resolution" sensors might not be obtained with relatively coarse resolution sensors that operate from orbiting platforms.

There are currently no passive microwave sensors in space that operate within the low microwave frequency range that have reasonable resolution dimensions. The Nimbus series of satellites have passive systems, but their lowest frequency is 4.9 GHz and the resolution at this frequency is on the order of 50 km to 60 km. The only 1.4 GHz passive system that has flown in space was aboard Skylab for a very brief period of time. However, it had a resolution of greater than 100 km. Even with this extremely coarse resolution, encouraging implications were obtained when comparing the data to available soil water information [8]-[10].

Since sensor systems that have design specifications applicable to soil moisture estimation are not currently in orbit, it is not possible to utilize measurements to directly determine the feasibility of estimating a soil water parameter from space. More importantly, if a system was currently in orbit, it would most likely have a fixed frequency, resolution, and look angle. It would not be possible to use such a system for a thorough analysis of the effects of frequency and resolution on the performance of a soil moisture estimation algorithm.

Objective

A sensor/scene simulation program is required in order to determine the effects of scene heterogeneity, resolution, frequency, look angle, and surface moisture and temperature relations on the performance of a spaceborne passive microwave system designed to estimate

soil water information. In addition, before the expenditures for an orbiting passive microwave sensor system can be justified, certain critical questions relating to its design parameters and expected performance must be answered. The first two objectives of the project documented herein were to 1) develop and 2) implement a computer program that could simulate the operation of a passive microwave sensor at L-band, C-band, and X-band frequencies for arbitrary antenna and orbit parameters. In addition, the model had to have the capability of simulating realistic scene configurations with arbitrary soil moisture and temperature spatial variations. A third objective was to utilize the model to perform soil moisture measurement feasibility studies. Specifically, to determine the maximum sensor resolution that would provide a reasonable sensitivity to soil moisture within the scene, and to determine the effects of scene makeup or the resolution/performance relationship.

Summary

To meet the three objectives, the effort consisted of three basic tasks: 1) model determination, 2) model implementation, and 3) soil moisture measurement feasibility studies. Each of these tasks are briefly summarized below.

Model Definition

The primary purpose of the model is to determine the effects of geometric and brightness temperature variations within the scene on the output of a radiometer. As a result, the model consists basically of a digital representation of the scene with algorithms capable of

integrating the brightness temperature of the scene weighted by the one way antenna pattern. By specifying both the horizontally and vertically polarized brightness temperatures for each element of the scene, effects of the cross polarized antenna pattern can also be computed.

The model is defined such that the orientation of the antenna with respect to the scene is arbitrary. In other words, the sensor altitude, incident angle, and azimuth angle with respect to the scene are input variables. The model is also implemented such that the scene can be updated after each over-flight. This feature can be used to simulate a flight path across the scene and demonstrate the effects of scene geometry. It is also useful in predicting the effect of changing scene parameters such as soil moisture, crop type, etc., on the radiometer output.

The model assumes a flat earth for both scene representation and flight path simulation. Atmospheric effects are not considered in this effort. However, atmospheric effects could be incorporated by modifying the brightness temperatures representing each element of the scene, or by implementing a subroutine that calculates the effect of the atmosphere on the brightness temperature corresponding to each differential solid angle involved in the antenna/scene integration.

Model Implementation

The model was implemented in FORTRAN for ease of implementation of most computer systems. The scene used in the model consists of an array of numbers corresponding to the percent of particular scene classifications contained in each pixel or array element. The array

corresponding to the scene was generated from actual Landsat scenes covering a large area of south-central Texas. Each array element or pixel represents a 240 meter square on the earth's surface.

The brightness temperature correspoinding to each ground scene pixel is calculated based upon the percentages of each scene component class contained therein and its relative position in the antenna beam. The estimated radiometer antenna temperature for each instantaneous antenna resolution element within the scene is calcualated by integrating the weighted contribution of each pixel within the antenna footprint.

Soil Moisture Measurement Feasibility Studies

After the simulation program was tested and verified, two flight lines were identified across the scene and used for all simulation computations. These flight lines were chosen so as to provide a representative sampling of all possible scene configurations and components. Numerous simulations were computed for L-, C-, and X-band frequencies over these flight lines and put into a data base for analysis. Resolution, soil moisture, soil temperature, surface roughness, and look angle were varied between simulation runs. Also, scene composition in terms of the percentage of each scene class within each resolution element was computed and maintained by the location of each resolution element within the scene.

The primary parameters investigated in this study were resolution or instantaneous field of view and soil moisture. The objective was to determine if the heterogeneity of the scene within the antenna resolution changes as a function of resolution size, to determine what

effect such a change would have on the antenna temperature soil moisture dependence, and to determine if there is a resolution that maximizes this dependence on soil moisture. In order to determine the effect of scene heterogeneity, soil moisture variations that would occur across a large scene due to precipitation patterns and soil composition were not addressed in this study. The effect of this moisture variability on the resolution requirements of an orbiting microwave system would be in addition to the resolution requirements due to scene heterogeneity. The intent was to address this question in the follow-on studies.

It was originally thought that as resolution was decreased the sensitivity of the antenna temperature to soil moisture would increase. This was based on the assumption that the scene "purity" within a resolution element would improve as resolution decreased. This turned out to be an erroneous assumption. As a result, it was determined that the average sensitivity of antenna temperature to soil moisture improves slightly as the antenna footprint size increased. Also, the precision (or variability) of the sensitivity changes as a function of resolution. Surprisingly, however, the highest variability occurs at middle resolutions, on the order of 20 km. Resolutions of 5 km and 60 km have approximately equal 95% confidence limits on the estimate of the sensitivity to soil moisture. At horizontal polarization, the average sensitivity to soil moisture at L-band is approximately -1.5°K/percent soil moisture; at C-band approximately -0.85°K/percent soil moisture; and X-band approximately -0.50°K/percent soil moisture. These computed sensitivities to soil moisture should be reasonable estimates of what can be expected from

an orbiting passive microwave system operating over non-mountainous land terrain, with the only limitation being that the pixels are less than 40% forest covered. Improvements in these sensitivities could be expected for pixels known to consist of agricultural features.

MODEL DEFINITION AND STRUCTURE

In order to produce a simulation model versatile enough to be of use in addressing the many unanswered questions concerning the viability and system measurement constraints on an orbiting passive microwave system designed for soil water measurement, the system model had to be capable (within limits) of: 1) handling arbitrary antenna gain patterns, 2) integration over both like and cross polarized antenna gain patterns, 3) arbitrary look angle, 4) arbitrary resolution, 5) arbitrary altitude, 6) antenna scanning, and 7) flight path simulation. In addition, the results obtained from the simulation model are only as good as the scene simulated. Thus, the scene characterization had to be realistic in both component make up, geometry, and component statistics. The capability of controlling certain scene parameters such as roughness, soil moisture, and temperature arbitrarily over the scene had to be available. And, methods of estimating the brightness temperature of each scene pixel had to be developed as a function of soil moisture, soil temperature, surface roughness, microwave frequency, polarization, and emission angle.

The simulation program generated met all of the above requirements. Although all of these capabilities were not utilized in this study, they are expected to be needed in future efforts. Of the two tasks described above, 1) space platform and antenna coordinate system

definition/implementation, and 2) ground scene definition and development, the latter proved to be the more difficult task and required the most effort.

Space Platform Coordinate System/Implementation

The center of each ground cell within the scene is defined by its position in the surface-based XYZ coordinate system, Figure 1. These coordinates are then linked to the satellite platform coordinates X"'Y"'Z"' by the system of equations:

$$\begin{vmatrix} X' \\ Y' \\ Z' \end{vmatrix} = \begin{vmatrix} X \\ Y \\ Z \end{vmatrix} - \begin{vmatrix} \alpha_0 \\ \beta_0 \\ \gamma_0 \end{vmatrix} \qquad (1)$$

and

$$\begin{vmatrix} X'' \\ Y'' \\ Z'' \end{vmatrix} = \begin{vmatrix} \cos\phi & \sin\phi & 0 \\ -\sin\phi & \cos\phi & 0 \\ 0 & 0 & 1 \end{vmatrix} \begin{vmatrix} X' \\ Y' \\ Z' \end{vmatrix} \qquad (2)$$

and

$$\begin{vmatrix} X''' \\ Y''' \\ Z''' \end{vmatrix} = \begin{vmatrix} 1 & 0 & 0 \\ 0 & \cos\theta & \sin\theta \\ 0 & -\sin\theta & \cos\theta \end{vmatrix} \begin{vmatrix} X' \\ Y' \\ Z' \end{vmatrix} \qquad (3)$$

This transformation is accomplished by first displacing the XYZ system by α_0, β_0, γ_0 to form the X'Y'Z' system. Next, the X'Y'Z' system is rotated about the Z' axis (angle ϕ) to form the X"Y"Z" system. Finally, this latter system is rotated about the Y" axis (angle θ) to form the X"'Y"'Z"' system. The angle ϕ (the first rotation of X'Y'Z' about Z') is defined as azimuth, while rotation about Y", angle θ is defined as the roll or incident angle.

ORIGINAL PAGE IS
OF POOR QUALITY

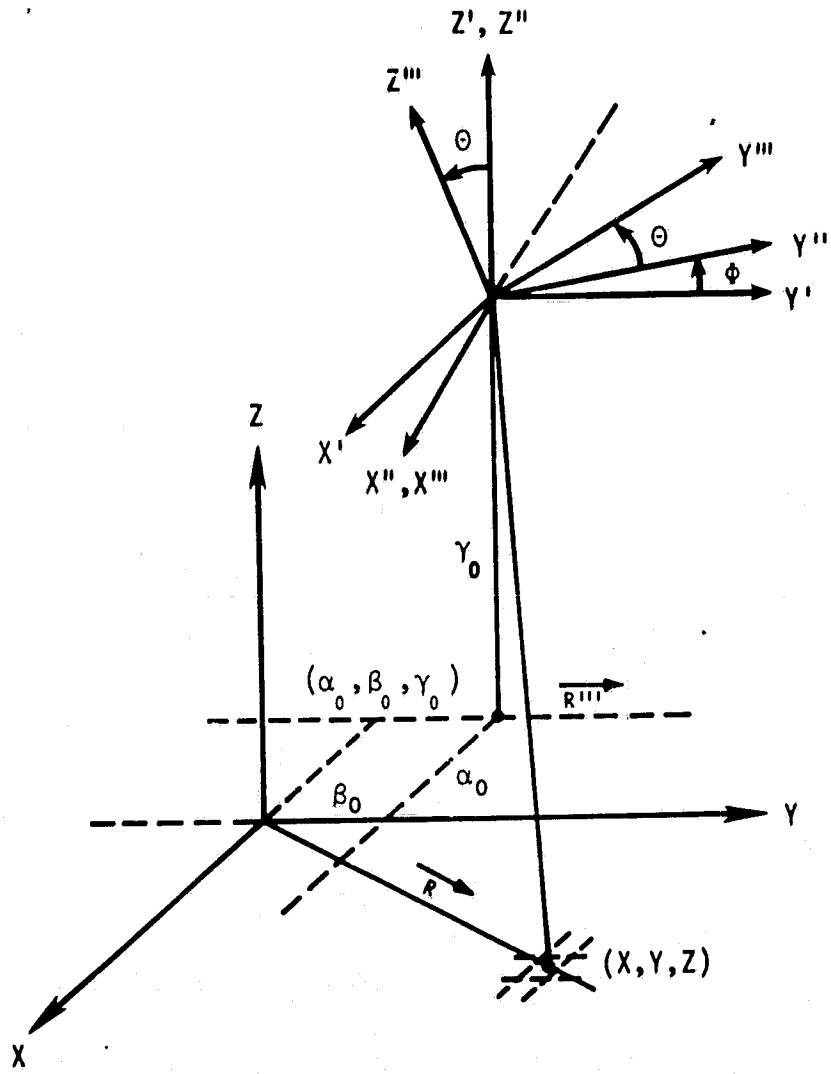

FIGURE 1. Relationship between the scene coordinate system and the satellite platform coordinate system

Antenna Temperature Equations

The computation of the radiometer antenna temperature of that portion of the scene at which the antenna is looking requires an integration of the product of the scene brightness temperature and the antenna gain pattern. This integral is performed for both horizontal and vertical linear polarizations and is denoted by:

$$BA_v = \frac{\int G_{VV}(\theta,\phi)BTV(\theta,\phi)d\Omega}{\int G_{VV}(\theta,\phi)d\Omega} + \frac{\int G_{VH}(\theta,\phi)BTH(\theta,\phi)d\Omega}{\int G_{VH}(\theta,\phi)d\Omega} \qquad (4a)$$

$$BA_h = \frac{\int G_{HH}(\theta,\phi)BTH(\theta,\phi)d\Omega}{\int G_{HH}(\theta,\phi)d\Omega} + \frac{\int G_{VH}(\theta,\phi)BTV(\theta,\phi)d\Omega}{\int G_{HV}(\theta,\phi)d\Omega} \qquad (4b)$$

where:

BA_V, BA_H - computed antenna temperature for vertical and horizontal polarizations, respectively.

$BTV(\theta,\phi)$, $BTH(\theta,\phi)$ - brightness temperature of the scene at vertical and horizontal polarizations, respectively

$G_{VV}(\theta,\phi)$, $G_{HH}(\theta,\phi)$ - like polarized antenna gain patterns for vertical and horizontal polarizations, respectively

$G_{VH}(\theta,\phi)$, $G_{HV}(\theta,\phi)$ - cross polarized antenna gain patterns for vertical and horizontal polarizations, respectively

$d\Omega$ - differential solid angle.

The angles θ and ϕ are identified in Figure 2. The second term in equations (4a) and (4b) constitute a cross polarized contribution to the antenna temperature. This contribution is small for good antennas. However, it is worth having the capability of computing this

ORIGINAL PAGE IS
OF POOR QUALITY

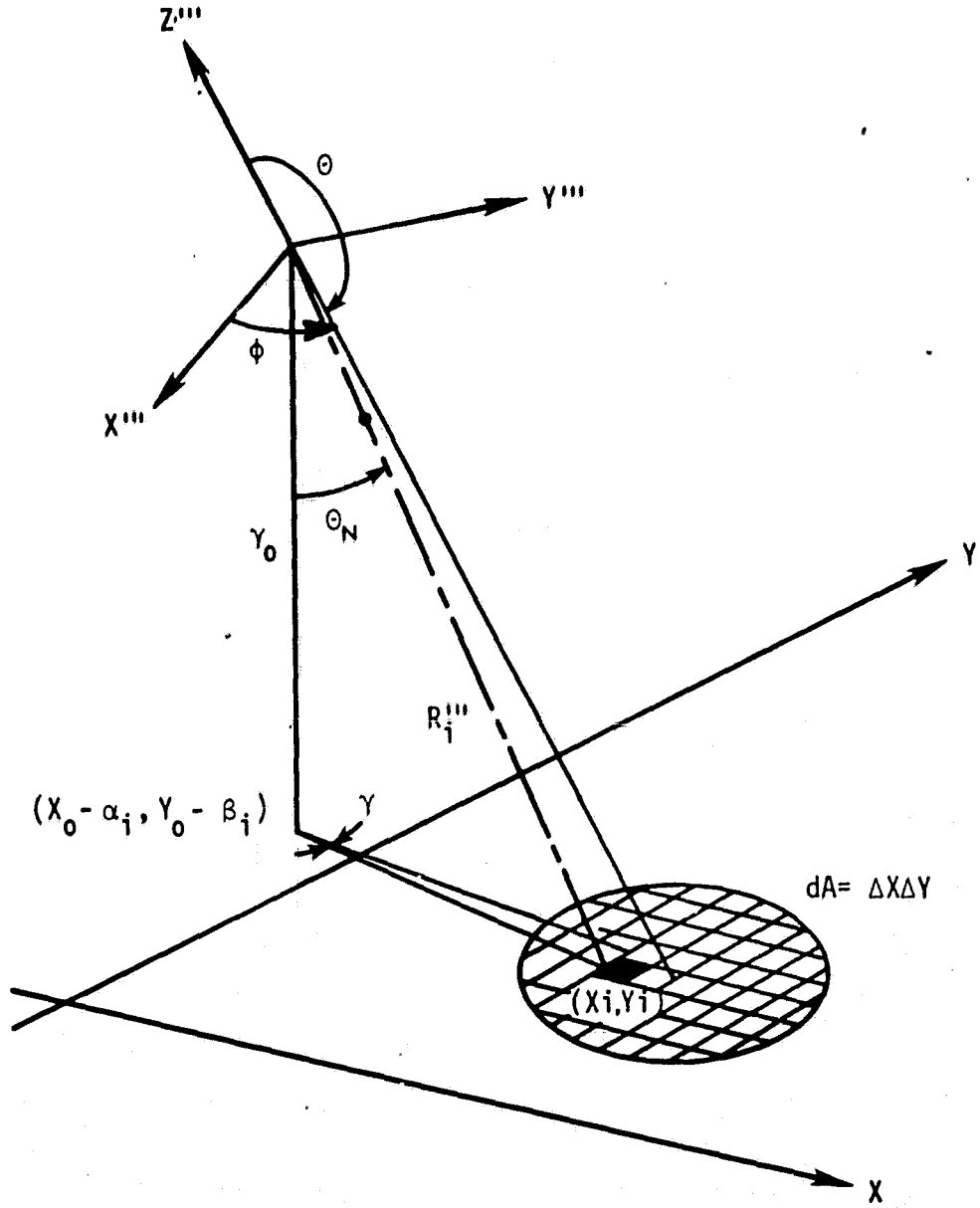

FIGURE 2. Definition of parameters used in model equations.

contribution in order to determine its effect on measurements by real antennas that might one day be flown in space.

Actual antenna patterns were not used in the program for the purpose of the study presented in this document. An idealized antenna gain pattern of the form:

$$G(\theta,\phi) = G(\theta) = \left|\frac{\sin x}{x}\right| f$$

where

$$x = \pi \frac{\theta}{\theta_n}$$

θ_n - half of null-to-null beamwidth of the main lobe

For this idealized antenna pattern, there is no cross polarized gain. The effect of the parameter f in the above expression is indicated in Table 1.

The horizontal brightness temperatures of the scene in equations (4a) and (4b) are also corrected for changes in the local plane of incidence within the antenna footprint. If γ is the angle between the plane determined by the sub-nadir line and the antenna axis, and the plane defined by the sub-nadir line and a line from the antenna and the pixel of interest in the scene (Figure 2), then the corrected scene brightness temperature is given by:

$$BTV(\theta,\phi) = TV(\theta')\cos^2\gamma + TH(\theta')\sin^2\gamma$$

$$BTH(\theta,\phi) = TH(\theta')\cos^2\gamma + TV(\theta')\sin^2\gamma$$

TABLE .. Effects of Parameter f on Gain Pattern Shape

f	Peak Value of First Sidelobe (db down)	3 db Beamwidth Compared to Null-to-Null Width
0.5	3.4	79
1.0	6.7	60
1.5	10.1	50
2.0	13.5	44
2.5	16.8	40
3.0	20.2	37
3.5	23.6	34
4.0	26.9	32
4.5	30.3	30
5.0	33.7	29

where

θ' - local incident angle at scene pixel defined by θ and ϕ

$TV(\theta')$ - vertical brightness temperature of pixel defined by θ and ϕ

$TH(\theta')$ - horizontal brightness temperature of pixel defined by θ and ϕ

The parameters TV and TH for each type of scene pixel are computed in subroutines BRIGHT and CORR described below.

Integral Evaluations

In order to evaluate the integrals in equations (4a) and (4b), they were transformed as follows:

$$\int G(\theta,\phi)T(\theta,\phi)d\Omega \simeq \sum_x \sum_y \frac{T(x,y,\theta_n,\phi,\rho)G(\theta,\phi)\cos\theta_n dA}{(R''')^2} \qquad (5)$$

and

$$\int G(\theta,\phi)d\Omega = \sum_x \sum_y \frac{G(\theta,\phi)\cos\theta_n dA}{(R''')^2} \qquad (6)$$

where

$$(R''')^2 \gg \Delta X \Delta Y$$

and

$$(R''')^2 = (X - \alpha_0)^2 + (Y - \beta_0)^2 + (Z - \gamma_0)^2 \qquad (7)$$

The angles θ and ϕ are given by:

$$\theta = \cos^{-1} \frac{Z'''}{R'''} \tag{8}$$

and

$$\phi = \mathrm{Tan}^{-1} \frac{Y'''}{X'''} \tag{9}$$

with X''', Y''', Z''' as defined in equations (1), (2) and (3).

The above system of equations was implemented on the Texas A&M computer. The computational algorithm was designed so that for each nadir position of the satellite, (α_j, β_j), equation (4) was evaluated over the antenna footprint, Figure 3. Equations (5) and (6) were used to calculate the value of the indefinite integrals in equation (4). The footprint limits were established as the area included within the antenna beamwidth projected onto the ground scene. The beamwidth of the antenna was selected as the angle included between the first two sidelobes. By design, these two sidelobes are 20 dB down from the gain at the center of the beam.

The basic system algorithm accomplishes the following:
For each X, Y, Z in the footprint, calculate

$$\theta = \cos^{-1} \frac{Z_i'''}{R_i'''} \tag{10}$$

or

$$\theta_i = \cos^{-1} \frac{(x_i - \alpha_j)\sin\theta\sin\phi - (y_i - \beta_j)\sin\theta\cos\phi}{R_i'''} \tag{10a}$$

ORIGINAL PAGE IS
OF POOR QUALITY

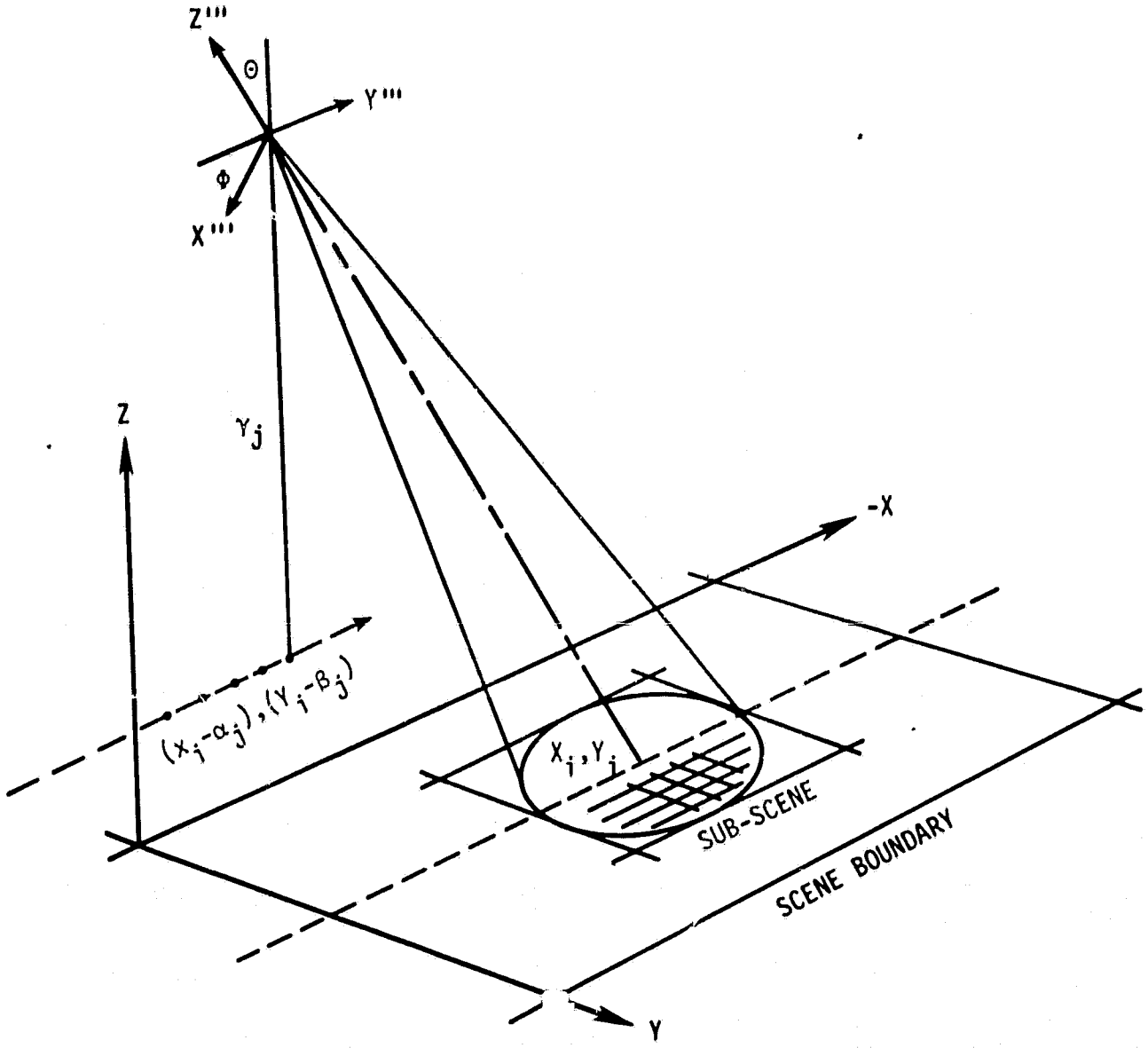

FIGURE 3. Antenna footprint relative to the nadir position and the scene boundary.

$$\phi_i = \sin^{-1}\left(\frac{Y_i'''}{R_i'''\sin\theta}\right) \tag{11}$$

or

$$\phi_i = \sin^{-1} \frac{-(x_i - \alpha_j)\sin\phi\cos\theta + (y_i - \beta_j)\cos\theta\cos\phi}{R_i'''\sin\theta} \tag{11a}$$

where

$$R_i''' = [(x_i - \alpha_j)^2 + (y_i - \beta_j)^2 + (z_i - \gamma_j)^2]^{1/2} \tag{12}$$

The i subscript indexes each pixel in the footprint and j indexes each position of the satellite nadir. As these parameters are evaluated for each pixel in the footprint, the two sums for the indefinite integrals, equations (5) and (6), are accumulated so that for each footprint, (or for each nadir position, (α_j, β_j)), there exists

$$N_j = \sum \sum \frac{(T_i G_i \cos\theta_n \Delta A_i)}{(R_j'''')^2} \tag{13}$$

and

$$D_j = \sum \sum \frac{(G_i \cos\theta_n \Delta A_i)}{(R''')^2} \tag{14}$$

which are used to evaluate apparent brightness temperature for that footprint,

$$BA_j = \frac{N_j}{D_j} \tag{15}$$

Simulated Ground Scene

Scene Construction

The dominant criteria used in constructing the ground scene was that it must be capable of being represented digitally on magnetic tape or some other peripheral storage medium. Next, the scene had to be large enough to accommodate satellite altitudes of up to 500 km with antenna beamwidths of 30 degrees or less, and incident angles of 50 degrees or less. As illustrated in Figure 4, these parameters yield a maximum field of view of 722 km. Finally, the minimum resolution desired was areas of approximately 40 acres. This turns out to be approximately 0.24 x 0.24 km; therefore, the ground scene was sized to be 1444 units wide.

To insure that the ground scene was as realistic as possible, actual fullframe classified Landsat images were used to build the scene. Eight Landsat images of central and east Texas classified into various vegetation, water, and urban classes by the Texas Parks and Wildlife Department were used. Figure 5 illustrates the area covered by the eight Landsat scenes. Appendix A contains the classified images as produced by the Texas Parks and Wildlife Department, along with descriptions of what the classifications mean.

Each classified Landsat image contained a maximum of 1824 by 2048 Landsat pixels. Further, each classified map had different classes. There was inconsistency in the definition format of the scene classes on different maps (i.e., the digital count representing grass would appear as a different value on each tape containing the classified

ORIGINAL PAGE IS
OF POOR QUALITY

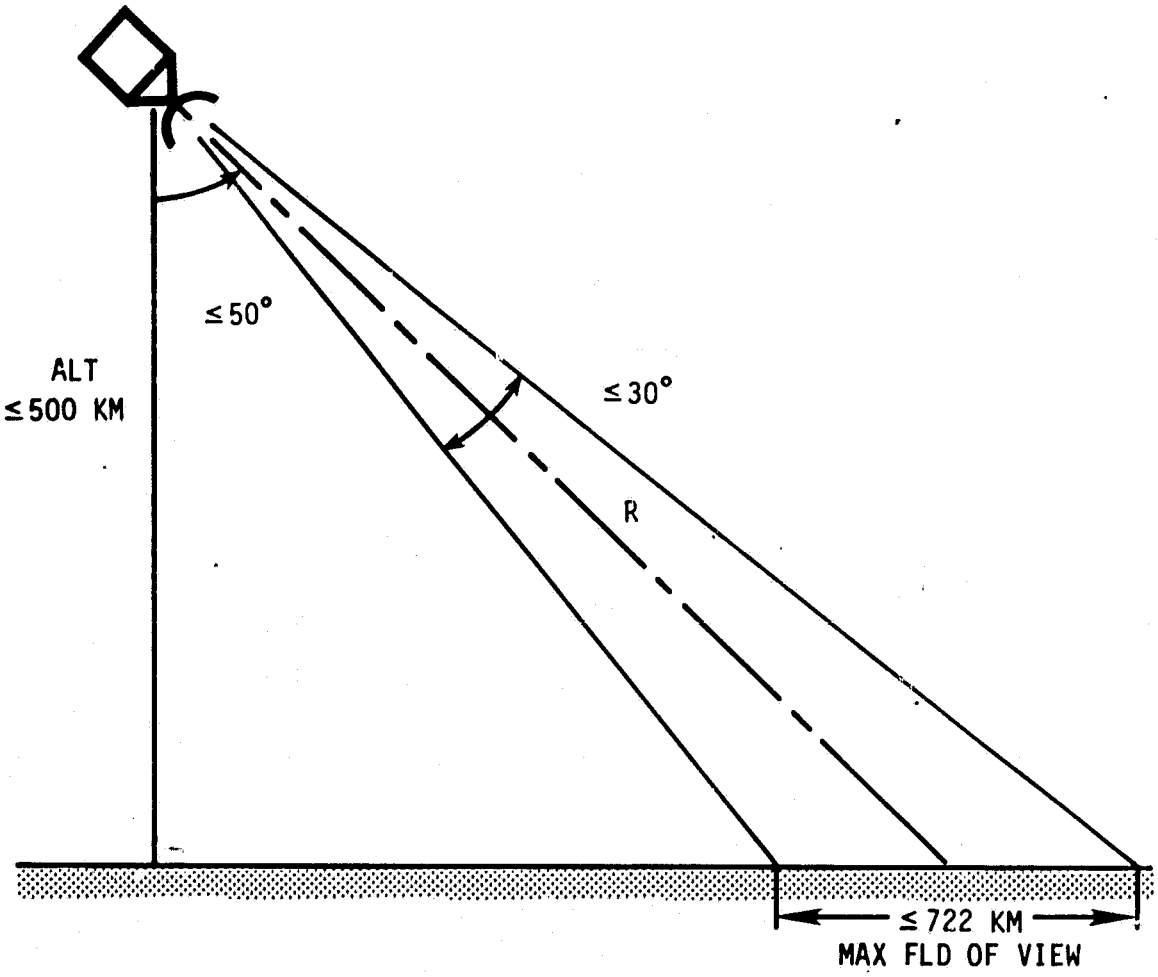

FIGURE 4. Limitations of the simulation model in terms of field of view requirements and scene size.

ORIGINAL PAGE IS
OF POOR QUALITY

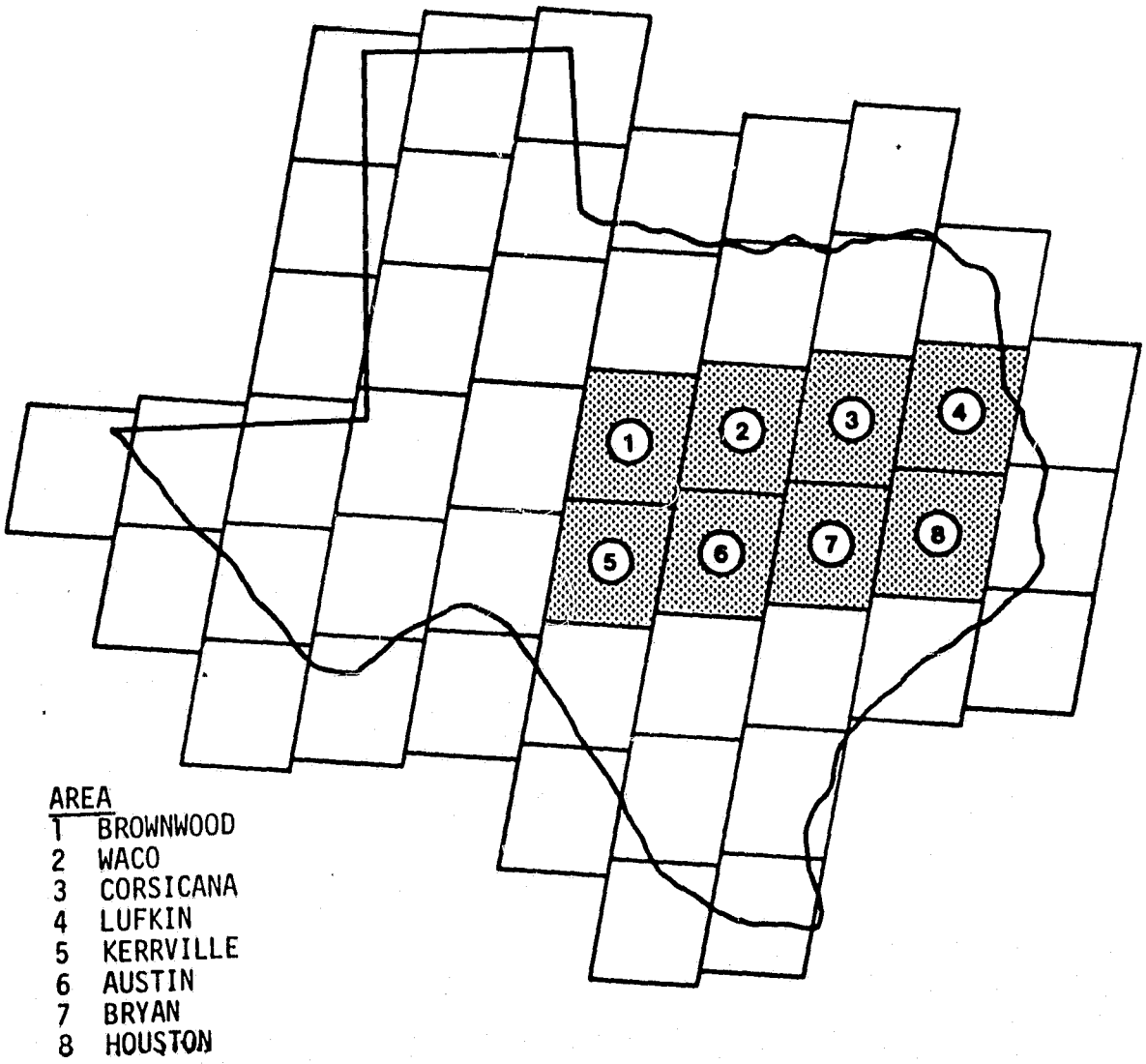

FIGURE 5. Areas covered by the eight Landsat scenes used to generate the simulated scene.

data from each scene). In order to use the Texas Parks and Wildlife classified Landsat images to produce a ground scene, the 80 m by 80 m Landsat pixels had to be aggregated to decrease the number of scene pixels. Also, the classes as defined by the Texas Parks and Wildlife Department had to be reassigned into classes meaningful to microwave emission computations. The class assignments in the Texas Parks and Wildlife classification were analyzed and transformed into the following six classes described in Table 2. The procedure for performing this reduction reclassification is described below. Models for computing the brightness temperature of each of the classes defined in Table 2 as a function of soil moisture, temperature, and roughness are also described below.

Converting Classified Landsat Types to TAMU Percent Class Types

Each pixel in the simulated scene was created by aggregating 3 by 3, 80 m by 80 m pixels in the classified Landsat maps to one 240 m by 240 m pixel in the simulated scene. In order to maintain the class composition of each aggregated 240 m by 240 m pixel, the percentage coverage of each class within the aggregated pixel was computed and maintained. These percentages were used to compute the proper brightness temperature for the mixture of classes within the aggregated pixel.

The Texas Parks and Wildlife tapes (MAPTAP) were formatted as scan lines of up to 2048 pixels per line such that each byte (8 bits) represented an 80 x 80 meter ground cell. Up to 1824 lines made up a single scene. The absolute binary value of each byte on the scan line was indicative of a land cover class (as defined by the Texas Parks

TABLE 2. Class Definitions.

Class	Description
1	Water
2	Bare Soil
3	Urban
4	Mixed Soil and vegetation
5	Fully vegetated
6	Forest

and Wildlife Service) within the respective ground cell. For example, in the Kerrville scene, MAPTAP No. 0068, the byte va ues range from 0 to 24 (decimal) as indicated in the legend for that scene in Appendix A. To convert these tapes to a more usable size and format, a reduction/reclassification transformation was performed. As indicated in Figure 6, each 6 x 6 set of bytes each byte representing one Landsat pixel on the MAPTAP was reduced into a set of 2 x 2 words (16 bits) of percent class data. Each word represents one 240 m x 240 m scene pixel.

Each MAPTAP was scanned to determine the percentage of the six pre-selected classes identified above that existed within each 3 x 3 Landsat pixel set. Since the MAPTAP vegetation classes did not match the 6 classes shown above and at the bottom of Figure 6, a selective transformation was made in the MAPTAP data. For example, on the Kerrville scene all MAPTAP values of 1, 2, 3, or 4 were considered to be TAMU Class 5; i.e., Fully Vegetated. The selected transformation that was used for each of the eight scenes varied according to the MAPTAP value assignments. Since each tape was different, a separate transformation scheme was selected for each tape (scene). The right-hand column of Appendix A shows the groupings used for each of the Texas Park and Wildlife scenes used.

Each 240 m by 240 m simulated scene pixel in the TAMU class data tape was represented by one 16 word bit. Each octal word within the 16 bits contained the percent of class coverage within that aggregated pixel for one of the six classes. In this manner, the 16 bit word contained the percentage coverages for five of the six classes. The percentage of the sixth class (forest) was implied by subtracting the

ORIGINAL PAGE IS
OF POOR QUALITY

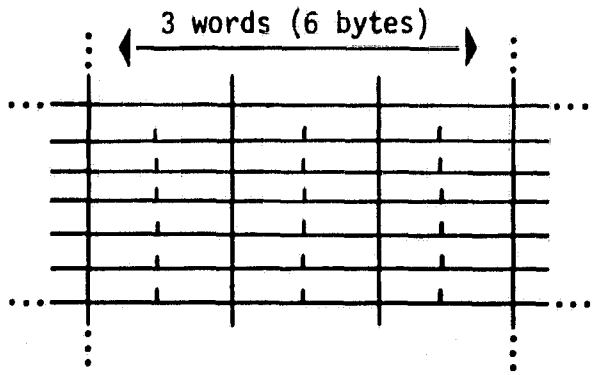

Texas Parks and Wildlife MAPTAP format. Each byte (≤ 255 counts) represents a Land cover class and corresponds to a Landsat 80 x 80 meter resolution element

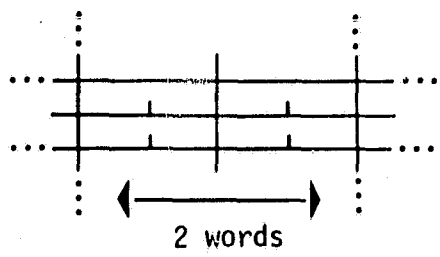

Each 6 x 6 bytes of MAPTAP information was mapped into 2 x 2 words. Each word represents percent class data for a 240 x 240 meter ground cell. Explanation of how each octal word represents class assignments is in Figure 7.

CLASS ASSIGNMENTS IN THE "CLASS DATA" TAPE

1 - WATER	4 - MIXED SOIL & VEGETATION
2 - BARE SOIL	5 - FULLY VEGETATED
3 - URBAN	6 - FOREST

FIGURE 6. Procedure for aggregating and mapping the Texas Parks and Wildlife Landsat classifications into the class used in the simulation program.

sum of the other five from 100. Encoding the percent class data into the 16 bit word describing each pixel of the simulated ground scene is illustrated in Figure 7. The [ ]$_i$ means the integer equivalent of the floating point expression.

Another problem was that the map tapes made no distinction between bare soil and urban area. Since these two areas have distinctly different brightness temperatures, adjustments had to be made. First, known urban areas were identified manually and their coordinates were given to the computer. These areas were then automatically changed from bare soil to urban as they were encountered during the transformation. Next, to get a more general mix of urban over the entire scene, whenever a 3 by 3 pixel set in the vegetation tapes was found to be fully bare soil, it was re-defined as urban. After each transformation, the resulting class map was plotted in grey-scale format to verify that an appropriate distribution had been achieved.

Using corner coordinates supplied with the Texas Parks and Wildlife sub-scene map tapes, the entire class data ground scene was grouped into one tape file as illustrated in Figure 8. The tape files contain 1650 records of 2496 words each. The process of constructing the composite class data scene was a nine step sequence. First, the entire scene was filled with Class 6 (forest) as a background. Each sub-scene of class data was over-layed starting in the upper right hand corner with the Lufkin sub-scene, and continuing with Houston, Corsicana, Bryan, Waco, Austin, Brownwood, and finally Kerrville. The entire class scene was then grey-scaled for each class. These maps are included in Appendix B.

ORIGINAL PAGE IS
OF POOR QUALITY

16 Bit word corresponding to one 240 x 240 m simulated scene pixel

0	1 - 3	4 - 6	7 - 9	10 - 12	13 - 15

CLASS 5

$$= \left[\left(\frac{\Sigma i}{9.}\right) * 7.\right]_I * 4096$$

CLASS 4

$$= \left[\left(\frac{\Sigma i}{9.}\right) * 7.\right]_I * 512$$

CLASS 3

$$= \left[\left(\frac{\Sigma i}{9.}\right) * 7.\right]_I * 64$$

CLASS 2

$$= \left[\left(\frac{\Sigma i}{9.}\right) * 7.\right]_I * 8$$

CLASS 1

$$= \left[\left(\frac{\Sigma i}{9.}\right) * 7.\right]_I$$

Notes:

1. Σi is the number of Landsat pixels in the 3 x 3 array of Landsat pixels corresponding to the ith class.

2. The subscript I indicates that the number in brackets is an integer.

- - - -CLASS 6 IMPLIED

FIGURE 7. Construction of the 16 bit word that describes the percentages of classes in each 240 x 240 meter simulated scene pixel.

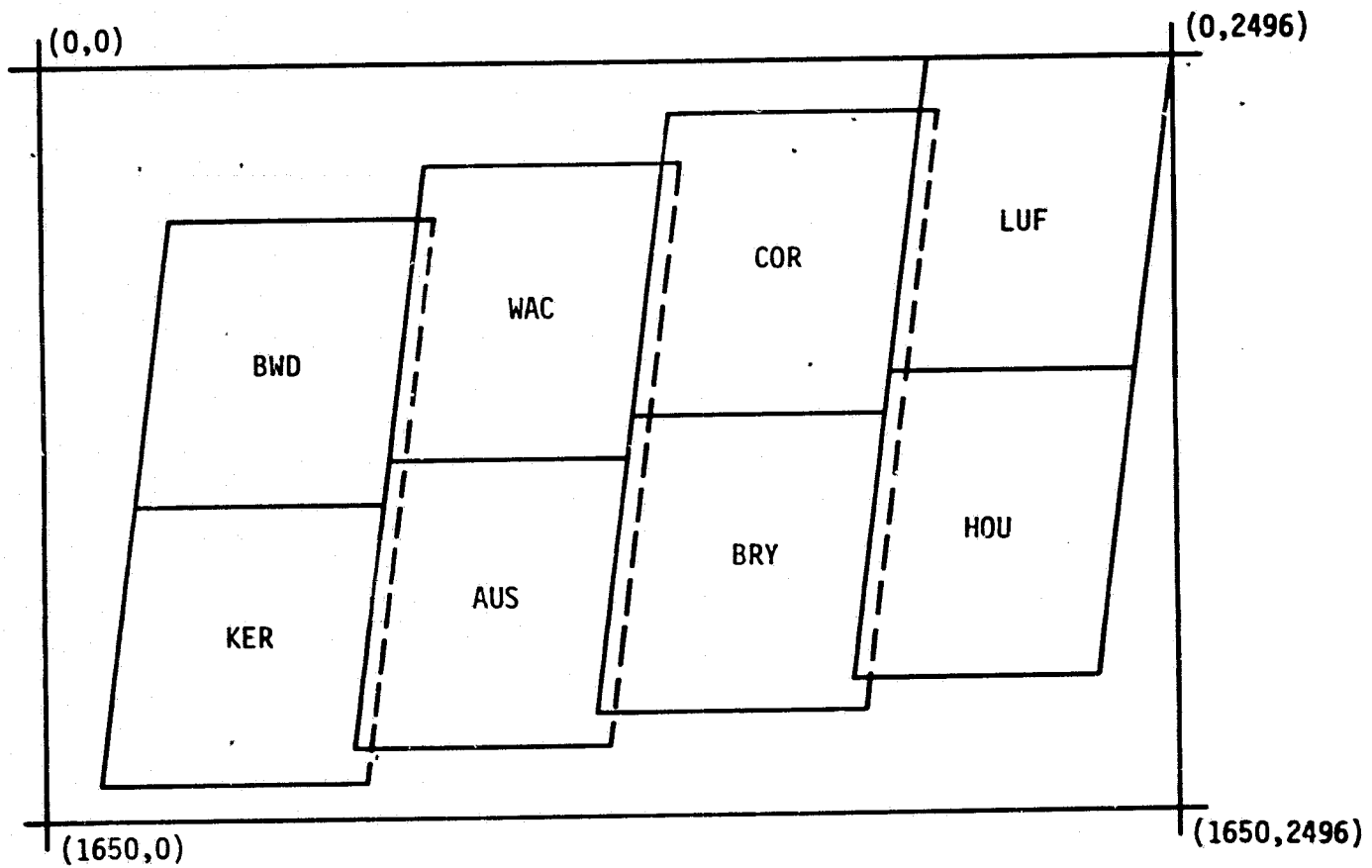

FIGURE 8. Relative locations of the Landsat scenes in relation to the entire simulated ground scene.

ORIGINAL PAGE IS
OF POOR QUALITY

Scene Utilization

Use of the composite ground scene and the related computer software has specific limits as implied in Figure 9. The altitude limits are related to antenna beamwidth. The scene pixels represent approximately 14 acres each. The entire scene represents a surface area of 396 by 599 km.

The system initialization and operation concept is illustrated in Figure 10. It is important to understand that the starting point is defined by the initial coordinates of the antenna beam footprint (center line); i.e., (X_0, Y_0). This, along with altitude, incident and azimuth angles, define the initial system geometry. Also required are beamwidth and displacement rates. During this phase of the project, zero rates were used for all variables except the nadir coordinates. Satellite movement was accomplished by stepping the nadir coordinate from (α_0, β_0) to (α_i, β_i) by the rates $\Delta\alpha$, $\Delta\beta$.

Since the initial position of the satellite is specified in terms of the antenna beam center line on the surface, the initial nadir point must be evaluated using the concept illustrated in Figure 11. At the beam center line,

$$X''' = Y''' = 0 \tag{16}$$

and

$$Z''' = \frac{-H}{\cos\phi} \tag{17}$$

then

$$R_S = Z'''\sin\theta = -H\tan\theta \tag{18}$$

so that

ORIGINAL PAGE IS
OF POOR QUALITY

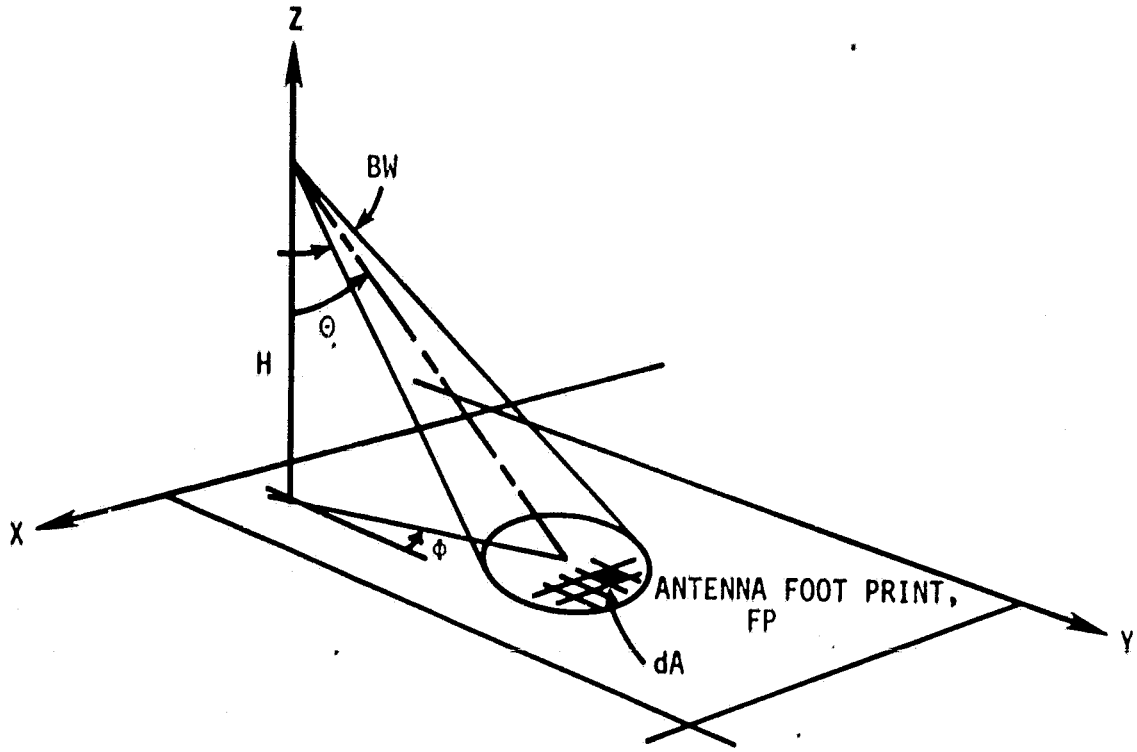

FIGURE 9. Major simulation parameters that must be specified properly in order to maintain consistency between the antenna footprint size and the simulated scene size.

ORIGINAL PAGE IS
OF POOR QUALITY

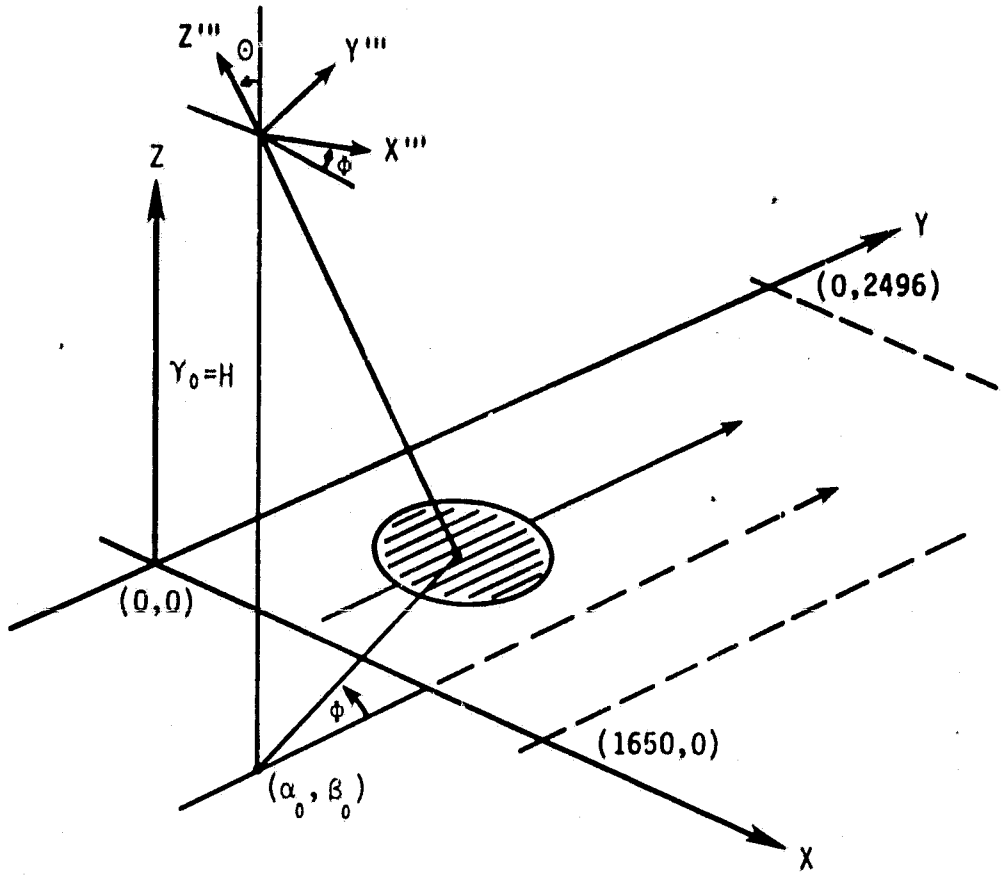

FIGURE 10. Simulation software initialization with respect to the ground scene coordinate system.

ORIGINAL PAGE IS
OF POOR QUALITY

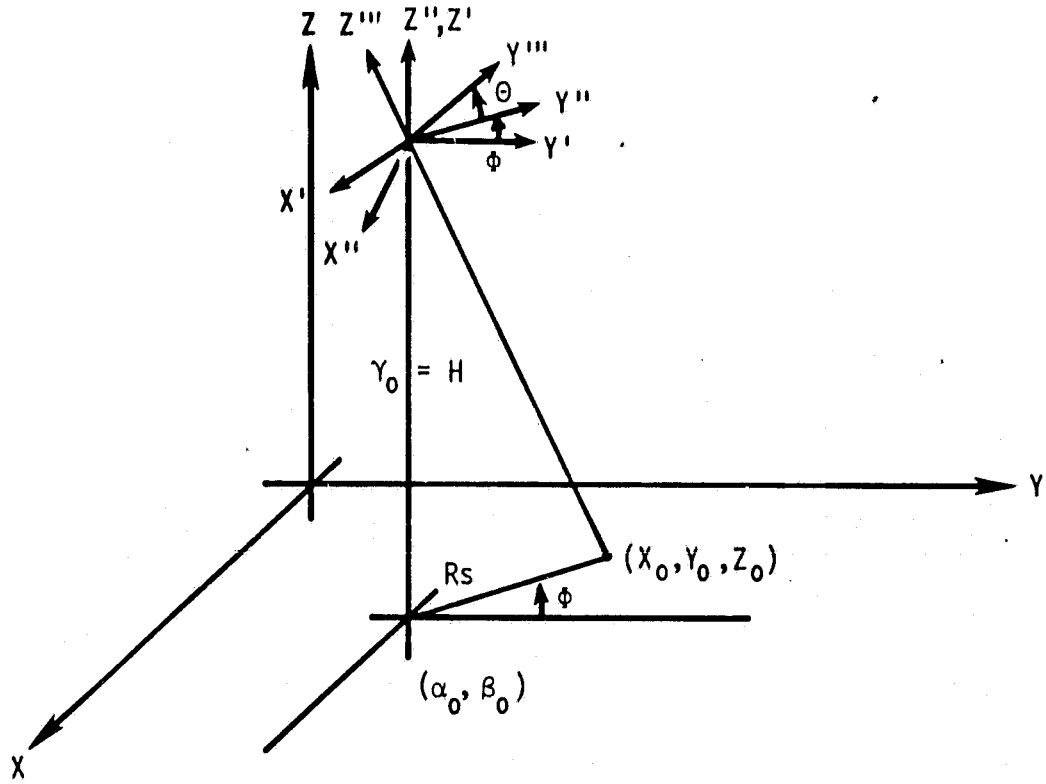

FIGURE 11. Calculation of the initial nadir point.

$$R_S \sin\Phi = \alpha_0 - X_0 \tag{19}$$

$$R_S \cos\Phi = Y_0 - \beta_0 \tag{20}$$

$$\alpha_0 = R_S \sin\Phi + X_0 \tag{21}$$

$$\beta_0 = Y_0 - R_S \cos\Phi \tag{22}$$

Now, knowing the starting condition it remains to determine reasonable limits on the integration over the antenna footprint. These limits were selected as upper and lower boundaries on a rectangle which always contains the smaller rectangle whose sides are parallel to the major and minor axis and tangent to the sides of the footprint ellipse, Figure 12. The lower and upper limits on X and Y are derived as follows (Figure 12):

$$a = -H \tan\Theta - c \tag{23}$$

$$b = (H/\cos\Theta)\tan BW/2 \tag{24}$$

$$c = H \tan(\Theta - BW/2) \tag{25}$$

$$d = H \tan(\Theta + BW/2) - a - c \tag{26}$$

then

$$YU = Y_i + d \cdot \cos\Phi + b \cdot \sin\Phi \tag{27}$$

$$YL = Y_i + a \cdot \cos\Phi - b \cdot \sin\Phi \tag{28}$$

$$XU = X_i + a \cdot \sin\Phi + b \cdot \cos\Phi \tag{29}$$

$$XL = X_i + d \cdot \sin\Phi - b \cdot \cos\Phi \tag{30}$$

Subsequent program steps in calculating the brightness temperature over the antenna footprint are outlined in the Computational Flow Chart in Appendix C. For each nadir position defined by ($\alpha_0 + k\Delta\alpha$, β_0

ORIGINAL PAGE IS
OF POOR QUALITY

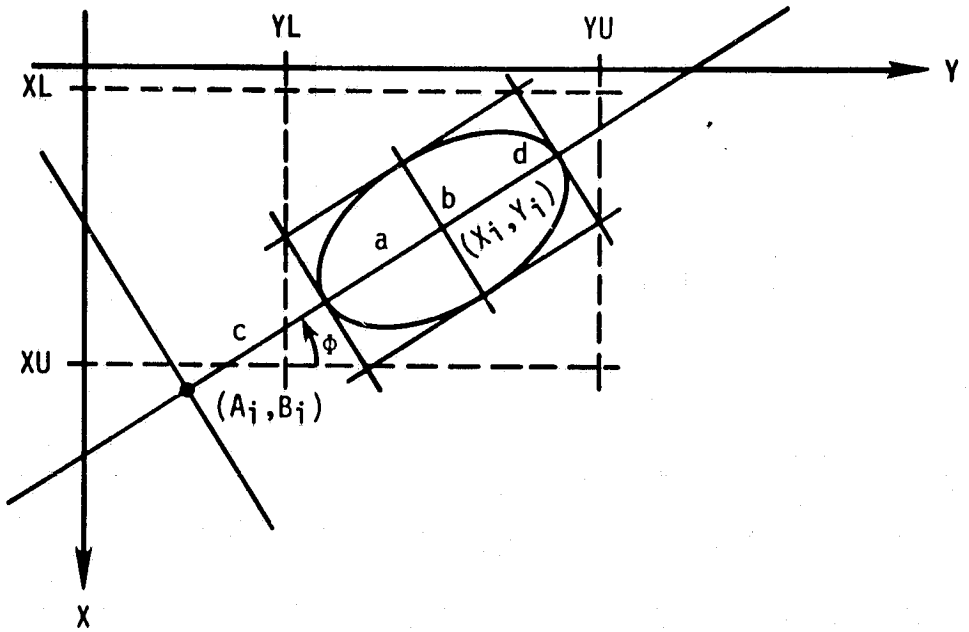

FIGURE 12. Definition of the parameters describing the limits of the antenna footprint integration.

$+ k\Delta\beta$), an apparent brightness temperature is calculated. Thus, the frequency of the data points calculated, as the satellite passes over the scene, and the direction of the movement across the scene, are governed by the selection of $\Delta\alpha$ and $\Delta\beta$. The index k simply increments from zero until the edge of the footprint encounters an edge of the composite scene.

The software system was implemented using the concept outlined in Figure 13. The main program was run either on the TI980 minicomputer or on the AMDAHL470 (IBM 360 Operating System). Coding was all in FORTRAN. Initialization was through the card reader or keyboard (TI980). Class data (ground scene) was on magnetic tape. The brightness temperatures and other associated data were output both in tabular form and on magnetic tape (compressed data set). All plots were made on the TI980 with output to a VERSATEC matrix printer.

All software code is included in Appendix D. These include the following:

STEP 1 PROGRAM - Maps vegetation 'type' data for each of 8 subscenes to each of 8 subscenes of '% class' data sets. Each unique mapping algorithm is included.

FILL DATA - Fills composite scene with forest background prior to performing individual overlays.

STEP 2 PROGRAM - Performs overlay operation; i.e., placing each subscene onto the composite scene at the correct position.

SATELLITE MODEL - Accepts initialization data and performs simulation of moving satellite over the scene, producing brightness temperature estimates for each position of the nadir point.

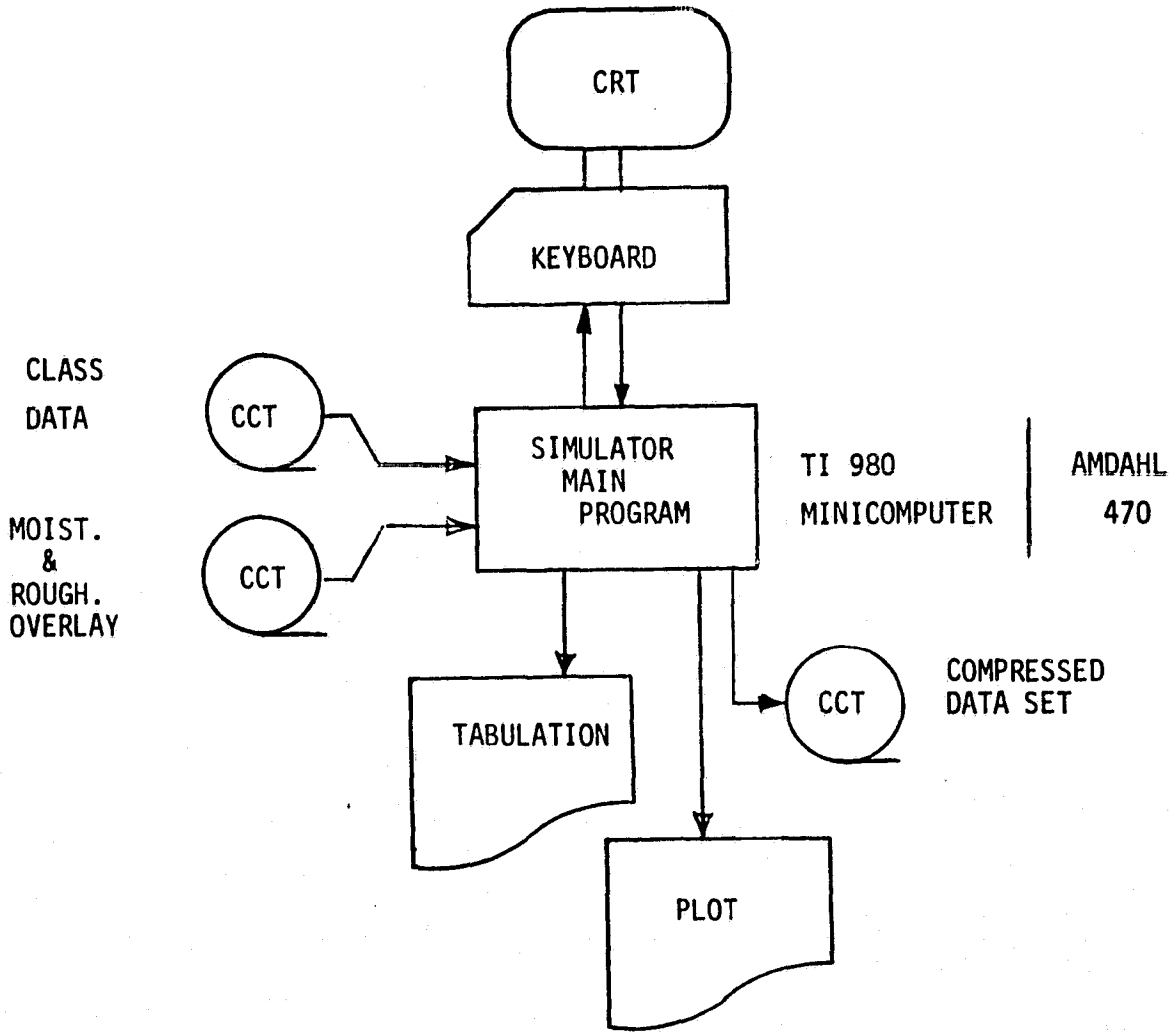

FIGURE 13. Implementation concept of the orbiting microwave radiometer simulation program.

COMPUTATION

The models used to compute the brightness temperature of each pixel in the simulated scene (BTH and BTV in equation (4)) were developed under subcontract to the University of Houston at Clear Lake City.

Objective and Approach

The objective of the research performed under the subcontract was to develop a mathematical model that can be used on a computer system to simulate passive microwave radiometer measurements over heterogeneous earth scenes under varying soil moisture, cultural feature, land cover, and atmospheric conditions. The algorithms that make up the mathematical model are limited to operating frequencies of 1.42 GHz (L-band), 4.8 GHz (C-band), and 10.7 GHz (X-band), and general land cover types of water, forest, grassland, partially vegetated, bare soil, and urban classes. The mathematical models predict the microwave emission of land or water surfaces for each of the six basic land cover types (i.e., water, fully vegetated (grassland), forest, mixed soil and vegetation, bare soil, and urban as specified in Table 2). The predicted emissions were designed to be valid at a nadir viewing angle of 50 degrees and for both horizontal and vertical polarization. Microwave emission at viewing angles other than 50 degrees was obtained through the use of yet another mathematical model.

To make the various computer models as realistic as possible, the class emission models were based upon empirical measurements with truck-mounted or airborne microwave radiometers where possible. In

most cases, such measurements existed and were documented in the open literature. Some gaps were evident, however. In these cases, theoretical models were used. As a matter of procedure, the information and models developed at the University of Houston at Clear Lake City were sent to the Remote Sensing Center throughout the contract period. The actual encoding of the algorithms on a computer system was done at the Remote Sensing Center at Texas A&M University.

The various mathematical models are described in detail in the following sections.

Subroutine BRIGHT

To provide a realistic data base of land cover types for the simulation program, as previously described, investigators at the Remote Sensing Center obtained a set of land cover themes based on classified Landsat images for the general area of central and eastern Texas. The area had been classified into several land cover categories which in turn could be assigned to one of the following six classes: open water, vegetation (total cover), bare soil, mixed vegetation and bare soil, forest, and urban. These data were given in a data base where each data cell represented one Landsat picture element having a spatial area of about 1.1 acre. It was determined by members of this current research effort that the given data base was too large to handle. So, it was decided to reduce the data base by combining 56 Landsat picture elements into one composite area. This procedure results in the basic information unit for land cover being heterogeneous, that is, many classes can be represented in the 40 acre data cell.

It was necessary to preserve some aspect of the mixture of classes within the composite data cell. Since a 16 bit word was available to encode the class type, it was decided to include some information about the percentage area of each class in the single data word used to represent the composite area in the reduced data base. After the leading sign bit, the data word was made up of five three-bit word slices. Each three-bit slice can be interpreted as follows:

Bit Pattern	Percent of Area Covered
000	0.0%
001	18.75
010	31.25
011	43.75
100	56.25
101	68.75
110	81.25
111	100.00

For example, suppose that 25% of the picture elements represented bare soil, 15% represented water, and the rest (60%) was mixed vegetation and soil. From left to right, the slices represent vegetation, mixed soil and vegetation, bare soil, urban, and open water. The class, forest, is included as a residual. The above percentages would then be encoded as follows (after the sign bit): 000100001000001. In turn, this particular pattern would be interpreted as follows:

Vegetation	0.0%
Mixed Soil & Vegetation	56.26
Bare Soil	18.75
Urban	0.0
Open Water	18.75
Subtotal	93.75

A residual of 6.25% would be assigned to the class of forest in this example. The example clearly shows the fact that errors exist

in the categorical way of expressing the percentage mixture of each subclass. The advantage gained is the increase in the speed of computation with a data base that has been reduced by a factor of 40.

FORTRAN Code for Subroutine BRIGHT

The FORTRAN code for Subroutine BRIGHT is given in Appendix D. The purpose of Subroutine BRIGHT is to calculate the horizontally and vertically polarized brightness temperature for a given composite data area at a viewing angle of 50 degrees from the nadir for given land cover types and conditions. The call for Subroutine BRIGHT is as follows:

```
CALL BRIGHT(SM,ICW,NB,TP,ROU,BTV50,BTH50)
```

The elements of the call are defined as follows:

SM - Soil moisture parameter taken to be the volumetric soil moisture content in percent for Miller Clay. A field capacity of 100% is reached when SM=38.

ICW - A 16-bit integer binary word that contains information about the distribution of ground cover types within the composite area cell, (see above for code)

NB - Frequency band number (NB=1 for L-band, NB=2 for C-band, and NB=3 for X-band)

TP - Temperature parameter (the temperature that dry, bare soil would have under the same weather conditions, given in degrees Celsius)

ROU - Roughness parameter (used for bare soil and mixed vegetation and soil calculations -- use ROU=0.0 for smooth fields and ROU=0.6 for rough soils)

BTV50 - Brightness temperature of the composite area cell for vertical polarization and for a zenith angle of 50 degrees (degrees Kelvin)

BTH50 - Brightness temperature of the composite area cell for horizontal polarization and for a zenith angle of 50 degrees (degrees Kelvin)

Subroutine BRIGHT uses several other subroutines in the process of the calculation of the brightness temperatures of the composite cell. Also, the information encoded in the parameter, ICW, is is unpacked and used in the calculation. Subroutine BRIGHT uses the following subroutines:

Subroutine WATER	Emission of open water
Subroutine URBAN	Emission of urban areas
Subroutine BARE	Emission of bare fields
Subroutine MIX	Emission of mixed vegetation and soil
Subroutine VEG	Emission of grassland
Subroutine FOREST	Emission of forest

The outputs from Subroutine BRIGHT (i.e., BTV50 and BTH50) are used in the Subroutine BCORR which estimates the polarized brightness temperature components at angles other than 50 degrees from the zenith.

The other subroutines mentioned above are discussed in detail in the following sections.

Brightness Temperature as Function of Angle (Subroutine BCORR)

Based upon the many measurements of the brightness temperature of various objects as reported throughout the literature, a simple extrapolation scheme was adopted to extend calculated brightness temperatures to angles of viewing needed in the program calculations. A program was developed to calculate the emissivity of a smooth, homogeneous dielectric material interfacing air. The calculations

were performed for viewing angles (measured from the normal to the interface surface) from 0 to 80 degrees in steps of one degree. The calculations were performed for a number of material types (liquid water, dry soil, wet soil). It was noted that the normalized distribution of emissivities with viewing angle was little affected by the choice of dielectric constant. Thus, it is possible to model the angular distribution with a tabular function as follows:

$$BTH = BTH50 + FH*DELBT$$

$$BTV = BTH50 + FV*DELBT$$

where

BTH - brightness temperature at some given angle for horizontal polarization

BTV - brightness temperature at some given angle for vertical polarization

FH - form factor for horizontal polarization which is a function of viewing angle (table lookup)

FV - form factor for vertical polarization which is a function of viewing angle (table lookup),

DELBT - difference between the brightness temperatures (vertical and horizontal polarization) at a viewing angle of 50 degrees, i.e.,

$$DELBT = BTV50 - BTH50$$

BTH50 - calculated brightness temperature for horizontal polarization and for a viewing angle of 50 degrees as given from Subroutine BRIGHT.

BTV50 - calculated brightness temperature for vertical polarization and for a viewing angle of 50 degrees as given from subroutine BRIGHT

The values for FH and FV adopted in the present algorithm are given in Table 3 and plotted in Figure 14.

The appropriate value for FH and FV is obtained by conversion of the angle to an integer index value. Using the index value, the

TABLE 3. Values for the form factors, FH and FV, as a function of nadir angle.

Angle (degrees)	FH	FV
0	0.540	0.540
1	0.540	0.540
2	0.539	0.540
3	0.538	0.541
4	0.537	0.542
5	0.535	0.544
6	0.534	0.546
7	0.531	0.548
8	0.529	0.551
9	0.526	0.554
10	0.522	0.557
11	0.519	0.561
12	0.515	0.565
13	0.510	0.569
14	0.506	0.574
15	0.500	0.579
16	0.495	0.584
17	0.489	0.590
18	0.483	0.596
19	0.476	0.602
20	0.469	0.609
21	0.461	0.617
22	0.453	0.624
23	0.445	0.632
24	0.436	0.641
25	0.426	0.649
26	0.417	0.659
27	0.406	0.668
28	0.395	0.378
29	0.384	0.689
30	0.372	0.699
31	0.360	0.711
32	0.347	0.722
33	0.333	0.734
34	0.319	0.747
35	0.305	0.759
36	0.289	0.773
37	0.274	0.787
38	0.257	0.801
39	0.239	0.815
40	0.222	0.830

TABLE 3. (con't). Values for the form factors, FH and FV, as a tabular function of nadir angle.

Angle (degrees)	FH	FV
41	0.203	0.845
42	0.184	0.861
43	0.164	0.877
44	0.143	0.894
45	0.121	0.911
46	0.099	0.928
47	0.075	0.945
48	0.051	0.963
49	0.026	0.982
50	0.000	1.000
51	-0.027	1.019
52	-0.055	1.038
53	-0.084	1.057
54	-0.114	1.076
55	-0.145	1.095
56	-0.177	1.115
57	-0.211	1.134
58	-0.245	1.153
59	-0.281	1.172
60	-0.316	1.190
61	-0.356	1.208
62	-0.396	1.225
63	-0.437	1.241
64	-0.480	1.256
65	-0.523	1.270
66	-0.569	1.282
67	-0.616	1.292
68	-0.664	1.300
69	-0.714	1.305
70	-0.766	1.306
71	-0.820	1.304
72	-0.875	1.297
73	-0.932	1.285
74	-0.991	1.266
75	-1.051	1.239
76	-1.114	1.203
77	-1.179	1.157
78	-1.246	1.098
79	-1.314	1.025
80	-1.385	0.933

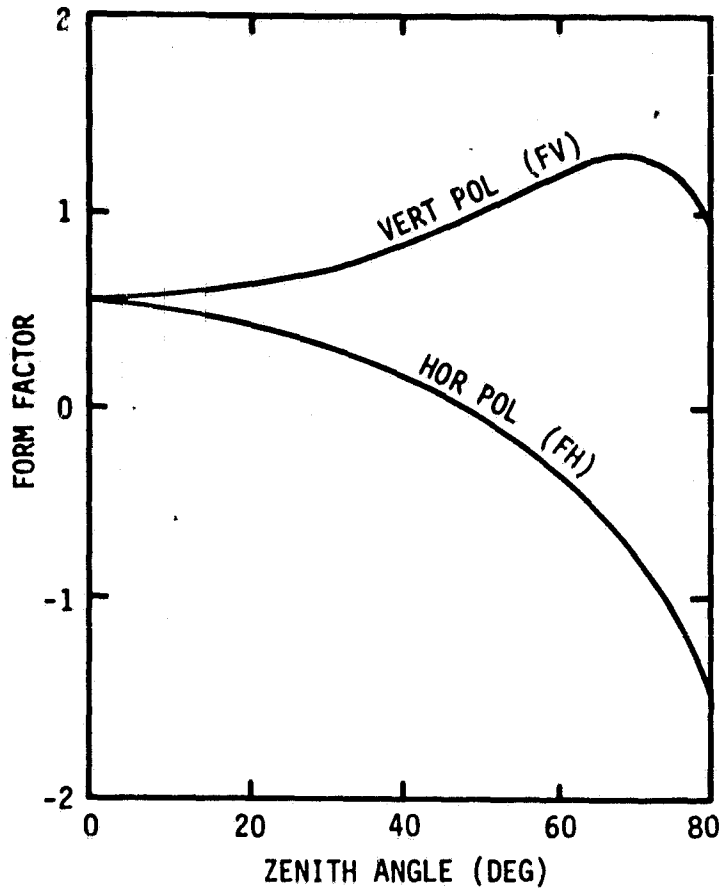

FIGURE 14. Plot of the form factor used to estimate brightness temperature as a function of incident angle.

needed value for FH and FV is looked up in the table of values of FH and FV. The brightness temperatures computed in subroutine BRIGHT at 50° (BTV50 and BTH50) are computed to the appropriate incident angle in subroutine BCORR. The listing of this subroutine is contained in Appendix D. The call for subroutine BCORR is as follows:

```
CALL BCORR(BTV50,BTH50,TN,BTV,BTH)
```

The elements of the call are determined as follows:

TN - incident angle at the pixel of interest

BTV - vertical brightness temperature at angle TN

BTH - horizontal brightness temperature at angle TN

Subroutine WATER

The emissivity of water at microwave frequencies is a function of water temperature, water salinity, frequency, angle of viewing, and polarization [12]. Linear relationships were derived between emissivity and water temperature at a 50 degree incident angle for both horizontal and vertical polarization based upon calculations made by Paris [2] in which the water surface was modeled as being a flat, homgeneous dielectric material overlain by air. These relationships were derived for the three frequency bands of interest to this research (i.e., L-, C-, and X-band). The results of the calculations are as follows:

L-band:

$$EH50 = 0.256 + TWC*0.000467$$

$$EV50 = 0.505 + TWC*0.000767$$

Note: EH50 is the horizontal emissivity at 50 degrees viewing angle, EV50 is the vertical emissivity at 50 degrees viewing angle, and TWC is the water temperature in degrees Celsius.

C-band:

EH50 = 0.265

EV50 = 0.522

X-band:

EH50 = 0.288 - TWC*0.0003

EV50 = 0.557 - TWC*0.0005

With the value of the emissivity, the brightness temperaure is calculated by the following formulas:

BTVW = EV50*TWK + (1. - EV50)*SKYT

BTHW = EH50*TWK + (1. - EH50)*SKYT

where

TWK - temperature in degrees Kelvin

SKYT - sky brightness temperature at 50 degrees viewing angle (SKYT = 6.0 for L-band, 8.0 for C-band and 10.0 for X-band)

BTVW - value of the brightness temperature of the water for vertical polarization and for a viewing angle of 50 degrees,

BTHW - the value of the brightness temperature of the water for horizontal polarization and for a viewing angle of 50 degrees.

The FORTRAN code for Subroutine WATER is given in Appendix D. The call for Subroutine WATER is as follows:

CALL WATER (NB,TP,BTN,BTHW)

The elements of the call are defined as follows:

NB - frequency band number (as before)

TP - temperature parameter (as before)

BTVW - brightness temperature of water for veritcal polarization and a viewing angle of 50 degrees

BTHW - brightness temperature of water for horizontal polarization and a viewing angle of 50 degrees.

Subroutine URBAN

An urban area is an extremely complex environment for which calculation of the brightness temperature is required. Water can pond on the tops of buildings. Many different types of materials are found in such areas. Also, natural vegetation and forest are mixed in such areas. A very simple approach was adopted in the face of such complexity. It was assumed that the emissivity of the urban area over all was simply the following:

$$EV50 = 0.96$$

$$EH50 = 0.86$$

Moreover, it was assumed that the temperature of the urban scene was the same as that of dry, bare soil under the same climatic conditions.

The assumed values for the emissivity of an urban area were based upon measurements over asphalt by Straiton and Talbert [13], over asphalt, gravel road, and other manmade materials by Straiton et al. [14], and on other such materials by Porter and Florance [15].

The FORTRAN code for Subroutine URBAN is given in Appendix D. The call for Subroutine URBAN is as follows:

```
CALL URBAN(TP,BTVU,BTHU)
```

The elements of the call are defined as follows:

TP - temperature parameter (as before)

BTVU - brightness temperature of an urban area for vertical polarization and for a viewing angle of 50 degrees

BTHU - brightness temperature of an urban area for horizontal

Subroutine BARE

The microwave emission of bare soil has been under study for many years by investigators in the Joint Soil Moisture Experiment sponsored by NASA. In general, they have found that the emissivity of soil is a function of soil moisture in the upper layers, soil roughness, soil type, angle of viewing, polarization, and frequency. The brightness temperature of soils is influenced by soil temperature as well as the forementioned parameters.

For the purpose of the algorithm reported in this report, the time of day is taken to be about 2 p.m. local time, a time when the surface of the soil is near its maximum temperature. For a given soil moisture condition, the microwave radiation that emerges from the soil surface is emitted from a zone of soil bounded on the top by the air-soil surface. The thickness of that zone is determined by soil moisture content itself and the frequency of the radiometer. Also, the relationship between emissivity and soil moisture is non-linear. In this algorithm, the non-linear function is approximated by two linear functions that are continuous. One function covers the range of soil moisture from 0 to 12% (by volume), and another function covers the range of soil moisture greater than 12% (by volume).

The most complete study of the microwave emissive properties of a soil type is that of Miller Clay near the Remote Sensing Center, Texas A&M University, College Station, Texas. The main results of several summers of measurements from truck-based microwave radiometers have been reported by Newton [4]. Recently, Choudhury et al. [11] found that the roughness effects on a field of bare soil can be

modeled by an exponential function. These results have been incorporated into the algorithms below.

Soil moisture itself has an effect on soil temperature. This fact is included in the algorithms proposed in this study. Figure 15 demonstrates the manner in which this is taken into account in the simulation for a temperature parameter (TP defined below) of 40°C.

X-band Algorithm

At X-band, the emission occurs from the uppermost layer for all ranges of soil moisture. The effect of soil moisture on soil temperature (TGK in degrees Kelvin) is given as:

$$TGK = 273.15 + TP - 0.87*SM$$

where TP is the temperature parameter (degrees Celsius), and SM is the soil moisture (percent by volume). For Miller Clay, SM ranges from zero to 38% at field capacity. Moisture contents greater than field capacity are possible. If SM is greater than 38%, TGK is set equal to TP plus 240.15.

The equations for the emissivity are as follows:

SM < 12%:

$$EH50 = 0.91 - 0.00917*SM$$

$$EV50 = 0.99 - 0.0025*SM$$

SM > 12%:

$$EH50 = 0.96 - 0.0135*SM$$

$$EV50 = 1.05 - 0.0077*SM$$

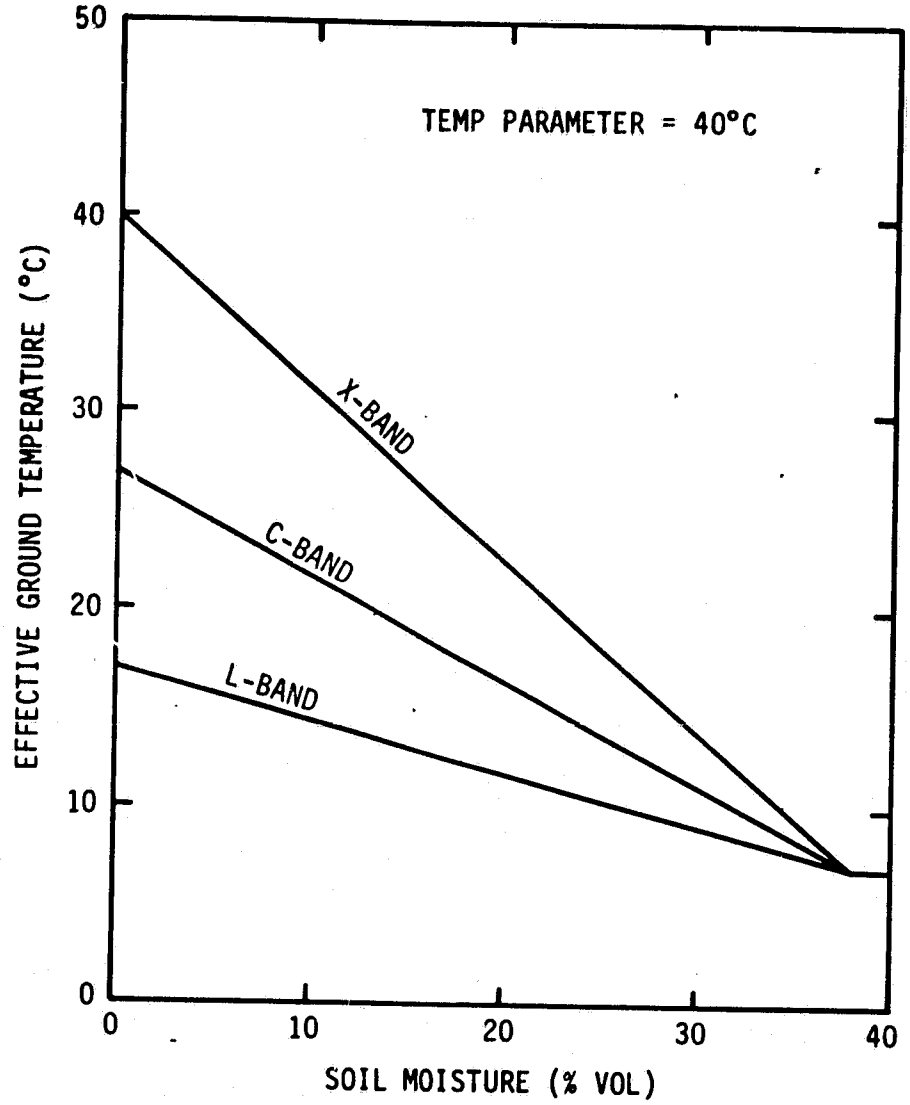

FIGURE 15. Plot of the assumed relationship between soil moisture and soil temperature for a temperature parameter of 40°C.

C-band Algorithm

Little work has been done at C-band in passive microwave remote sensing of soils. It is assumed here that the effects of soil moisture lie halfway between the effects at L-band and at X-band. The main departure is the modeling of dielectric constant from which emissivities are gathered. The algorithm at C-band is as follows:

TGK = 260.15 - 0.53*SM + TP

SM < 12%:

EH50 = 0.86 - 0.00833*SM

EV50 = 0.97 - 0.0025*SM

SM > 12%:

EH50 = 0.92 - 0.0135*SM

EV50 = 1.04 - 0.00846*SM

L-band Algorithm

The algorithm at L-band is as follows:

TGK = 250.15 + TP - 0.26*SM

SM < 12%:

EH50 = 0.90 - 0.00917*SM

EV50 = 0.98 - 0.0025*SM

SM > 12%:

EH50 = 0.96 - 0.0139*SM

EV50 = 1.047 - 0.00808*SM

FORTRAN Code for Subroutine BARE

The FORTRAN code for Subroutine BARE is given in Appendix D. The call for Subroutine BARE is as follows:

```
CALL BARE(NB,TP,SM,ROU,BTVB,BTHB,RH,RV)
```

The elements of the call are defined as follows:

NB - Frequency band number (as before)

TP - Temperature parameter (as before)

SM - Soil moisture parameter -- the soil moisture for a Miller Clay soil in percent by volume. For other soils, translate the soil moisture to that of Miller Clay by use of wilting point (12%) and field capacity (38%).

ROU - Roughness parameter (as before)

BTVB - Brightness temperature for bare soil for vertical polarization and for a viewing angle of 50 degrees.

BTHB - Brightness temperature for bare soil for horizontal polarization and for a viewing angle of 50 degrees.

RH - Reflectivity for horizontal polarization and for a viewing angle of 50 degrees (parameter is needed for Subroutines MIX and VEG)

RV - Reflectivity for vertical polarization and for a viewing angle of 50 degrees

Roughness Algorithm

A rough surface has a higher emissivity than does a smooth surface. The algorithm used to account for the effect of surface roughness is as follows:

```
RH = 1.0 - EH50

RV = 1.0 - EV50

RFAC = EXP(-ROU*0.4132)

RHnew = RHold*RFAC

RVnew = RVold*RFAC

EH50new = 1.0 - RHnew

EV50new = 1.0 - RVnew
```

Then, to complete the calculation for BTHB and BTVB:

BTHB = EH50*TGK

BTVB = EH50*TGK

An example of this effect is seen in Figure 16.

Subroutine VEG

In this subroutine, it is assumed that a 100 percent grass type vegetal cover exists on the land. In such cases, the temperature of the vegetal canopy is moderated by the processes of evaporation and transpiration. The algorithm below attempts to allow for this effect. Figure 17 illustrates the dependence of the plant canopy temperature on the temperature parameter.

The brightness temperature of vegetation is computed using the reflectivities and brightness temperatures obtained from Subroutine BARE under smooth surface conditions (i.e., ROU=0.0). The reflectivity is modified according to a computed vegetation factor, VFAC, which depends upon the soil moisture content. This factor is based upon measurements made by Newton [4]. The FVAC reduces the computed reflectivity. The vegetation factor is applied fully for L-band calculations, partially for C-band calculations, and is not used for X-band calculations. This means that at X-band, no penetration of the vegetal canopy occurs. In the case of X-band, a constant set of emissivities is assumed, viz., EH50=0.92 and EV50=0.95. The L-band algorithm is given below:

```
TVC = (TP - 25.0)*0.24 + 25.0  (Correction for canopy
                                temperature)
TVK = TVC + 273.15
CALL BARE(NB,TVC,SM,0.0,BTVB,BTHB,RH,RV)
```

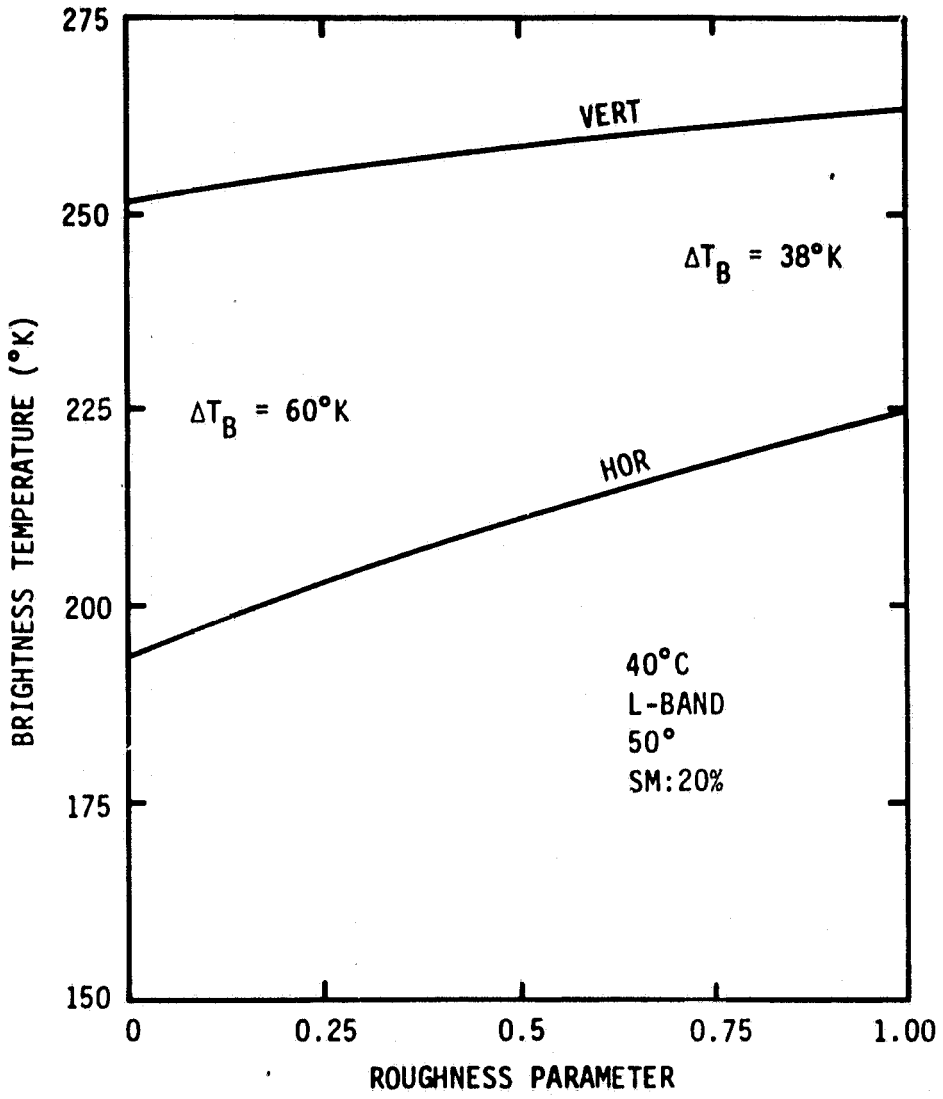

FIGURE 16. Example of the roughness parameter effect on brightness temperature.

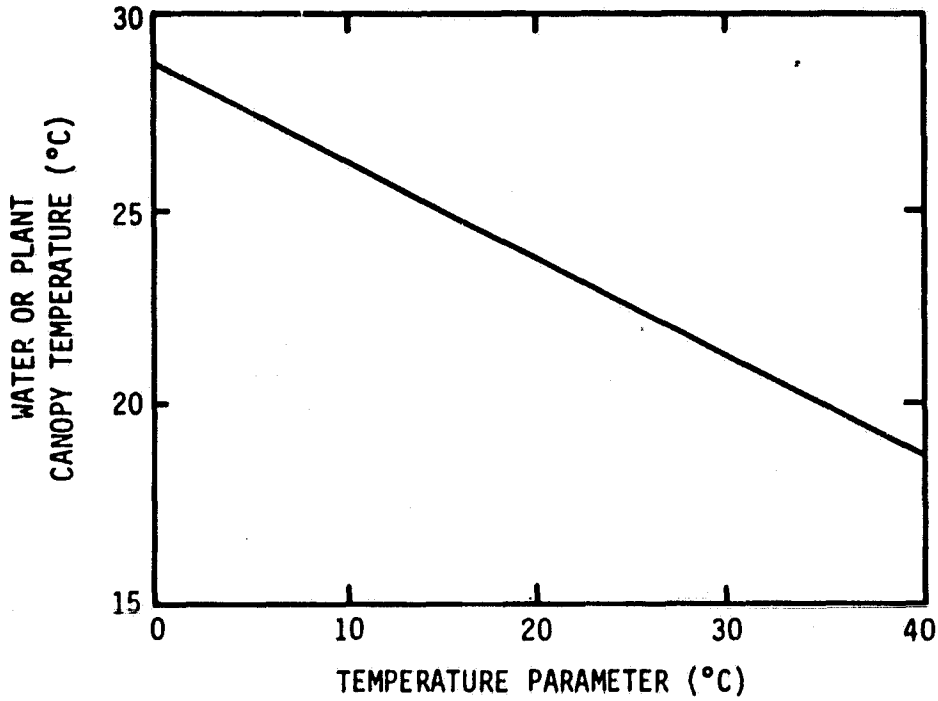

FIGURE 17. Example of how the temperature parameter is assumed to effect the water or plant canopy temperature.

VFAC = 0.8 - 0.00395*SM

XRH = RH*VFAC

XRV = RV*VFAC

The FORTRAN code for Subroutine VEG is given in Appendix D. The call for Subroutine VEG is as follows:

```
CALL VEG(NB,TP,SM,BTVV,BTHV)
```

The elements of the call are defined as follows:

NB - Frequency band number (as before)

TP - Temperature parameter (as before)

SM - Soil moisture parameter (as before)

BTVV - Brightness temperature of the vegetal canopy for vertical polarization and for a viewing angle of 50 degrees

BTHV - Brightness temperature of the vegetal canopy for horizontal polarization and for a viewing angle of 50 degrees.

Subroutine MIX

Subroutine MIX is a subroutine that calculates the brightness temperatures for a partially vegetated field. Subroutines BARE and VEG are called in the program. The results are averaged together to get the mixed result.

The FORTRAN code for Subroutine MIX is given in Appendix D. The call for Subroutine Mix is a follows:

```
CALL MIX(NB,TP,SM,ROU,BTVM,BTHM)
```

The elements of the call are defined as follows:

NB - Frequency band number (as before)

TP - Temperature parameter (as before)

SM - Soil moisture parameter (as before)

ROU - Roughness parameter (as before)

BTVM - Brightness temperature for the partially vegetated field for horizontal polarization and for a viewing angle of 50 degrees

BTHM - Brightness temperature for the partially vegetated field for horizontal polarization and for a viewing angle of 50 degrees.

Subroutine FOREST

Subroutine FOREST simply treats the surface as a thick vegetated canopy. Subroutine VEG is used with NB=3 regardless of the band used.

The FORTRAN code for Subroutine FOREST is given in Appendix D. The call for Subroutine FOREST is as follows:

```
CALL FOREST(TP,BTVF,BTHF)
```

The elements of the call are as follows:

TP - Temperature parameter (as before)

BTVF - Brightness temperature of the forest for vertical polarization and for a viewing angle of 50 degrees

BTHF - Brightness temperature of the forest for horizontal polarization and for a viewing angle of 50 degrees.

Summary

Examples of the brightness temperatures for the different classes and the effect of soil moisture and soil temperature are shown in Figures 17 thorugh 21. Note in Figures 18 and 19 that the brightness temperature of only three classes are dependent on soil moisture. These figures are for L-band and also demonstrate the effect of vegetation in decreasing the dependence on soil moisture. Figures 20 and 21 show that at X-band there are only two classes that have a dependence on soil moisture. Also, the mixed bare and vegetative class is significantly less sensitive to sol moisture than the bare

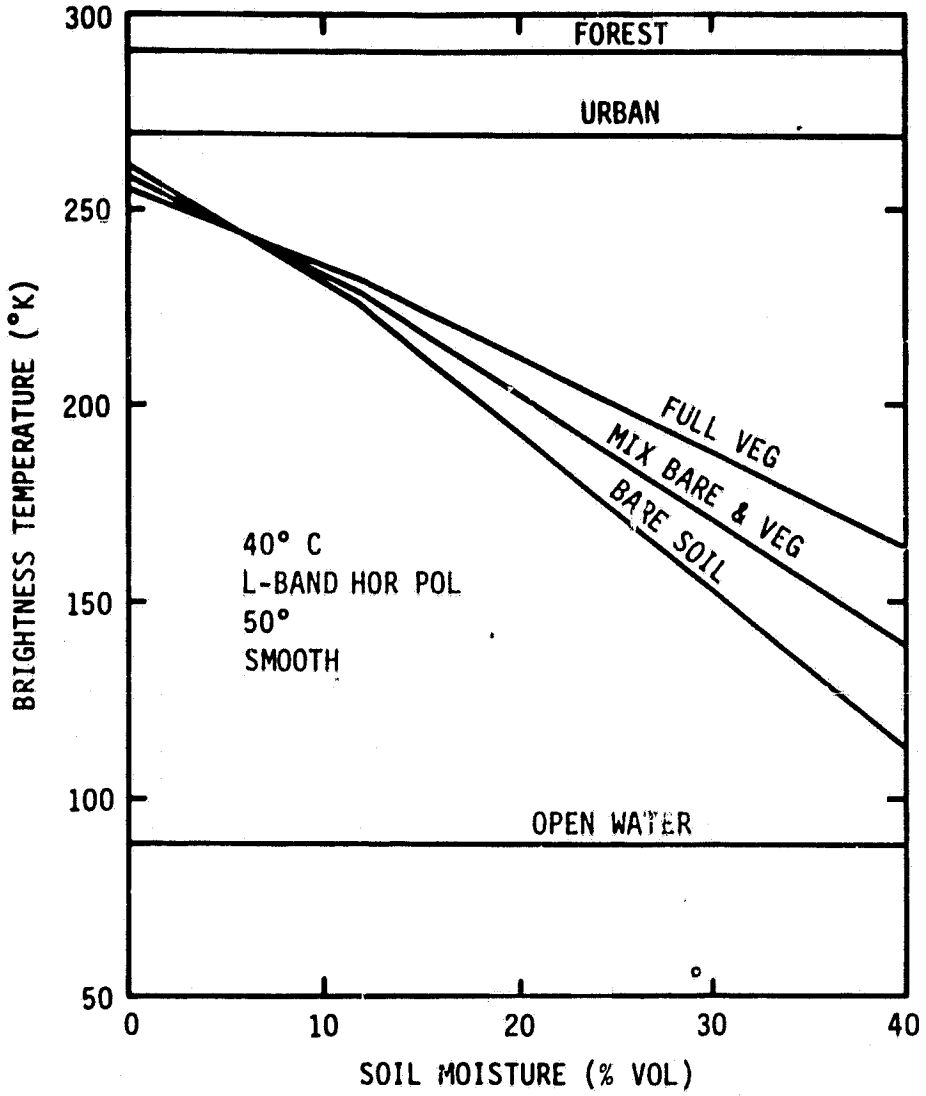

FIGURE 18. Example of the dependence of brightness temperature on soil moisture for all classes at L-band horizonal polarization.

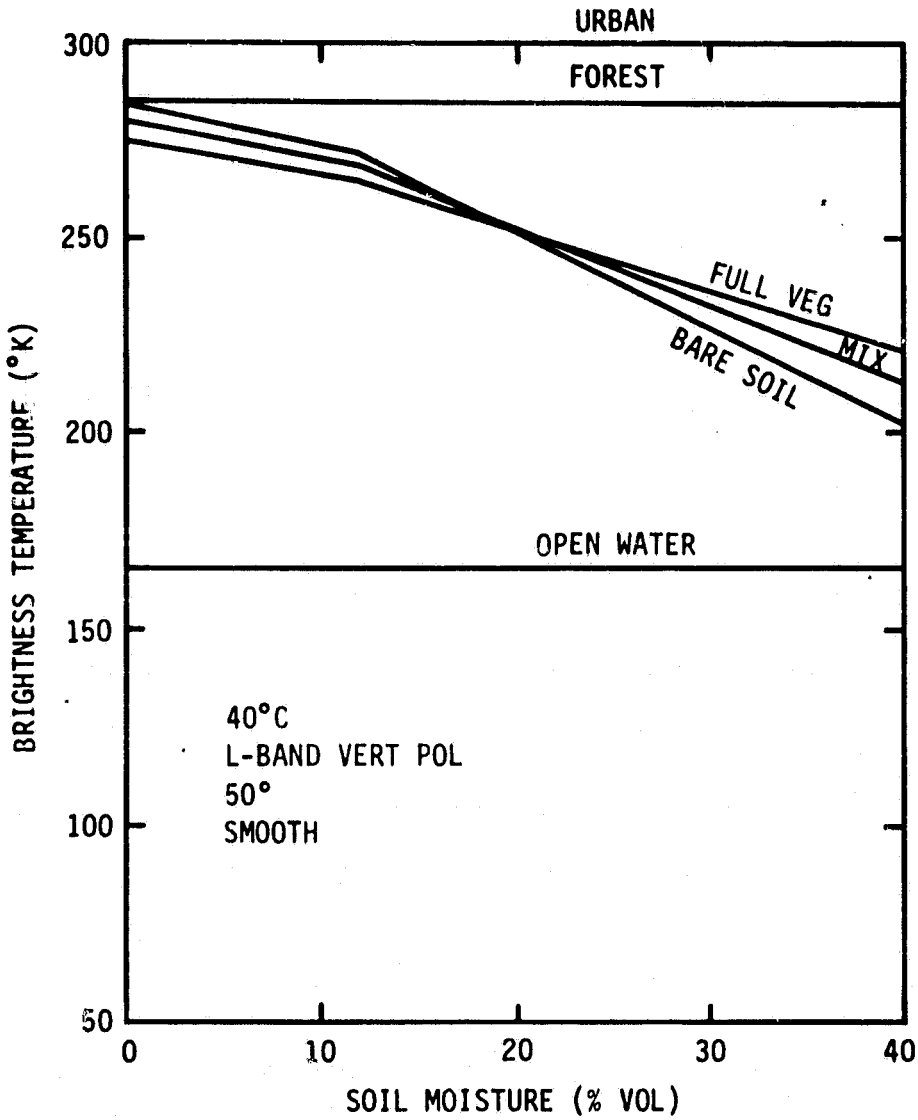

FIGURE 19. Example of the dependence of brightness temperature on soil moisture for all classes at L-band vertical polarization.

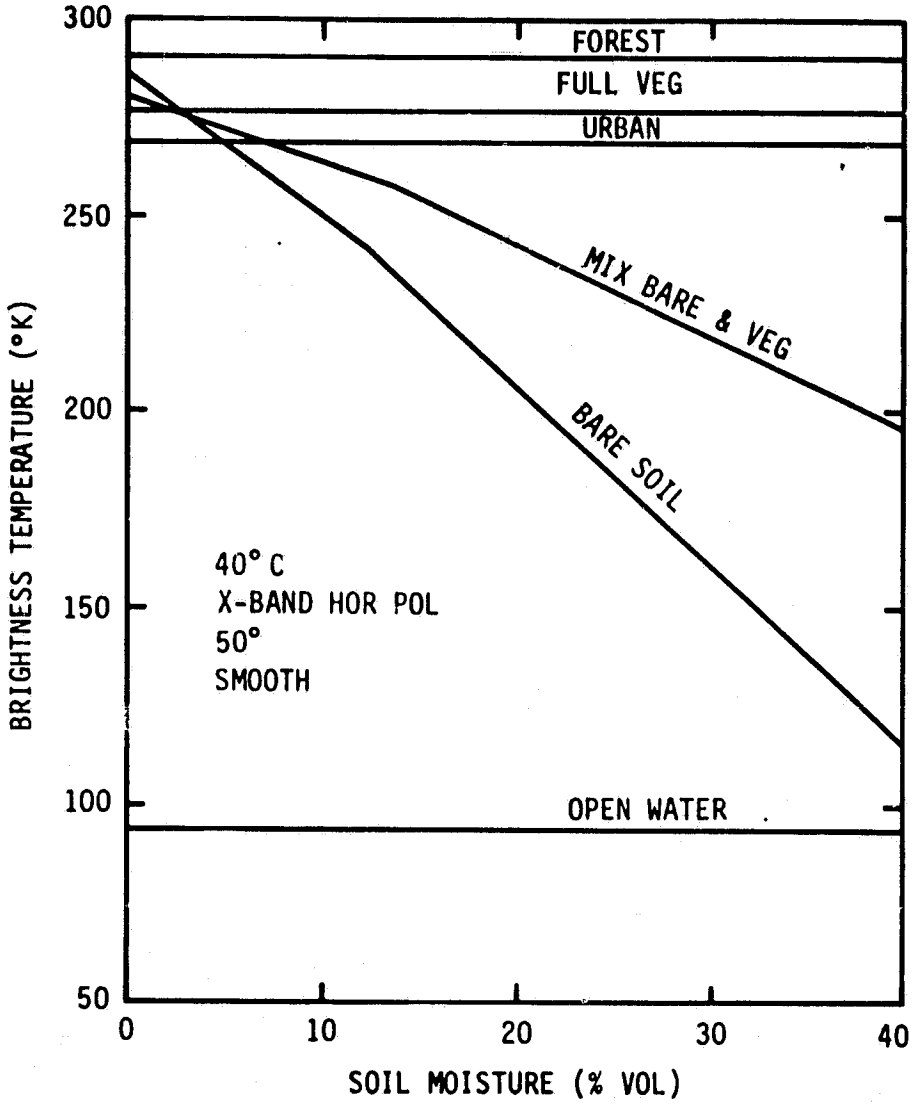

FIGURE 20. Example of the dependence of brightness temperature on soil moisture for all classes at X-band horizonal polarization.

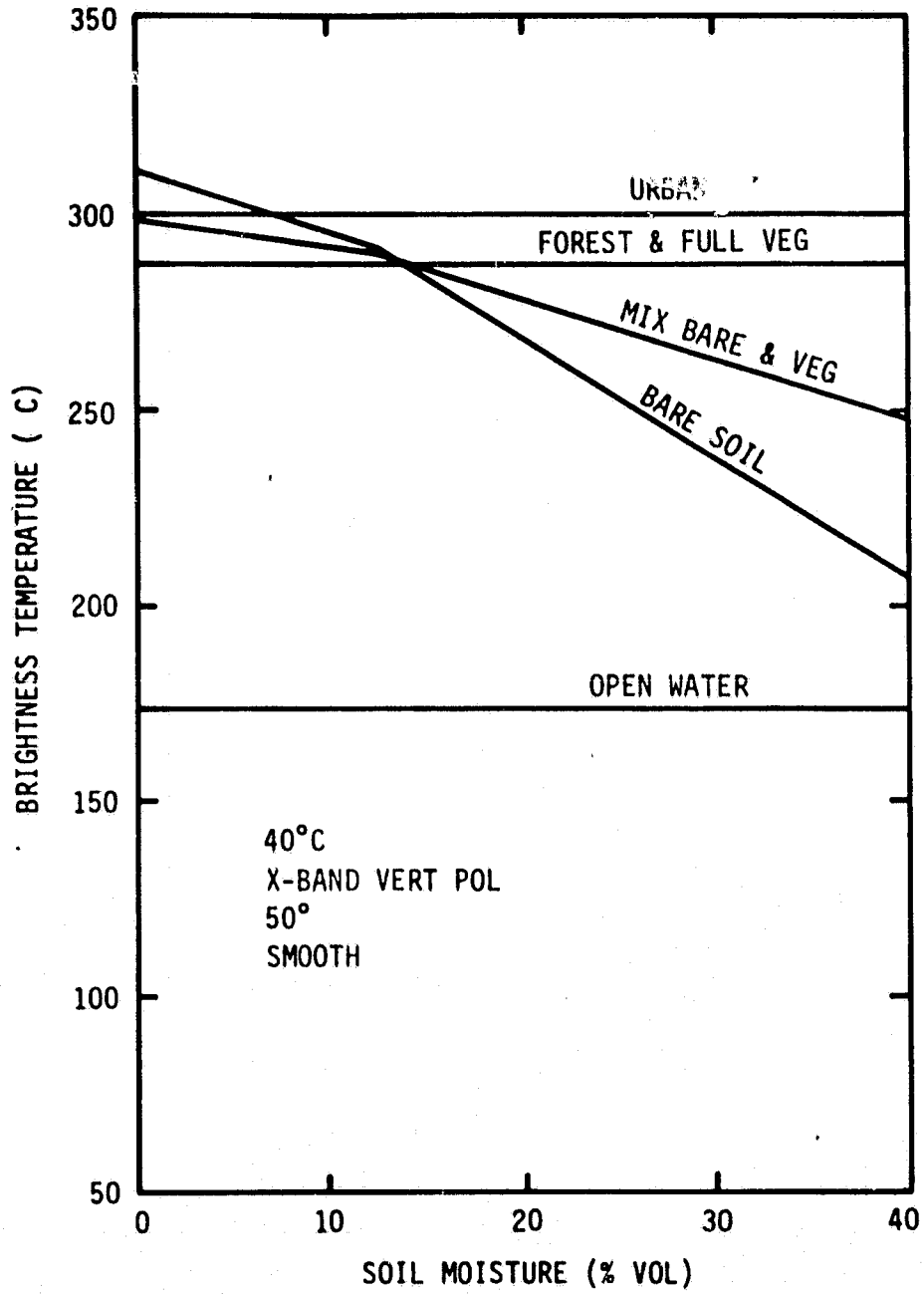

FIGURE 21. Example of the dependence of brightness temperature on soil moisture for all classes at X-band vertical polarization.

soil class. The effect of soil moisture on the brightness temperature of these classes at C-band lies between the effects shown at L-band and X-band. Figure 22 shows the effect of the soil temperature parameter on the brightness temperature of each class at X and L-band and 12% soil moisture.

SIMULATION RESULTS

Simulation Description

Rationale

There are several scene and system parameters that can affect the ability to use a microwave radiometer for estimating soil moisture over extended scenes. This study was only concerned with the problems associated with the estimation of soil moisture assuming a spatially uniform soil moisture distribution over the scene under consideration. No consideration was given to the effects of soil moisture profile on the emission at the various microwave frequencies. This is a separate problem and is handled in another study. In addition, the spatial soil moisture distributions that naturally occur due to precipitation patterns and variations in soil properties were considered to impose separate restrictions on the resolution of an orbiting microwave radiometer and were not considered in this study. However, these spatial variations are important and could very well be the limiting factor on resolution. Their effect can easily be considered using the simulation model. This should be investigated in a follow-on study.

The scene and sensor parameters that were of concern to this study were scene heterogeneity and its relationshp to sensor resolution, surface roughness, soil temperature, and sensor incident angle.

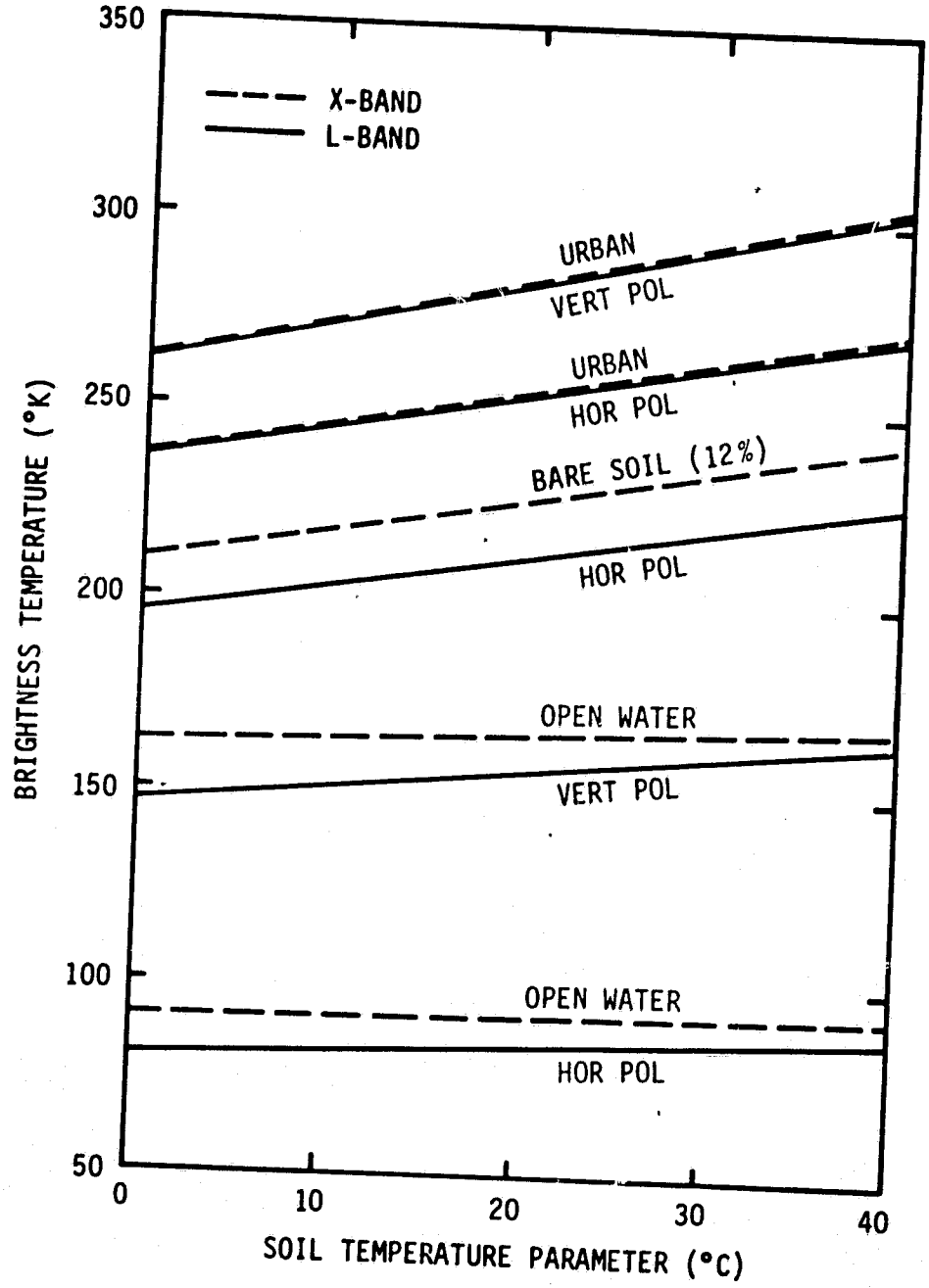

FIGURE 22. Example of the dependence of brightness temperature on the soil temperature parameter for both X-band and L-band.

Specific simulation runs were made to provide data to address each of these factors. However, the most emphasis in this study centered around the effect of scene heterogeneity and resolution since these are the most critical parameters about which the least is currently known.

The simulation of realistic scene geometry and composition were vital to the accuracy of the results of this study. As a result, the scene was simulated based on full frame Landsat images classified into six categories. These categories were water, bare soil, urban, mixed bare and vegetation, fully vegetated and forest. The description of how the original classifications were aggregated into these six, and the problems of classification consistency between Landsat frames is described in the section entitled Model Definition and Structure. These classes were chosen as being representative of the scene parameters that are important in affecting the relationship between microwave emission and soil moisture. The pixel size over which the antenna integration was performed was 0.24 by 0.24 km.

Test Runs

In utilizing the simulated scene to simulate microwave radiometer measurements for analyses of the effects of scene heterogeneity, it was necessary to be careful in choosing the ground tracts of the radiometer flight path. The simulated scene contains very diverse ground cover from very dense forest in East Texas to sparse vegetation in Central Texas. Analysis of simulated radiometer measurements to determine the ability to estimate soil moisture from space can be

severely biased by the amount of vegetation contained in the radiometer resolution elements. As a result, two ground tracts were chosen based on two general criteria. The first criteria was that the ground tract pass over areas of heavy forest vegetation as well as areas of sparser vegetation, and that the ground tracts pass over features that would be recognizable from the simulated radiometer measurement. One ground tract runs from just north of Waco, Texas southeastward to Lake Livingston, Texas. The other ground tract runs east and west from approximately Kerrville, Texas eastward to Houston, Texas and out into the Trinity Bay area. These ground tracts are shown on the urban class map contained in Appendix B. It will be shown below and can be seen in the class maps contained in Appendix B that these ground tracts cover areas that are predominantly vegetation.

Numerous radioeter measurement simulations were computed for the two ground tracts described above. These simulations were run using the parameters documented in Table 4. The choice of parameters in Table 4 was based on the desire to determine the effects of resolution and frequency on the ability to estimate soil moisture with microwave radiometers over realistic and heterogeneous scenes. The simuation model computed both the vertical and horizontal brightness temperature for nadir angles from 0° to 50° in 10° increments.

In order to quantify the effect of scene makeup on the microwave radiometer brightness temperature computation, the model was constructed to compute and keep track of the percentage of each class contained in each radioemter footprint. These percentages are plotted as a function of range down the ground tract from west to east in Figures 23 through 28. Figures 23 and 24 contain the percentages of

TABLE 4. Simulation parameters used in Test Runs.

Parameter	Value
Frequency	L, C, X-band
Soil Moisture	0%, 35%
Temperature Parameter	10°C, 60°C
Roughness Parameter	0.3
Antenna Footprint	5 km, 20 km, 60 km

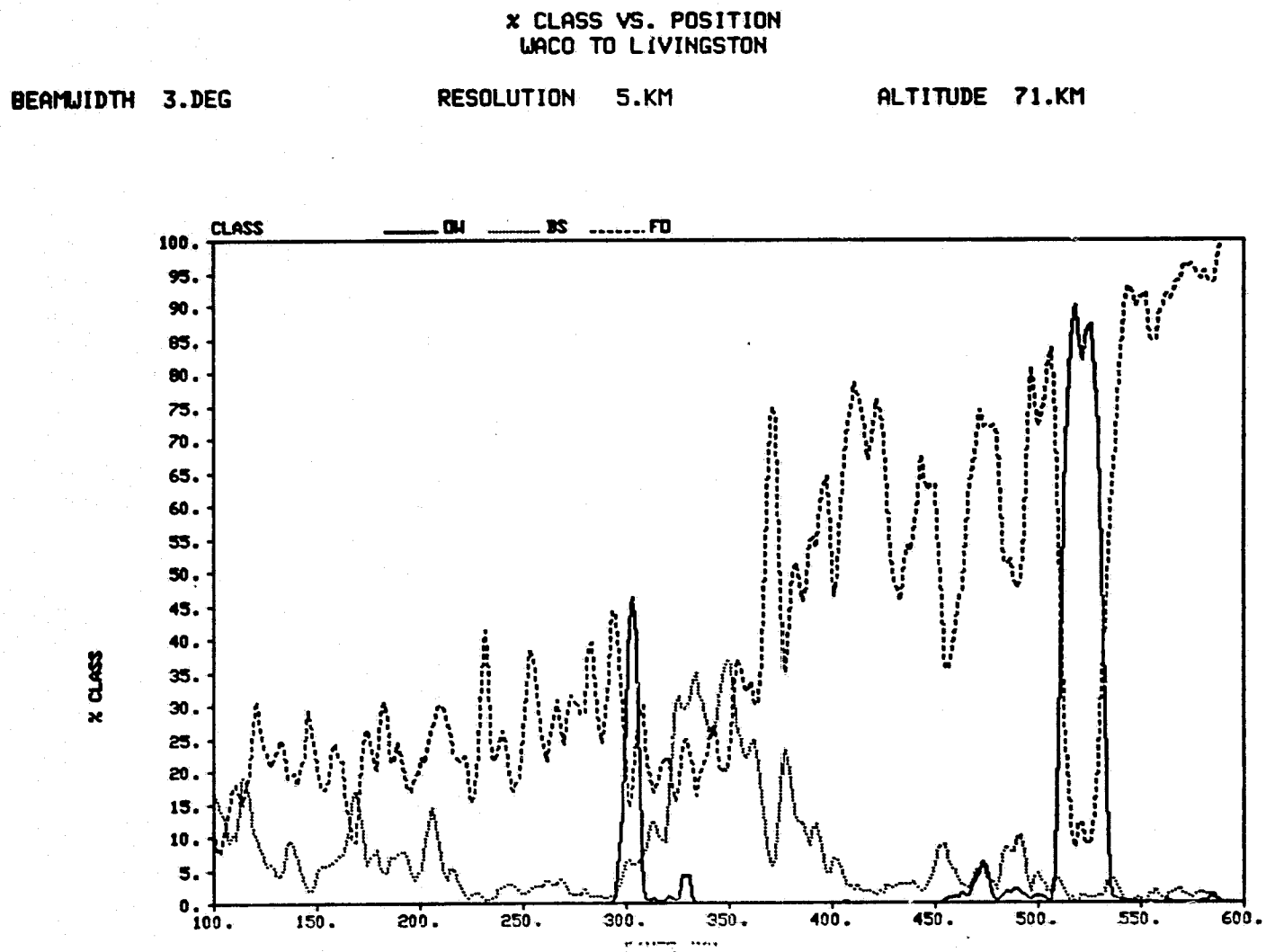

FIGURE 23. Percent of water, bare soil and forest classes in each antenna footprint as a function of range for the Waco to Livingston ground track at a resolution of 5 kilometers.

ORIGINAL PAGE IS
OF POOR QUALITY

ORIGINAL PAGE IS
OF POOR QUALITY

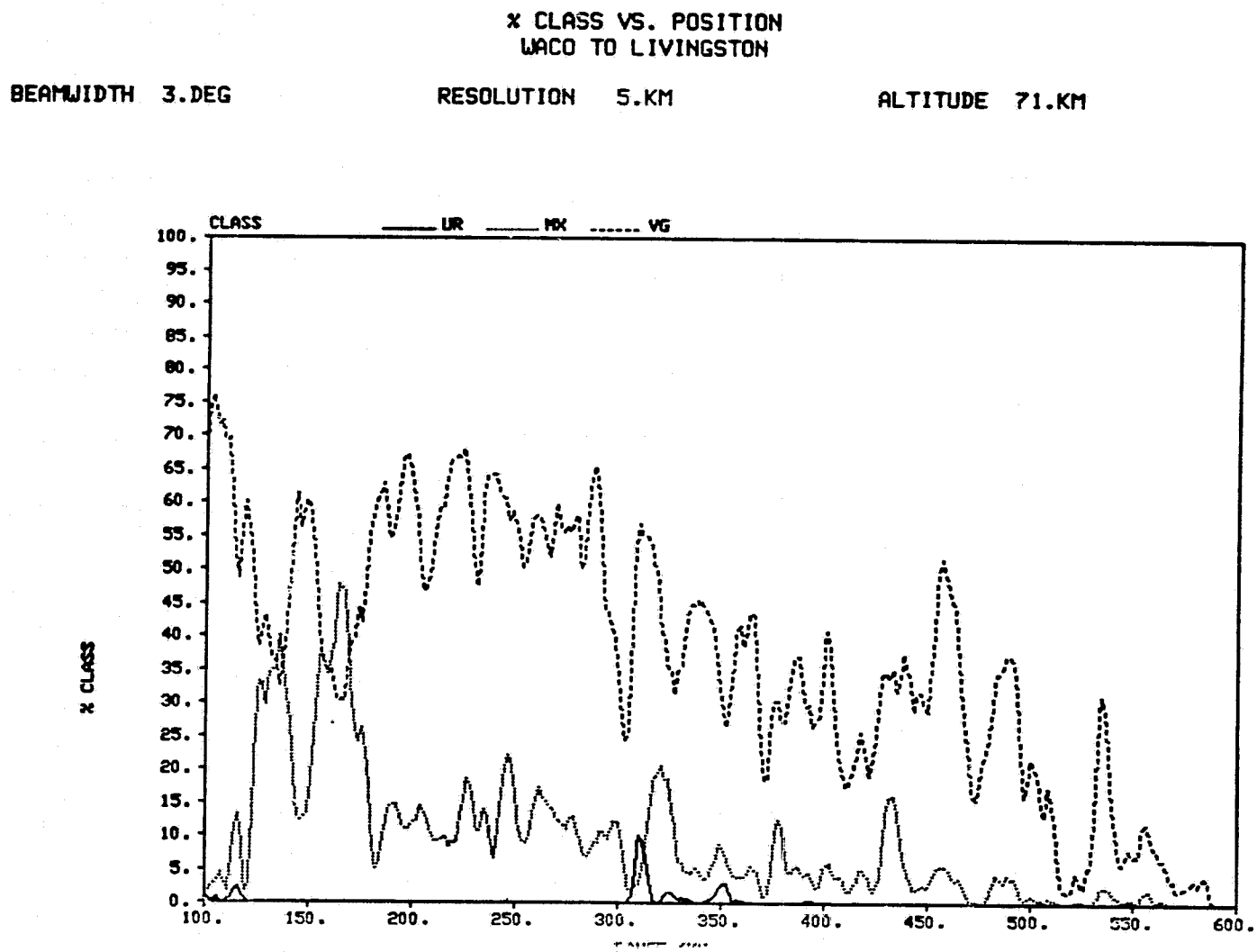

FIGURE 24. Percent of urban, mixed bare and vegetated and fully vegetated classes in each antenna footprint as a function of range for the Waco to Livingston ground track at a resolution of 5 kilometers.

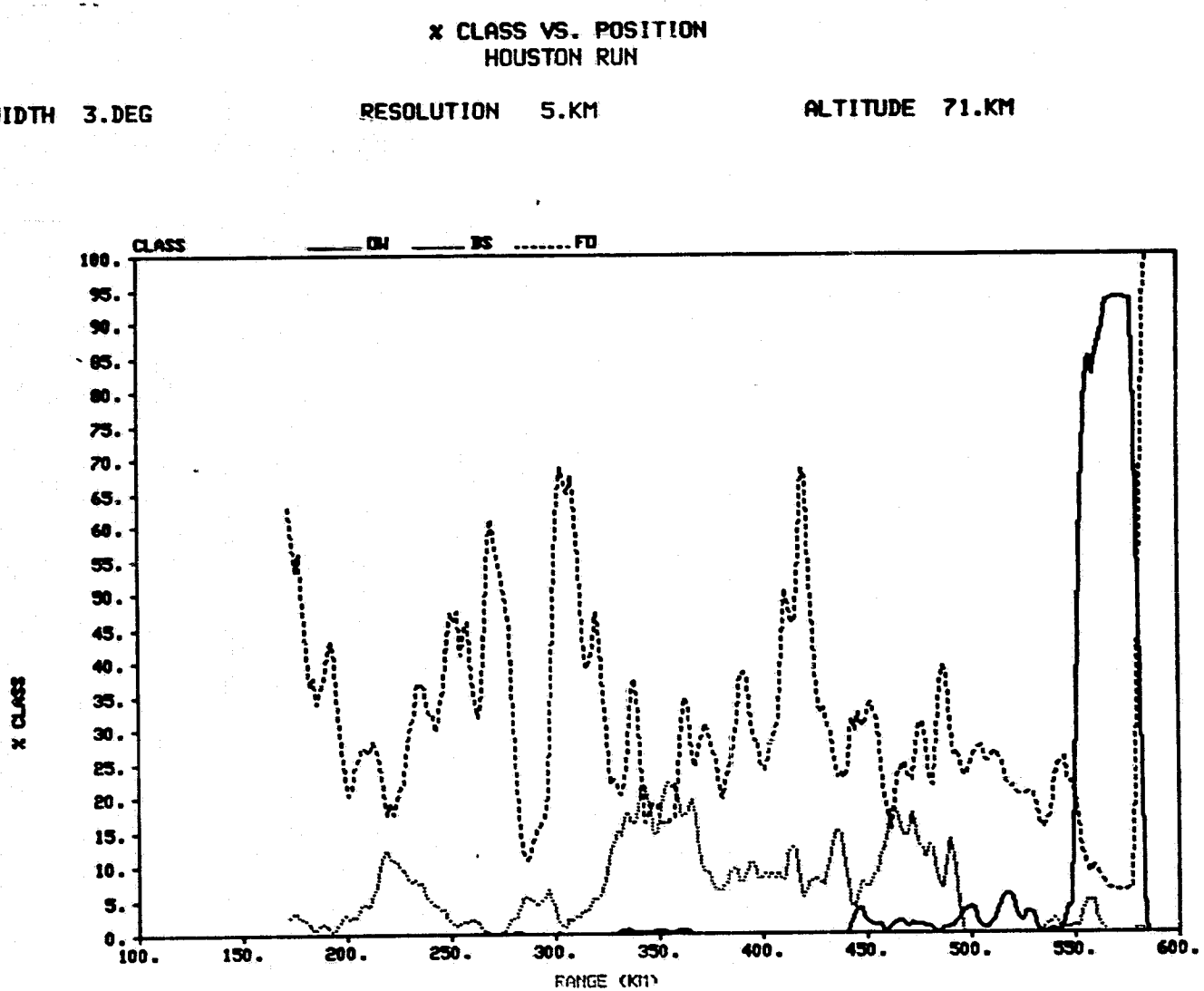

FIGURE 25. Percent of water, bare soil and forest classes in each antenna footprint as a function of range for the Kerrville to Houston ground track at a resolution of 5 kilometers.

ORIGINAL PAGE IS
OF POOR QUALITY

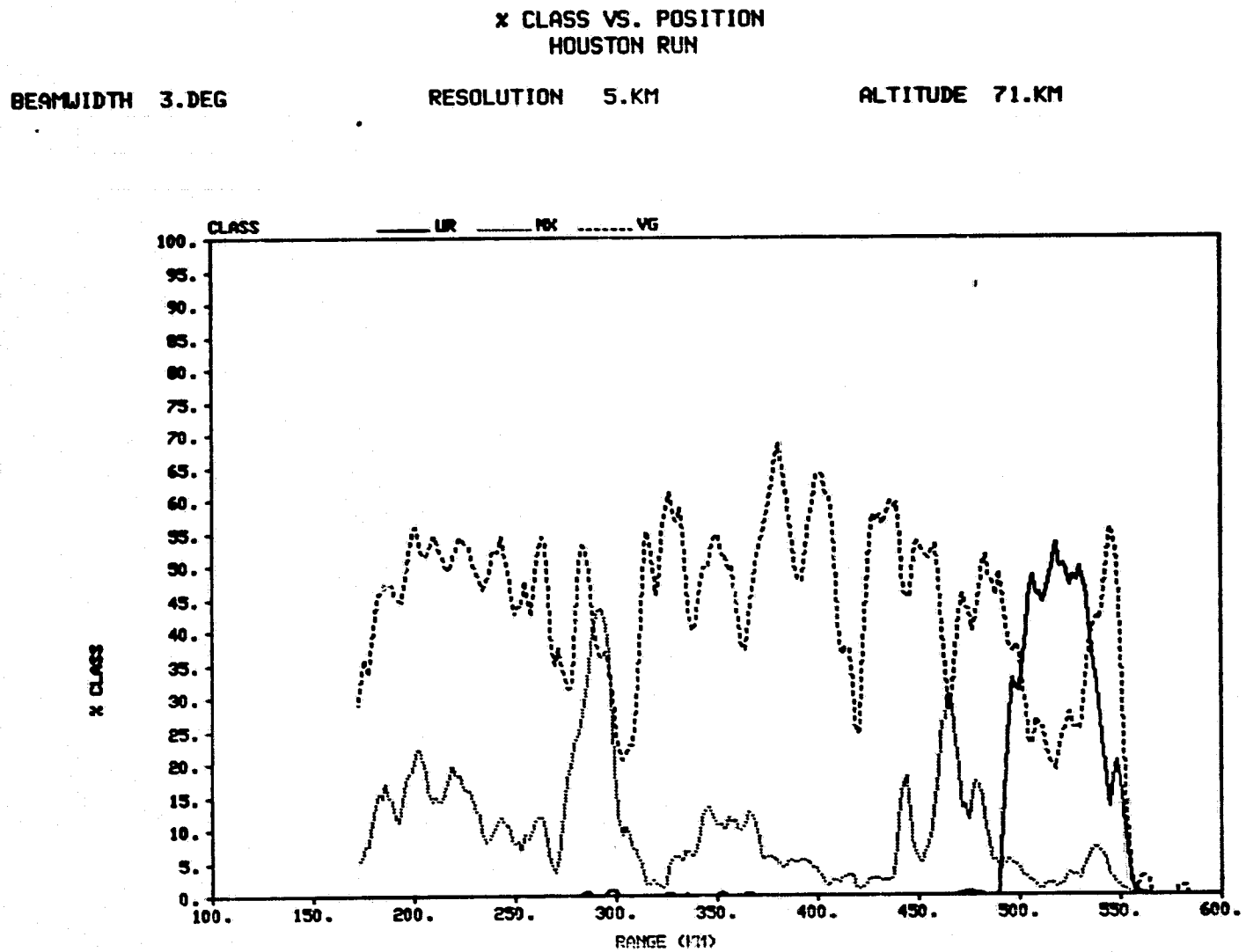

FIGURE 26. Percent of urban, mixed bare and vegetated and fully vegetated classes in each antenna footprint as a function of range for the Kerrville to Houston ground track at a 5 kilometer resolution.

ORIGINAL PAGE IS
OF POOR QUALITY

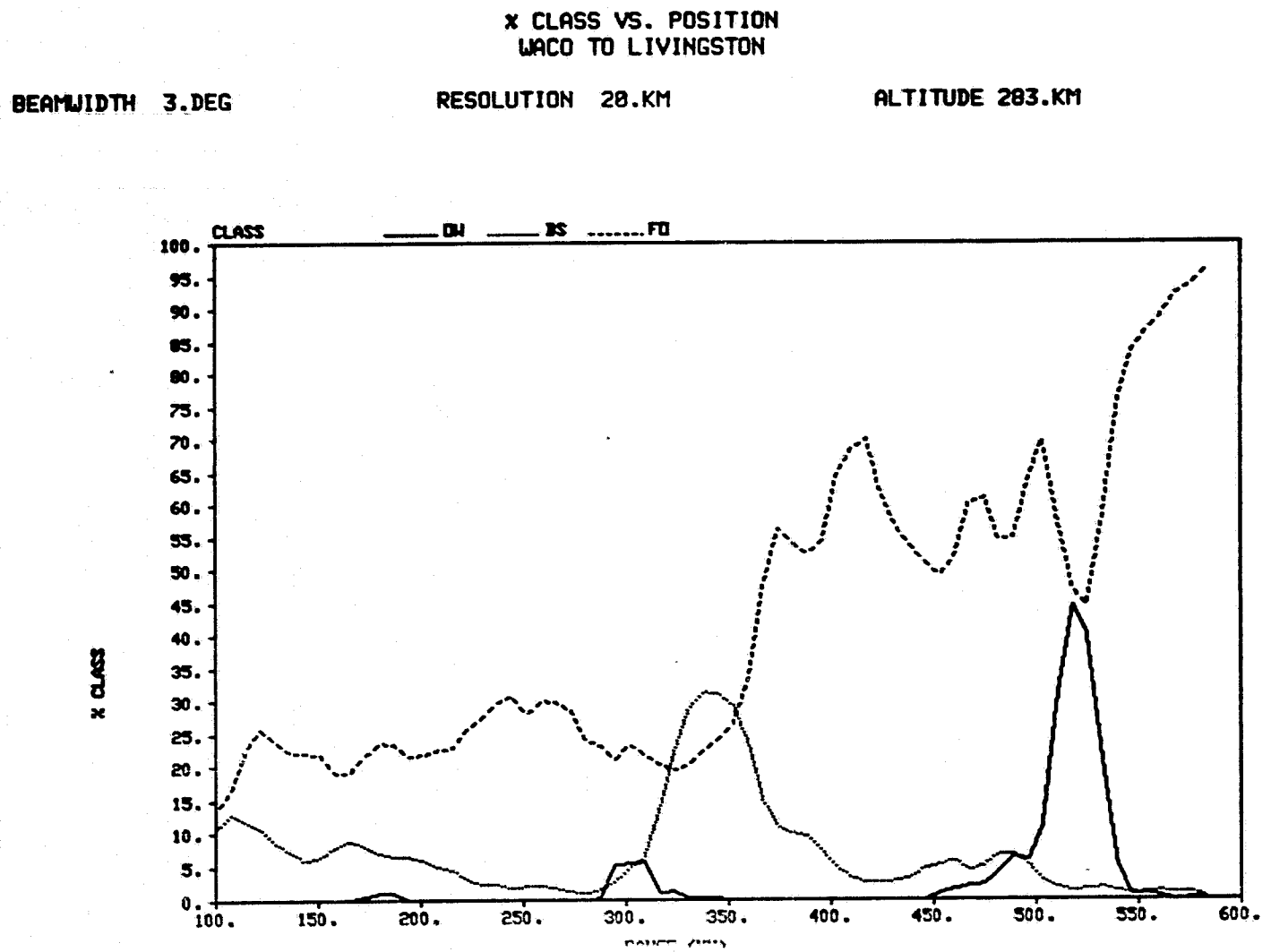

FIGURE 27. Percent of water, bare soil and forest classes in each antenna footprint as a function of range for the Waco to Livingston ground track at a 20 kilometer resolution.

ORIGINAL PAGE IS
OF POOR QUALITY

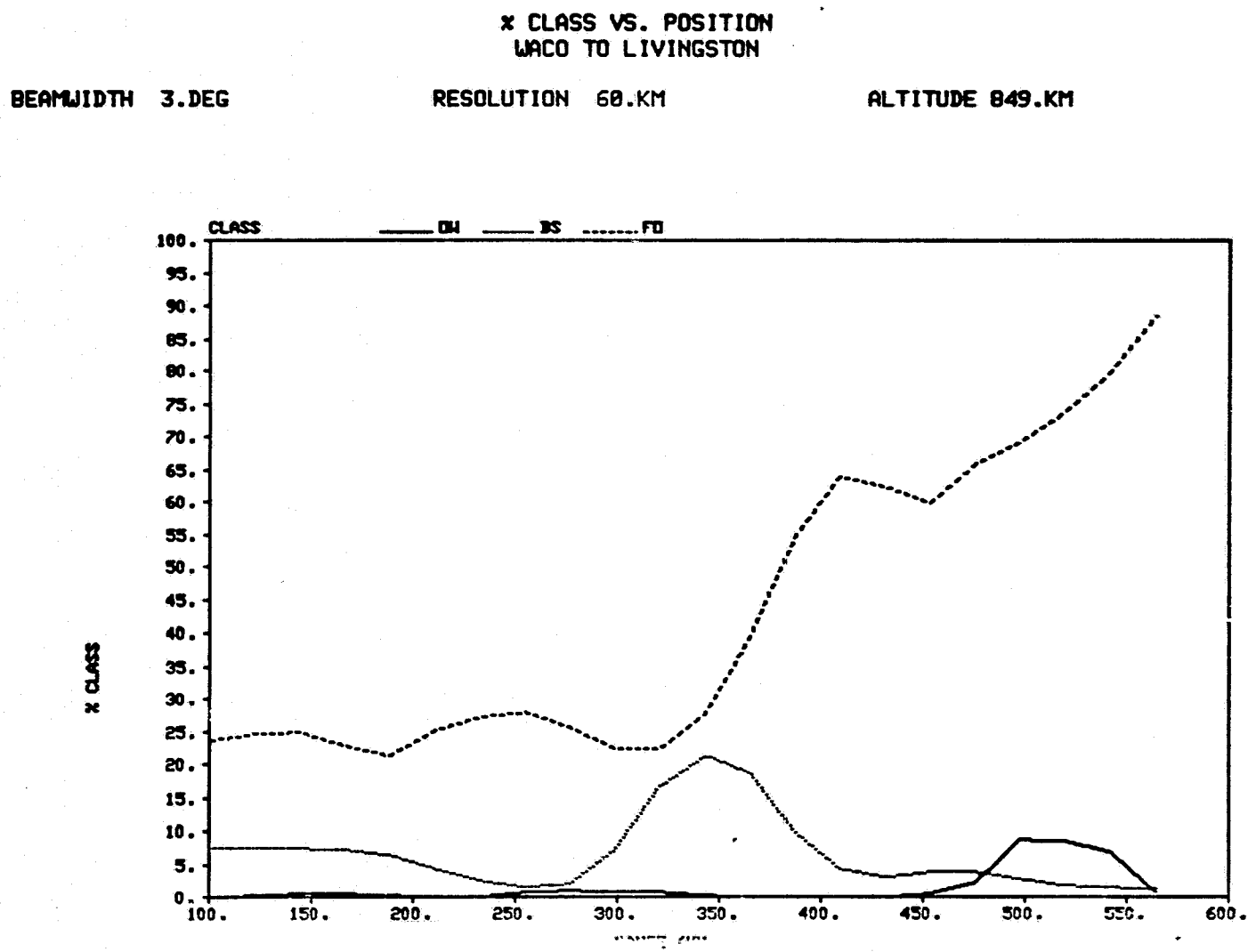

FIGURE 28. Percent of water, bare soil and forest classes in each antenna footprint as a function of range for the Waco to Livingston ground track at a 60 kilometer resolution.

ORIGINAL PAGE IS
OF POOR QUALITY

each of the classes in each antenna footprint for a 5 kilometer radiometer resolution for the Waco to Livingston ground tract. Two water features show up distinctly on the plot in Figure 23. At a range of approximately 300 kilometers Lake Conroe shows up distinctly and at a range of approximately 525 kilometers Lake Livingston shows up distinctly. In addition, it can be seen that near Waco, the percentage of forest in each footprint is on the order of 20% to 25%, while the percentage of forest begins to increase at approximately 375 kilometers of range and approaches 100% beyond 550 kilometers of range. Also in Figure 23, it can be seen that the amount of bare soil is very small, never going above approximately 10% of each footprint, except in the range of 325 kilometers to 374 kilometers where it averages approximately 25% of the footprint. In Figure 24, it can be seen that although the ground tract is over several cities, the percentage of urban area in each footprint is very small. It can also be seen in Figure 24 that the mixed bare and vegetated class and the fully vegetated class made up a significant percentage of each footprint on the western end of the ground tract and decreases as a function of range.

The same type of observations are made concerning Figures 25 and 26 which show the percentage class of each 5 kilometer footprint for the Houston ground tract. Distinguishing features in this case are Trinity Bay which begins approximately 550 kilometers of range and the Houston urban area which spans the area from approximately 490 kilometers to 550 kilometers of range. It can be seen that the Houston urban area does constitute approximately 40% to 50% of each footprint within the 500 to 550 kilometer range for the 5 kilometers antenna footprint.

Another factor of importance is to note that as the antenna footprint size is increased the percentage of each class making up each radiometer footprint remains approximately the same. Figures 27 and 28 demonstrate this fact for an antenna footprint of 20 kilometers and 60 kilometers for the Waco to Livingston ground tract and the water, bare soil and forest classes. It can be seen that the increased radiometer resolutions produce an averaging affect on the percent of class plots. It should also be pointed out that for a fixed ground tract length, the number of brightness temperature simulations decreases significantly as radiometer resolution is increased.

Figure 23 through 28 illustrate the make-up of the simulated scene within the radiometer footprint spatially along the ground tracts. Figures 29 through 40 provide some additional statistical data concerning the make-up of the simulated scene along the ground tracts, but without the spatial information. These figures are frequency bar charts that show distribution of footprints along the ground tract in terms of the ground cover make up with the footprints. This distribution is computed in terms of 5% increments of total ground cover within each footprint. Figures 29 through 34 are for the Waco to Livingston ground tract, while Figures 35 through 40 are for the Houston ground tract. All are computed for an antenna footprint of 5 kilometers. Again, it can be seen that by far the highest percentage of radioemter footprints is vegetation. The highest percentage of bare soil in any footprint along the Houston ground tract is 25%, while the highest percentage of bare soil along the Waco to Livingston ground tract is 35%. In addition, by far the largest number of footprints contain 5% or less of bare soil.

ORIGINAL PAGE IS
OF POOR QUALITY

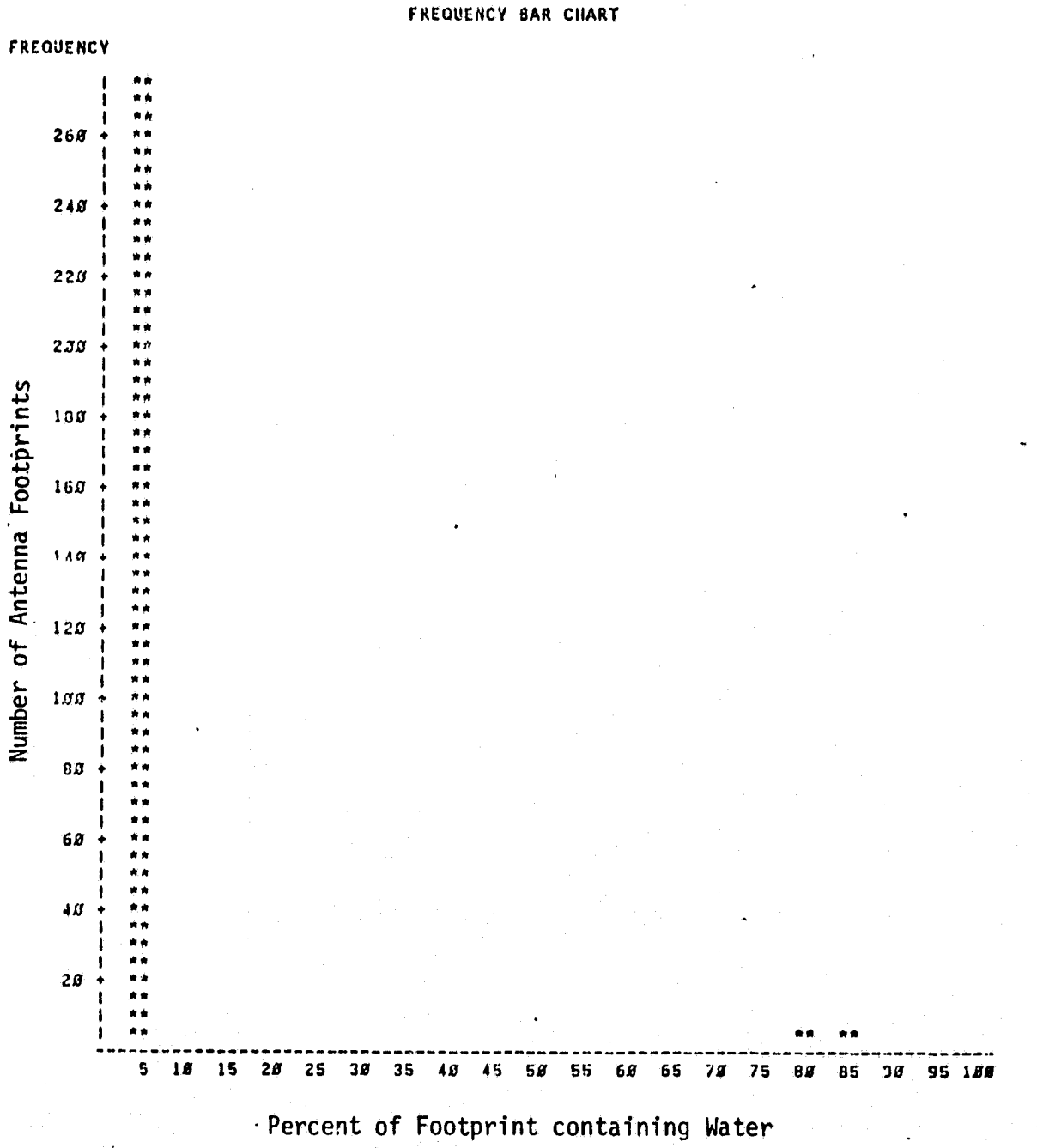

FIGURE 29. Histogram of the percentage of the antenna footprint containing water for the Waco to Livingston ground track at a 5 kilometer resolution.

ORIGINAL PAGE IS
OF POOR QUALITY

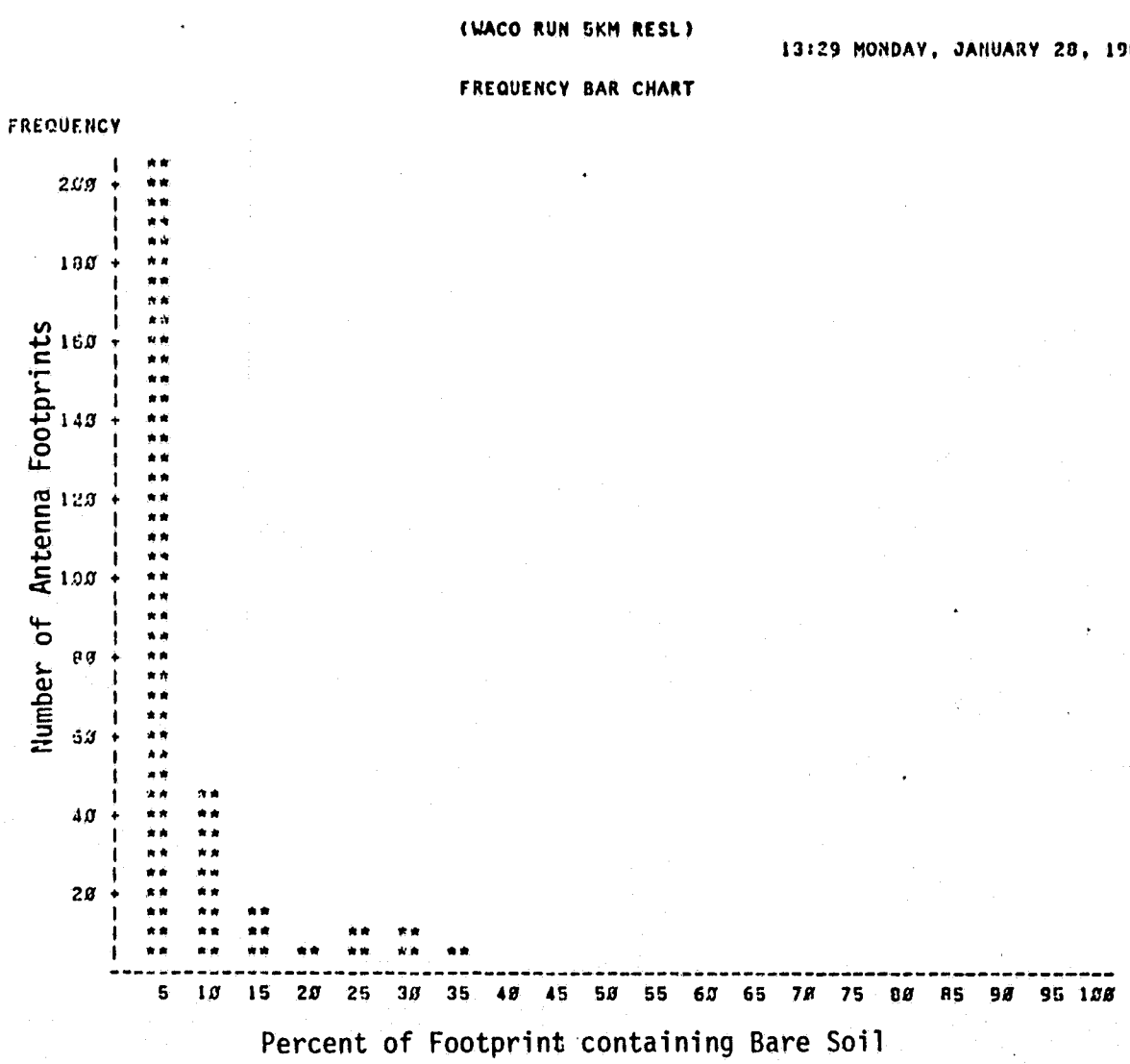

FIGURE 30. Histogram of the percentage of the antenna footprint containing bare soil for the Waco to Livingston ground track at a 5 kilometer resolution.

ORIGINAL PAGE IS
OF POOR QUALITY

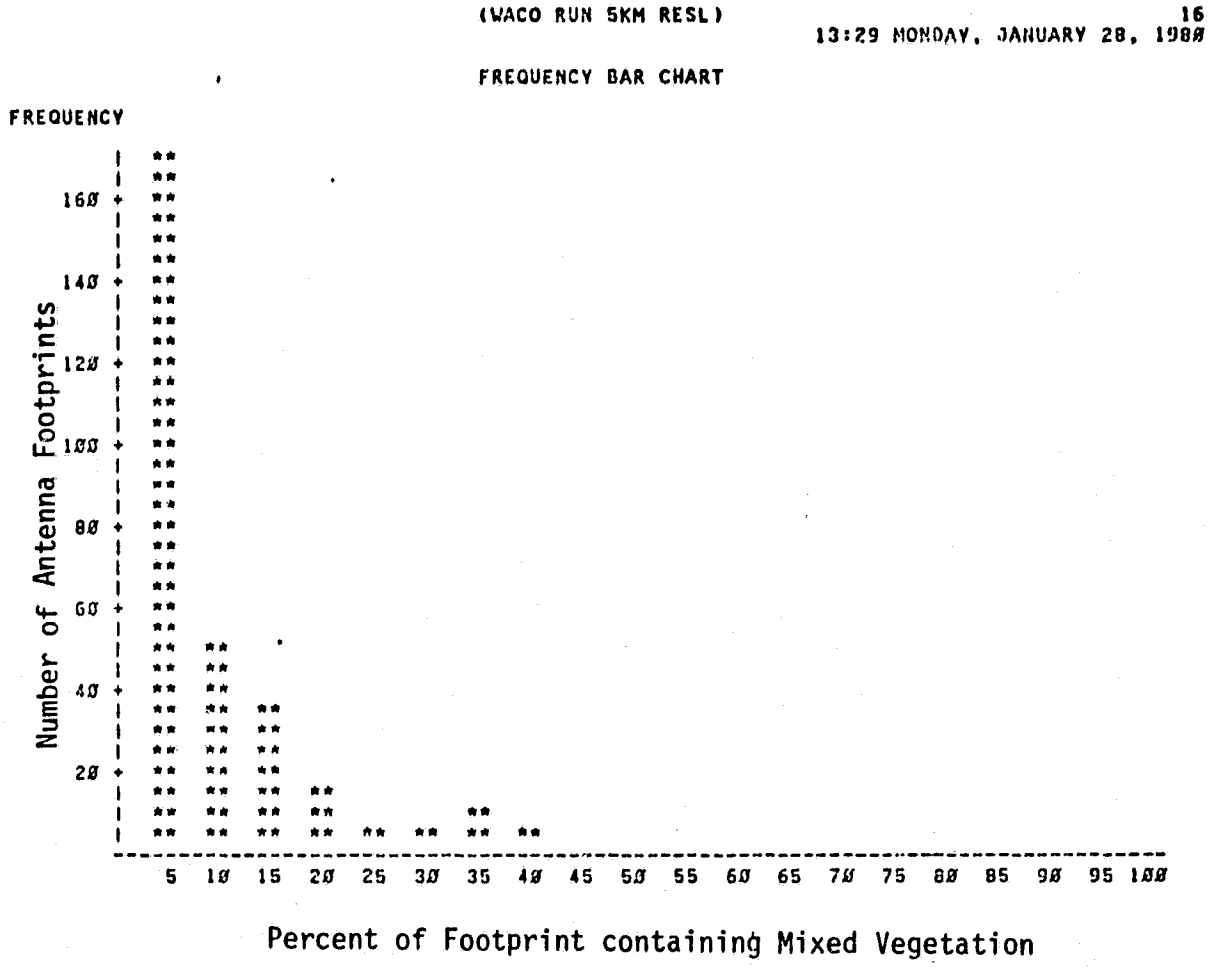

FIGURE 31. Histogram of the percentage of the antenna footprint containing mixed bare and vegetation for the Waco to Livingston ground track at a 5 kilometer resolution.

ORIGINAL PAGE IS
OF POOR QUALITY

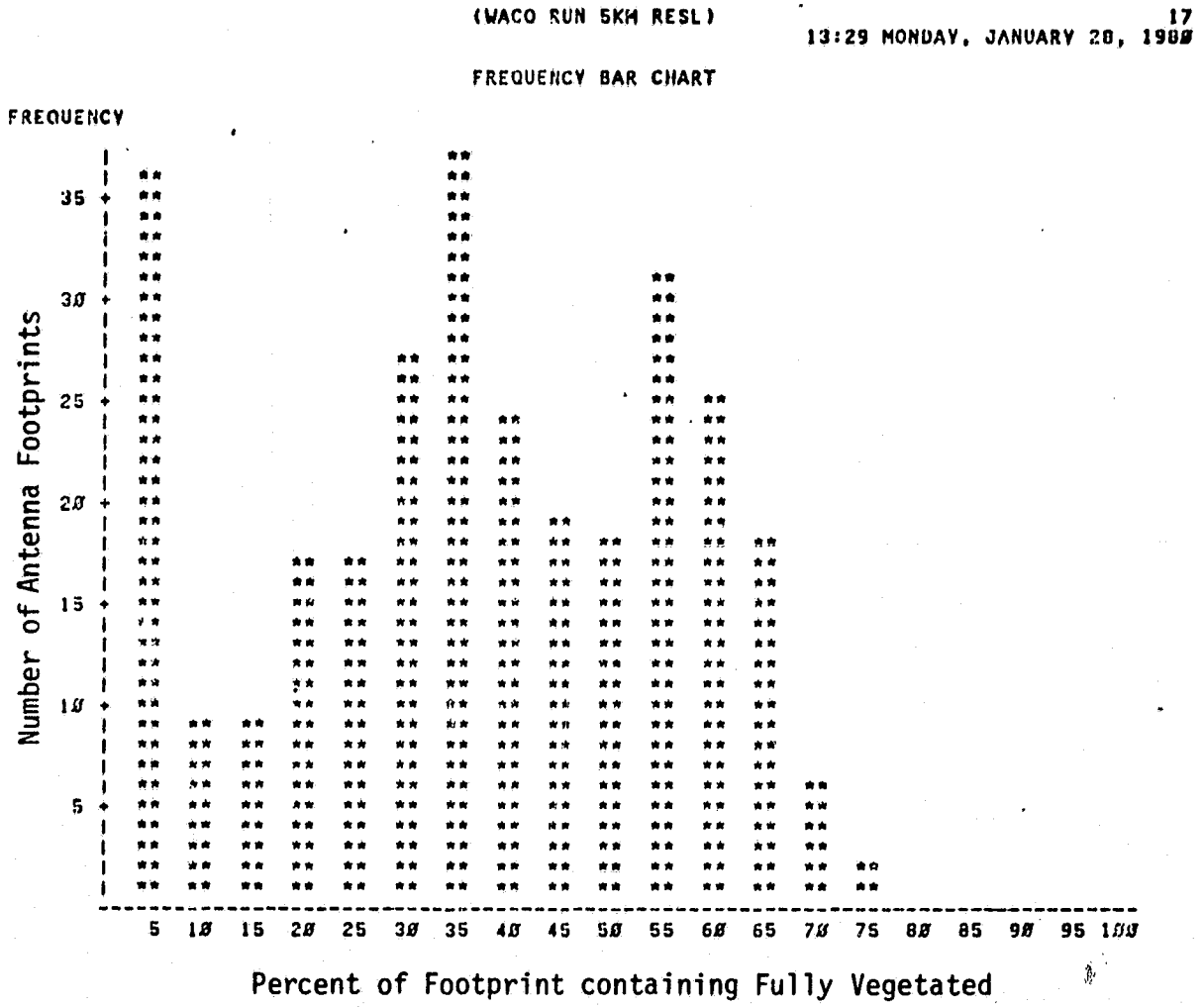

FIGURE 32. Histogram of the percentage of the antenna footprint containing full vegetation for the Waco to Livingston ground track at a 5 kilometer resolution.

ORIGINAL PAGE IS
OF POOR QUALITY

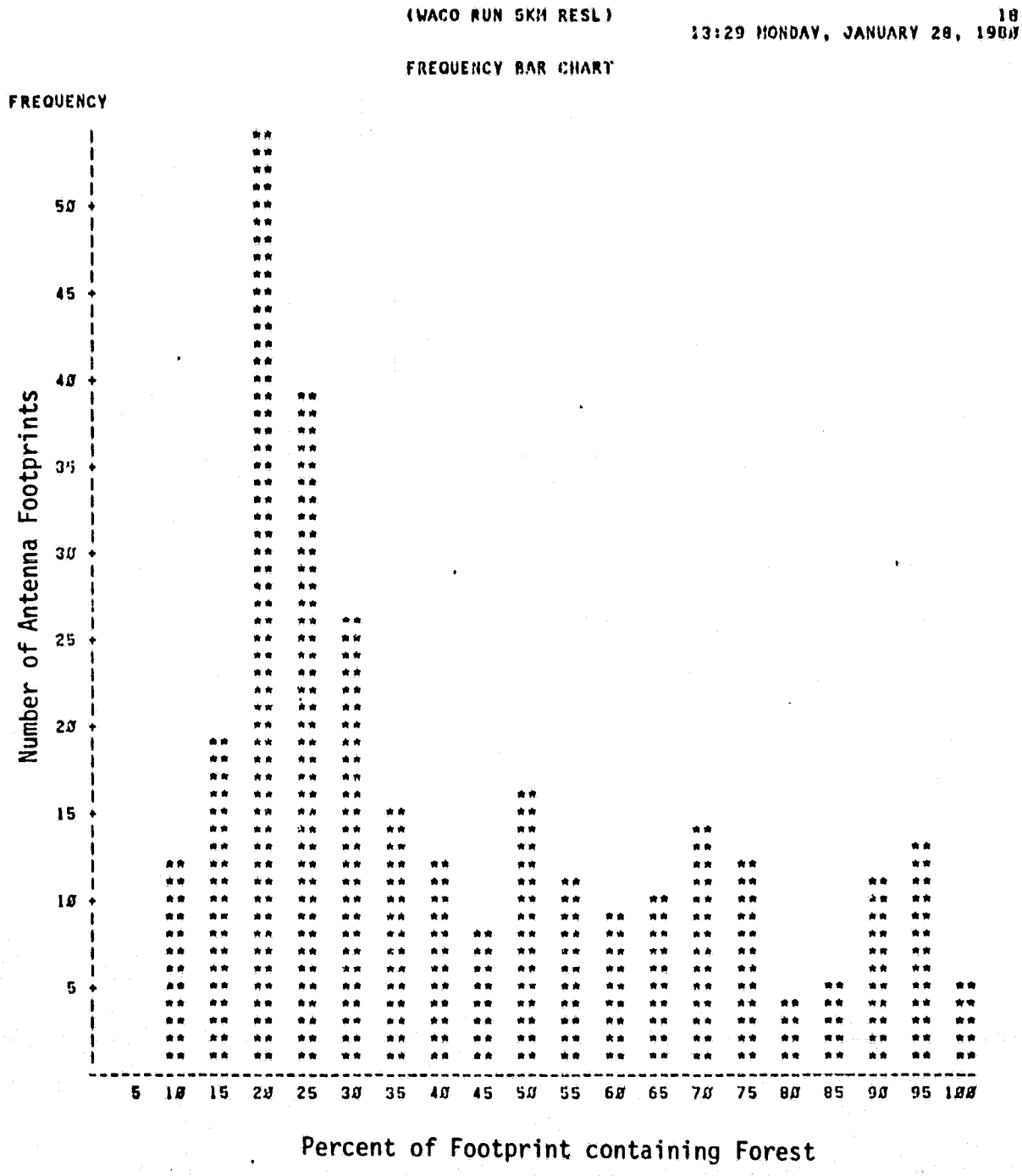

FIGURE 33. Histogram of the percentage of the antenna footprint containing forest for the Waco to Livingston ground track at a 5 kilometer resolution.

ORIGINAL PAGE IS
OF POOR QUALITY

(WACO RUN 5KM RESL) 15
13:29 MONDAY, JANUARY 20, 1980

FREQUENCY BAR CHART

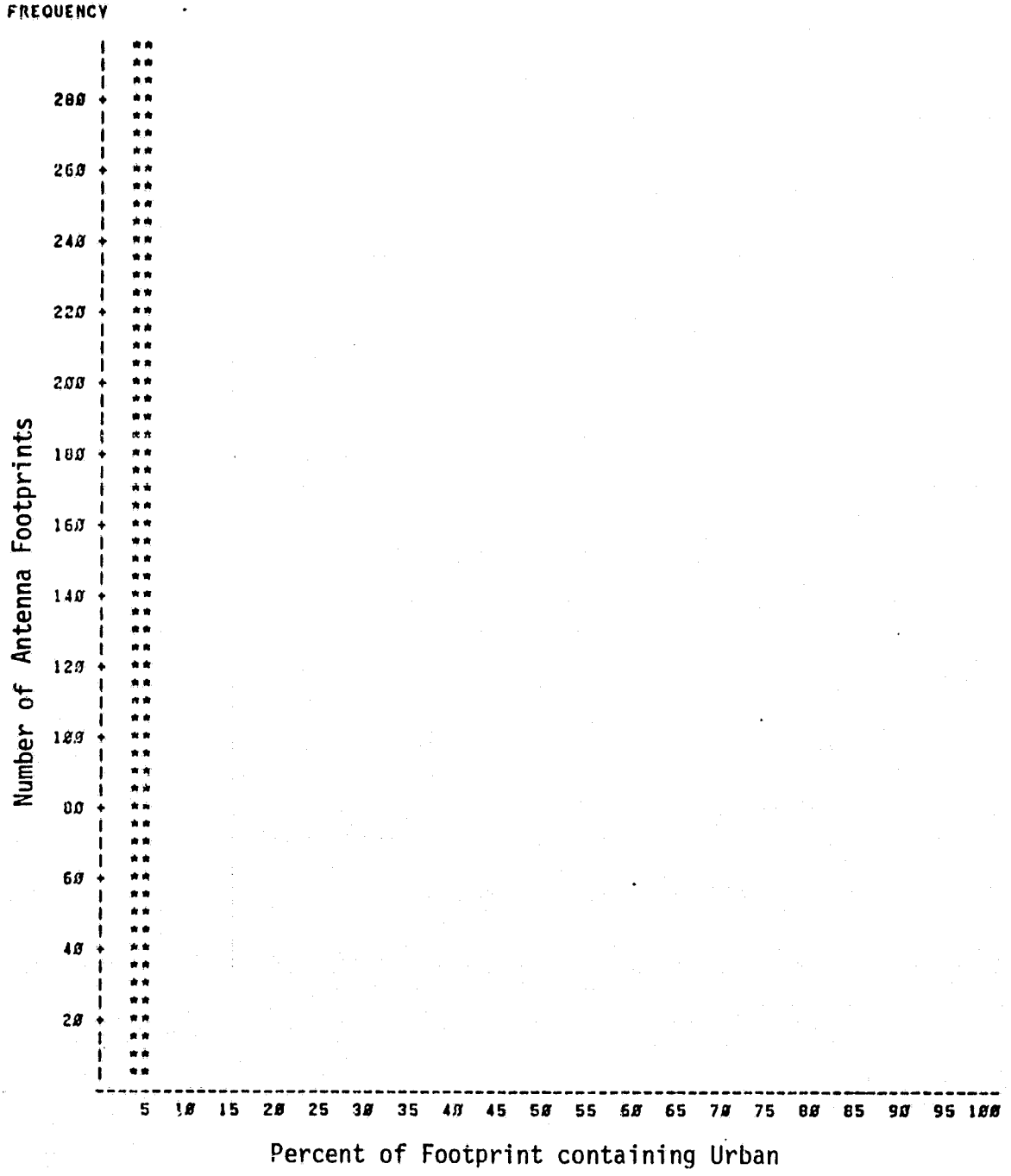

FIGURE 34. Histogram of the percentage of the antenna footprint containing urban for the Waco to Livingston ground track at a 5 kilometer resolution.

ORIGINAL PAGE IS
OF POOR QUALITY

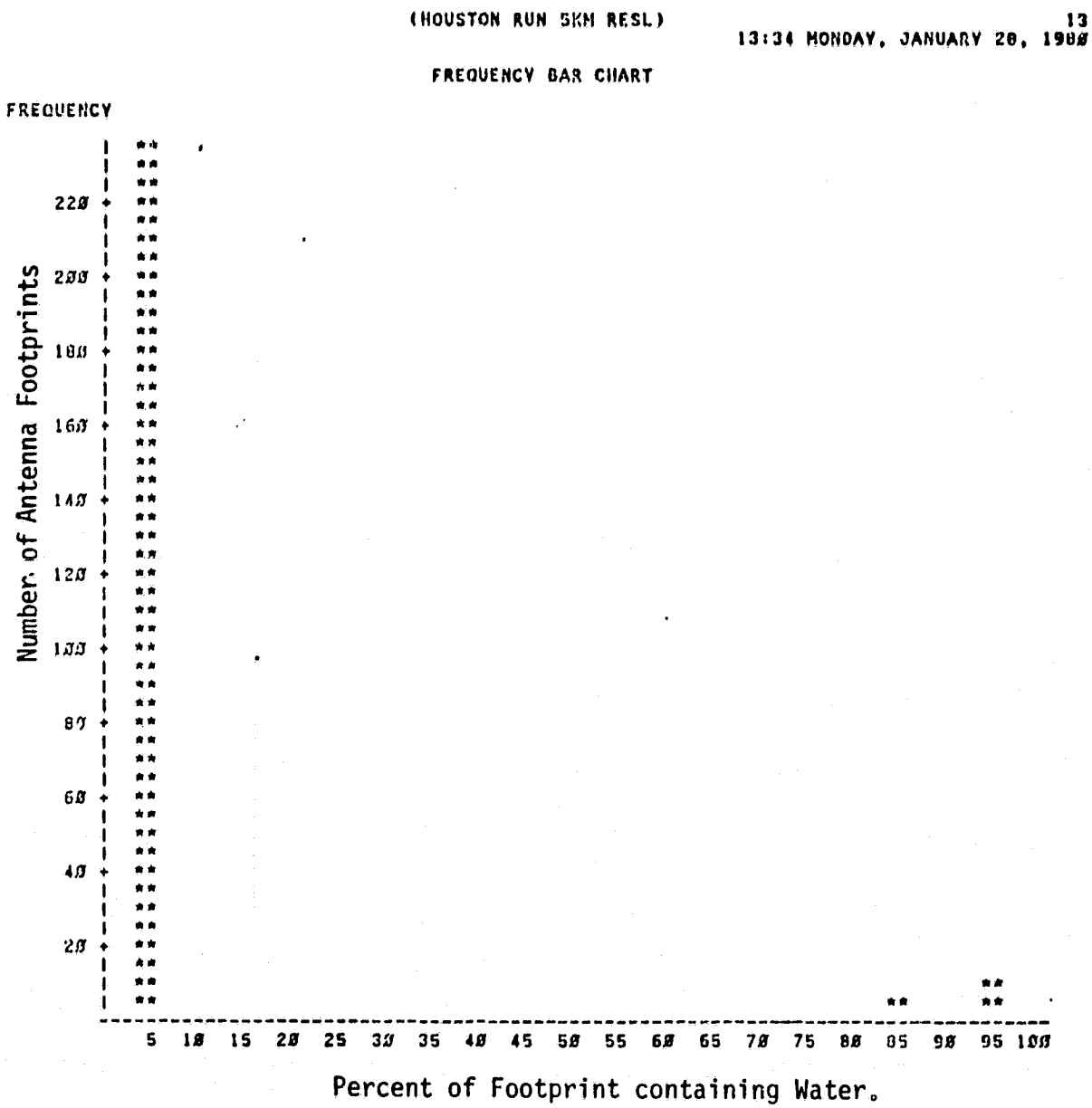

FIGURE 35. Histogram of the percentage of the antenna footprint containing water for the Waco to Livingston ground track at a 5 kilometer resolution.

FREQUENCY BAR CHART

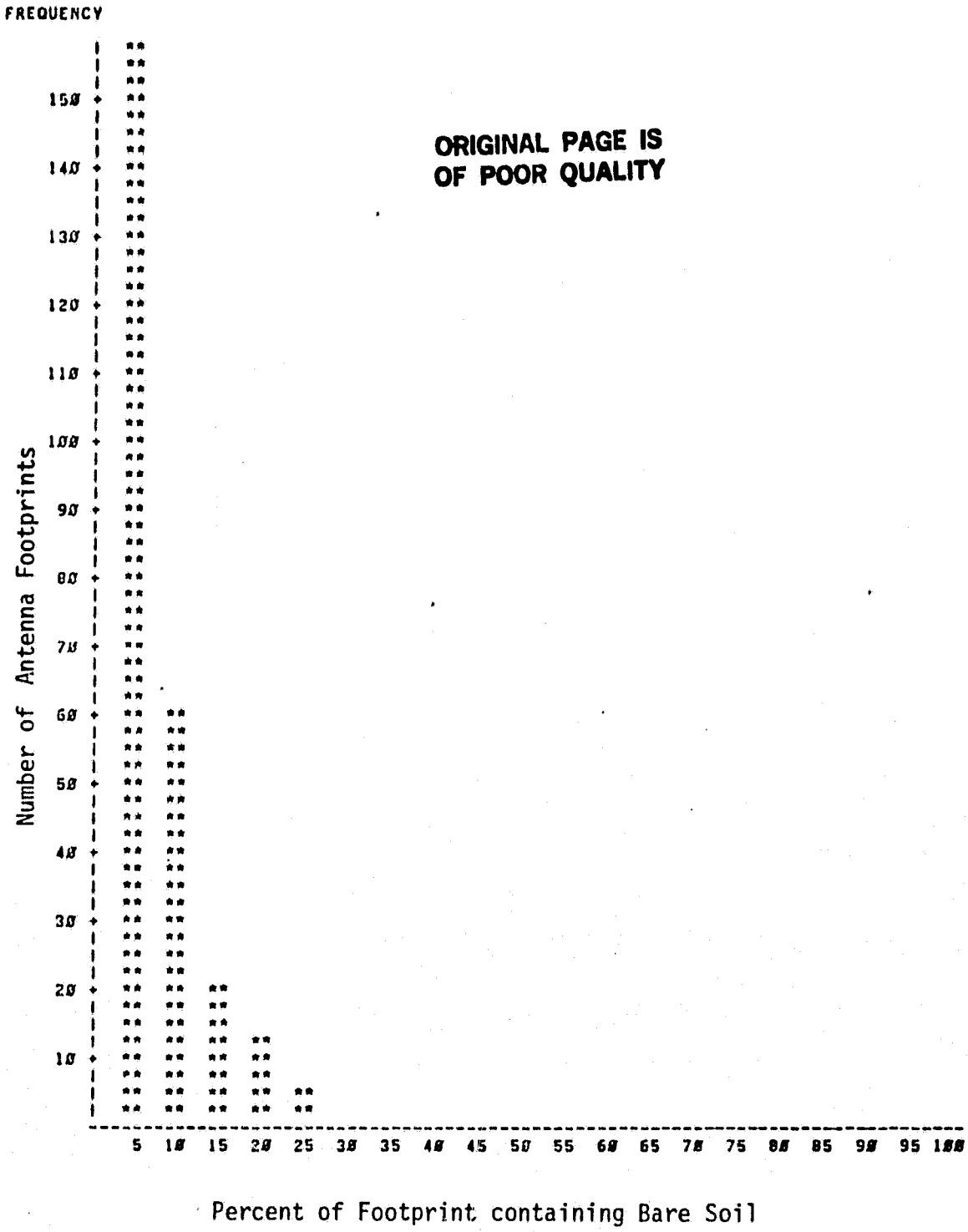

ORIGINAL PAGE IS
OF POOR QUALITY

FIGURE 36. Histogram of the percentage of the antenna footprint containing bare soil for the Kerrville to Houston ground track at a 5 kilometer resolution.

ORIGINAL PAGE IS
OF POOR QUALITY

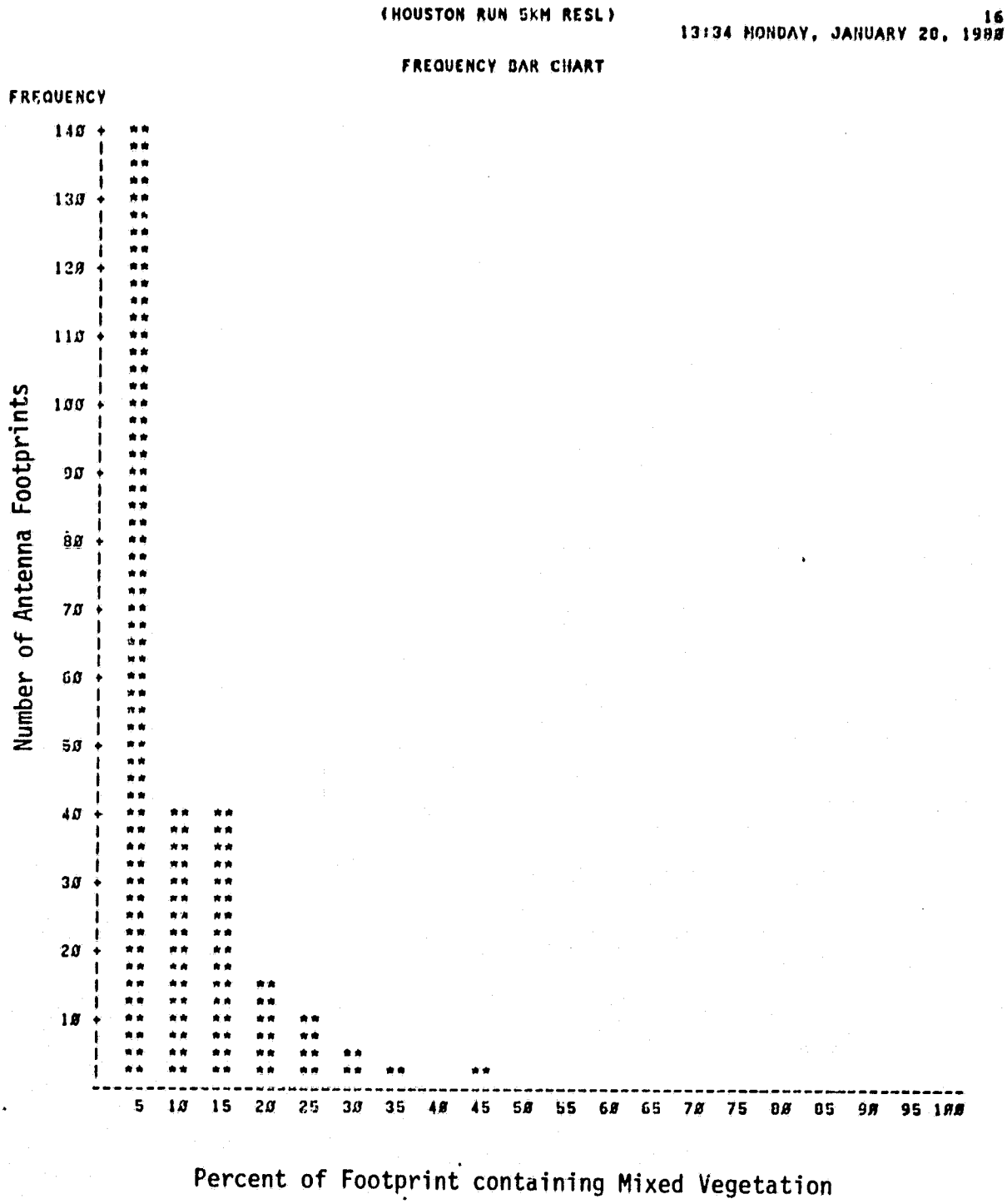

FIGURE 37. Histogram of the percentage of the antenna footprint containing mixed bare and vegetation for the Kerrville to Houston ground track at a 5 kilometer resolution.

ORIGINAL PAGE IS
OF POOR QUALITY

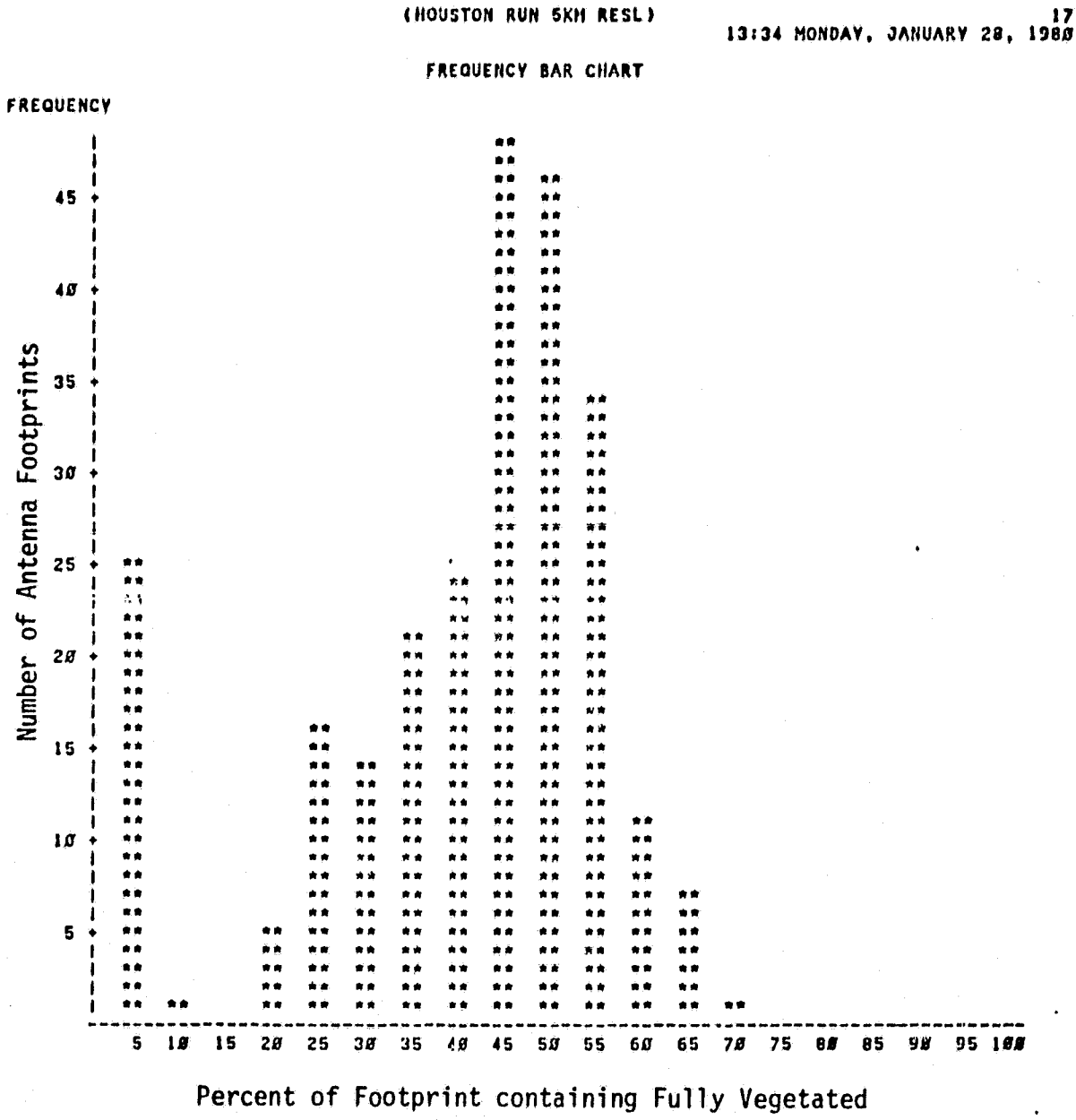

FIGURE 38. Histogram of the percentage of the antenna footprint containing full vegetation for the Kerrville to Houston ground track at a 5 kilometer resolution.

ORIGINAL PAGE IS
OF POOR QUALITY

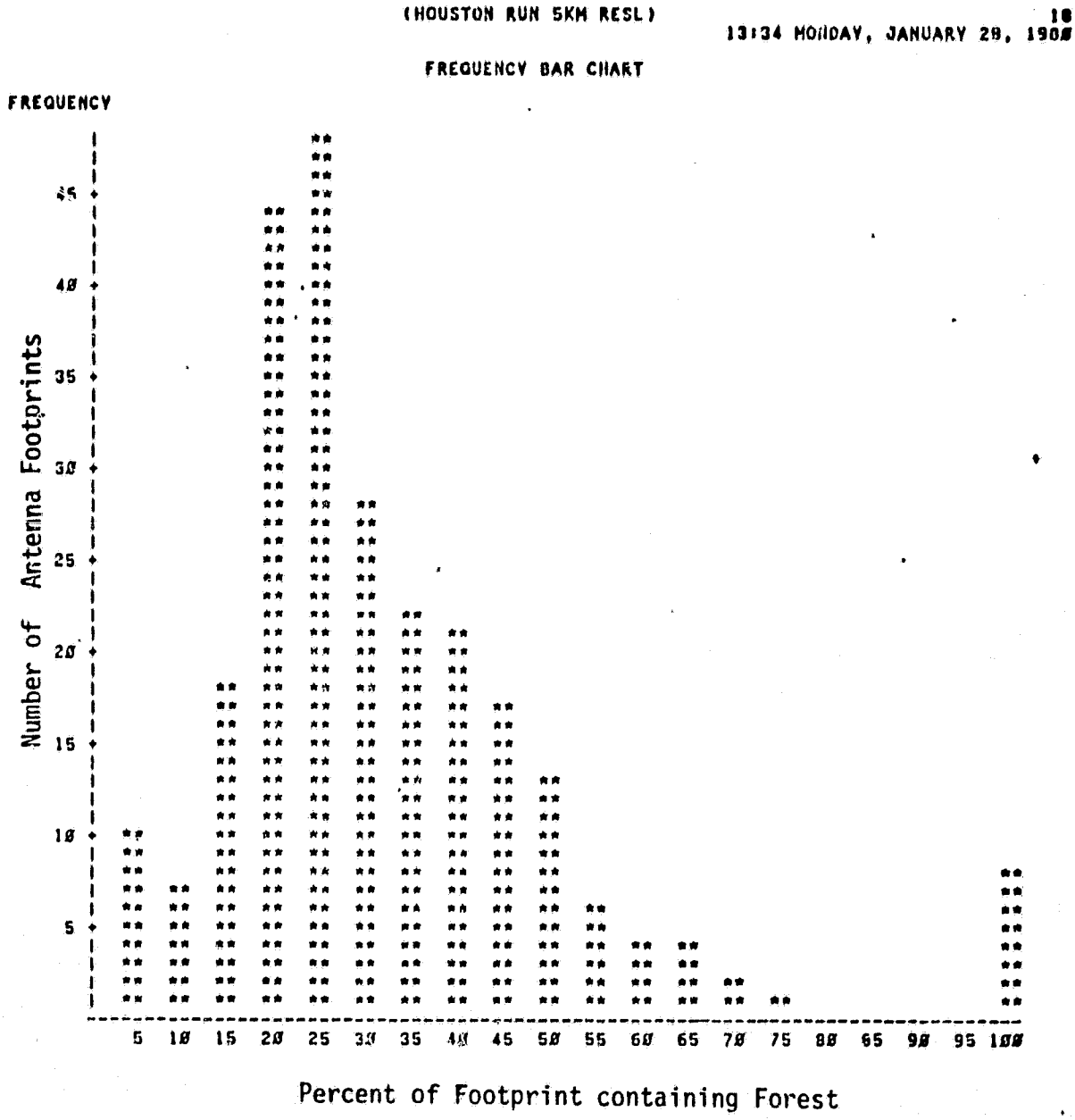

FIGURE 39. Histogram of the percentage of the antenna footprint containing forest for the Kerrville to Houston ground track at a 5 kilometer resolution.

ORIGINAL PAGE IS OF POOR QUALITY

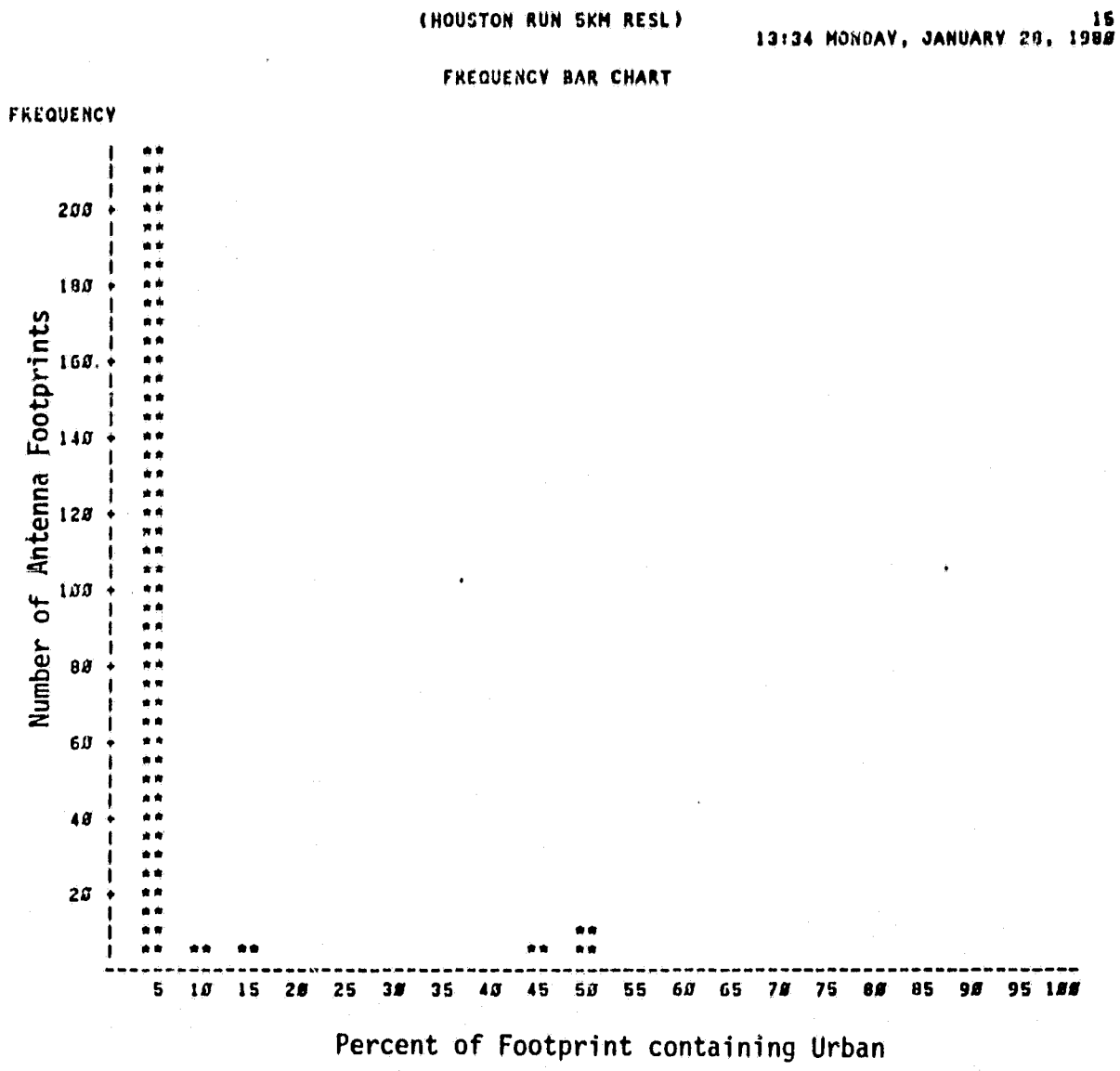

FIGURE 40. Histogram of the percentage of the antenna footprint containing urban for the Kerrville to Houston ground track at a 5 kilometer resolution.

Since the simulation model is reasonably expensive to run on the Texas A&M University Amdahl computers, only the two ground tracts were simulated in this study. However, in the interest of future analysis, all simulated outputs were recorded on magnetic tape and stored for future reference.

Analysis

Model Validity

The steps in analyzing the simulated radiomter measurements were to verify that the simulation program behaves properly. It was important to demonstract that the brightness temperature computations were properly dependent on incident angle, temperature, surface roughness, soil moisture, and resolution. Figure 41 demonstrates the brightness temperature computation vs. incident angle at L-band for both horizontal and vertical polarizations from nadir to 50°. It can be seen in Figure 23 that the antenna footprint containing the largest percentage of bare soil occurred at a range of 350 kilometers in the Waco to Livingston ground track. In addition, it can also be seen in the same figure that the antenna footprint containing the largest percentage of water occurred at the range of 525 kilometers. Figure 41 demonstrates that the simulation model adequately predicts angular behavior of the brightness temperature in that the brightness temperature adequately responds to the scene makeup within the antenna footprint as computed by the simulation model.

Figure 42 demonstrates the effect of the temperature parameter computed by the simulation model. Figure 42 shows the horizontal brightness temperature computer for L-band at nadir for a 20 kilometer

ORIGINAL PAGE IS
OF POOR QUALITY

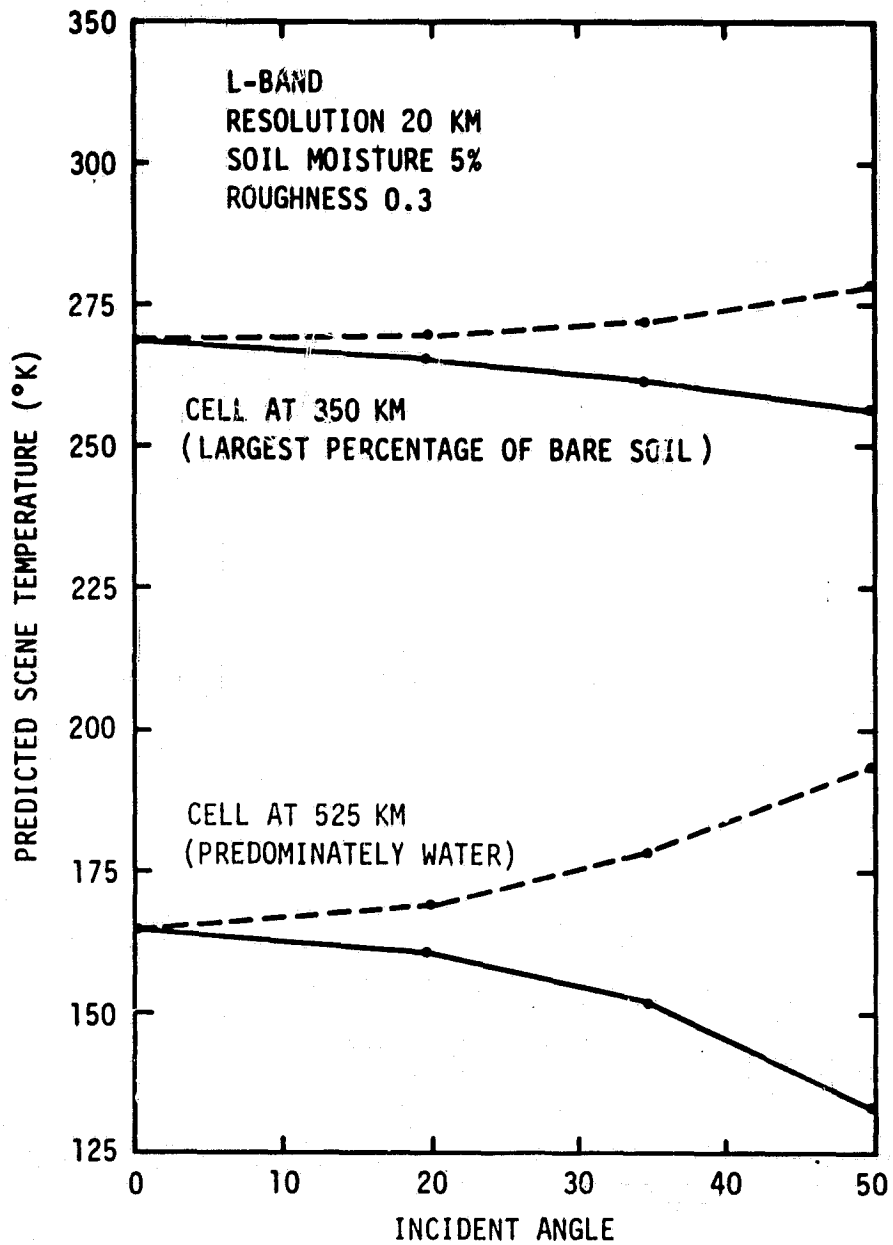

FIGURE 41. Computation of brightness temperature as a function of incident angle for L-band and a 20 kilometer resolution for an antenna footprint containing predominantly bare soil and one containing predominantly water.

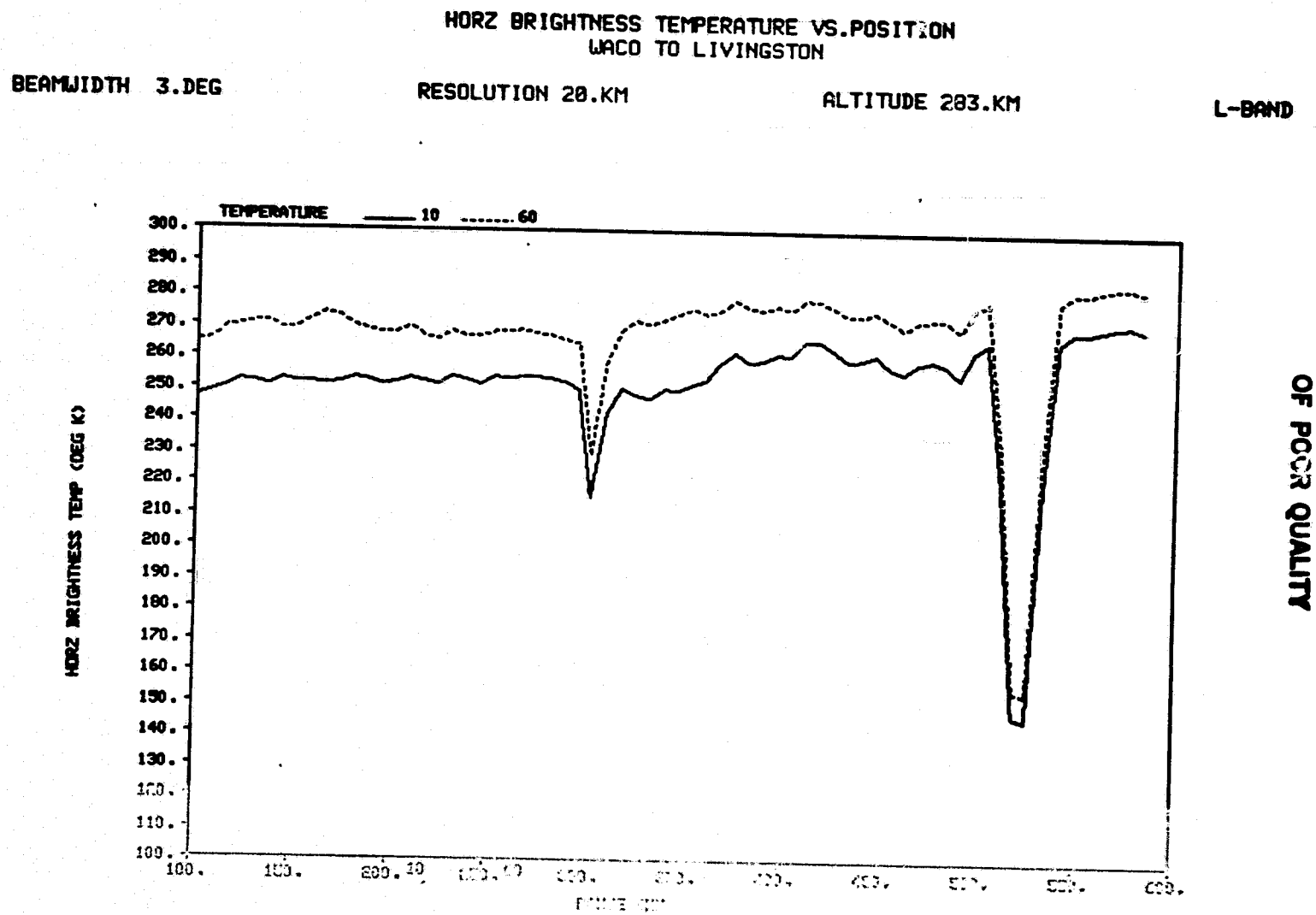

FIGURE 42. Horizontal brightness temperature computed at L-band and a 20 kilometer resolution as a function of range along the Waco to Livingston ground track for a temperature parameter of 10°C and 60°C.

ORIGINAL PAGE IS
OF POOR QUALITY

antenna footprint along the Waco to Livingston ground track for a temperature parameter of 10°C and a temperature parameter of 60°C. The effect of the 50° difference in temperature parameter is apparent. Also, the effect of two large water bodies are readily visible in the brightness temperature computation. Lake Conroe occurs at approximately the 300 kilometer range and Lake Livingston occurs at approximately the 525 kilometer range. It can also be seen that the effect of the temperature is different between footprints containing predominantly forest and footprints with large percentages of bare soil. This is apparent by the difference in the two brightness temperature computations at a range of approximately 325 kilometers where the highest percent of bare soil occurs, and a range of approximate 550 kilometers where the highest percentage of forest occurs.

Figures 43 through 48 demonstrate the performance of the simulation model as a function of microwave frequency, antenna footprint size, and soil moisture. Figures 43, 44, and 45 are plots of horizontal brightness temperature computed at 35° incidence for an antenna footprint of 5 kilometers for L, C, and X-band respectively as a function of range along the Waco to Livingston ground track for two values of soil moisture, 5% and 35%. These computations were made using a roughness factor of 0.3 which corresponds to a medium scale roughness. There are several observations which can be made concerning these three figures. First, in Figure 43, the effect of the increasing density of the forest from a range of approximately 350 kilometers to 600 kilometers is obvious. The large difference between the horizontal brightness temperature at 5% soil moisture and 35% soil moisture decreases as the forest cover density increases. Beyond the

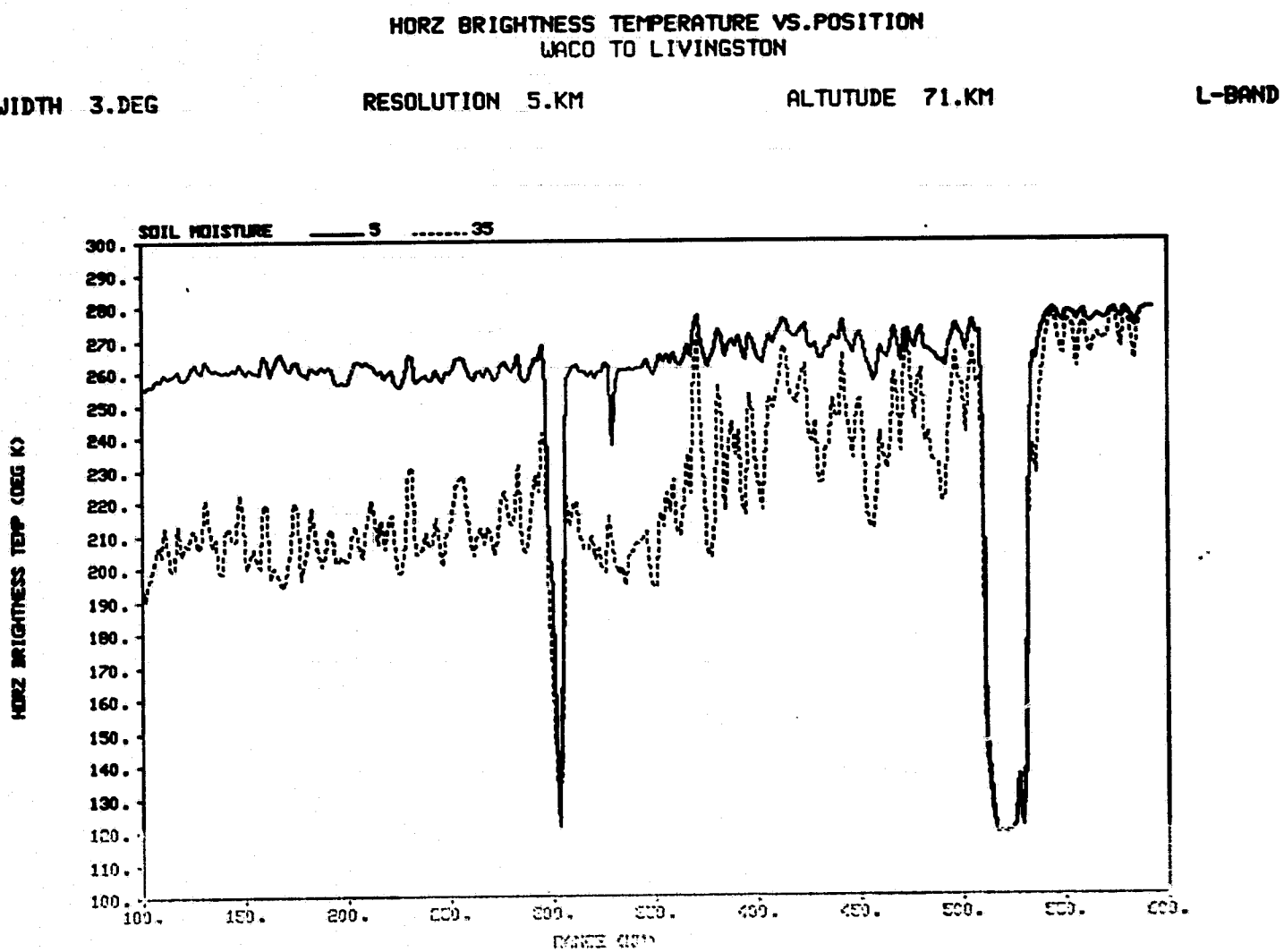

FIGURE 43. Horizontal brightness temperature computed at L-band and a 5 kilometer resolution for the Waco to Livingston ground track at two soil moistures, 5% and 35%.

ORIGINAL PAGE IS
OF POOR QUALITY

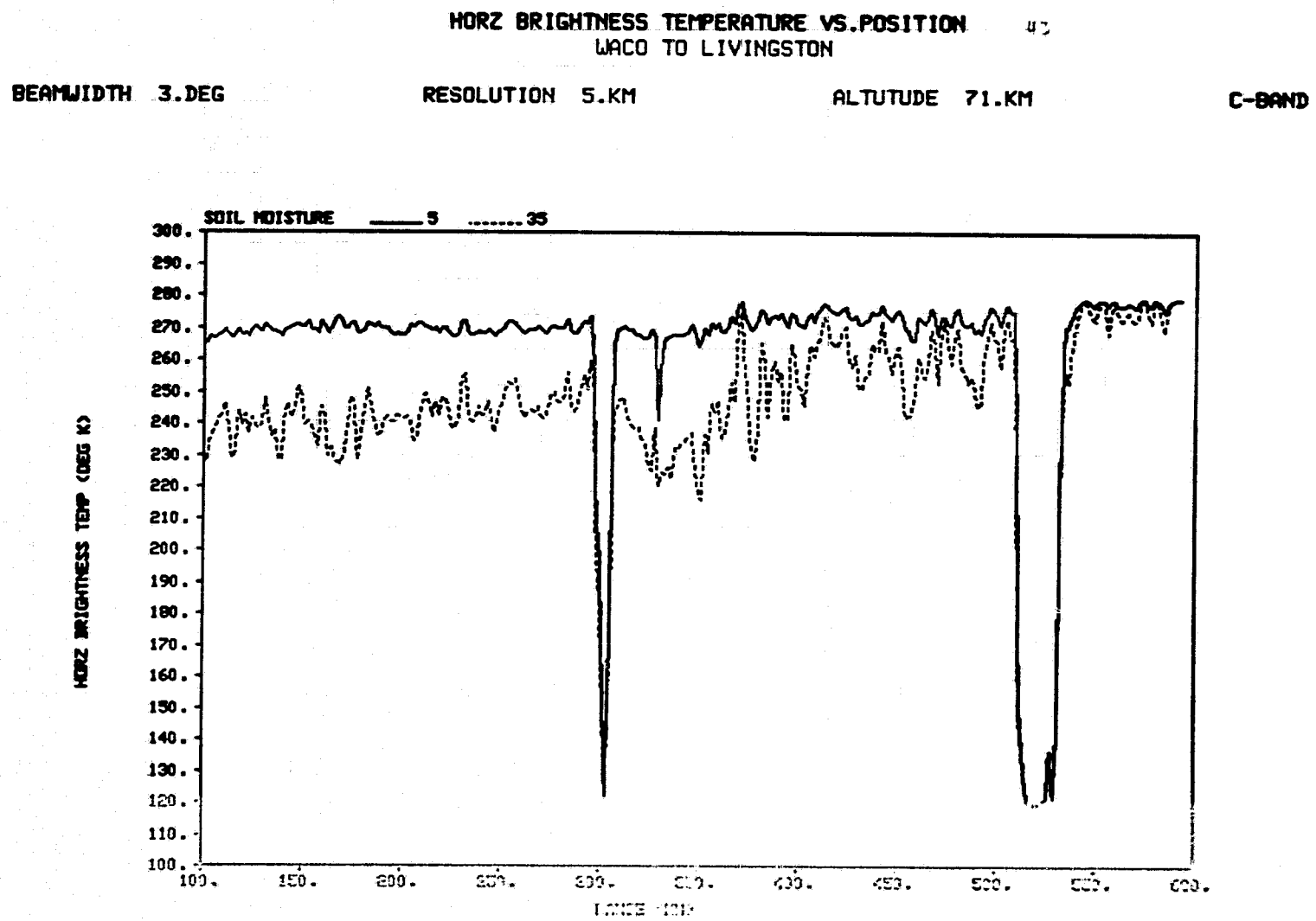

FIGURE 44. Horizontal brightness temperature computed at C-band and a 5 kilometer resolution for the Waco to Livingston ground track at two soil moistures, 5% and 35%.

ORIGINAL PAGE IS
OF POOR QUALITY

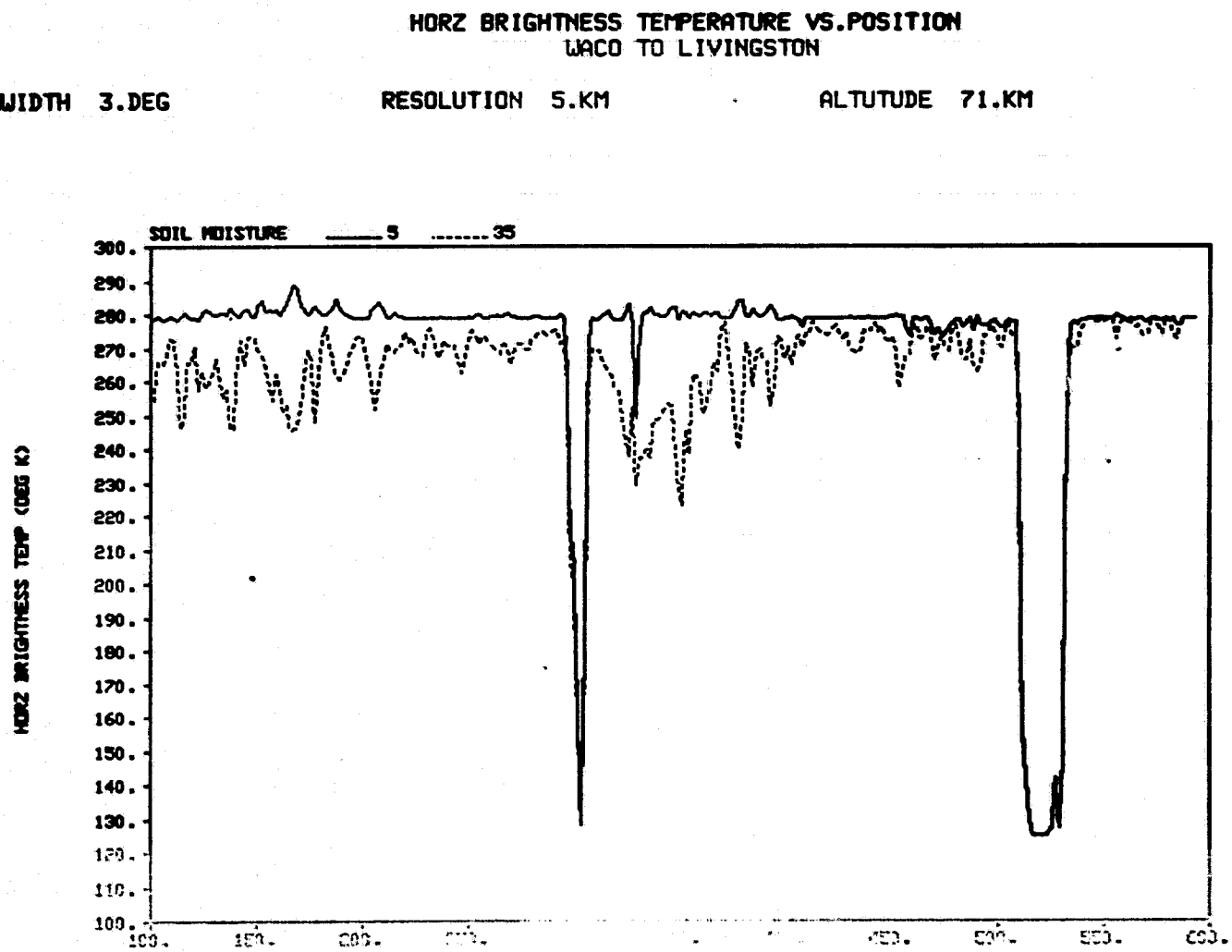

FIGURE 45. Horizontal brightness temperature computed at X-band and a 5 kilometer resolution for the Waco to Livingston ground track at two soil moistures, 5% and 35%.

ORIGINAL PAGE IS
OF POOR QUALITY

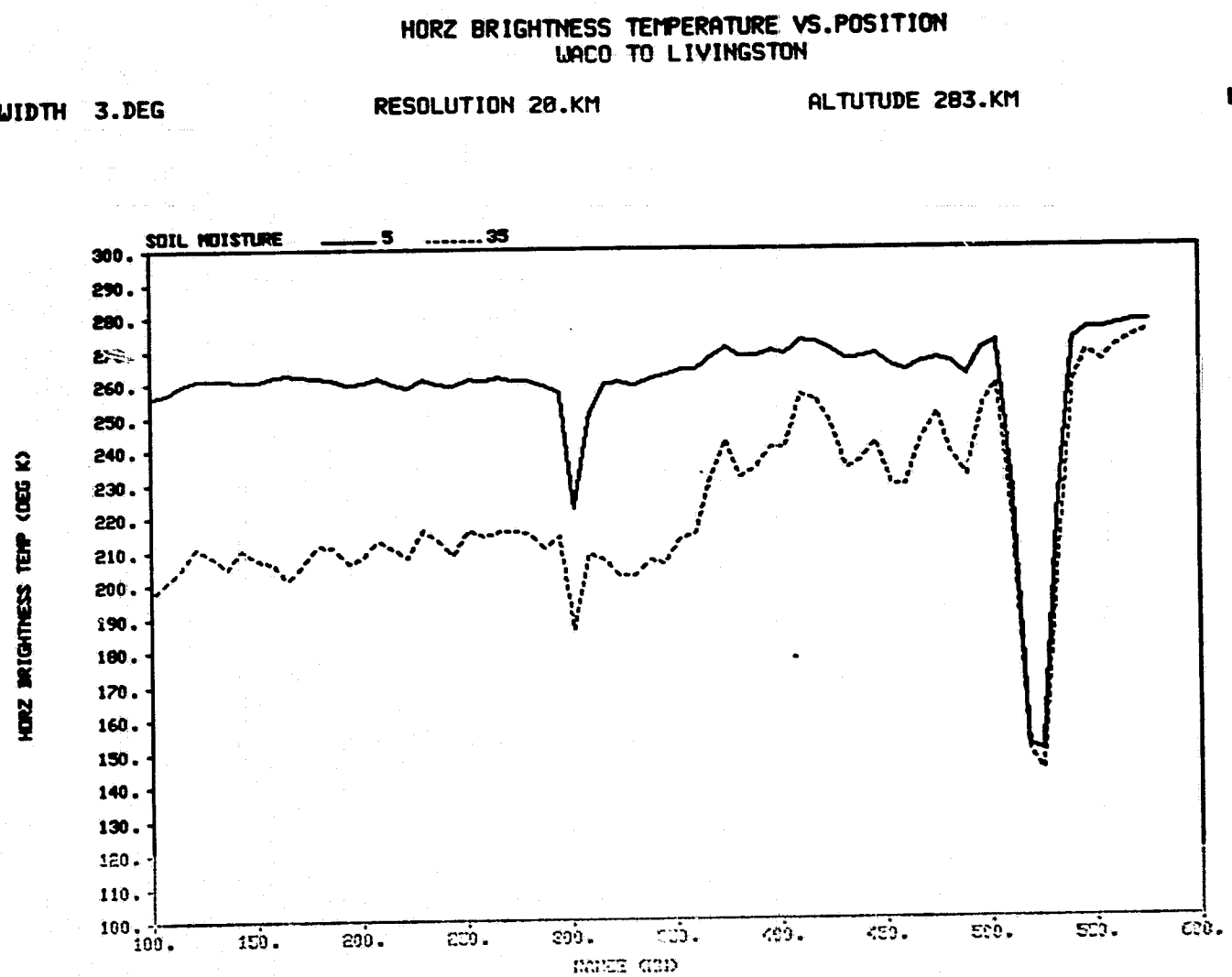

FIGURE 46. Horizontal brightness temperature computed at L-band and a 20 kilometer resolution for the Waco to Livingston ground track at two soil moistures, 5% and 35%.

ORIGINAL PAGE IS OF POOR QUALITY

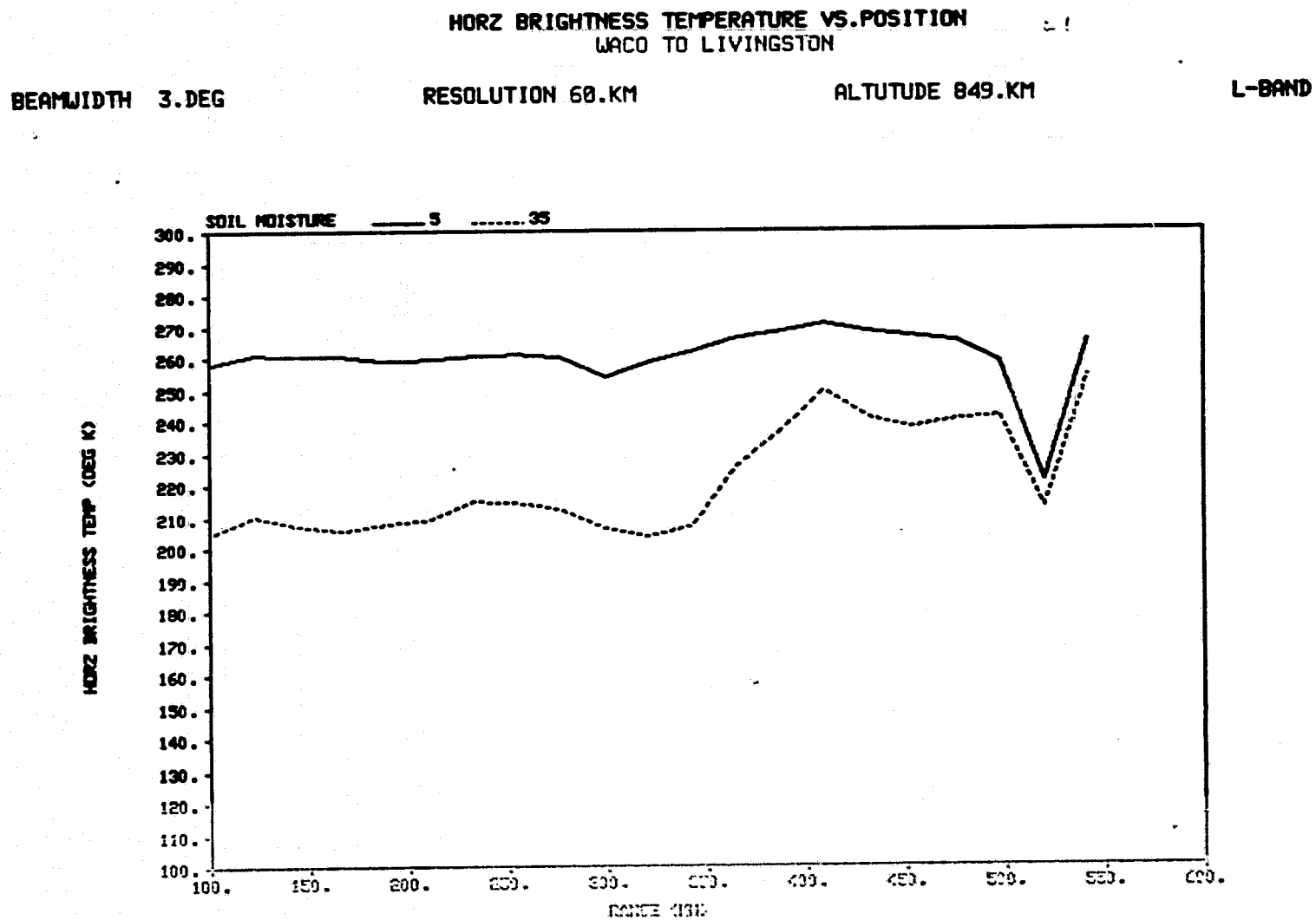

FIGURE 47. Horizontal brightness temperature computed at L-band and a 60 kilometer resolution for the Waco to Livingston ground track at two soil moistures, 5% and 35%.

ORIGINAL PAGE IS
OF POOR QUALITY

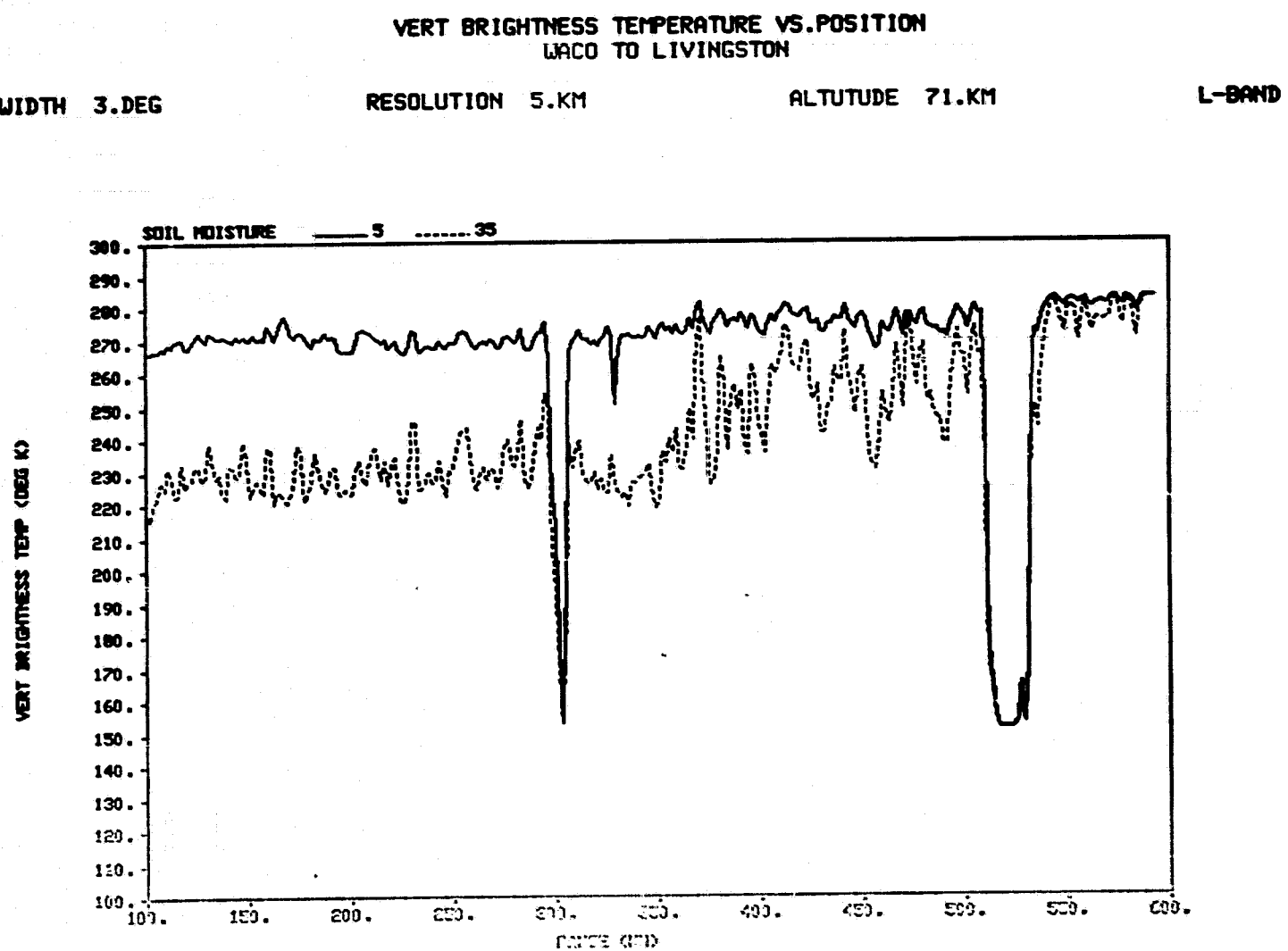

FIGURE 48. Vertical brightness temperature computed at L-band and a 5 kilometer resolution for the Waco to Livingston ground track at two soil moistures, 5% and 35%.

ORIGINAL PAGE IS
OF POOR QUALITY

range of 550 kilometers, where the percent of forest cover is in the 90% range, the sensitivity to soil moisture is practically eliminated. By comparing Figure 43, 44, and 45 the effect of microwave frequency can easily be seen. It is obvious from these figures that as the frequency goes higher, a difference between the brightness temperature at 5% soil moisture and 35% soil moisture decreases. This is due primarily to the effect of the vegetation cover that exists in the simulation scene. The largest percentages of bare soil occur around the range of 350 kilometers. Again, this is obvious in Figures 43, 44, and 45 since it is in this range interval that the largest difference occurs between the 5% soil moisture computation and the 35% soil moisture computation for all microwave frequencies.

The effect of antenna footprint size can be seen by comparing Figure 43, 46, and 47. The parameters used in generating these figures are identical except for the fact that the antenna footprint was increased from 5 kilometers to 20 kilometers and 60 kilometers, respectively. The effect of the largest footprint is obvious in the smoothing effect of the brightness temperature computations as a function of range. In addition, the ability to resolve physical features is diminished. In Figure 46, Lake Conroe and Lake Livingston are still visible, however, in Figure 47, Lake Conroe is practically unresolvable. However, the effect of the higher percentages of bare soil in the range around 350 kilometers still is visible in Figure 47 for the 60 kilometer antenna footprint size.

Figures 43 and 48 demonstrate the capability of the simulation model to compute horizontal and vertically polarized brightness temperatures. Figure 48 is identical to Figure 43 except that it pre-

sents vertically polarized brightness temperature computations. It can be seen by comparing these two figures that the vertical polarized brightness temperature at both the 5% soil moisture and 35% soil moisture are several degrees higher than the horizontal brightness temperature.

Analysis Approach

As stated earlier, the objective of this study was to investigate the effects of scene heterogeneity on the ability of a microwave radiometer system to estimate soil moisture and to determine if the effects of scene heterogeneity are dependent upon the size of the antenna footprint. The most pleasing appraoch to accomplishing this objective is to quantify the effect of the percent ground cover of each class on the sensitivity of the brightness temperature computation to soil moisture. Unfortunately, it is impossible to quantify the effects of each class independently of one another due to the dimensionality of the problem. Therefore, the approach was to quantify the effects of each ground cover class on the sensitivity of the brightness temperature to soil moisture individually without regard to the other classes, and do this as a function of antenna footprint size. Care must be exercised in analyzing results presented in the manner. Obviously at low percentages of the ground cover class being investigated, there will be larger influences of other classes that have higher ground cover percentages. This will cause scatter in the results <u>not</u> due to the class being investigated. It is possible, however, to document the <u>mean</u> sensitivity to soil moisture for the two ground tracks considered and to approximate a quantitative description

of the effects of each individual ground cover class on that sensitivity.

Analysis Results

In this section the simulation results will be analyzed to demonstrate the effect of each scene class, microwave frequency, and antenna resolution on the sensitivity of brightness temperature to soil moisture. This will be done by first considering horizontal brightness temperature plotted as a function of percent class for two soil moistures, 5% and 35%. Figures 49 through 52 contain brightness temperature computation for the Waco to Livingston ground track at a 35° incident angle and a 5 kilometer resolution. These plots demonstrate the scatter in the brightness temperature computations when the computations for each ground resolution cell are viewed independently.

Figure 49 shows L-band horizontal brightness temperatures for bare soil plotted as a function of percent class of bare soil. The general effect of the soil moisture difference is obvious. However, between 0% and 8% bare soil there are some very low brightness temperatures. These particular footprints are those that occurred over Lake Conroe and Lake Livingston, thus these low brightness temperatures are due to water. Note also, that the largest amounts of scatter in the brightness temperatures occur in the low percentage range of bare soil, and that as the percentage of bare soil increases the scatter in the brightness temperature computation decreases. In addition, the largest scatter occurs for the brightness temperature computations at 35% soil moisture. These effects are due to the fact that at low percentages of bare soil the primary class consitutents within the

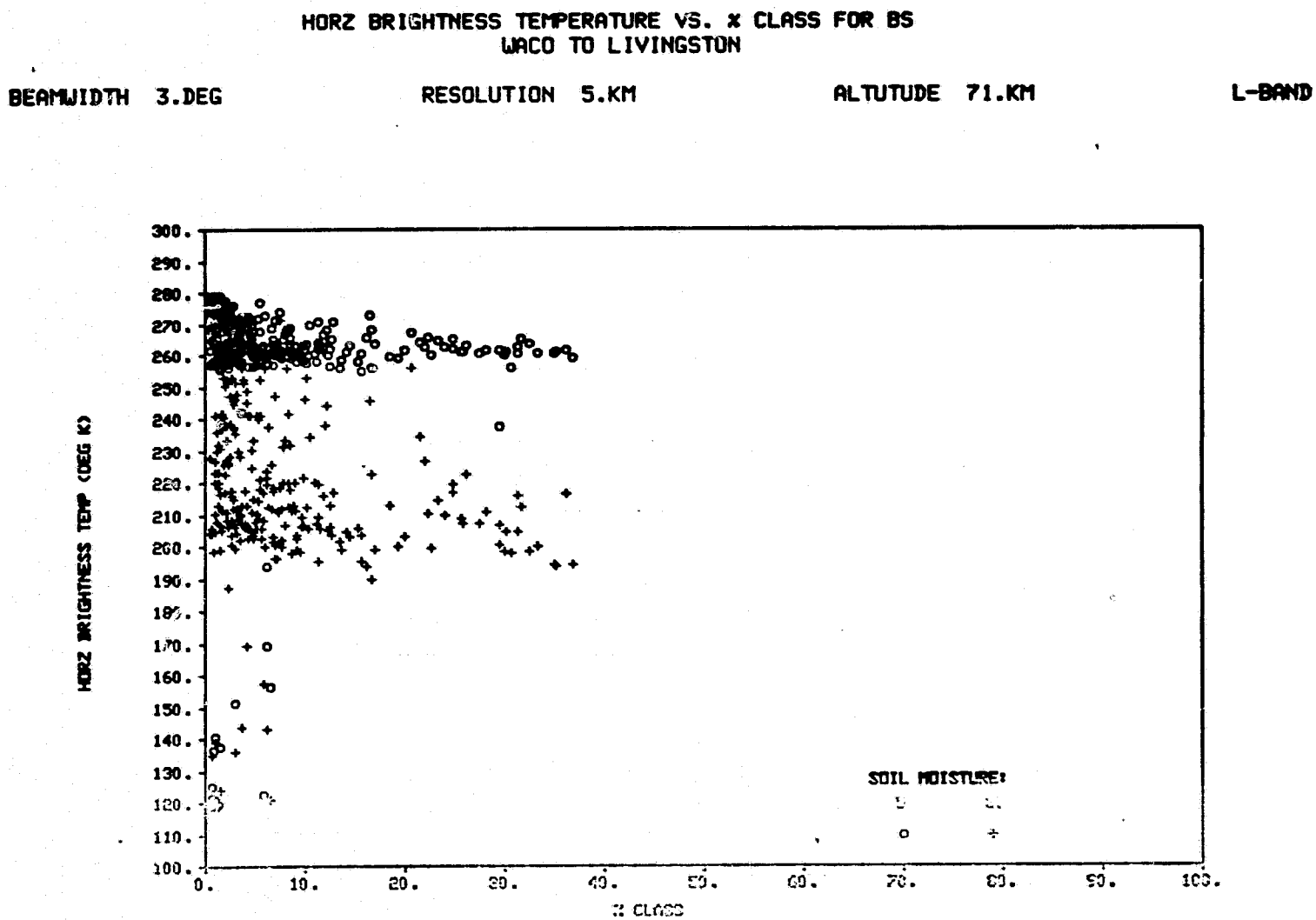

FIGURE 49. Horizontal brightness temperature computed at L-band for the Waco to Livingston ground track at a 5 kilometer resolution plotted as a function of percent class of bare soil at two soil moistures, 5% and 35%.

ORIGINAL PAGE IS
OF POOR QUALITY

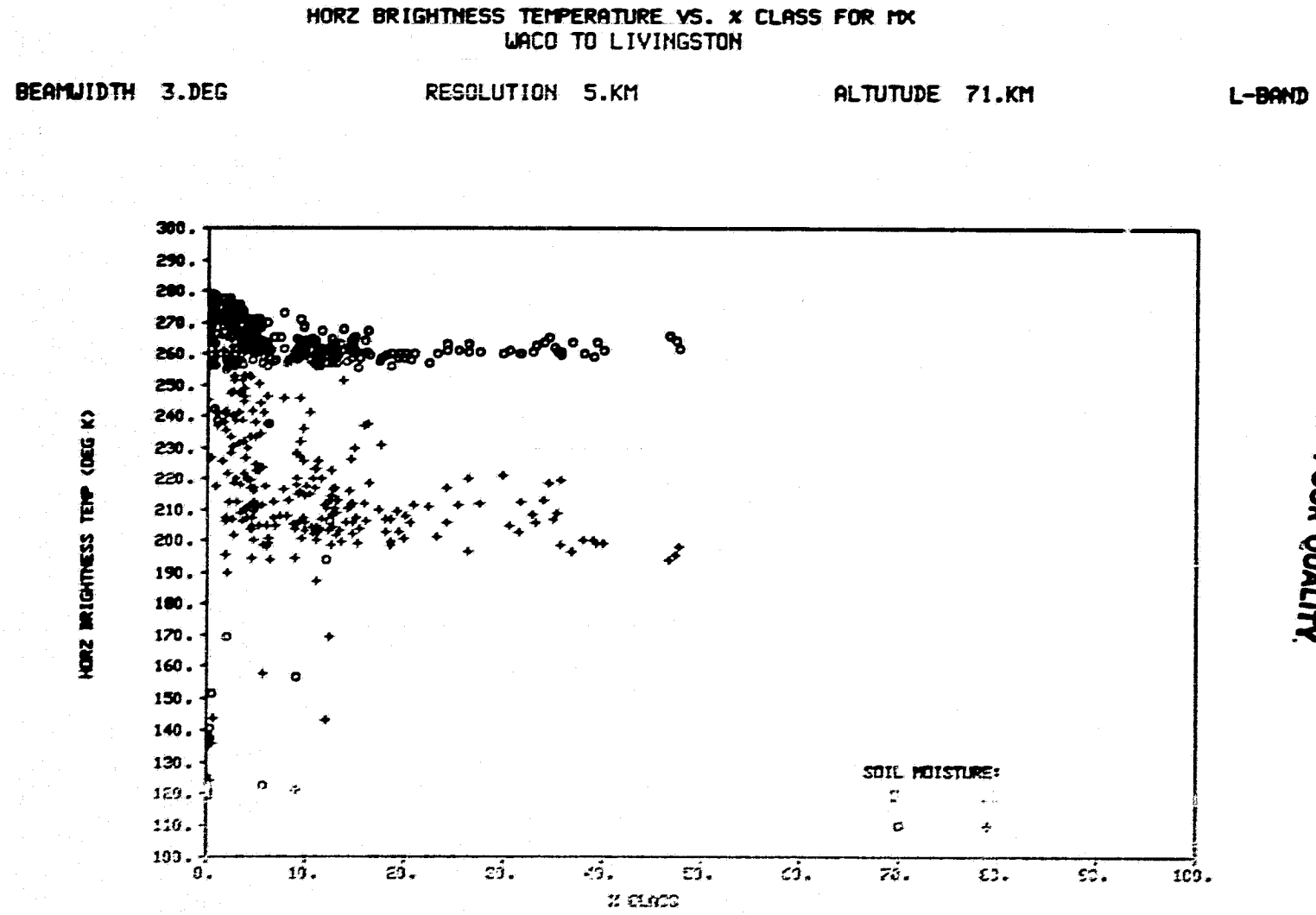

FIGURE 50. Horizontal brightness temperature computed at L-band for the Waco to Livingston ground track at a 5 kilometer resolution plotted as a function of percent class of mixed bare and vegetation at two soil moistures, 5% and 35%.

ORIGINAL PAGE IS OF POOR QUALITY

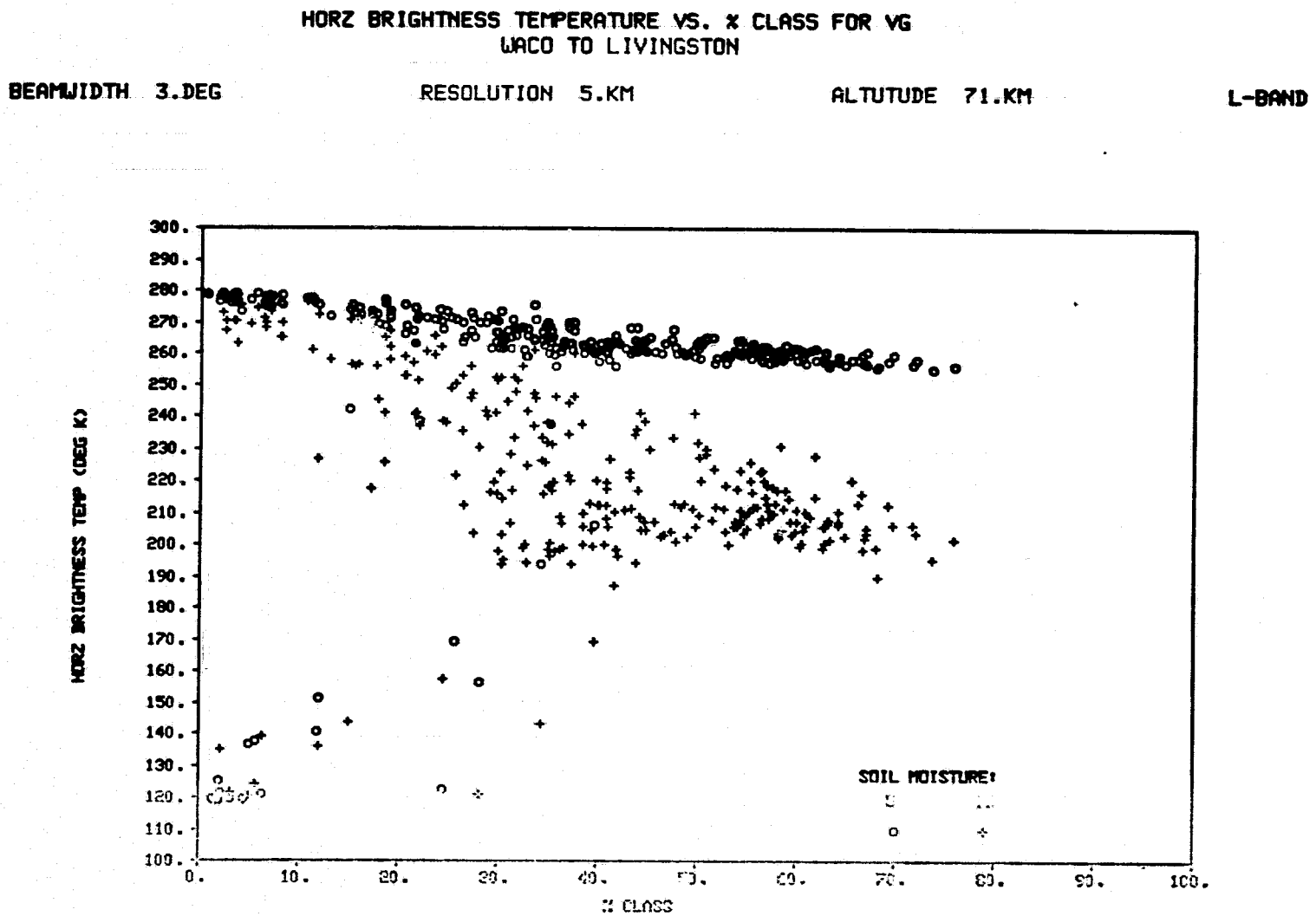

FIGURE 51. Horizontal brightness temperature computed at L-band for the Waco to Livingston ground track at a 5 kilometer resolution plotted as a function of percent class of fully vegetated at two soil moistures, 5% and 35%.

ORIGINAL PAGE IS
OF POOR QUALITY

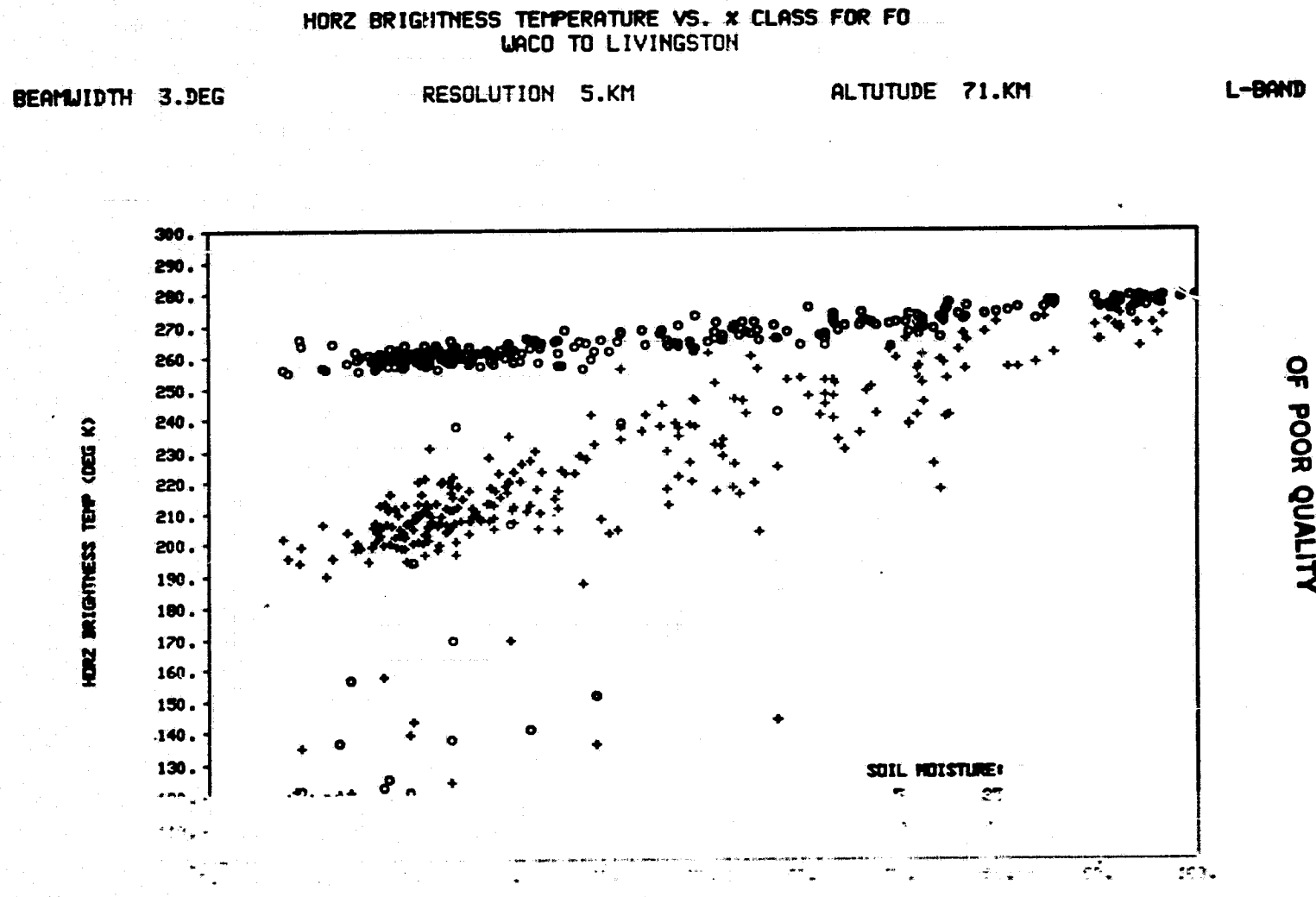

FIGURE 52. Horizontal brightness temperature computed at L-band for the Waco to Livingston ground track at a 5 kilometer resolution plotted as a function of percent forest class at two soil moistures, 5% and 35%.

ORIGINAL PAGE IS
OF POOR QUALITY

resolution footprint is some other class. No information is provided on which class in this particular plot. However, by looking at Figures 23 and 24 that show the percentage class distribution as a function of range down the Waco to Livingston ground track, it is obvious that the majority of the footprint for the low percentage of bare soil resolution are some form of vegetation, primarily, fully vegetated and forested.

Figure 50 shows the same type of information except for the mixed vegetation class. It can be seen that above approximately 20% mixed bare soil and vegetation the scatter in the brightness temperature computations are significantly decreased. Figure 51 shows the brightness temperatures for 5% and 35% soil moisture plotted as a function of the fully vegetated class. Note that there are antenna footprints where the percentage of this class is much higher than that for bare soil and the mixed vegetation class. Also, the scatter for the 35% soil moisture brightness temperature computation continues to much higher percentages of the fully vegetated class than previously seen for the mixed vegetation class or the bare soil class. This is due to the fact that the resolution elements that contained less than approximately 40% of the fully vegetated class contain very high percentages of the forest class, usually above 50% as can be seen in Figures 23 and 24.

Figure 52 shows the same type of plot for the forest class. The effect of increasing the percentage forest in each resolution element is obvious. It can be seen that above approximately 35% to 40% of the forest class there is severe degradation in the ability to distinguish

between the two soil moisture contents. In addition, below approximately the 40% point there are some extremely low brightness temperature computations. Again, this is due primarily to Lake Livingston and Lake Conroe.

Plots such as those shown in Figure 49 through 52 will not be provided for the urban and water class since there was not a good enough distribution of resolution elements with different percent classes to present the data in this manner.

Figures 49 through 52 show brightness temperature computations for L-band at 5 kilometers for each of the four major classes. Figures 53 and 54 show the same type computations for the class mixed vegetation at C-band and X-band, respectively. In Figure 53 it can be seen that the same general comments that were made concerning Figure 50 (which showed mixed vegetation class for L-band) can be made. The only difference is that the magnitude difference between the horizontal brightness temperature computed at 5% soil moisture and the brightness temperature computed at 35% soil moisture is less at C-band than it was at L-band. In addition, the percent of the mixed vegetation class must get above approximately 20% in order for the scatter in the brightness temperature for the 35% soil moisture to decrease significantly. In Figure 54, which is the same plot for X-band, it can be seen that the effect of the vegetation is more severe. In fact, the percent class of the mixed vegetation must be above approximately 35% for the scatter to significantly decrease. It should also be noted that the ability to discriminate soil moisture increases as the percent of the mixed vegetation class increases at all three frequencies. This is due to the fact that the forest class predomi-

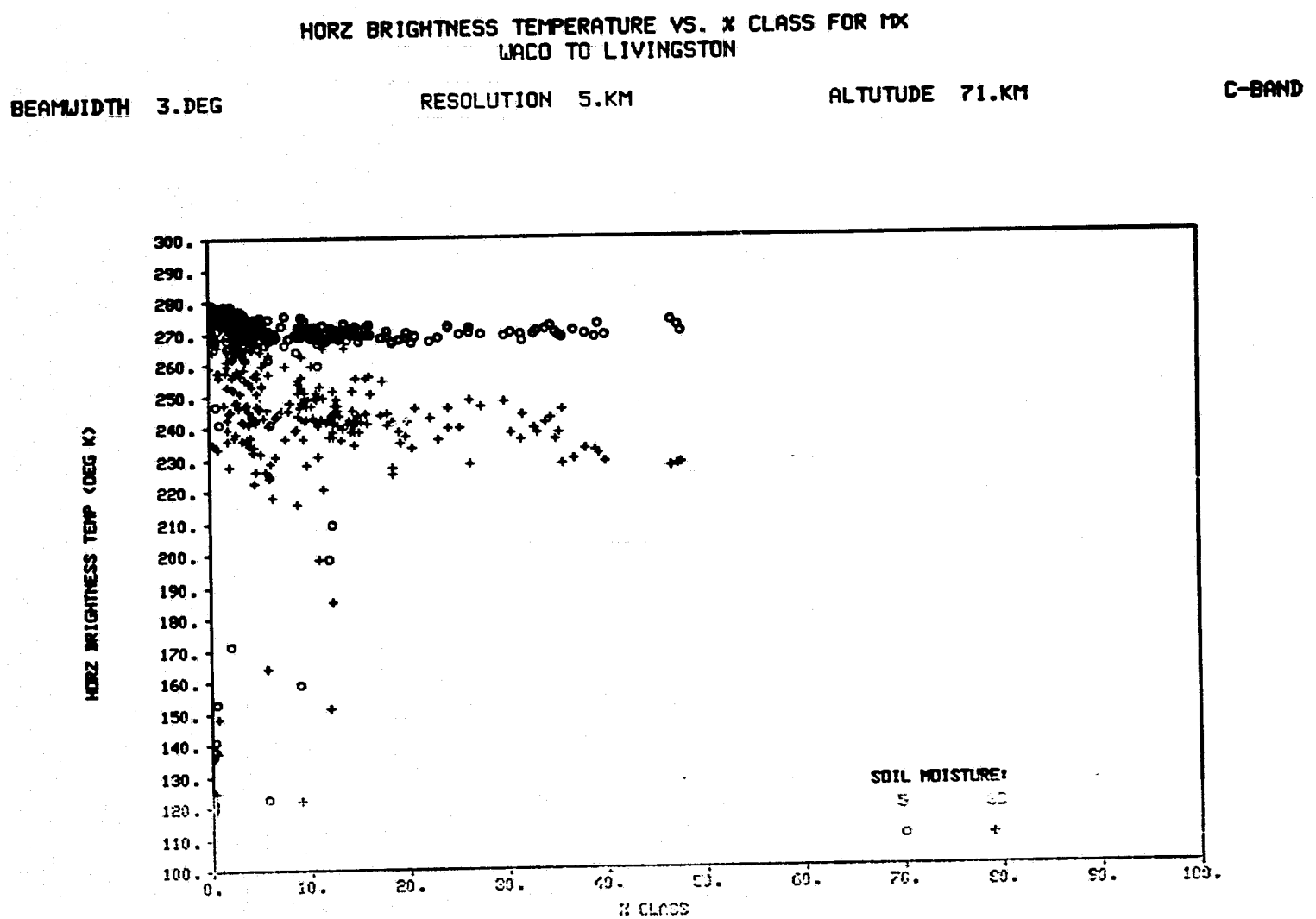

FIGURE 53. Horizontal brightness temperature computed at C-band for the Waco to Livingston ground track at a 5 kilometer resolution plotted as a function of percent mixed bare and vegetation class at two soil moistures, 5% and 35%.

ORIGINAL PAGE IS
OF POOR QUALITY

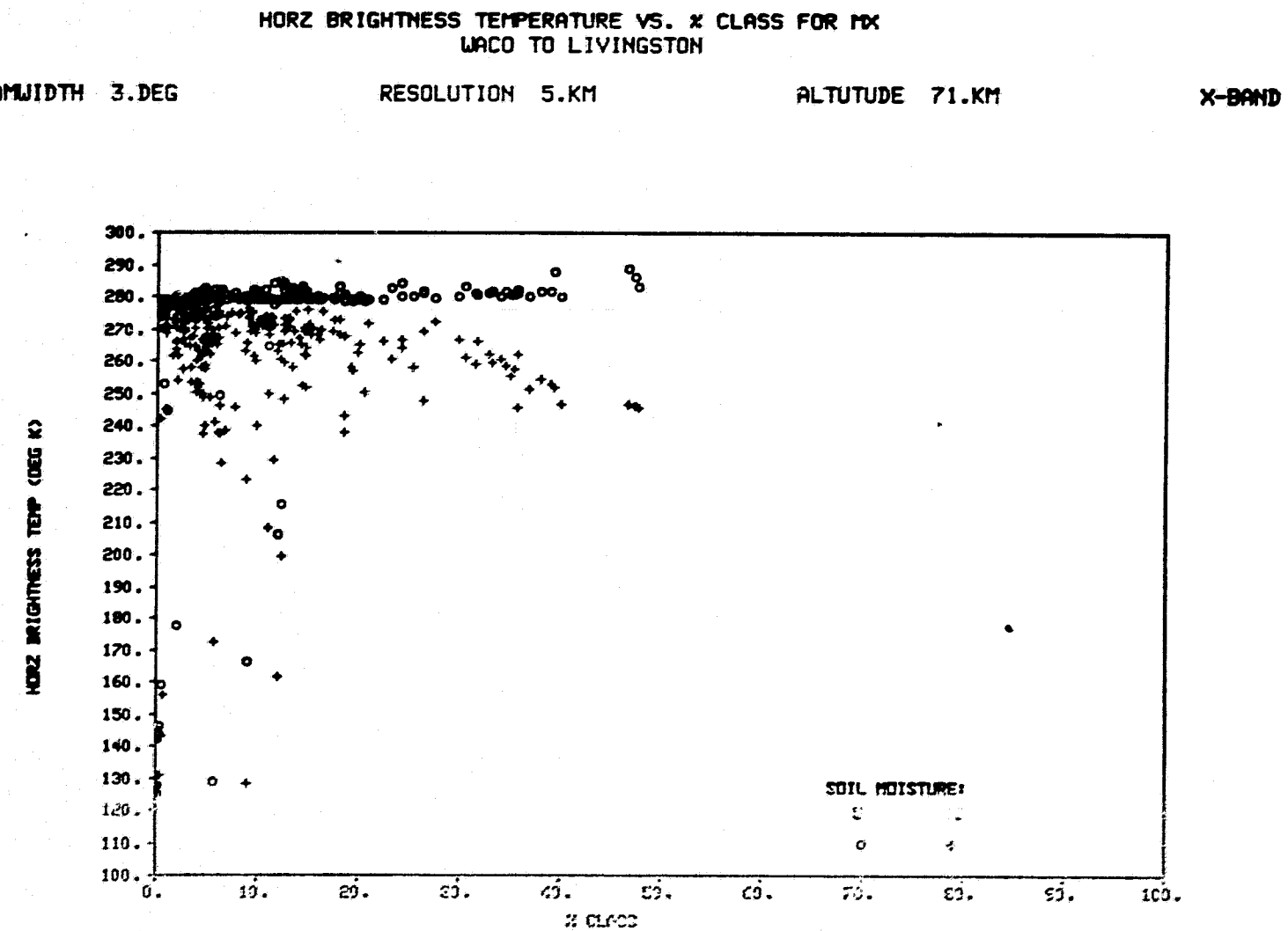

FIGURE 54. Horizontal brightness temperature computed at X-band for the Waco to Livingston ground track at a 5 kilometer resolution plotted as a function of percent mixed bare and vegetation class at two soil moistures, 5% and 35%.

ORIGINAL PAGE IS
OF POOR QUALITY

nates the make of the resolution elements for the low percentages of the mixed vegetation class.

Figures 55 and 56 will be used to demonstrate the effect of resolution on the scatter seen in the brightness temperature computations. Figure 55 shows the horizontal brightness temperature computed for L-band at 5% and 35% soil moisture for the mixed vegetation class and a 20 kilometer resolution. This figure can be compared to Figure 50 which is the same plot for the 5 kilometer resolution size. It can be seen that the general trends in both figures are the same although the scatter in the data for the 20 kilometer footprint is significantly less. Although there is less scatter, there is a corresponding fewer number of points in Figure 55 than in Figure 50. This demonstrates the averaging effect of simply increasing the resolution size of the antenna. Increasing resolution is very nearly equivalent to averaging measurements taken at smaller resolution. The effect of going to a 60 kilometer resolution element is essentially the same, additional averaging and fewer points. This result indicates that in general the ground cover classes behave as if they are randomly oriented over the scene. Figure 56 demonstrates the same phenomena as Figure 55. The four points at the 45% forest class correspond to calculations made over Lake Livingston as can be seen from Figure 27.

Figures 49 through 56 provide a qualitative indication of the distribution of the brightness temperature computations as a function of scene class. It is informative to investigate the distribution of the brightness temperature computations for 5% soil moisture and 35% soil moisture for the entire scene without regard to individual

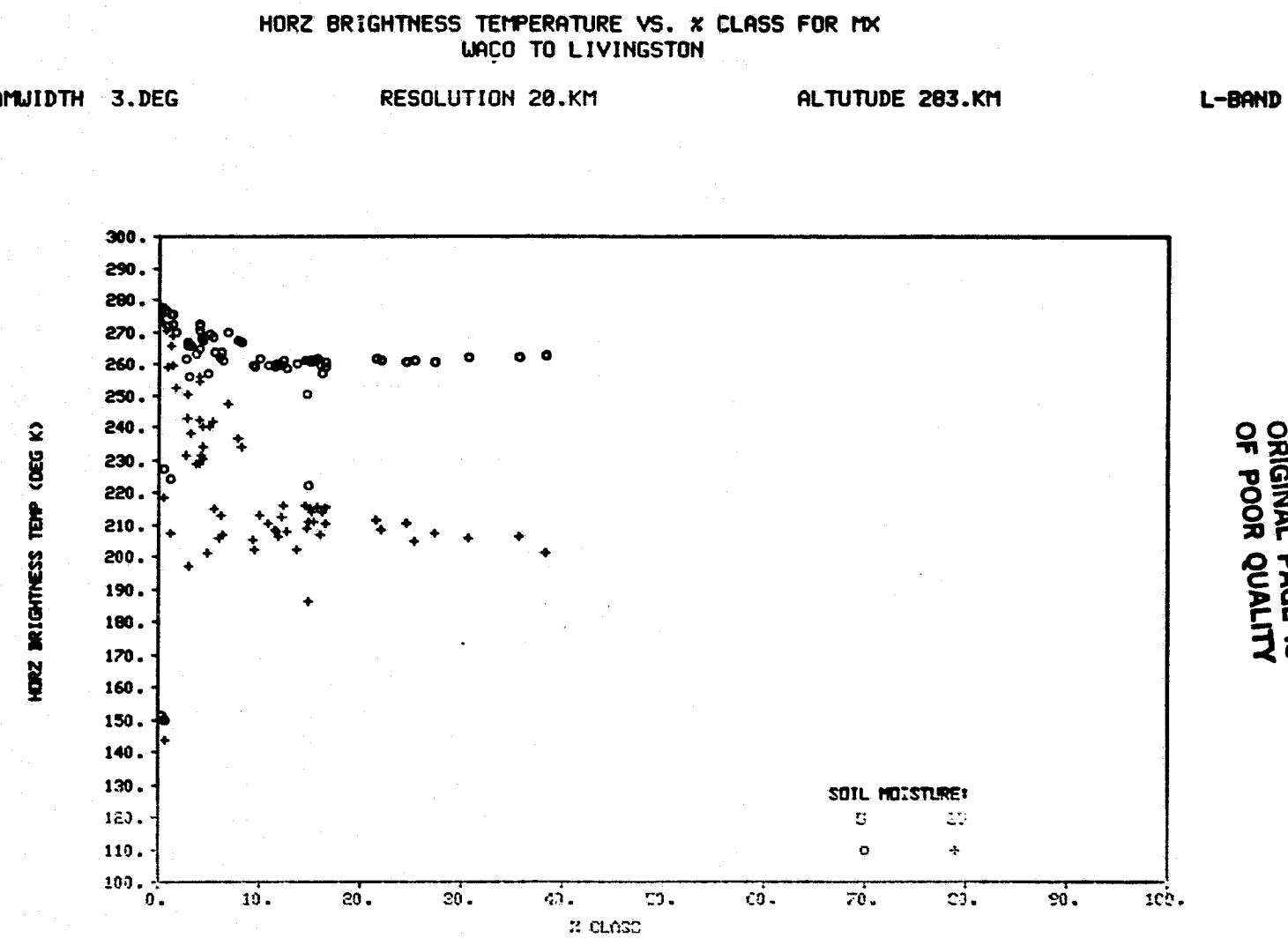

FIGURE 55. Horizontal brightness temperature computed at L-band for the Waco to Livingston ground track at a 20 kilometer resolution plotted as a function of percent mixed bare and vegetation class at two soil moistures, 5% and 35%.

ORIGINAL PAGE IS
OF POOR QUALITY

ORIGINAL PAGE IS
OF POOR QUALITY

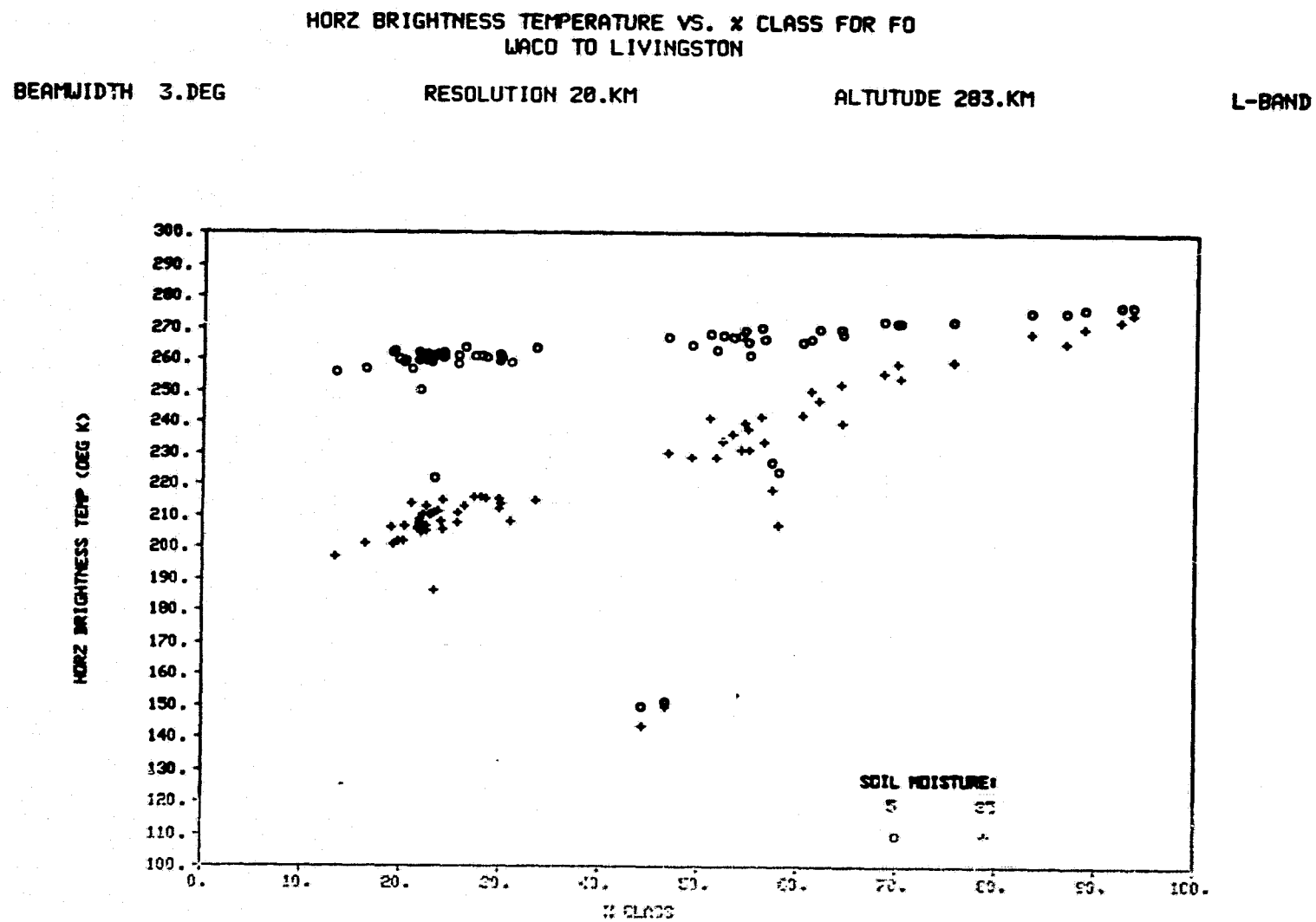

FIGURE 56. Horizontal brightness temperature computed at L-band for the Waco to Livingston ground track at a 20 kilometer resolution plotted as a function of percent forest class at two soil moistures, 5% and 35%.

classes. Figures 57 and 58 are frequency histograms for the brightness temperature computed at L-band at an incident angle of 35° for the Waco to Livingston ground track at horizontal polarization. Figure 57 was computed for a 5 kilometer ground resolution. It can be seen that the distribution of brightness temperatures for a 5% soil moisture tightly clusters between 250°K and 275°K. The brightness temperatures for the 35% soil moisture has a peak at 200°K but spreads up to 275°K. It will be seen later that this spreading effect causes the confidence interval on the sensitivity of the brightness temperature to soil moisture to be larger than that for the 60 kilometer resolution. Figure 58 shows the same frequency histogram for the 60 kilometer resolution. Again, for the 5% soil moisture the brightness temperature cluster tightly between 250 and 275°K. However, for the 35% soil moisture, brightness temperature is a multimodal distribution. One peak occurs at 250°K while the other occurs at approximately 230°K.

Up to now we have only qualitatively investigated the dependence of brightness temperature on soil moisture by analyzing brightness temperature computations for 5% soil moisture and 35% soil moisture over the same ground track. One method of quantifying the sensitivity of the brightness temperature to soil moisture is to compute the slope of the best fit straight line between the brightness temperatures computed for 5% soil moisture and 35% soil moisture. Since it is known from other investigations that the microwave brightness temperature is linearly related to soil moisture, this slope can be termed the sensitivity of the brightness temperature to soil moisture in °K per percent soil moisture. Figures 59 through 61 are plots of the sensi-

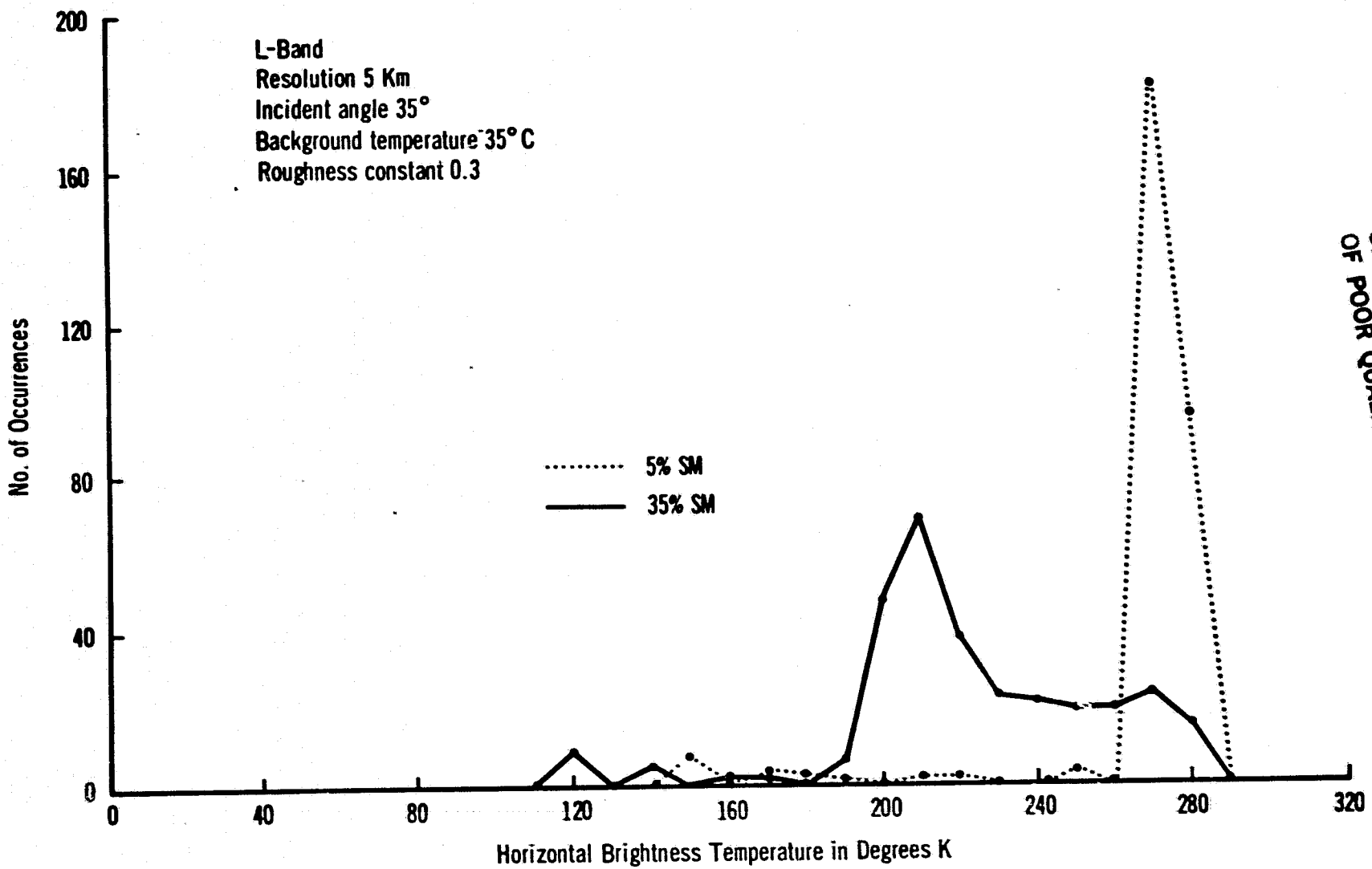

ORIGINAL PAGE IS
OF POOR QUALITY

FIGURE 57. Histogram of the horizontal L-band brightness temperature computed for the Waco to Livingston ground track at 5% and 35% soil moisture and a 5 kilometer resolution.

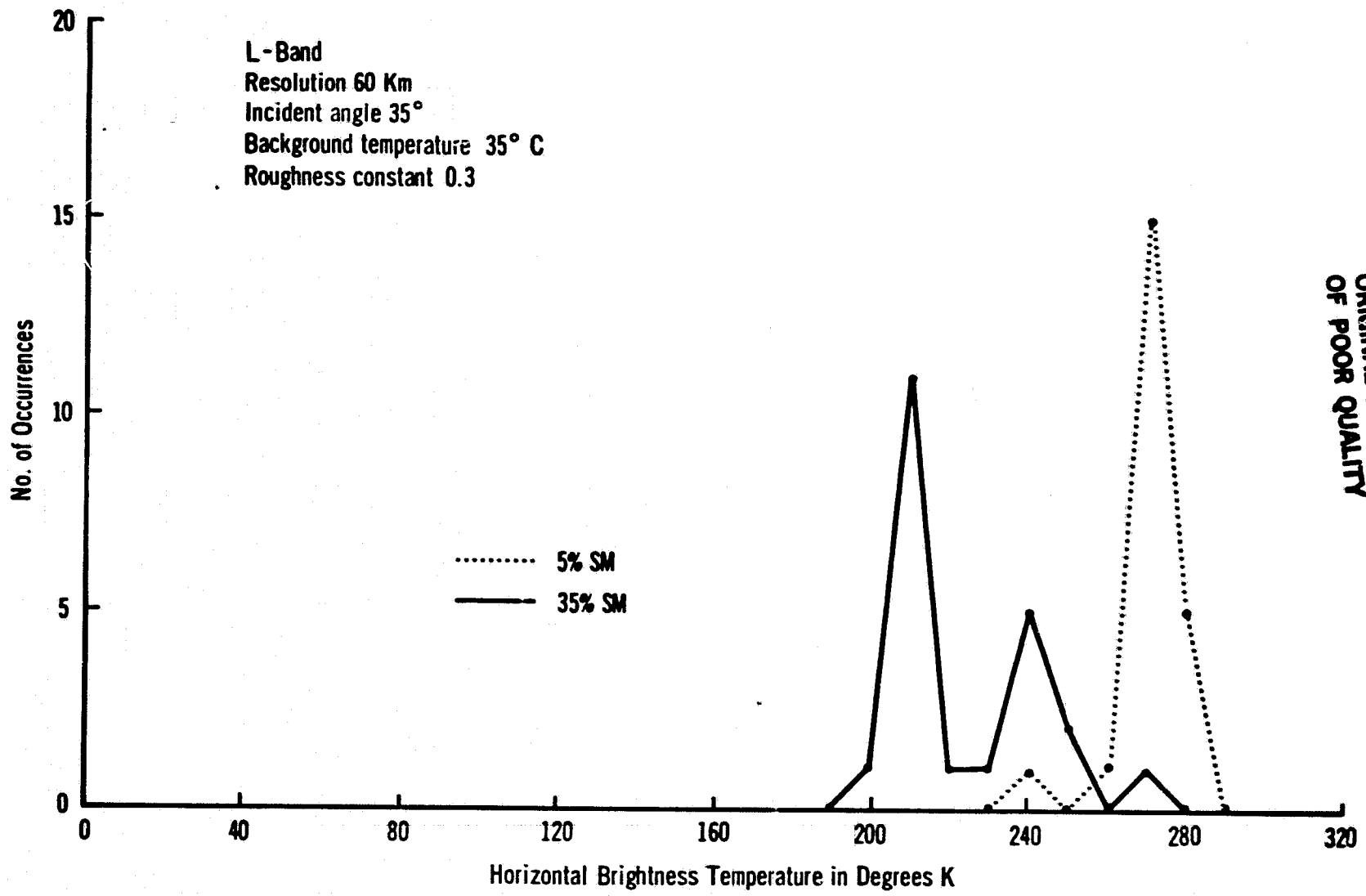

ORIGINAL PAGE IS
OF POOR QUALITY

FIGURE 58. Histogram of the horizontal L-band brightness temperature computed for the Waco to Livingston ground track at 5% and 35% soil moisture and a 60 kilometer resolution.

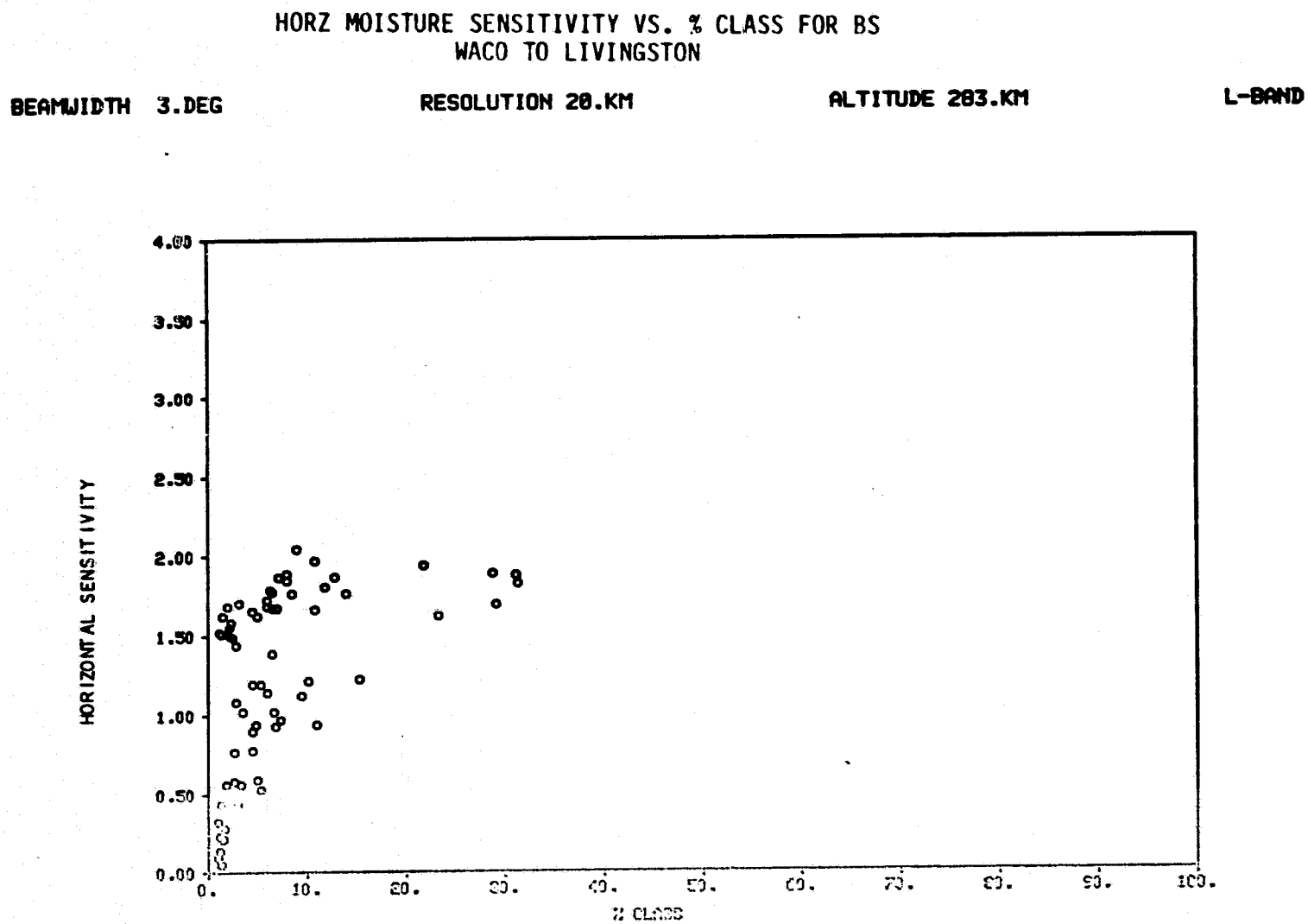

FIGURE 59. Soil moisture sensitivity of the L-band horizontally polarized brightness temperature for the Waco to Livingston ground track at a 20 kilometer resolution plotted as a function of percent bare soil.

ORIGINAL PAGE IS
OF POOR QUALITY

ORIGINAL PAGE IS
OF POOR QUALITY

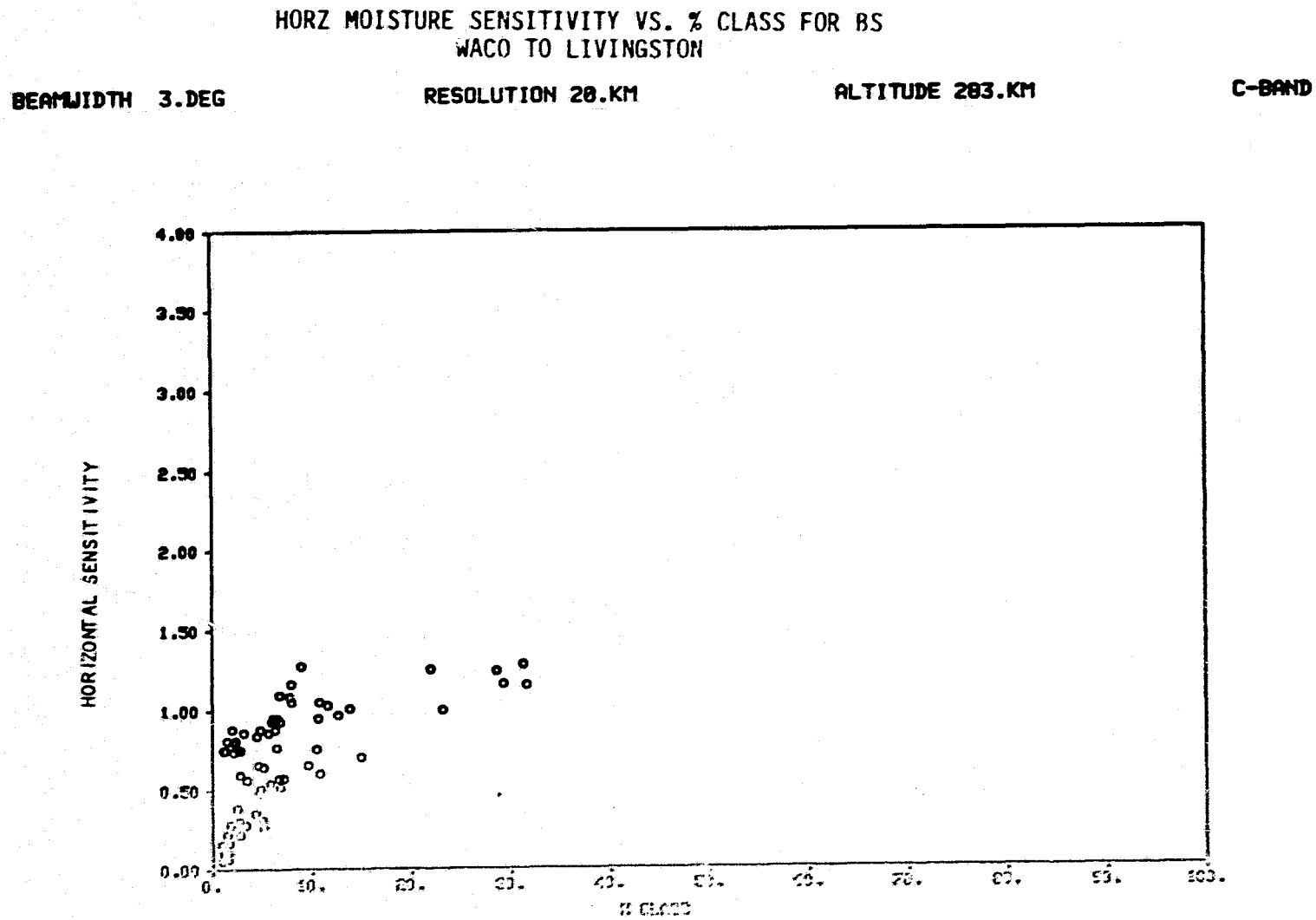

FIGURE 60. Soil moisture sensitivity of the C-band horizontally polarized brightness temperature for the Waco to Livingston ground track at a 20 kilometer resolution plotted as a function of percent bare soil.

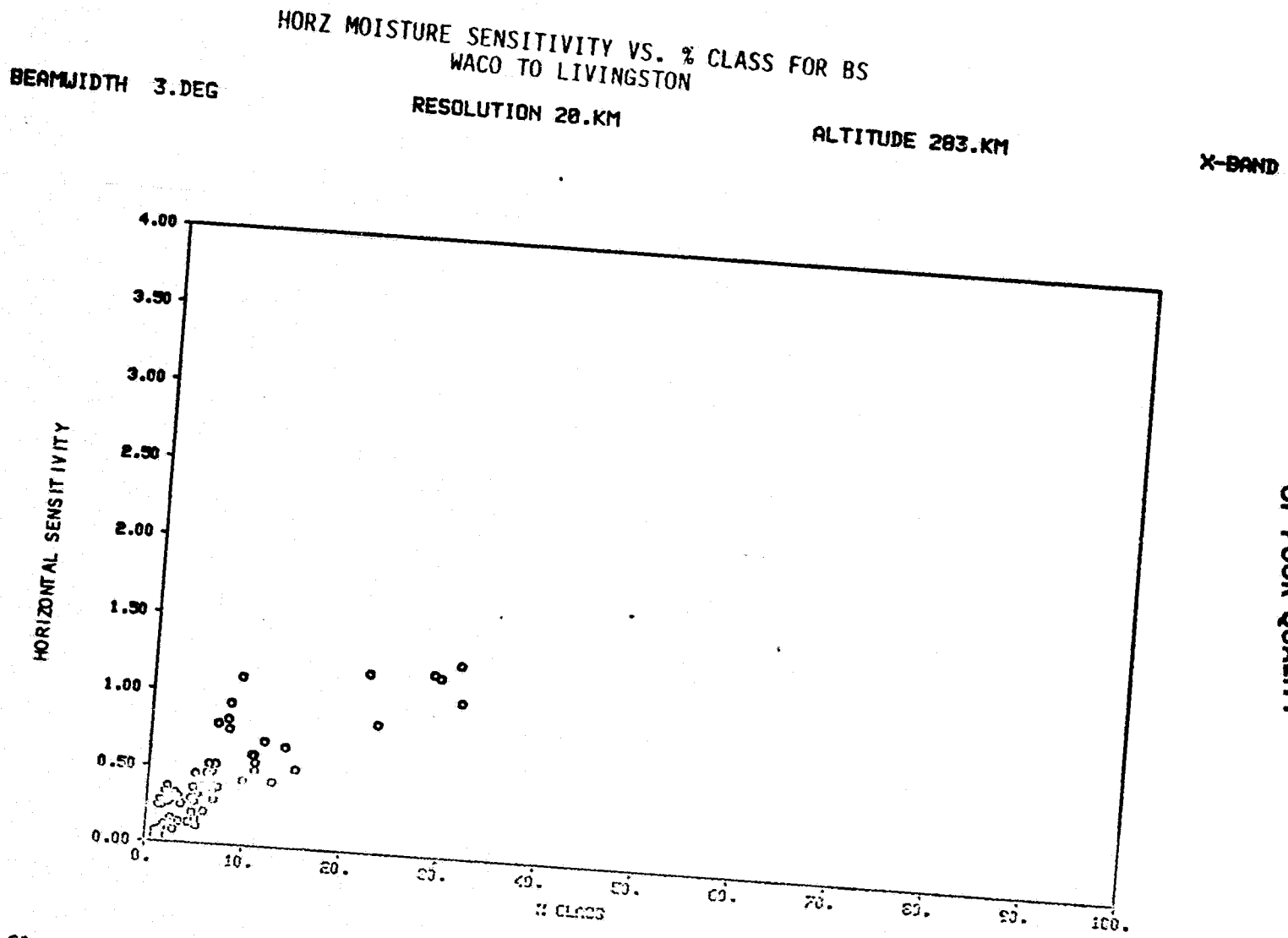

FIGURE 61. Soil moisture sensitivity of the X-band horizontally polarized brightness temperature for the Waco to Livingston ground track at a 20 kilometer resolution plotted as a function of percent bare soil.

ORIGINAL PAGE IS
OF POOR QUALITY

tivity of the brightness temperature to soil moisture as a function of percent class of bare soil for the 20 kilometer resolution along the Waco to Livingston ground track computed at horizontal polarization for L-band, C-band, and X-band respectively. It can seen that there is considerable scatter in the sensitivity up to approximately 20% bare soil. Above approximately 20% bare soil the sensitivity at L-band is approximately 1.75°K for percent soil moisture. Again it can be noted that the scatter in the sensitivity below 20% bare soil is due to a very high percentage of forest and fully vegetated in the ground resolution elements (individual antenna footprints). This can be verified from Figures 23 and 24. In Figure 23 it can be seen that only between the range of 325 kilometers and 375 kilometers does the bare soil go above approximately 20% of the antenna footprint. Also in Figure 23 it can be seen that above a range of approximately 375 kilometers the majority of the footprint is forest and in Figure 24 below a range of approximatey 325 kilometer the majority of the footprint is fully vegetated. The same plot for C-band is shown in Figure 60. The same effects are seen to exist, however, the sensitivity of the brightness temperature to soil moisture above approximately 20% bare soil only reaches approximately 1.25°K/percent soil moisture. This is due to the stronger effect of the vegetation at C-band than at L-band. Figure 61 shows the same information for X-band. Again, the same effects are seen to exist, but effects of other classes besides bare soil are obviously more severe. There is more scatter in the sensitivity computations than for L-band and C-band above 20% bare soil. The average sensitivity at 30% bare soil is approximately 1.1°K/percent soil moisture.

Figures 59 through 61 demonstrated the effect of microwave frequency on the sensitivities to soil moisture using the bare soil class as an example. Figure 62 through 64 will be used to demonstrate the effect of the classes on the sensitivity to bare soil using L-band horizontal polarization, 20 kilometer footprint size and the Waco to Livingston ground track. Figure 62 shows the sensitivity plotted as the function of percent class for L-band and the mixed vegetation class. By comparing this figure to Figure 59 it can be seen that the results are nearly identical to bare soil except that the percentage of the mixed vegetation class within the footprint goes up to nearly 40% while the percentage of bare soil only went slightly above 30%. In addition, the sensitivity climbs to approximately 2°K/percent soil moisture. This sensitivity is fairly large since the 40% mixed vegetation class occurs between the ranges of 125 kilometers to 140 kilometers and a 150 kilometers to 175 kilometers as seen in Figures 23 and 24. In these range intervals the percentage of forest is somewhere between 20% and 25%.

Figure 63 shows the same information except for the fully vegetated class. The character of this plot looks slightly different than the previous ones in that it appears that the sensitivity linearly climbs as a function of percent class although there is some scatter between 38% and 48% class. This is due to the fact that below 38% class of fully vegetated soil the primary other component of the ground resolution footprint is forest as can be seen from Figure 23 and 24. This occurs at a range of above 350 kilometers where the percent of forest ranges anywhere from 50 to 90%. The scatter in Figure 63 toward higher sensitivities between 38% class and 48% class

ORIGINAL PAGE IS
OF POOR QUALITY

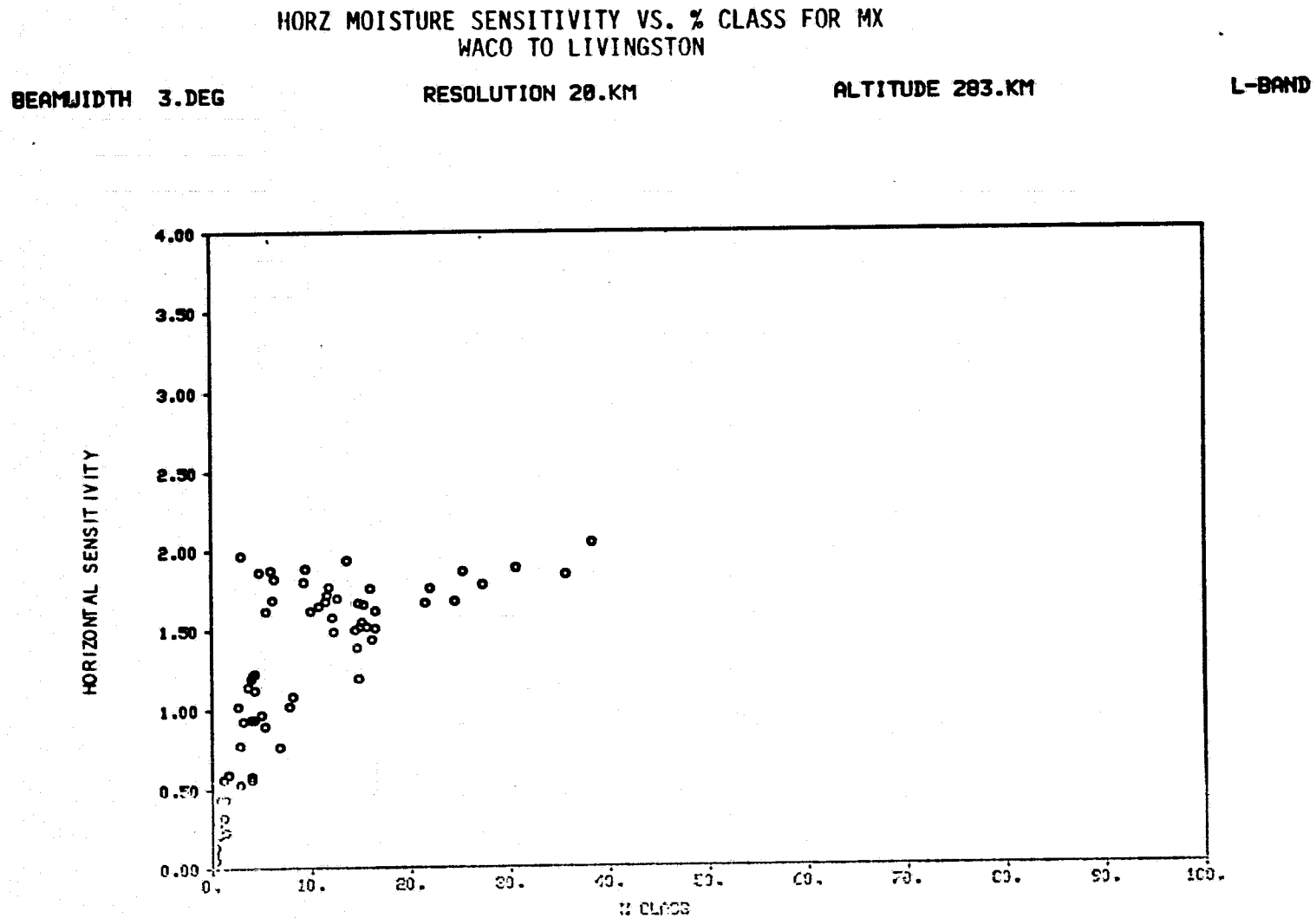

FIGURE 62. Soil moisture sensitivity of the L-band horizontally polarized brightness temperature for the Waco to Livingston ground track at a 20 kilometer resolution plotted as a function of percent mixed bare and vegetated class.

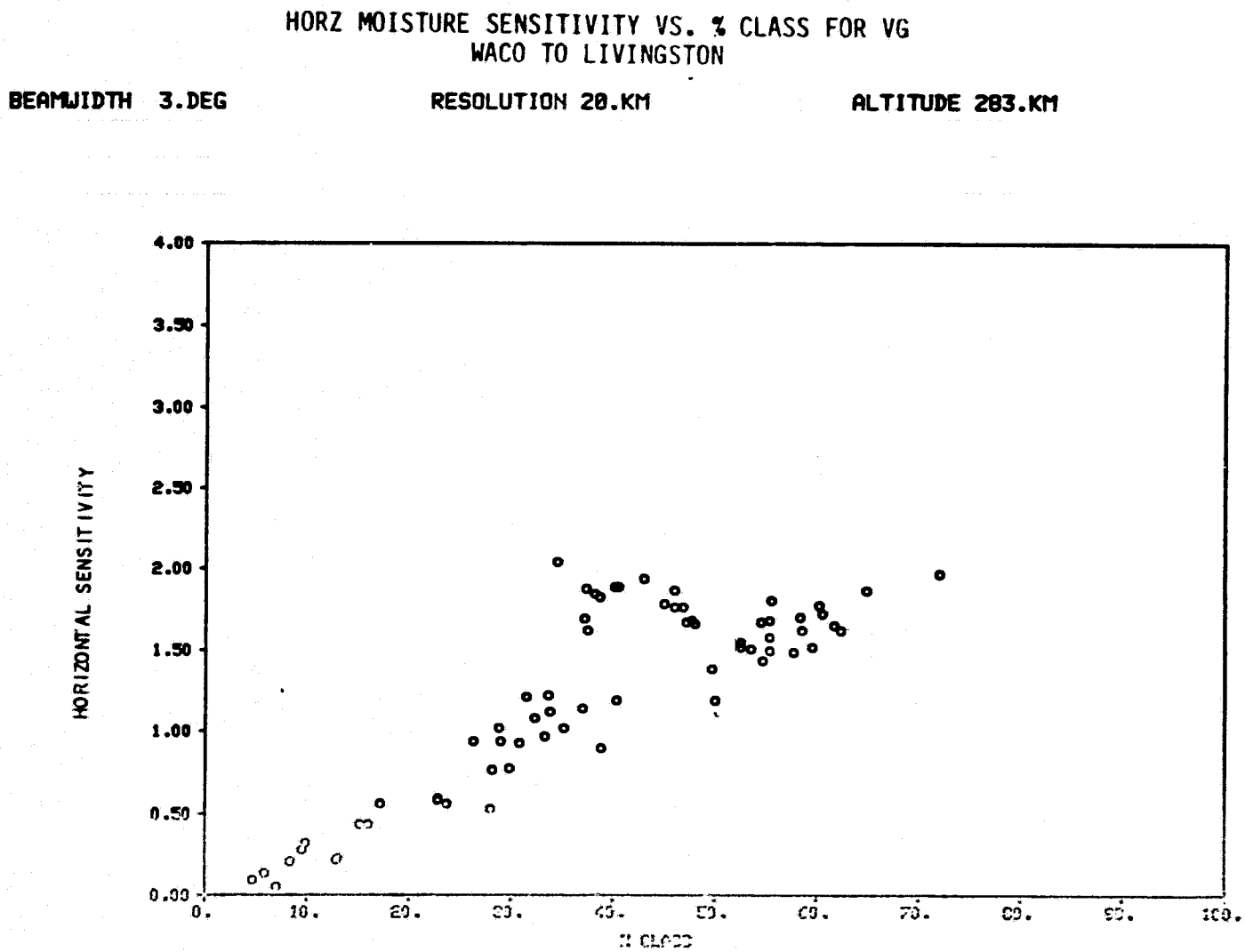

FIGURE 63. Soil moisture sensitivity of the L-band horizontally polarized brightness temperature for the Waco to Livingston ground track at a 20 kilometer resolution plotted as a function of percent fully vegetated class.

ORIGINAL PAGE IS
OF POOR QUALITY

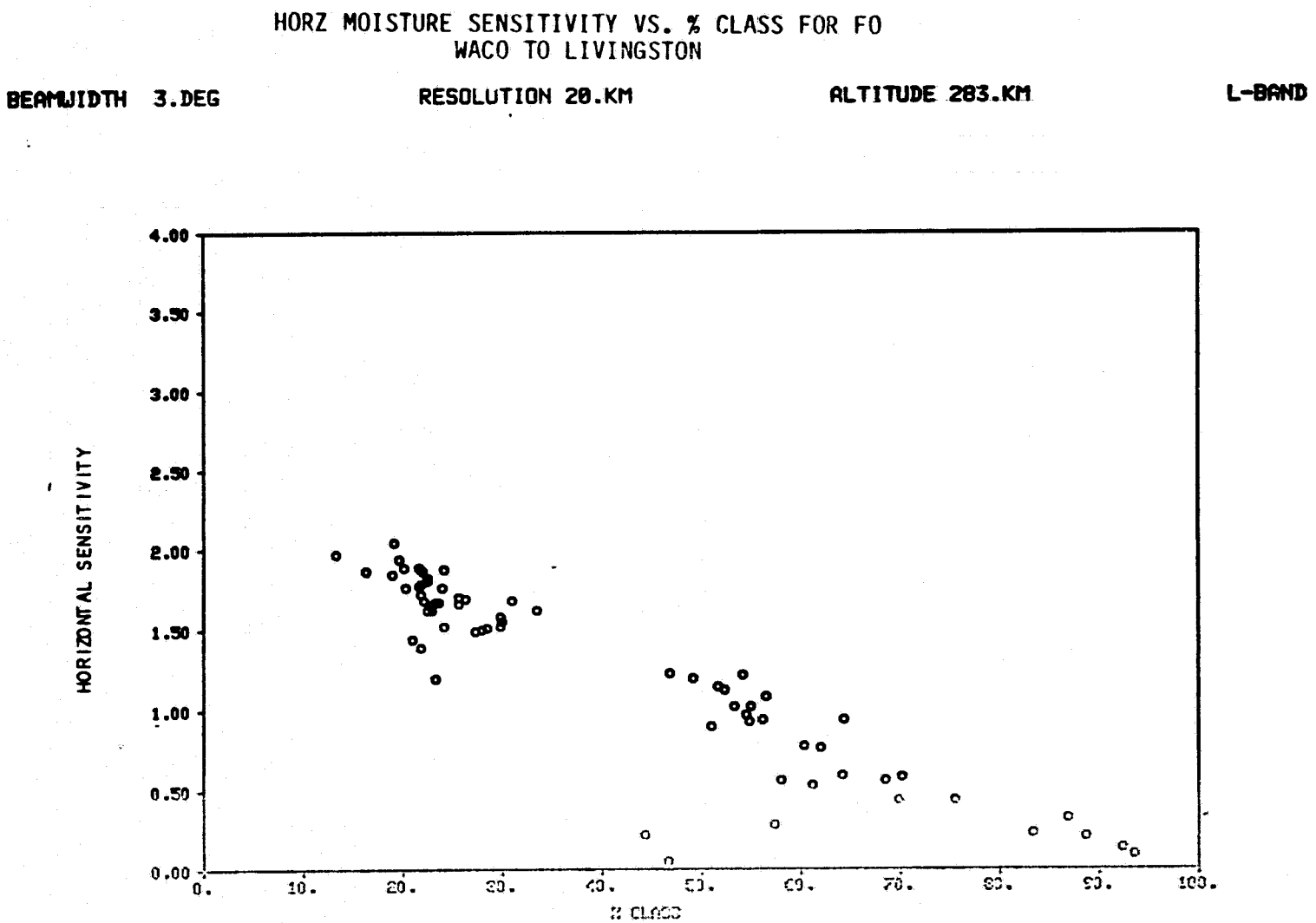

FIGURE 64. Soil moisture sensitivity of the L-band horizontally polarized brightness temperature for the Waco to Livingston ground track at a 20 kilometer resolution plotted as a function of percent forest class.

ORIGINAL PAGE IS
OF POOR QUALITY

occurs due to the significant percentage of bare soil within those resolution footprints. The 38% to 48% of fully vegetated soil occurs between the ranges of approximately 300 to 350 kilometers where the bare soil approaches its maximum. At any rate, it can be seen that since the sensitivity above 50% of the fully vegetated class is greater than 1.5°K percent soil moisture, the fully vegetated class is not the controlling effect on the sensitivity of brightness temperature to soil moisture at least for L-band.

Figure 64 shows the same information for the forest class. In the models used to compute the brightness temperature for each class, it was assumed that the forest class had no sensitivity to soil moisture. As a result Figure 64 is an expected result. As the percent of forest increases the sensitivity to soil moisture linearly decreases from approximately 2°K/percent soil moisture at 15% of the forest class to zero at 100% of the forest class. There were so few resolution elements with a significant percentage of urban or water class that it was pointless to attempt to make similar plots for those classes. The general conclusion that can be drawn from Figures 59 through 64 is that the forest class is probably the controlling effect on the sensitivity of the brightness temperture to soil moisture.

Figures 59 through 64 were used to show the sensitivity of the brightness temperature to soil moisture as a function of the percentages of each scene constituent within an antenna footprint. It is also instructive to compare the sensitivity of the brightness temperature to soil moisture for all ground resolution elements without regard to the constituency of the scene within each antenna footprint as a function of frequency and resolution. Figure 65 is a

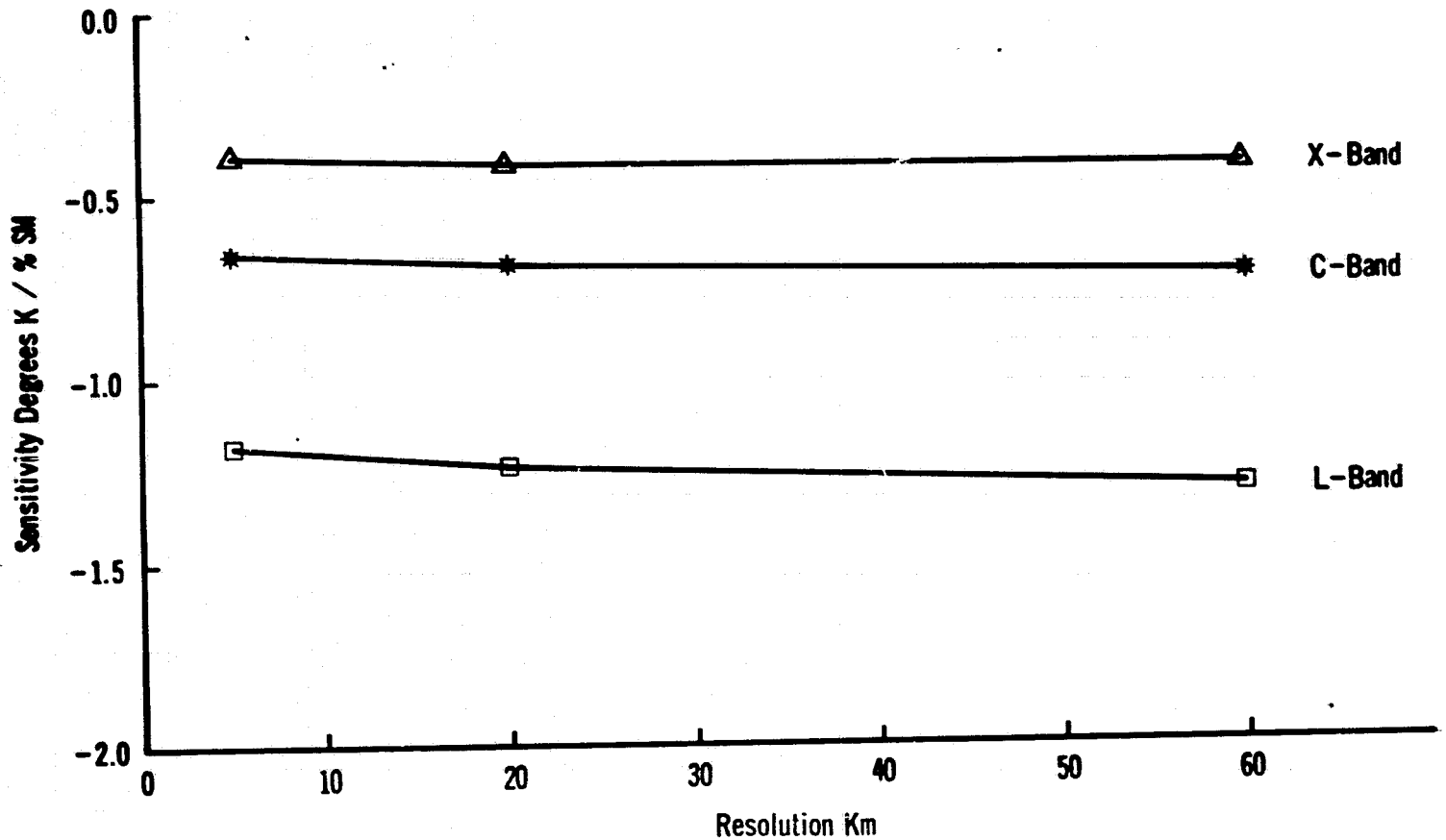

FIGURE 65. Average soil moisture sensitivity plotted as a function of frequency and resolution without regard to class constituency within the antenna footprints.

ORIGINAL PAGE IS
OF POOR QUALITY

plot of the sensitivity of the horizontally polarized brightness temperature to soil moisture as a function of resolution and frequency without regard to the class make up of the scene.

Since it was previously shown that the forest class is the controlling effect on the sensitivity of the brightness temperature to soil moisture, there is obviously significant effects of the high percentages of forest with the simulated scene on the average sensitivity to soil moisture presented in Figure 65. In an operational satellite system put up for the purpose of estimating soil moisture using a microwave radiometer, the location of each antenna footprint should be known. It would not be difficult to map the areas of significant forest cover such that footprints containing percentages of forest cover over a certain threshold are neglected.

The improvement in sensitivity to soil moisture when it is possible to partition ground resolution elements by the percentage of forest within each element is investigated in Figures 66 and 67. In order to obtain enough points to be statistically significant, both the Waco to Livingston and Houston ground tracks were used to compute the numbers shown in Figures 66 and 67. Figure 66 shows a plot of sensitivity in °K per percent soil moisture plotted as a function of resolution and frequency. The sensitivity plotted in Figure 66 is an average computed only for antenna footprints containing less than 40% forest cover. In addition, 95% confidence intervals for these average

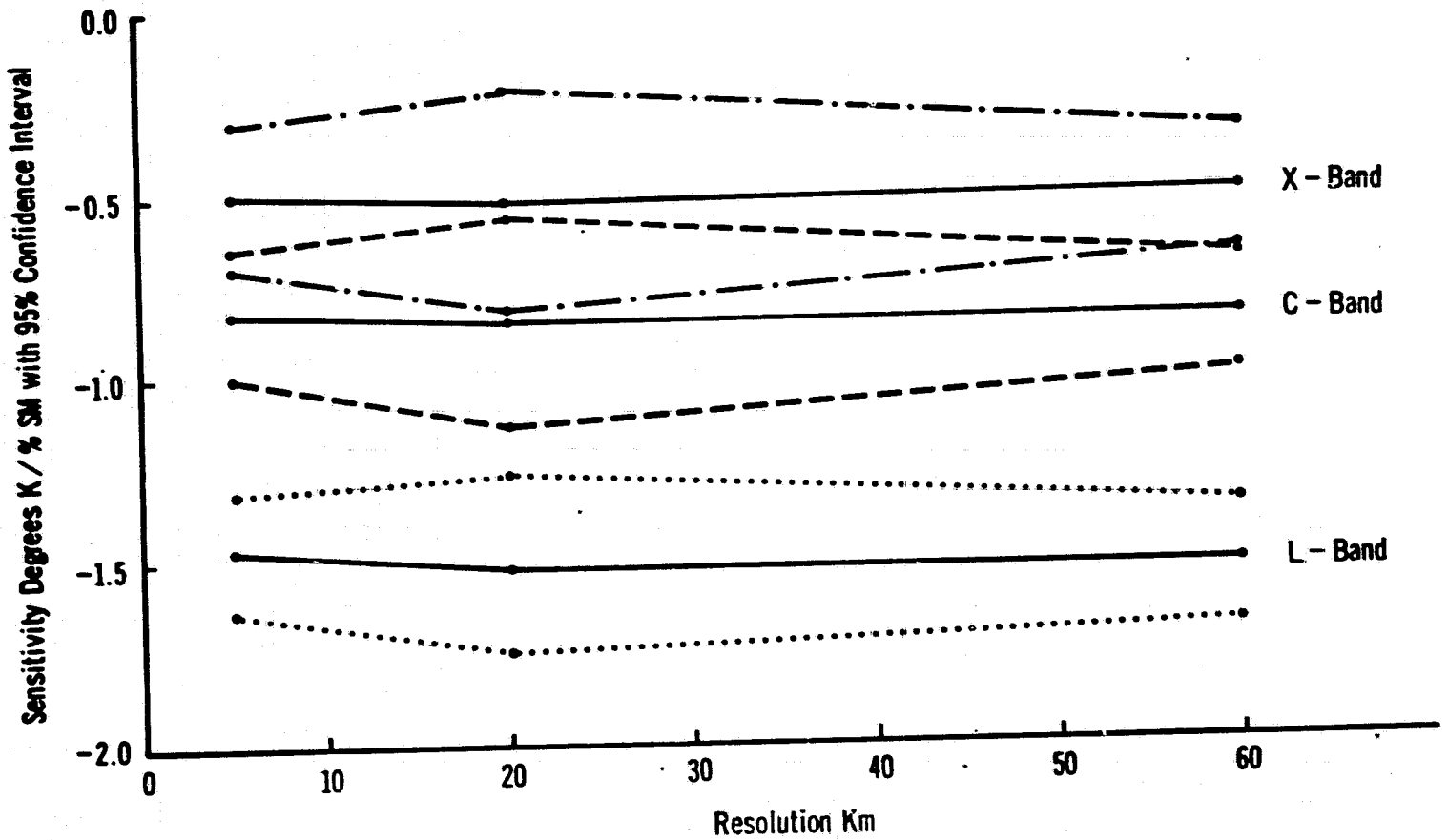

FIGURE 66. Soil moisture sensitivity plotted as a function of resolution and frequency for antenna footprints containing less than 40% forest class with the 95% confidence intervals indicated.

ORIGINAL PAGE IS
OF POOR QUALITY

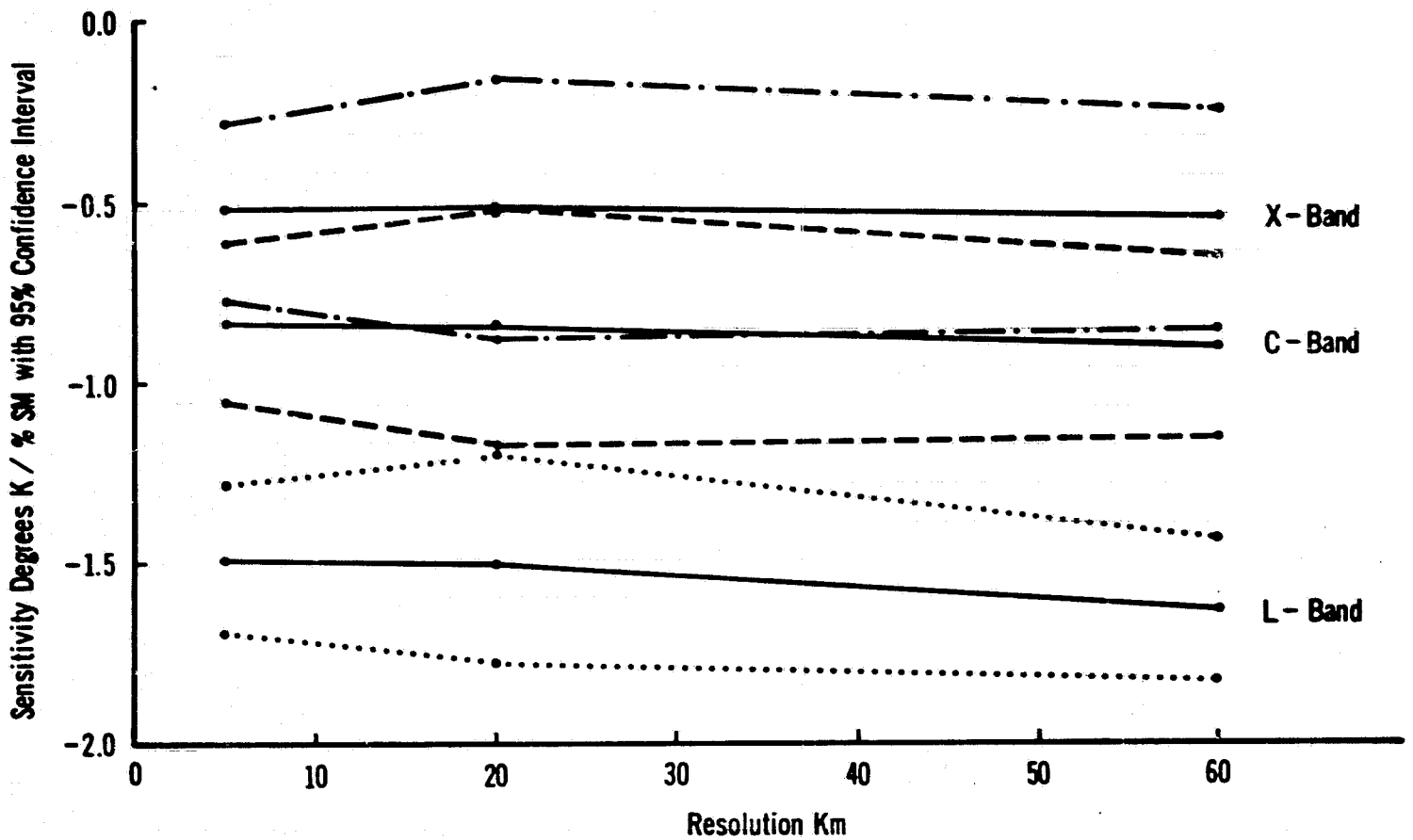

FIGURE 67. Soil moisture sensitivity plotted as a function of resolution and frequency for antenna footprints containing less than 30% forest class with the 95% confidence intervals indicated.

ORIGINAL PAGE IS
OF POOR QUALITY

sensitivities are also provided. It can be seen that at L-band the sensitivity is approximately 1.5°K/percent soil moisture for all resolution with a very slight increase as the resolution increases. At C-band the sensitivity is approximately 0.8°K/percent soil moisture and at X-band approximately 0.5°K/percent soil moisture. Figure 68 provides the same information except at the sensitivities plotted in figure 68 were computed only for antenna footprints containing less than 30 percent forest cover. A major effect is that the sensitivity at L-band increases from approximately 1.5°K/percent soil moisture to 1.64°K/percent soil moisture from the 5 kilometer resolution to the 60 kilometer reslution. Similar effects occur at C-band and X-band but to a lesser degree. In both Figure 66 and 67 the tremendous sensitivity reduction at C-band and X-band relative to L-band is due to the effects of vegetation. Another very important fact to notice is that the confidence interval computed for the average sensitivity is the largest at the 20 kilometer resolution. For all frequencies the confidence intervals are comparable at the 5 kilometer and 60 kilometer resolutions. There were not enough data points for antenna footprints containing only 10% and 20% forest cover to provide similar plots based on these partitioning percentages.

CONCLUSIONS

A simulation model of an orbiting microwave radiometer has been implemented and demonstrated. A realistic scene was also constructed over which the radiometer could be arbitrarily flown in a line scan or side to side scanning mode. The ground scene is based on classified Landsat images and thereby provides realistic ground classes as well

as geometries. It was shown that the realism of the scene make up in both ground cover class and geometry is critical to the accuracy of the simulation results. The model is capable of computing brightness temperatures for L-band, C-band and X-band frequencies as a function of orbit and antenna characteristics.

An analysis of the effects of scene heterogeneity and antenna resolution on the sensitivity to soil moisture was performed. It was assumed in executing this analysis that the soil moisture was uniform over the entire scene (i.e. no precipitation patterns were overlaid on the scene) such that effects of the different scene components on the sensitivity to soil moisture could be investigated. A sensitivity to soil moisture as a function of the percentage of each ground cover class was shown. It was demonstrated that the forest cover class was the limiting factor on the sensitivity of brightness temperature to soil moisture. The average sensitivity to soil moisture as a function of frequency and resolution without regard to ground cover classes was also shown. In addition, since the forest cover class was the limiting factor on sensitivity to soil moisture, average sensitivities for each frequency and resolution were computed based on partitioning out antenna footprints containing greater than 40% of the forest cover class. It was shown under this condition that the L-band frequency could achieve a resolution of 1.5°K/percent soil moisture, C-band a sensitivity of 0.8°K/percent soil moisture and X-band a sensitivity of 0.5°K/percent soil moisture. The significant reduction as frequency increases is due to the effects of vegetation. It should be pointed out that the scene was made up primarily of the fully vegetated and forest cover classes. The largest percentage of the bare soil class

was in the range of 30% to 35% for only approximately 10% of the ground track simulated.

Another important result was that the effect of increasing resolution size (antenna footprint size) is to provide a data averaging effect. However, it was seen that increasing resolution did improve the average sensitivity. This is most likely due to the manner in which the larger antenna footprint size averages the forest and fully vegetated classes. In addition, it was seen that the confidence interval on the average sensitivity computation was the largest for the 20 kilometer footprint and smallest for the 5 kilometer and 60 kilometer footprints, which were approximately the same.

This model is a very useful tool for a very wide ranging set of investigations. Although atmospheric effects were not considered in this study, the model is well suited for including an atmospheric model. In addition, the model would be well suited for quantitatively testing soil moisture estimation algorithms derived from other studies. It can also be used to develop test efficient soil moisture estimators based on the Kalmen filtering approach.

REFERENCES

[1] Blinn, J. C. and J. G. Quade, "Microwave properties of geological materials: Studies of penetration depth and moisture effects," 4th Annual Earth Resource Program Review, NASA Johnson Space Center, Houston, Texas, January 17-21, 1972.

[2] Newton, R. W., S. L. Lee, J. W. Rouse, and J. F. Paris, "On the feasibility of remote monitoring of soil moisture with microwave sensors," 9th International Symposium on Remote Sensing of Environment, University of Michigan, Ann Arbor, Mich., April 1974.

[3] Newton, R. W. and E. A. Tesch, "Joint Soil Moisture Experiment: Ground-based measurements at Texas A&M University, July 13-25, 1975," Technical Report RSC-71, Remote Sensing Center, Texas A&M University, College Station, Texas, 1976.

[4] Newton, R. W., "Microwave remote sensing and its application to soil moisture detection," Technical Report RSC-81, Remote Sensing Center, Texas A&M University, College Station, Texas, 1976.

[5] Poe, G. and A. T. Edgerton, "Determination of soil moisture content using microwave radiometry," Final Report, 1684FR-1 DOC contract 0-35239, Aerojet General Corp., El Monte, California, 1971.

[6] Schmugge, T. J., P. Gloersen, T. Wilheit, and F. Geiger, "Remote sensing of soil moisture with microwave radiometers," Journal of Geophysical Research, vol. 79, pp. 317-323, 1974.

[7] Schmugge, T. J., T. Wilheit, W. Webster, and P. Gloersen, "Remote sensing of soil moisture with microwave radiometers II," NASA Technical Note TN D-8321, 1976.

[8] Eagleman, J. R., and W. C. Lin, "Remote Sensing of Soil Moisture by a 21 cm Passive Radiometer," Journal of Geophysical Research, vol. 81, pp. 3660-3666, 1976.

[9] McFarland, M. J. and B. J. Blanchard, "Temporal correlation of antecedent precipitation with Nimbus 5 ESMR brightness temperatures," 2nd Hydrometeorology Conference, Toronto, Canada, October 1977.

[10] McFarland, M. J., "The correlation of Skylab L-band brightness temperatures with antecedent precipitation," Proceedings of the Conference on Hydrometeorology, Fort Worth, Texas, April 1976.

[11] Choudhury, B. J., T. J. Schmugge, R. W. Newton, and A. Chang, "Effect of Surface roughness on the microwave emission from soils," Tech Memo 79606, NASA Goddard Space Flight Center, Greenbelt, Md, 1978.

[12] Paris, J. F., "Transfer of thermal microwaves in the atmosphere," Ph.D. dissertation, Dept. Meteorology, Texas A&M University, College Station, Texas, 1971.

[13] Straiton, A. W. and C. W. Tolbert, "Factors affecting earth-satellite millimeter wavelength communications," IEEE Proc. Microwave Theory Tech., MTT-11, pp. 296-301, 1963.

[14] _____, _____, and Britt, "Apparent temperatures of some terrestial materials and the sun at 4.3 millimeter wavelengths," J. Appl. Phys., vol. 29, pp. 776-782, 1958.

[15] Porter, R. A., "An analytical study of measured radiometer data," prepared under Contract 952397 for Jet Propulsion Laboratory, Accession No. N70-20193, December 12, 1969.

APPENDIX A

TEXAS PARKS & WILDLIFE MAPTAP VALUES

VS

TAMU CLASS ASSIGNMENTS

A limited number of vegetation type maps were produced in color. Additional information contained on the maps may be obtained by contacting the authors of this report.

Vegetation Type Map

Corsicana, TX

ORIGINAL PAGE IS
OF POOR QUALITY

Legend Nomenclature and Color Assignments for Respective Values on MAPTAP 0062

MAPTAP Value	Legend Nomenclature	TAMU CLASS
0	Unclassified	
1	Grasses	5
2	Grasses	5
3	Grasses	5
4	Post Oak-Black Hickory Forest	6
5	Mesquite-Elm Parks	6
6	Post Oak-Black Hickory Forest	6
7	Mesquite Woods	6
8	Pecan-Elm/Water Oak-Elm/Elm-Hackberry Forest	6
9	Pecan-Elm/Water Oak-Elm/Elm-Hackberry Forest	6
10	Pecan-Elm/Water Oak-Elm/Elm-Hackberry Forest	6
11	Pecan-Elm/Water Oak-Elm/Elm-Hackberry Forest	6
12	Loblolly Pine-Sweetgum Forest	6
13	Post Oak-Black Hickory Forest	6
14	Post Oak-Black Hickory Forest	6
15	Post Oak-Black Hickory Forest	6
16	Loblolly Pine-Sweetgum Forest	6
17	Water	1
18	Water	1
19	Water	1
20	Water	1
21	Crops	4

MAPTAP Value	Legend Nomenclature	TAMU CLASS
22	Crops	4
23	Crops	4
24	Crops	4
25	Crops	4
26	Crops	4
27	Crops	4
28	Crops	4
29	Sparsely Vegetated/Urban	2
30	Sparsely Vegetated/Urban	2
31	Sparsely Vegetated/Urban	2
32	Sparsely Vegetated/Urban	2
33	Sparsely Vegetated/Urban	2
34	Sparsely Vegetated/Urban	2
35	Sparsely Vegetated/Urban	2
36	Sparsely Vegetated/Urban	2
126	Latitude-Longitude Tick Marks	
127	Background	

Vegetation Type Map
Kerrville, TX

ORIGINAL PAGE IS
OF POOR QUALITY

Legend Nomenclature and Color Assignments for Respective Values on MAPTAP 0068

MAPTAP Value	Legend Nomenclature	TAMU CLASS
0	Unclassified	-
1	Grasses	5
2	Grasses	5
3	Grasses	5
4	Live Oak-Ashe Juniper/Live Oak-Mesquite Parks (Sparse)	5
5	Sparsely Vegetated/Urban	2
6	Live Oak-Mesquite Park (Sparse)	5
7	Live Oak-Ashe Juniper/Live Oak-Mesquite Parks (Sparse)	5
8	Live Oak-Ashe Juniper/Live Oak-Texas Oak/Live Oak-Mesquite Parks (Dense)	6
9	Live Oak-Ashe Juniper/Live Oak-Texas Oak/Live Oak-Mesquite Parks (Dense)	6
10	Live Oak-Ashe Juniper/Live Oak-Texas Oak/Live Oak-Mesquite Parks (Dense)	6
11	Live Oak-Ashe Juniper Woods	6
12	Live Oak-Ashe Juniper Woods	6
13	Live Oak-Ashe Juniper Woods	6
14	Pecan-Elm Forest	6
15	Pecan-Elm Forest	6
16	Live Oak-Ashe Juniper/Live Oak-Texas Oak/Live Oak-Mesquite Parks (Dense)	6
17	Crops	4
18	Crops	4
19	Crops	4

MAPTAP Value	Legend Nomenclature	TAMU CLASS
20	Water	1
21	Sparsely Vegetated/Urban	2
22	Sparsely Vegetated/Urban	2
23	Cloud Cover	-
24	Cloud Cover	-

To be designated by specified colors but not included in the legend

126	Latitude-Longitude Tick Marks	-
127	Background	-

Class Arrangement as Desired on Map Legend
(MAPTAP No. 0059)

NOTE: Class names and color assignment now occur only once on the MAPTAP and follow the Legend.

MAPTAP Value	Legend Nomenclature	TAMU CLASS
1	Grasses	5
2	Oak/Mesquite/Juniper/Mixed Parks (Sparse)	5
3	Oak/Mesquite/Juniper/Mixed Parks (Dense)	6
4	Oak/Mesquite/Juniper/Mixed Woods	6
5	Crops	4
6	Water	1
7	Sparsely Vegetated/Urban/Crops	2,3
8	Unclassified	

To be designated by colors but not included in the Legend.

126	(Latitude-Longitude Tick Marks)
127	(Background)

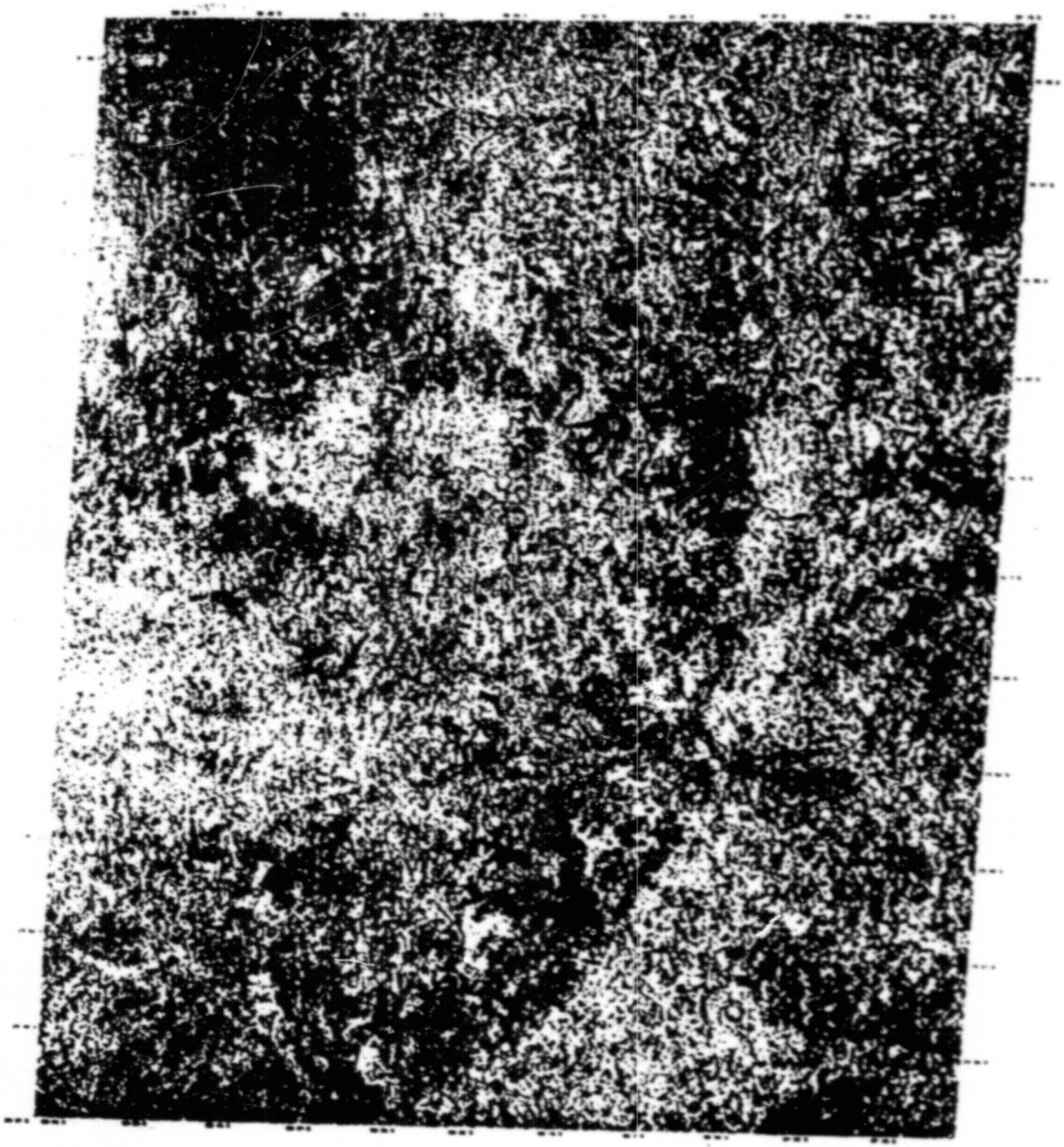

Vegetation Type Map

Austin, TX

ORIGINAL PAGE IS
OF POOR QUALITY

Legend Nomenclature and Color Assignments for Respective Values on MAPTAP 0060

MAPTAP Value	Legend Nomenclature	TAMU CLASS
0	Unclassified	
1	Grasses	5
2	Grasses	5
3	Grasses	5
4	Live Oak-Ashe Juniper/Post Oak-Live Oak Parks (Dense)	6
5	Live Oak-Ashe Juniper/Post Oak-Live Oak Elm-Hackberry Parks (Sparse)/Grasses	5
6	Live Oak-Ashe Juniper/Post Oak-Live Oak/Elm-Hackberry Parks (Sparse)/Grasses	5
7	Live Oak-Mesquite Parks (Sparse)	5
8	Live Oak-Ashe Juniper/Post Oak-Live Oak/Elm-Hackberry Parks (Sparse)/Grasses	5
9	Ashe Juniper Parks (Dense)	6
10	Live Oak-Ashe Juniper/Post Oak-Live Oak/Elm-Hackberry Parks (Sparse)/Grasses	4
11	Live Oak-Ashe Juniper/Post Oak-Live Oak/Elm-Hackberry Parks (Sparse)/Grasses	4
12	Live Oak-Ashe Juniper Woods	6
13	Post Oak-Blackjack Oak/Elm-Hackberry Woods	6
14	Pecan-Elm/Live Oak Forest	6
15	Crops	4
16	Crops	4
17	Crops	4
18	Crops	4
19	Sparsely Vegetated/Urban	2

MAPTAP Value	Legend Nomenclature	TAMU CLASS
20	Crops	4
21	Crops	4
22	Live Oak-Ashe Juniper Woods	6
23	Cloud Cover	0
24	Cloud Cover	0
25	Water	1
26	Water	1
27	Water	1
28	Sparsely Vegetated/Urban	2
29	Sparsely Vegetated/Urban	2
30	Sparsely Vegetated/Urban	2
31	Sparsely Vegetated/Urban	2
32	Sparsely Vegetated/Urban	2
33	Post Oak-Eastern Redcedar Woods	6
34	Post Oak-Eastern Redcedar Parks (Dense)	6

To be designated by specified colors but not included in legend.

126 Latitude-Longitude Tick Marks

127 Background

Class Arrangement as Desired on
Map Legend (MAPTAP No. 0086)

NOTE: Class names and color assignnment now occur only once on the MAPTAP and follow the Legend.

MAPTAP Value	Legend Nomenclature	TAMU CLASS
1	Grasses	5
2	Oak/Mesquite/Juniper/Mixed Parks (Sparse)/ Grasses	5
3	Oak/Mesquite/Juniper/Mixed Parks (Dense)	6
4	Oak/Mesquite/Juniper/Mixed Woods	6
5	Pecan-Elm/Live Oak Forest	6
6	Crops	4
7	Water	1
8	Sparsely Vegetated/Urban	2,3
9	Cloud Cover	
10	Unclassified	

To be designated by colors but not included in the Legend.

126 (Latitude-Longitude Tick Marks)

127 (Background)

ORIGINAL PAGE IS
OF POOR QUALITY

Vegetation Type Map
Lufkin,TX

Legend Nomenclature and Color Assignments for Respective Values on MAPTAP 0046

MAPTAP Value	Legend Nomenclature	TAMU CLASS
0	Unclassified	0
1	Grasses	5
2	Grasses	5
3	Water Oak-Elm Forest	6
4	Shortleaf Pine-Post Oak/Loblolly Pine-Sweetgum/Post Oak-Black Hickory Forest	6
5	Shortleaf Pine-Post Oak/Loblolly Pine-Sweetgum/Post Oak-Black Hickory Forest	6
6	Shortleaf Pine-Post Oak/Loblolly Pine-Sweetgum/Post Oak-Black Hickory Forest	6
7	Loblolly Pine-Shortleaf Pine Forest	6
8	Loblolly Pine-Shortleaf Pine Forest	6
9	Loblolly Pine-Slash Pine Young Forest/ Eastern Mixed Hardwood Brush/Woods	6
10	Water	1
11	Sparsely Vegetated/Urban	2,3
12	Crops	4
13	Crops	4
14	Crops	4

To be designated by specified colors but not included in the legend.

126	Latitude-Longitude Tick Marks
127	Background

Vegetation Type Map

Houston, TX

ORIGINAL PAGE IS
OF POOR QUALITY

Legend Nomenclature and Color Assignments for Respective Values on MAPTAP 0031

MAPTAP Value	Legend Nomenclature	
0	Unclassified	0
1	Grasses	5
2	Grasses	5
3	Grasses	5
4	Water Oak-Elm/Pecan-Elm/Willow Oak-Blackgum Forest	6
5	Post Oak-Black Hickory Forest	6
6	Post Oak-Black Hickory Forest	6
7	Loblolly Pine-Sweetgum/Loblolly Pine-Shortleaf Pine Forest	6
8	Loblolly Pine-Sweetgum/Loblolly Pine-Shortleaf Pine Forest	6
9	Loblolly Pine/Sweetgum/Loblolly Pine-Shortleaf Pine Forest	6
10	Water Oak-Elm/Pecan-Elm/Willow Oak-Blackgum Forest	6
11	Loblolly Pine-Sweetgum/Loblolly Pine-Shortleaf Pine Forest	6
12	Water Oak-Elm/Pecan-Elm/Willow Oak-Blackgum Forest	6
13	Loblolly Pine-Slash Pine Young Forest/Eastern Mixed Hardwood Brush/Woods	6
14	Loblolly Pine-Sweetgum/Loblolly Pine-Shortleaf Pine Forest	6
15	Crops	4
16	Crops	4
17	Crops	4

MAPTAP Value	Legend Nomenclature	TAMU CLASS
18	Crops	4
19	Crops	4
20	Crops	4
21	Crops	4
22	Cloud Cover	0
23	Elm-Hackberry Woods/Baccharis Brush	5
24	Elm-Hackberry Woods/Baccharis Brush	5
25	Urban/Sparsely Vegetated	2
26	Urban/Sparsely Vegetated	2
27	Urban/Sparsely Vegetated	2
28	Urban/Sparsely Vegetated	2
29	Urban/Sparsely Vegetated	2
30	Urban/Sparsely Vegetated	2
31	Urban/Sparsely Vegetated	2
32	Urban/Sparsely Vegetated	2
33	Urban/Sparsely Vegetated	2
34	Marsh/Cultivated Wetlands	1
35	Marsh/Cultivated Wetlands	1
36	Loblolly Pine-Sweetgum/Loblolly Pine-Shortleaf Pine Forest	6
37	Water	1
38	Loblolly Pine-Sweetgum/Loblolly Pine-Shortleaf Pine Forest	6
39	Urban/Sparsely Vegetated	2
40	Cloud Cover	0
41	Cloud Cover	0

To be designated by specified colors but not included in the legend.

126	Latitude-Longitude Tick Marks
127	Background

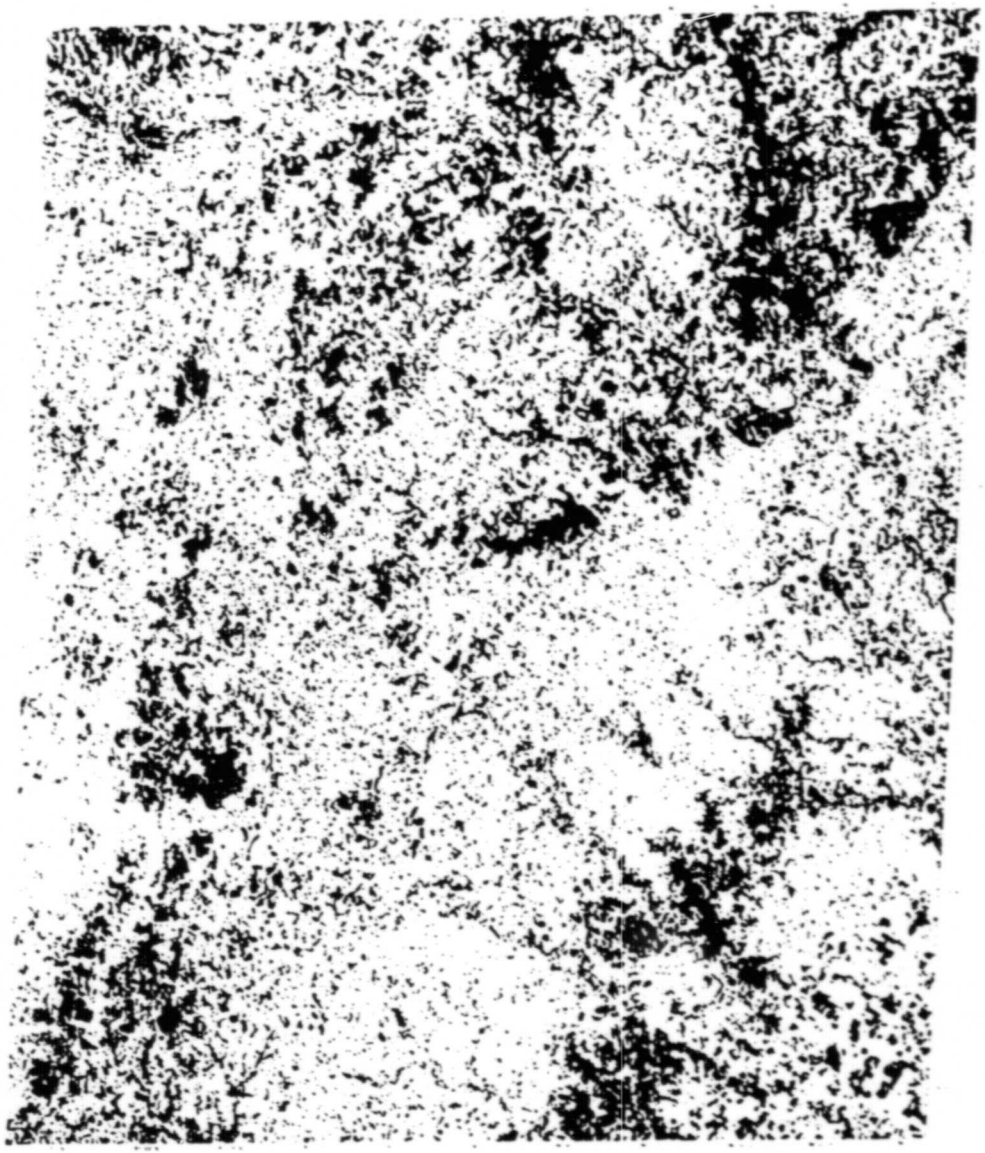

Vegetation Type Map

Bryan, TX

ORIGINAL PAGE IS
OF POOR QUALITY

Legend Nomenclature and Color Assignments for Respective Values on MAPTAP 0067

MAPTAP Value	Legend Nomenclature	TAMU CLASS
0	Unclassified	0
1	Grasses/Elm-Hackberry Parks	5
2	Post Oak-Blackjack Oak/Elm-Hackberry Woods/Forest	6
3	Grasses/Elm-Hackberry Parks	5
4	Grasses/Elm-Hackberry Parks	5
5	Grasses/Elm-Hackberry Parks	5
6	Grasses/Elm-Hackberry Parks	5
7	Post Oak-Blackjack Oak/Elm-Hackberry Woods/Forest	6
8	Sparsely Vegetated/Urban	2
9	Crops	4
10	Post Oak-Blackjack Oak/Elm-Hackberry Woods/Forest	6
11	Water Oak-Elm/Pecan-Elm Forest	6
12	Post Oak-Blackjack Oak/Elm-Hackberry Woods/Forest	6
13	Crops	4
14	Grasses/Elm-Hackberry Parks	5
15	Crops	4
16	Water Oak-Elm/Pecan-Elm Forest	6
17	Loblolly Pine-Pinst Oak Forest	6
18	Crops	4
19	Crops	4

MAPTAP Value	Legend Nomenclature	TAMU CLASS
20	Water Oak-Elm/Pecan-Elm Forest	6
21	Sparsely Vegetated/Urban	2
22	Sparsely Vegetated/Urban	2
23	Sparsely Vegetated/Urban	2
24	Water	1
25	Loblolly Pine-Post Oak Forest	6
26	Water	1
27	Crops	4
28	Loblolly Pine-Post Oak Forest	6
29	Crops	4
30	Crops	4
31	Crops	4
32	Grasses/Elm-Hackberry Parks	5
33	Sparsely Vegetated/Urban	2
34	Sparsely Vegetated/Urban	2
35	Crops	4
36	Crops	4
37	Crops	4
38	Sparsely Vegetated/Urban	2
39	Crops	4

To be designated by specified colors but not included in the legend.

126	Latitude-Longitude Tick Marks
127	Background

APPENDIX B

FULL SCENE GREY-SCALE MAPS BY CLASS

ORIGINAL PAGE IS
OF POOR QUALITY

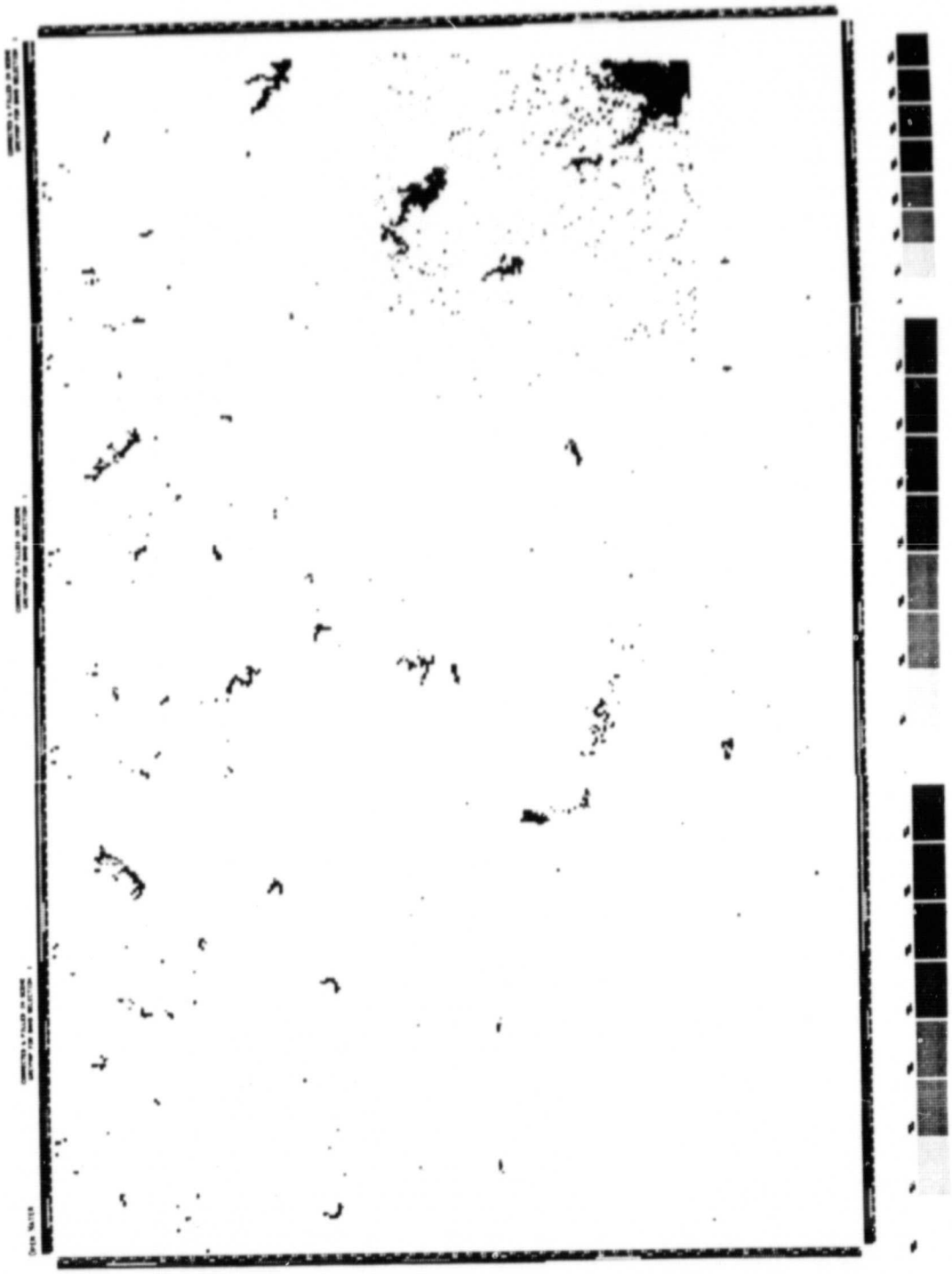

Figure B-1. Image of ground scene high-lighting pixels classified as "open water".

ORIGINAL PAGE IS
OF POOR QUALITY

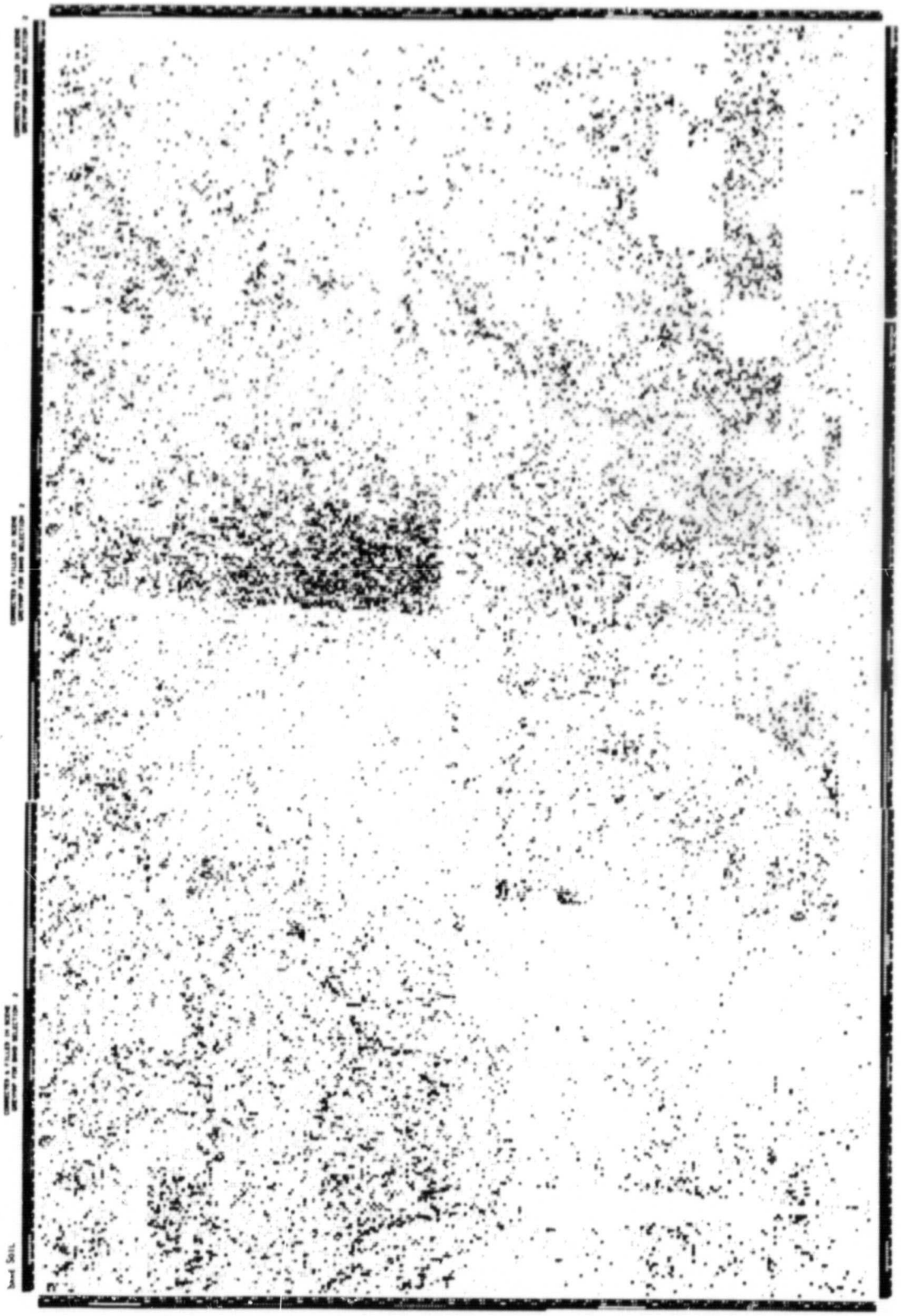

Figure B-2. Ground scene image showing pixels classified as "bare soil".

ORIGINAL PAGE IS
OF POOR QUALITY

Figure B-3. Ground scene grey-map displaying pixels classified as "mixed bare soil and vegetation" areas.

ORIGINAL PAGE IS
OF POOR QUALITY

Figure B-4. Ground scene image of pixels classified as "forested" areas.

ORIGINAL PAGE IS
OF POOR QUALITY

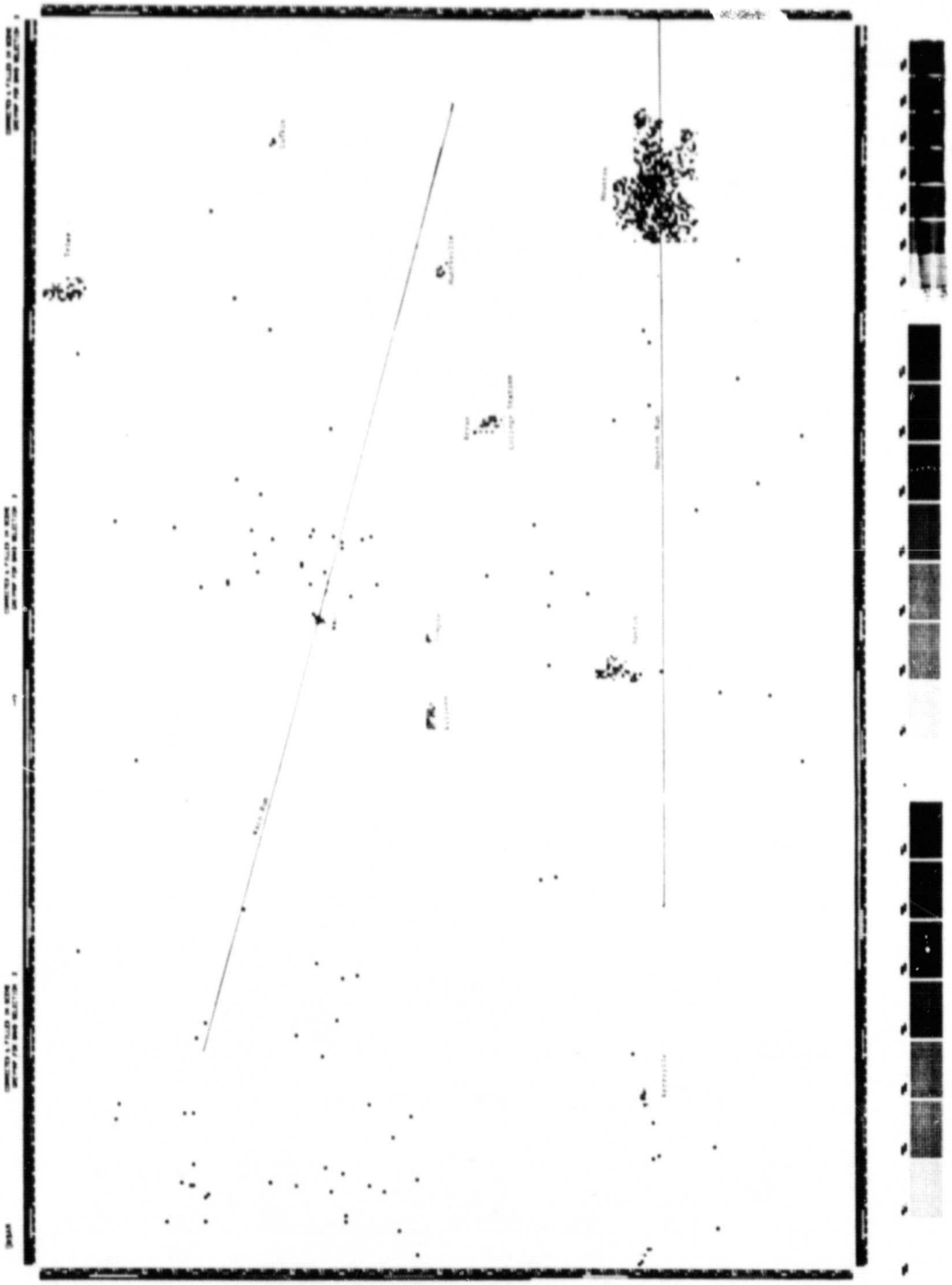

Figure B-5. Full scene pixels classified as "urban" areas; e.g., cities and towns.

**Note: The two lines are the ground-track of the satellite pass for the "run" indicated.

ORIGINAL PAGE IS
OF POOR QUALITY

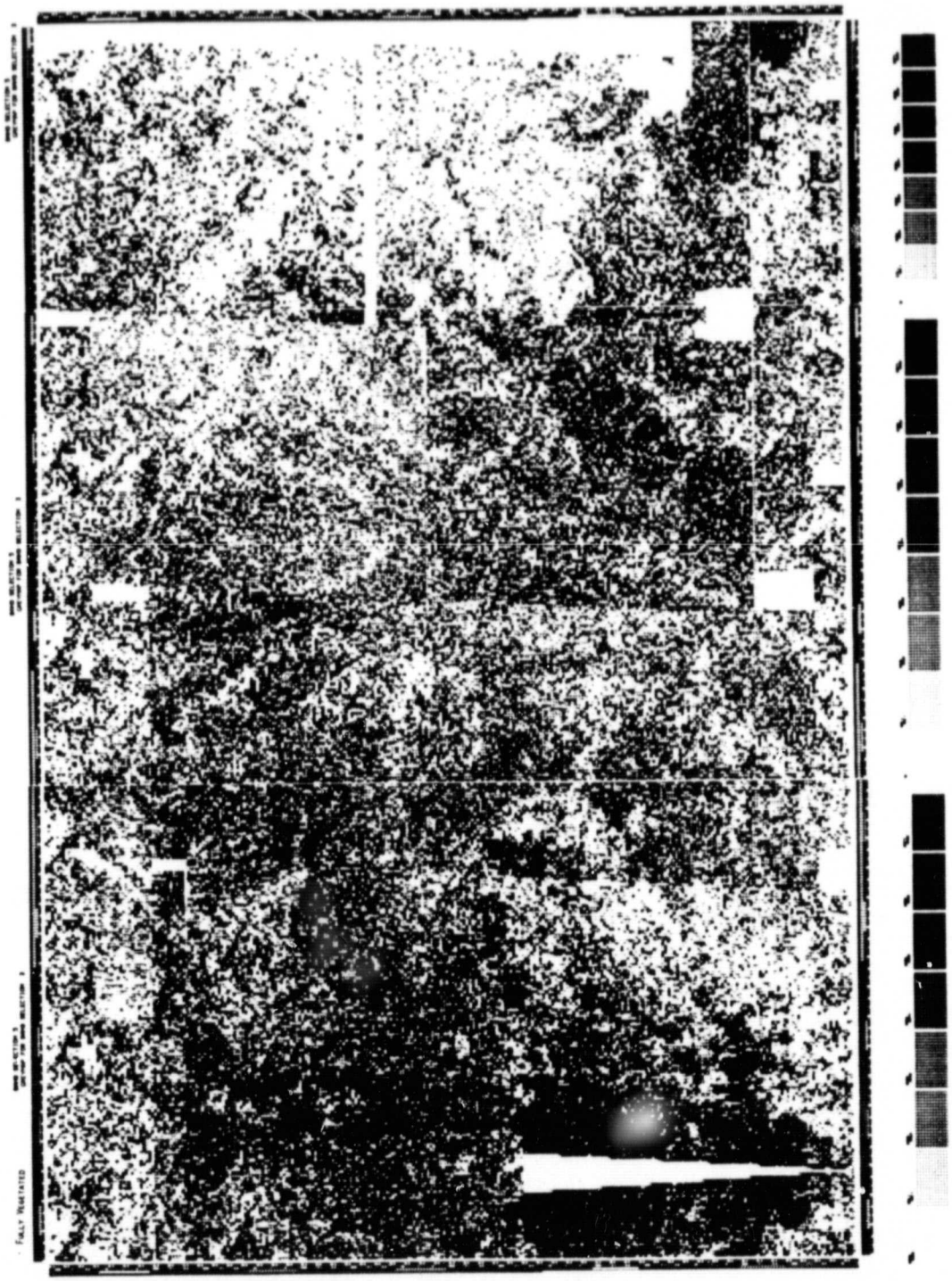

Figure B-6. Grey-scale map of pixels classified as "fully vegetated".

APPENDIX C

COMPUTATION FLOW OF COMPUTER ALGORITHM

ORIGINAL PAGE IS
OF POOR QUALITY

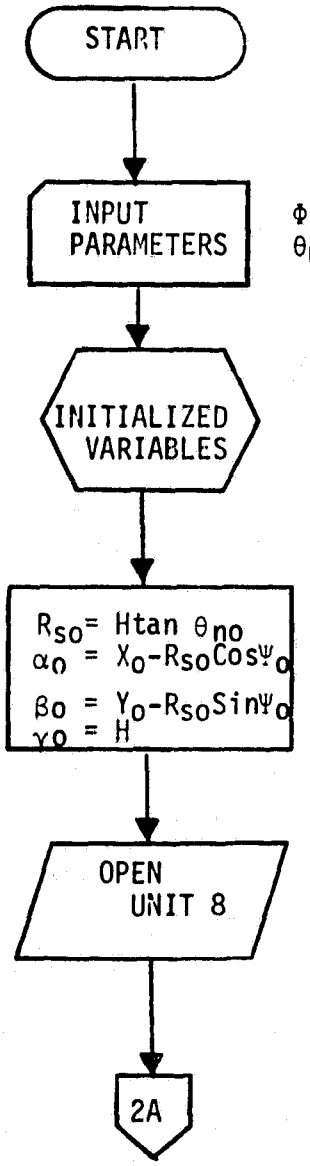

Φ, Θ, B,
θ_{no}, Ψ_o, H, II

$X_o = 825.$, $Y_o = 0.$, $Z_o = 0$
$\Delta X = \Delta Y = 1.$, $\Delta Z = 0.$
$\Delta\alpha = \Delta\gamma = 0.$, $\Delta\beta = 1.$
$\Delta\theta = 1./57.3$, $C = 273.$
$N = 2496$, $M = 1650$,
$S = 0.24$

EVALUATE INITIAL NADIR COORDINATES

KEY

Φ, azimuth, $-90° \leq \Phi \leq 90°$
Θ, roll, $-90° \leq \Theta \leq 90°$
B, beam width, $1° \leq B \leq 30°$
θ_{no}, incidence, $0° \leq \Theta_{no} \leq 50°$
Ψ_o, radial, $0° \leq \Psi_o \leq 359°$
H, altitude, $50 \leq \gamma_o \leq 500$ KM
N, scene length, 2496 units
M, scene width, 1650 units
C, background temp., 273°K
S, scale factor, 0.24 KM/unit
II, nadir step, $1 \leq II \leq 16$

ORIGINAL PAGE IS
OF POOR QUALITY

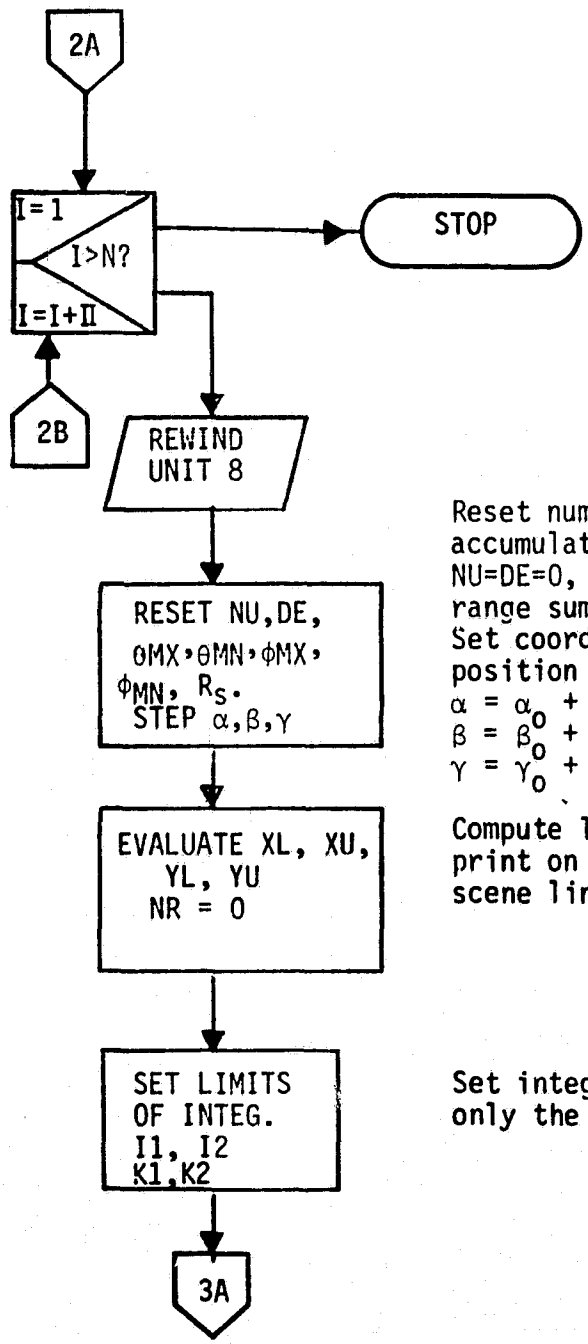

Reset numerator & denominator accumulators
NU=DE=0, Reset max/min angles & range sum
Set coordinates of nadir to next position
$\alpha = \alpha_o + (I-1)\Delta\alpha$
$\beta = \beta_o + (I-1)\Delta\beta$
$\gamma = \gamma_o + (I-1)\Delta\gamma$

Compute limits of antenna foot-print on the ground plane. Reset scene line count.

Set integration limits to cover only the antenna foot-print.

ORIGINAL PAGE IS
OF POOR QUALITY

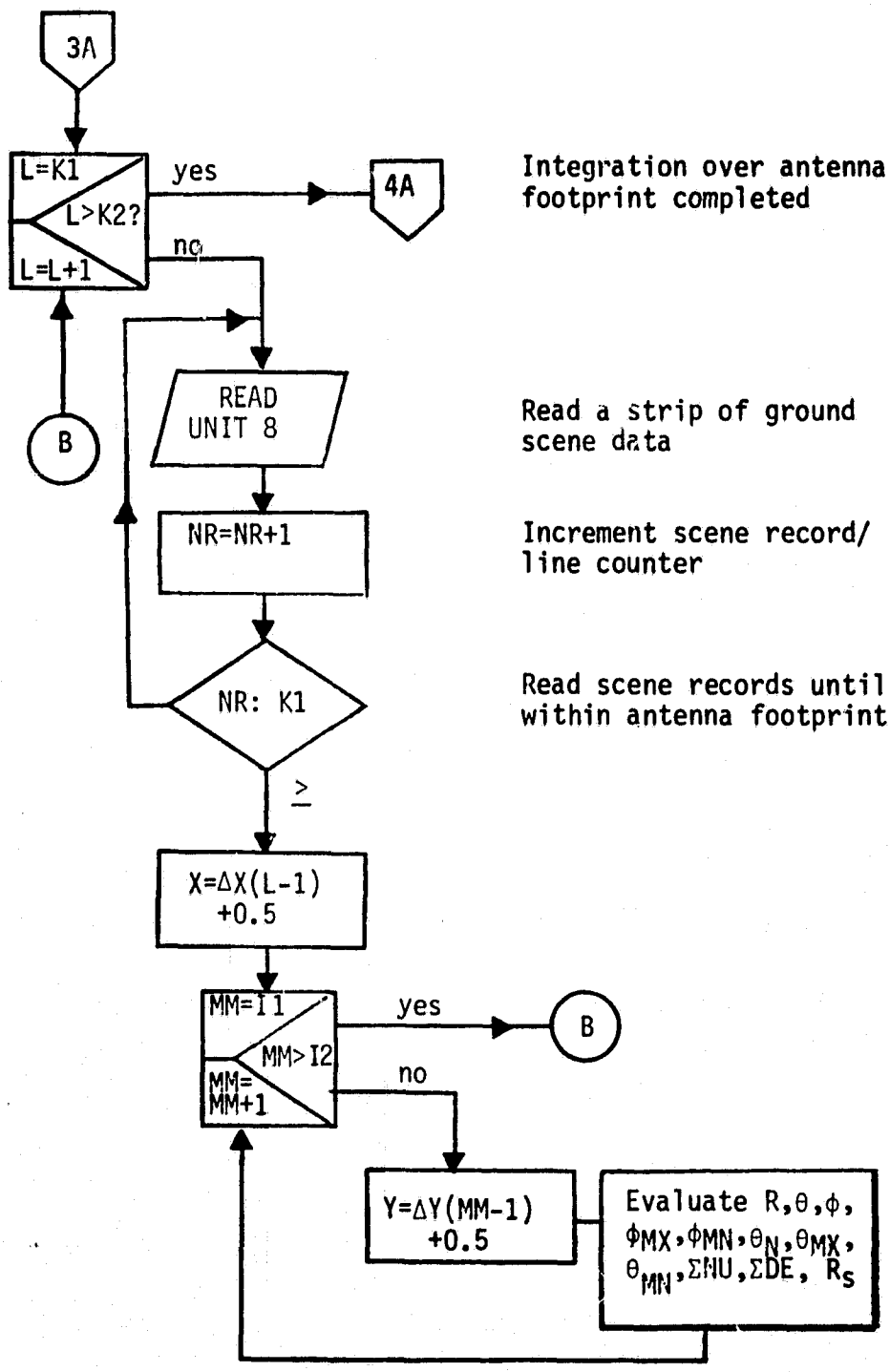

ORIGINAL PAGE IS
OF POOR QUALITY

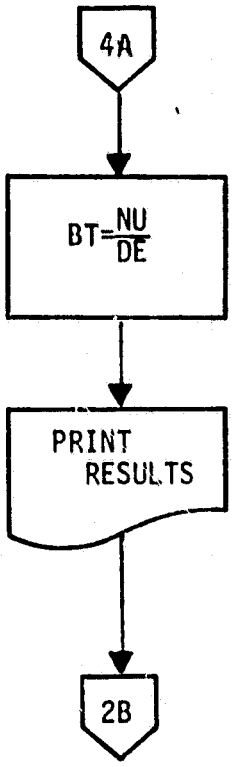

Display BT, R, X, Y, XL, XU, YL, YU
and Satellite Characteristics;
i.e., Φ, Θ, B, θ_{no}, Ψ_o, H, II

APPENDIX D

SOFTWARE LISTINGS

ORIGINAL PAGE IS
OF POOR QUALITY

```
C   >>>> STEP - 1 PROGRAM    <<<
C
C         **  VEGETATION-CLASS SUB-SCENE TO MODEL CLASS COUNT SUB-SCENE
C
C
      INTEGER ASGR
      DIMENSION ITBUFF( 912,6),ASGR(6,6),CCLAS(6,4),IWORD(4)
      DIMENSION MSLINE(608,2)
C
C   UNIT ASSIGNMENTS FOR THE TI-980:
C        B4 = CRT
C        B5 = CRT OR CDR (RECORD COUNT INPUT)
C        B6 = LP (MSG FILE)
C        B7 = INPUT(VEGETATION MAP) TAPE, <1824 BYTE RECORDS
C        B8 = OUTPUT(MODEL SCENE) TAPE, 1216 BYTE RECORDS
C        B9 = LP OR CRT DIAGNOSTICS PRINT OUT
C
C
C   RESET CYCLE COUNTER AND END-OF-FILE FLAG
      ICYC=0
      IEND=0
      ICNT=0
      IEOF=0
C   OPEN TAPE UNITS FOR INPUT AND OUTPUT
      CALL SVC(183,7,1824,ITBUFF)
      CALL SVC(184,7,1216,MSLINE)
C
C   CALL FOR  INPUT DATA
      WRITE(4,3)
    3 FORMAT(1H ,'INPUT RCD COUNT AND DUMP FLAG(2I5)',/,1X)
C
C   READ IN THE NUMBER OF TAPE RECORDS EXPECTED AND DUMP FLAG
C
      READ(5,10) IREC,ID
   10 FORMAT(2I5)
      WRITE(6,11) IREC,ID
   11 FORMAT(1H ,'EXPECT',I6,' RCDS',5X,'DUMP FLAG',I6)
      IRM5=IREC-50
    5 CONTINUE
      ITRCD=0
      IF(IEND.LT.0) GO TO 16
C   RESET END OF BUFFER LINES BEFORE READING TAPE
C
      DO 8 M=1,6
      DO 7  L=800, 912
    7 ITBUFF(L,M)=32639
    8 CONTINUE
C
C   GET A TAPE RECORD 6-TUPLE, EACH <=912 BYTE PAIRS
C
```

ORIGINAL PAGE IS
OF POOR QUALITY

```
    6 DO 15 N=1,6
      IF(ICNT.EQ.IREC) GO TO 150
C
C   INPUT A TAPE RECORD FROM UNIT NBR 7
      CALL SVC(183,1,1824,ITBUFF(1,N))
      IF(ICNT.GT.IRM5) CALL TCK(IEOF)
      IF(IEOF.NE.0) GO TO 150
C
      ICNT=ICNT+1
      ITRCD=ITRCD+1
   15 CONTINUE
   16 CONTINUE
C
C   BUILD 2 LINES OF MODEL SCENE DATA
      DO 125 K=1,304
      I=1+(K-1)*3
C
C   BUILD 6-BY-6 WORD-BOX FROM 6-BY-6 VEGETATION BYTE-BOX
      DO 30 J=1,6
      DO 29 L=1,3
      LK=L-1
      LL=LK*2+1
      TEMP=ITBUFF(I+LK,J)
C   RIGHT JUSTIFY L-H BYTE
      ASQR(LL,J)=TEMP/256
C   FIND VALUE OF R-H BYTE
      ASQR(LL+1,J)=TEMP-(ASQR(LL,J)*256)
   29 CONTINUE
   30 CONTINUE
C
C
C   RESET THE COUNTERS FOR CLASSES IN EACH MODEL SCENE BOX
      DO 35 J=1,4
      DO 34 IK=1,6
      CCLAS(IK,J)=0
   34 CONTINUE
   35 CONTINUE
C
C   COUNT CLASSES IN 6-BY-6 BYTE-BOX FOR  4-BY-4 WORD-BOX
      DO 44 JI=1,6
      DO 43 KI=1,6
      IK=KI/4+1+(JI/4)*2
C
C   VALUE OF JI INDEXES LINE NBR
C   VALUE OF IK     "      COLM NBR
C   COUNT NUMBER OF VALUES IN EACH OF 6 CLASSES FOR EACH
C     OF 4 BOXES IN ASQR (INDEXED BY IK)
      CALL COUNT(JI,KI,IK,ASQR,CCLAS)
   43 CONTINUE
   44 CONTINUE
```

ORIGINAL PAGE IS
OF POOR QUALITY

```
C
C  BUILD 2 MODEL SCENE WORDS FOR EACH OF TWO LINES
C
      DO 75 IK=1,4
      IWORD(IK)=0
C
C       BUILD MODEL SCENE DATA SUB-WORD INDEXED BY IK
      DO 70 KK=1,5
      KP=KK-1
      IWORD(IK)=IWORD(IK)+IFIX((CCLAS(KK,IK)/9.)*7.+0.5)*IFIX(8.**KP)
   70 CONTINUE
   75 CONTINUE
C  PUT 4 SUBWORDS INTO TWO MODEL SCENE LINES
C
      II=1+(K-1)*2
      DO 80 LL=1,2
      MSLINE(II,LL)=IWORD(2*LL-1)
      MSLINE(II+1,LL)=IWORD(2*LL)
   80 CONTINUE
C *****   DIAGNOSTICS ***
      IF(ID.EQ.0) GO TO 125
      IF((K.GT.265).AND.(K.LE.270).AND.(ICYC.GE.  5).AND.(ICYC.LE.10))
     $ GO TO 140
C
      IF((K.LE.265).OR.(K.GT.270).OR.(ICYC.LE.252).OR.(ICYC.GT.267))
     $ GO TO 125
C
  140 CONTINUE
      IP3=I+2
      IIP1=II+1
      WRITE(9,142)((ITBUFF(L,N),L=I,IP3),N=1,6),ASQR,CCLAS,
     $IWORD,((MSLINE(MM,NN),MM=II,IIP1),NN=1,2),K,ICYC
  142 FORMAT(1H ,'TRCD: ',/,6(1X,3I7,/),1X,'BYTE-BOX',/,6(1X,6I7,/),1X,/,
     $1X,'CLASS CNT',/,4(1X,6I7,/),1X,/,
     $1X,'WORD BITS',/,1X,4I8,/,
     $1X,'TAPE RCD WORDS',/,    2(1X,2I7,/),1X,/,
     $1X,'K=',I7,5X,'CYCLE=',I7,/,1X)
C
C ***   END OF DIAGNOSTICS    ***
  125 CONTINUE
      ICYC=ICYC+1
C  COMPLETED 2 LINES OF MODEL SCENE 608 WORDS/LINE
C  WRITE 2 LINES TO TAPE UNIT NBR 2
      CALL SVC(184,3,1216,MSLINE(1,1))
      CALL SVC(184,3,1216,MSLINE(1,2))
      WRITE(4,141)ICNT
  141 FORMAT(1H ,5X,'RCD CNT',I6)
      IF(IEND.LT.0) GO TO 151
      GO TO 5
  150 IF(ITRCD.NE.0) GO TO 300
```

ORIGINAL PAGE IS
OF POOR QUALITY

```
C  COMPLETED TAPE FILE AND MODEL SUB-SCENE
  151 IRCD=ICYC*6
      ILINES=ICYC*2
      ENDFILE 8
      WRITE(6,200) IRCD,ILINES,ICYC,ITRCD,IREC,ICNT
  200 FORMAT(10X,'...END OF INPUT TAPE: ',I6,' RECORDS',
     $5X,I6,' MODEL SCENE LINES',5X,I6,' LINE-PAIR CYCLES',/,
     $5X,I6,' TAPE RECORD RESIDUE',/,
     $5X,I6,' RECORDS EXPECTED, RECORD COUNT=',I6)
      STOP
  300 CONTINUE
C
C  FINISH OFF MODEL-SCENE WITH BACKGROUND DATA, >7F7F
      NXL=ITRCD+1
      DO 310 LL=NXL,6
      DO 309 LC=1, 912
      ITBUFF(LC,LL)=32639
  309 CONTINUE
  310 CONTINUE
      IEND=-1
      GO TO 5
      END
```

ORIGINAL PAGE IS
OF POOR QUALITY

```
      SUBROUTINE TCK(IEOF)
      IBK=0
A      DATA     >C385            ;TURN OFF MPB
A 200  LDM      %10              ;GET STATUS WORD
A      DATA     >C38D
A      RMO      M,A              ;MOVE IT TO ACCUM
A      STA      %23,I            ;STORE AT ISTAT
A      CPL      %11              ;>8000, COMPLETE?
A      SEQ
A      BRU      %500             ;NOT COMPLETE, CHECK FOR EOF
A      BRU      %777             ;OP COMPLETE
A 500  SNZ      A                ;SKIP IF NOT ZERO STATUS
A      BRU      %200             ;WAIT FOR CHANGE
A      CRA      8                ;PUT EOF 7-BIT INTO LOC 15
A      SEV      A                ;SKIP IF NOT EOF
A      BRU      %666             ;EOF FOUND
A      CRA      2                ;NOT EOF, CK PARITY
A      SEV      A                ;SKIP IF NO  "   ERROR
A      BRU      %999             ;SIGNAL ERROR
A      BRU      %777             ;RETURN
  999  WRITE(4,1000)
 1000  FORMAT(5X,'TAPE ERROR')
  600 CONTINUE
A      DATA     >C386            ;TURN ON MPB
       WRITE(6,900) ISTAT
  900 FORMAT(5X,'STATUS',I6)
A      BRU      %777             ;RETURN
C
  666  IEOF=1
  667  CONTINUE
A      DATA     >C386            ;TURN ON MPB
  800 RETURN
  777 IEOF=0
       GO TO 667
A  10  DATA     >009C
A  11  DATA     >8000
A  23  DATA     ISTAT
C
       END
```

ORIGINAL PAGE IS
OF POOR QUALITY

```
      SUBROUTINE COUNT(J,K,I,ASQ,CCL)
      INTEGER ASQ
      DIMENSION ASQ(6,6) ,CCL(6,4)
C  ***   ***   ***   ***   ***   ***   *
C
C  INSERT COUNTING RULES FOR VEGETATION SCENE HERE
C
C   ***   KERRVILLE   KERRVILLE   ***
C
      IF((ASQ(K,J).LE.0).OR.(ASQ(K,J).GE.23)) GO TO 100
      GO TO (1,2,3,4,5,6,7,8,9,10,11,12,13,14,15,16,17,18,19,20,21,22),
     $ASQ(K,J)
  100 RETURN
C
C   WATER - - - - - - - - - - - - - - - - - -  -- -CLASS1
C
   20 CCL(1,I)=CCL(1,I)+1
      GO TO 100
C
C   URBAN & BARE SOIL - - - - - - - - - - - - - - - --CLASS 2, 3
C
    5 CONTINUE
   21 CONTINUE
   22 CCL(2,I)=CCL(2,I)+1
      GO TO 100
C
C   MIXED SOIL AND VEGETATION - - - - - - - - - - -CLASS 4
C
   17 CONTINUE
   18 CONTINUE
   19 CCL(4,I)=CCL(4,I)+1
      GO TO 100
C
C    FULLY VEGETATED(NON-FOREST) - - - - - - - - --CLASS 5
C
    1 CONTINUE
    2 CONTINUE
    3 CONTINUE
    4 CONTINUE
    6 CONTINUE
    7 CCL(5,I)=CCL(5,I)+1
      GO TO 100
C
C   FOREST LAND -- - - - - - - - - - - - - - - - - - CLASS 6
C
    8 CONTINUE
    9 CONTINUE
   10 CONTINUE
   11 CONTINUE
   12 CONTINUE
```

ORIGINAL PAGE IS
OF POOR QUALITY

```
   13 CONTINUE
   14 CONTINUE
   15 CONTINUE
   16 CCL(6,I)=CCL(6,I)+1
      GO TO 100
C
C  END OF COUNTING RULES
C   ***   ***   ***   ***   ***   ***   ***
      END
```

ORIGINAL PAGE IS
OF POOR QUALITY

```
C    ***   AUSTIN   AUSTIN   ***
C
       IF((ASQ(K,J).LE.0).OR.(ASQ(K,J).GE.34)) GO TO 100
       GO TO (1,2,3,4,5,6,7,8,9,10,11,12,13,14,15,16,17,18,19,20,
     $21,22,23,24,25,26,27,28,29,30,31,32,33),ASQ(K,J)
  100 RETURN
C
C    WATER -- -- -- -- -- -- -- -- -- ---- - - - -CLASS 1
C
   25 CONTINUE
   26 CONTINUE
   27 CCL(1,I)=CCL(1,I)+1
      GO TO 100
C
C    URBAN & BARE SOIL - - - - - - - - - - - - - ---CLASS 2, 3
C
   19 CONTINUE
   28 CONTINUE
   29 CONTINUE
   30 CONTINUE
   31 CONTINUE
   32 CCL(2,I)=CCL(2,I)+1
      GO TO 100
C
C    MIXED SOIL & VEGETATION - - - - - - - - - - - - CLASS 4
C
   10 CONTINUE
   11 CONTINUE
   15 CONTINUE
   16 CONTINUE
   17 CONTINUE
   18 CONTINUE
   20 CONTINUE
   21 CCL(4,I)=CCL(4,I)+1
      GO TO 100
C
C    FULLY VEGETATED(NON-FORESTED)- - - - - - - - - - - CLASS 5
C
    1 CONTINUE
    2 CONTINUE
    3 CONTINUE
    5 CONTINUE
    6 CONTINUE
    7 CONTINUE
    8 CCL(5,I)=CCL(5,I)+1
      GO TO 100
C
C    FOREST LAND - - - - - - - - - - - - - - - - - - - CLASS 6
C
    4 CONTINUE
```

ORIGINAL PAGE IS
OF POOR QUALITY

```
    9 CONTINUE
   12 CONTINUE
   13 CONTINUE
   14 CONTINUE
   22 CONTINUE
   33 CONTINUE
   34 CCL(6,I)=CCL(6,I)+1
   23 CONTINUE
   24 CONTINUE
      GO TO 100
C
```

ORIGINAL PAGE IS
OF POOR QUALITY

```
C    ***    BROWNWOOD    BROWNWOOD    ***
C
       IF((ASQ(K,J).LE.0).OR.(ASQ(K,J).GE.8)) GO TO 100
       GO TO (1,2,3,4,5,6,7),ASQ(K,J)
  100 RETURN
C
C    WATER - - - - - - - - - - - - - - - - - - - - - -CLASS 1
C
     6 CCL(1,I)=CCL(1,I)+1
       GO TO 100
C
C    URBAN & BARE SOIL - - - - - - - - - - - - - - - - CLASS 2, 3
C
     7 CCL(2,I)=CCL(2,I)+1
       GO TO 100
C
C    MIXED SOIL & VEGETATION  - - - - - - - - - - - CLASS 4
C
     5 CCL(4,I)=CCL(4,I)+1
       GO TO 100
C
C    FULLY VEGETATED(NON-FOREST) - - - - - - - - - -CLASS 5
C
     1 CONTINUE
     2 CCL(5,I)=CCL(5,I)+1
       GO TO 100
C
C    FOREST-LAND - - - - - - - - - - - - - - - - - - -CLASS 6
C
     3 CONTINUE
     4 CCL(6,I)=CCL(6,I)+1
       GO TO 100
C
       END
```

ORIGINAL PAGE IS
OF POOR QUALITY

```
C    ***    WACO    WACO    ***
C
       IF((ASQ(K,J).LE.0).OR.(ASQ(K,J).GE.9)) GO TO 100
       GO TO (1,2,3,4,5,6,7,8),ASQ(K,J)
  100 RETURN
C
C    WATER - - - - - - - - - - - - - - - - - - - - - -CLASS 1
C
     7 CCL(1,I)=CCL(1,I)+1
       GO TO 100
C
C    URBAN & BARE SOIL - - - - - - - - - - - - - - - -CLASS 2,3
C
     8 CCL(2,I)=CCL(2,I)+1
       GO TO 100
C
C    MIXED SOIL & VEGETATION --------- - - - - - -CLASS 4
C
     6 CCL(4,I)=CCL(4,I)+1
       GO TO 100
C
C    FULLY VEGETATED(NON-FOREST)- - - - - -  - - -CLASS 5
C
     1 CONTINUE
     2 CCL(5,I)=CCL(5,I)+1
       GO TO 100
C
C    FOREST-LAND - - - - - - - - - - - - - - - - - - CLASS 6
C
     3 CONTINUE
     4 CONTINUE
     5 CCL(6,I)=CCL(6,I)+1
       GO TO 100
C
C
       END
```

ORIGINAL PAGE IS
OF POOR QUALITY

```
C    ***    BRYAN    BRYAN    ***
C
C
      IF((ASQ(K,J).LE.0).OR.(ASQ(K,J).GT.39))GO TO 100
      GO TO (1,2,3,4,5,6,7,8,9,10,11,12,13,14,15,16,17,18,19,20,
     *21,22,23,24,25,26,27,28,29,30,31,32,33,34,35,36,37,38,39),ASQ(K,J)
  100 RETURN
C
C    OPEN WATER ---    --- --- - -- - - - - - - - -  CLASS 1
C
   24 CONTINUE
   26 CCL(1,I)=CCL(1,I)+1
      GO TO 100
C
C    URBAN AND BARE SOIL------ - - - - -  - - - - CLASS 2, 3
C
    8 CONTINUE
   21 CONTINUE
   22 CONTINUE
   23 CONTINUE
   33  CONTINUE
   34 CONTINUE
   38 CCL(2,I)=CCL(2,I)+1
      GO TO 100
C
C    MIXED SOIL AND VEGETATION
C
C    MIXED SOIL AND VEGETATION-------------- - -  --CLASS 4
C
    9 CONTINUE
   13 CONTINUE
   15 CONTINUE
   18 CONTINUE
   19 CONTINUE
   27 CONTINUE
   29 CONTINUE
   30 CONTINUE
   31 CONTINUE
   35 CONTINUE
   36  CONTINUE
   37  CONTINUE
   39 CCL(4,I)=CCL(4,I)+1
      GO TO 100
C
C    FULLY VEGETATED ( NON-FOREST) ------ - - - - CLASS 5
C
    1 CONTINUE
    3 CONTINUE
    4 CONTINUE
    5 CONTINUE
```

ORIGINAL PAGE IS
OF POOR QUALITY

```
    6 CONTINUE
   14 CONTINUE
   32 CCL(5,I)=CCL(5,I)+1
      GO TO 100
C
C    FOREST-LAND    ------ - - - - - - - - - - - - - - - CLASS 6
C
    2 CONTINUE
    7 CONTINUE
   10 CONTINUE
   11 CONTINUE
   12 CONTINUE
   16 CONTINUE
   17 CONTINUE
   20 CONTINUE
   25 CONTINUE
   28 CCL(6,I)=CCL(6,I)+1
      GO TO 100
C
C    END OF BRYAN RULES
      END
```

ORIGINAL PAGE IS
OF POOR QUALITY

```
C    ***    CORSICANA    CORSICANA    ***
C
       IF((ASQ(K,J).LE.0).OR.(ASQ(K,J).GT.36))GO TO 100
       GO TO(1,2,3,4,5,6,7,8,9,10,11,12,13,14,15,16,17,18,19,20,
      $21,22,23,24,25,26,27,28,29,30,31,32,33,34,35,36),ASQ(K,J)
  100 RETURN
C
C    WATER--------------------     CLASS 1
C
   17 CONTINUE
   18 CONTINUE
   19 CONTINUE
   20 CCL(1,I)=CCL(1,I)+1
      GO TO 100
C
C    URBAN & BARE SOIL       -------------CLASS 2, 3
C
   29 CONTINUE
   30 CONTINUE
   31 CONTINUE
   32 CONTINUE
   34 CONTINUE
   33 CONTINUE
   35 CONTINUE
   36 CCL(2,I)=CCL(2,I)+1
      GO TO 100
C
C    MIXED SOIL & VEGETATION ------------CLASS 4
C
   21 CONTINUE
   22 CONTINUE
   23 CONTINUE
   24 CONTINUE
   25 CONTINUE
   26 CONTINUE
   27 CONTINUE
   28 CCL(4,I)=CCL(4,I)+1
      GO TO 100
C
C    FULLY VEGETATED (NON-FOREST)    -----CLASS 5
C
    1 CONTINUE
    2 CONTINUE
    3 CCL(5,I)=CCL(5,I)+1
      GO TO 100
C
C    FOREST LAND        ----------------  CLASS 6
C
    4 CONTINUE
    5 CONTINUE
```

ORIGINAL PAGE IS
OF POOR QUALITY

```
    6 CONTINUE
    7 CONTINUE
    8 CONTINUE
    9 CONTINUE
   10 CONTINUE
   11 CONTINUE
   12 CONTINUE
   13 CONTINUE
   14 CONTINUE
   15 CONTINUE
   16 CCL(6,I)=CCL(6,I)+1
      GO TO 100
C  END OF RULES FOR CORSICANA  ****
      END
```

ORIGINAL PAGE IS
OF POOR QUALITY

```
C    ***    HOUSTON    HOUSTON    ***
C
       IF((ASQ(K,J).LE.0).OR.(ASQ(K,J).GT.39))GO TO 100
       GO TO (1,2,3,4,5,6,7,8,9,10,11,12,13,14,15,16,17,18,19,20,21,22,
     $23,24,25,26,27,28,29,30,31,32,33,34,35,36,37,38,39),ASQ(K,J)
  100 RETURN
C
C    ***    WATER    ***    ---    ---    ---    ---    --- CLASS 1
C
   34 CCL(1,I)=CCL(1,I)+1
      GO TO 100
   35 GO TO 34
   37 GO TO 34
C
C    ***    URBAN & BARE SOIL    ---    ---    ---    ---    CLASS 2, 3
C
   25 CCL(2,I)=CCL(2,I)+1
      GO TO 100
   26 CONTINUE
   27 CONTINUE
   28 CONTINUE
   29 CONTINUE
   30 CONTINUE
   31 CONTINUE
   32 CONTINUE
   33 CONTINUE
   39 GO TO 25
C
C  MIXED SOIL & VEGETATION-----------------------CLASS 4
   15 CONTINUE
   16 CONTINUE
   17 CONTINUE
   18 CONTINUE
   19 CONTINUE
   20 CONTINUE
   21 CCL(4,I)=CCL(4,I)+1
   22 GO TO 100
C
C  FULLY VEGETATED(NON/FOREST)-------------------CLASS 5
C
    1 CONTINUE
    2 CONTINUE
    3 CONTINUE
   23 CONTINUE
   24 CCL(5,I)=CCL(5,I)+1
      GO TO 100
C
C   FOREST-LAND-----------------------------------CLASS6
    4 CONTINUE
    5 CONTINUE
```

ORIGINAL PAGE IS
OF POOR QUALITY

```
    6 CONTINUE
    7 CONTINUE
    8 CONTINUE
    9 CONTINUE
   10 CONTINUE
   11 CONTINUE
   12 CONTINUE
   13 CONTINUE
   14 CONTINUE
   36 CONTINUE
   38 CCL(6,I)=CCL(6,I)+1
      GO TO 100
C
      END
```

ORIGINAL PAGE IS
OF POOR QUALITY

```
C    ***   LUFKIN   LUFKIN   ***
C
C
      IF((ASQ(K,J).LE.0).OR.(ASQ(K,J).GT.14)) GO TO 100
      GO TO (1,2,3,4,5,6,7,8,9,10,11,12,13,14),ASQ(K,J)
  100 RETURN
C
C  WATER- - - - - - - - - - - - - - - - - - - - - - -CLASS 1
C
   10 CCL(1,I)=CCL(1,I)+1
      GO TO 100
C
C  URBAN & BARE SOIL  - - - - - - - - - - - - - - - -CLASS 2, 3
C
   11 CCL(2,I)=CCL(2,I)+1
      C  CLASS 3 = SAME AS CLASS 2
      GO TO 100
C
C  MIXED SOIL & VEGETATION  - - - - - - - - - - - -CLASS 4
   12 CCL(4,I)=CCL(4,I)+1
      GO TO 100
   13 GO TO 12
   14 GO TO 12
C
C  VEGETATED(NON-FOREST) -  - - - - - - - - - - - -CLASS 5
C
    1 CCL(5,I)=CCL(5,I)+1
      GO TO 100
    2 GO TO 1
C
C  FOREST- - - - - - - - - - - - - - - - - - - - - -CLASS 6
C
    3 CCL(6,I)=CCL(6,I)+1
      GO TO 100
    4 GO TO 3
    5 GO TO 3
    6 GO TO 3
    7 GO TO 3
    8 GO TO 3
    9 GO TO 3
      END
C
```

**ORIGINAL PAGE IS
OF POOR QUALITY**

```
C   FILL TAPE DATA SCENE WITH BACKGROUND
C
C
C   ASSIGN B7 TO MT
C    ASSIGN B4 CRT
C
       INTEGER ISCENE(2496)
C   FILL SUPER-SCENE   LINE BUFFER WITH BACKGROUND
       DO 12 IC=1,2496
       ISCENE(IC)    =0
   12 CONTINUE
C   OPEN TAPE UNIT FOR 2496 WORDS PER RECORD
       CALL SVC(183,7,4992,ISCENE(1))
       ICNT=0
       WRITE(4,10)ICNT
   10 FORMAT(1H ,'TAPE UNIT OPEN, RCD CNT=',I6)
       DO 24 KR=1,1650
C   OUTPUT A RECORD FROM THE BUFFER FILLED WITH ZERO
       CALL SVC(183,3,4992,ISCENE(1))
       ICNT=ICNT+1
   24 CONTINUE
C   OUTPUT TWO END OF FILE MARKS ON THE TAPE
       CALL SVC(183,10,4992,ISCENE(1))
       WRITE(4,30)ICNT
   30 FORMAT(1H ,'TAPE UNIT CLOSED, RCD CNT=',I6)
       STOP
       END
```

C-3

**ORIGINAL PAGE IS
OF POOR QUALITY**

```
C   *********   STEP 2 PROGRAM   *********
C
C         MODEL SUPERSCENE FROM MODEL SUBSCENES
C
C         UNIT ASSIGNMENTS:
C              8 = INPUT MODEL SCENE
C              9 = INPUT SUPERSCENE
C             10 = OUTPUT SUPERSCENE
C
C   ISCN = (INPUT SCENE SEQ NBR: 1 THROUGH 8)
C              1 = LUFKIN
C              2 = HOUSTON
C              3 = CORSICANA
C              4 = BRYAN
C              5 = WACO
C              6 = AUSTIN
C              7 = BROWNWOOD
C              8 = KERRVILLE
C   IMSL = NBR OF LINES IN THE SCENE BEING PROCESSED
C
C   SYSTEM OPERATION:
C         1. READS UNIT 5 FOR OPERATION PARAMETERS
C         2.  OVERLAYS SUPER-SCENE WITH MODEL SUB-SCENE SPECIFIED BY ISCN
C         THREE TAPES SHOULD BE MOUNTED, INPUT = MODEL SUBSCENE
C                                        INPUT = OLD SUPERSCENE
C                                        OUTPUT = NEW SUPERSCENE
C
      INTEGER*2 ISCENE,MSCENE
      DIMENSION ISCENE(2496,2),MSCENE(608,2)
      COMMON/FILLER/ISCENE
C
C    GET RUN PARAMETERS FROM CARD READER
C
      READ(5,10)          ISCN,IMSL
   10 FORMAT(3I5)
C
C   BACKGROUND FILLED WITH >0000
      WRITE(6,12) ISCN,IMSL
   12 FORMAT(1H1,10X,'STEP 2 PROGRAM RUN PARAMETERS:',/,
     *20X,'INPUT SCENE=',I6,10X,'INPUT SCENE LINE COUNT=',I6,/)
C
C    CHECK MODEL SUB-SCENE SEQ NBR
C
   15 CONTINUE
      GO TO (100,200,300,400,500,600,700,800) ,ISCN
C
C    THIS SECTION FOR LOADING MODEL SUBSCENE
  100 CONTINUE
C
      LCOL=1888
```

ORIGINAL PAGE IS
OF POOR QUALITY

```
      LNBR=0
      LN=0
      WRITE(6,110) ISCN,LNBR,LCOL
  110 FORMAT(1H ,10X,'BEGINNING SCENE',I6,', LUFKIN  AT LINE',I6,
     *', COLUMN',I6,/)
C
  225 CONTINUE
C  GET LINE FROM MODEL-SCENE INTO BUFFER PAIR NBR 1
      READ(8,226,END=1777)(MSCENE(M,1),M=1,608)
  226 FORMAT(19(32A2))
C
C   GET LINE FROM  SUPER-SCENE INTO NBR 1 BUFFER PAIR
      READ(9,227)(ISCENE(II,1),II=1,2496)
  227 FORMAT(39(64A2))
C
C   OVER-LAY 1ST SUB-SCENE LINE ONTO 1ST SUPER-SCENE LINE
C
      DO 230 MC=1,608
      IC=LCOL+MC-1
      IF(ISCENE(IC,1).EQ.0)ISCENE(IC,1)=MSCENE(MC,1)
  230 CONTINUE
C   OUTPUT THE REFORMATTED SUPER-SCENE LINE FROM BUFFERS 1
C
      WRITE(10,227)(ISCENE(II,1),II=1,2496)
      LNBR=LNBR+1
      LN=LN+1
      IF(LN  .GE.IMSL) GO TO 1777
C   GET ANOTHER PAIR OF LINES INTO NBR 2 BUFFERS
C
      READ(8,226,END=1777)(MSCENE(M,2),M=1,608)
      READ(9,227)(ISCENE(II,2),II=1,2496)
C
C    OVER-LAY 2ND SUB-SCENE LINE ONTO 2ND SUPER-SCENE LINE
      DO 240 MC=1,608
      IC=LCOL+MC-1
      IF(ISCENE(IC,2).EQ.0)ISCENE(IC,2)=MSCENE(MC,2)
  240 CONTINUE
C  OUTPUT THE REFORMATTED SUPER-SCENE LINE FROM BUFFERS 2
      WRITE(10,227)(ISCENE(II,2),II=1,2496)
      LNBR=LNBR+1
      LN=LN+1
C   COMPLETED  TWO LINES INTO THE NEW SUPER-SCENE
      IF(LN  .GE.IMSL) GO TO 1777
      GO TO 225
C
C  FINISH WRITING THE SUPER-SCENE ONTO NEW TAPE
C   POINT TO THE NEXT LINE TO PROCESS
 1777 LAST = LNBR
 1800 IF(LNBR.GE.1650) GO TO 1801
      READ(9,227)(ISCENE(II,1),II=1,2496)
```

ORIGINAL PAGE IS
OF POOR QUALITY

```
      WRITE(10,227)(ISCENE(II,1),II=1,2496)
      LNBR=LNBR+1
      GO TO 1800
 1801 CONTINUE
C
C    SUPER-SCENE NOW ON (NEW) TAPE
      ENDFILE 10
      WRITE(6,1900) LAST,LNBR,LN
 1900 FORMAT(10X,'---LAST MODEL SCENE LINE=',I6,' ON SUPERSCENE',
     $/,11X,'--- LAST LINE NBR=',I6,' LAST MODEL SCENE LINE=',I6,/)
      STOP
C
C  FOR LOADING HOUSTON SUBSCENE ONTO SUPER SCENE
  200 LNBR=680
      LCOL=1848
      WRITE(6,210) ISCN,LNBR,LCOL
  210 FORMAT(1H ,10X,'BEGINNING SCENE',I6,', HOUSTON   AT LINE',I6,
     *', COLUMN',I6,/)
  250 CALL SKIP(LNBR)
C
C  INITIALIZE MODEL SCENE LINE NUMBER
      LN=0
      GO TO 225
C
C  FOR LOADING SUB-SCENE FROM CORSICANA
  300 LNBR=99
      LCOL=1330
      WRITE(6,310) ISCN,LNBR,LCOL
  310 FORMAT(1H ,10X,'BEGINNING SCENE',I6,', CORSIC. AT LINE',I6,
     *', COLUMN',I6,/)
      GO TO 250
C
C  FOR LOADING SUB-SCENE FROM BRYAN
  400 LNBR=780
      LCOL=1292
      WRITE(6,410) ISCN,LNBR,LCOL
  410 FORMAT(1H ,10X,'BEGINNING SCENE',I6,', BRYAN   AT LINE',I6,
     *', COLUMN',I6,/)
      GO TO 250
C
C  FOR LOADING SUB-SCENE FROM WACO
  500 LNBR=212
      LCOL=772
      WRITE(6,510) ISCN,LNBR,LCOL
  510 FORMAT(1H ,10X,'BEGINNING SCENE',I6,', WACO    AT LINE',I6,
     *', COLUMN',I6,/)
      GO TO 250
C
C  FOR LOADING SUB-SCENE FROM AUSTIN
  600 LNBR=892
```

ORIGINAL PAGE IS
OF POOR QUALITY

```
      LCOL=734
      WRITE(6,610) ISCN,LNBR,LCOL
  610 FORMAT(1H ,10X,'BEGINNING SCENE',I6,', AUSTIN  AT LINE',I6,
     *', COLUMN',I6,/)
      GO TO 250
C
C  FOR LOADING SUB-SCENE FROM BROWNWOOD
  700 LNBR=281
      LCOL=216
      WRITE(6,710) ISCN,LNBR,LCOL
  710 FORMAT(1H ,10X,'BEGINNING SCENE',I6,', BROWNW.  AT LINE',I6,
     *', COLUMN',I6,/)
      GO TO 250
C
C  FOR LOADING SUB-SCENE FROM KERRVILLE
  800 LNBR=963
      LCOL=170
      WRITE(6,810) ISCN,LNBR,LCOL
  810 FORMAT(1H ,10X,'BEGINNING SCENE',I6,', KERRVI.  AT LINE',I6,
     *', COLUMN',I6,/)
      GO TO 250
C
      END
      SUBROUTINE SKIP(LCNT)
      INTEGER*2 ISCENE(2496,2)
      COMMON/FILLER/ISCENE
C
      DO 310 K=1,LCNT
      READ(9,10)(ISCENE(J,1),J=1,2496)
      WRITE(10,10)(ISCENE(L,1),L=1,2496)
   10 FORMAT(32(78A2))
  310 CONTINUE
      RETURN
      END
```

ORIGINAL PAGE IS
OF POOR QUALITY

```
C    MODEL OF ORBITING MICROWAVE RADIOMETER
C
C INPUT 3 CARDS FOR EACH PASS:
C     CARD #1:
C       5F5.0--AZIM,BMWID,INCID,ALT,TEMP
C                DEG    DEG    DEG   KM DEG C
C       2I5--DOWN & CROSS RANGE SCENE SIZE
C    CARD#2:
C       4F5.0--SOIL MOIST X & Y DELTA
C              ROUGHNESS  X & Y DELTA
C       2I5--NADIR MOTION STEP SIZE,
C              BAND IDENTIFICATION #
C       2F6.1--SOIL MOIST & ROUGHNESS
C    CARD #3:
C       2F5.0--X & Y STARTING COORD. OF ANTENNA FOOT PRINT
C
C INPUT UNITS:
C    5=CDR
C    7=MT1(MOIST,ROUGH)
C    8=MT2(VEG CLASS)
C OUTPUT UNITS:
C    6=LP(BT HISTORY)
C    9=MT3(BT HISTORY & PARMS)
C
C     SYSTEM BAND:  1=L,2=C,3=X
C     AZIM-AZIMUTH(=>0,=<90)  ALT-SATELLITE ALTITUDE
C     BWID-BEAMWIDTH          TEMP-BACKGROUND TEMP.(DEG C)
C     ANGI-INCIDENT ANGLE     SCENE BOUNDARY LIMITS:
C          (=>0,=<45)            LMDR-DOWNRANGE
C                                LMCR-CROSSRANGE
C     TARGET COORDINATES:     SCENE INTEGRATION STEPS:   NADIR DISPLACEMENT
C       TOP-X COORDINATE         DOWN-DOWNRANGE STEP        DNAD-DOWNRANGE
C       CENT-Y COORDINATE        CROS-CROSSRANGE STEP       CNAD-CROSSRANGE
C       SFC-SURFACE              ELEV-ELEVATION STEP        ENAD-ELEVATION
C ***********************************************************************
      DOUBLE PRECISION RSUM,RCNT
      INTEGER*2 ILINE,IMOIST
      DIMENSION ILINE(2496),IMOIST(2496), BY(325),BRITV(325),BRITH(325)
      EQUIVALENCE(X,TOP),(Y,CENT),(ANGI,ROLL)
      COMMON/COORD/X,XL,XU,Y,YL,YU,X1,X2,Y1,Y2
      COMMON/DAT/ILINE,IMOIST
      COMMON/ROUGH/RH,RV
      COMMON/GAN/BWID,XPI,IF
      COMMON/ORIEN/ROLL,AZIM,ALT,A,B
      COMMON/TRIG/COSR,SINR,COSA,SINA
      COMMON/CLAS/CLASUM(6)
C
      CONRAD(ANGLE)=ANGLE/57.2957
      IF=3
      XPI=3.14159
```

ORIGINAL PAGE IS
OF POOR QUALITY

```
C INITIALIZE RECORD NBR
C SCAN PARAMETERS READ IN, VARIABLES INITIALIZED
      IRCD=0
  200 CALL INPUT(AZIM,BWID,ANGI,LMDR,LMCR,ALTO,TEMP)
C
C READ MOISTURE ROUGHNESS RATES, INTEGRATION STEP SIZE, BAND
      READ(5,8)DSMY,DSMX,RUFY,RUFX,ISTEP,NBND,SOILK,ROUK
C
C INITIALIZE SATELLITE NADIR COORDINATES
      READ(5,13)X,Y,RESL,DNAD
   13 FORMAT(3F5.0,F5.4)
C
C INITIALIZE SURFACE ELEVATION(MSL)
      SFCO=0.0
C
C SET DOWN AND CROSS RANGE INTEGRATION UNIT SIZE, SET ELEV. UNIT STEP
      DOWN=1.0
      CROS=1.0
      ELEV=0.0
C INITIALIZE ALTITUDE FOR SPECIFIED RESOLUTION
      IF(RESL.NE.0.)CALL CALT(RESL,ALTO)
C SET NADIR DISPLACEMENT UNIT SIZES
      CNAD=1.0
      ENAD=0.0
      DELZ=0.0
C INITIALIZE LINE COUNTER,
C   AND SET DELTA-THETA STEP
      II=0
C INITIALIZING COMPUTATIONAL VARIABLES
      DA=DOWN*CROS
C
C SET UNIT SCALE FACTOR & SCALE ALTITUDE
      S=0.24
      SALT=ALTO
      ALTO=ALTO/S
      WRITE(6,2)AZIM,TEMP,BWID,ANGI,LMDR,LMCR,SALT,TOP,DOWN,
     $DNAD,CENT,CROS,CNAD,SFCO,ELEV,ENAD
      WRITE(9,210)AZIM,TEMP,BWID,ANGI,LMDR,LMCR,SALT,TOP,DOWN,
     $DNAD,CENT,CROS,CNAD,SFCO,ELEV,ENAD
      ANGSV=ANGI
C CONVERT ANGLES TO RADIANS
      AZSV=AZIM
      BWSV=BWID
      TPSZ=TEMP
      ANGI=CONRAD(ANGI)
      AZIM=CONRAD(AZIM)
      BWID=CONRAD(BWID)
      COSR=COS(ROLL)
      SINR=SIN(ROLL)
      COSA=COS(AZIM)
```

ORIGINAL PAGE IS
OF POOR QUALITY

```
      SINA=SIN(AZIM)
C EVALUATE SURFACE RANGE, AND INITIALIZE NADIR COORDINATES
      SFRG=ALTO*TAN(ROLL)
      SRSINA=SFRG*SINA
      AO=TOP+SRSINA
      SRCOSA=SFRG*COSA
      BO=CENT-SRCOSA
      IF(ISTEP.NE.0)GO TO 53
      ISTEP=IFIX(ALTO*TAN(BWID/2.))
   53 WRITE(6,3)SFRG,AO,BO,SOILK,ROUK
      WRITE(6,9)ISTEP,NBND,RESL
C BEGIN COMPUTATION ***************************************************
      DO 10 J=1,LMDR,ISTEP
C RESET NUMERATOR & DENOMINATOR ACCUMULATOR
      D=0.0
      XNH=0.0
      XNV=0.0
      II=II+1
      DO 57 LL=1,6
   57 CLASUM(LL)=0.0
C INCREMENT NADIR COORDINATES TO NEXT POSITION
      L=J-1
      A=AO+L*DNAD
      B=BO+L*CNAD
C PUT NADIR POINT IN PLOT BUFFER
      BY(II)=B+SRCOSA
C STEP ALTITUDE AND SURFACE
      ALT=ALTO+L*ENAD
      SFC=SFCO+L*DELZ
C INITIALIZE RANGE SUMMATION REGISTER
      RSUM=0.0
C FIND UPPER AND LOWER LIMITS OF ANTENNA SPOT SIZE
      X=A-SRSINA
      Y=BY(II)
      CALL XYLMIT(DX,DY)
      IF(J.NE.1)GO TO 101
      WRITE(6,12)XU,YU,XL,YL,DX,DY
      WRITE(9,211)SFRG,AO,BO,SOILK,ROUK,ISTEP,NBND,RESL,
     @XU,YU,XL,YL,DX,DY
      WRITE(6,5)
  101 CONTINUE
C SET LIMITS ON INTEGRATION IN X-DIRECTION
      K1=IFIX(XL-.5)
      IF(K1.LE.0)K1=1
      IF(K1.GT.1650)K1=1650
      K2=IFIX(XU+.5)
      IF(K2.LT.1)K2=1
      IF(K2.GT.1650)K2=1650
C SET LIMITS ON Y-DIRECTION
      I1=IFIX(YL-.5)
```

```
      IF(I1.LE.0)I1=1
      IF(I1.GT.2496)I1=2496
      I2=IFIX(YU+.5)
      IF(I2.LE.0)I2=1
      IF(I2.GT.LMDR)GO TO 110
C INITIALIZE RANGE AVERAGING COUNTER
C SKIP DOWN GRND SCENE TO FOOT-PRINT
      RCNT=0.0
      IF(IRCD.LT.(K1-1)) CALL ISKIP(IRCD,K1)
      IF(IRCD.GT.(K1-1))CALL IBACK(IRCD,K1)
C  SCAN DOWN FOOT-PRINT, LINE-BY-LINE
      DO 30 K=K1,K2
C
C INPUT SCENE DATA
C READ STRIP OF DATA FROM GROUND SCENE AND MOISTURE OVERLAY
C     READ(7,300)IMOIST
      READ(8,300,END=110)ILINE
C INCREMENT OVER ANTENNA-FOOT-PRINT
      IRCD=IRCD+1
      TOP=(K-1)*DOWN+0.5
C SCAN ACROSS FOOT-PRINT
      DO 20 I=I1,I2
C  SCAN SCENE,ACCUMULATE BRIGHTNESS COMPONENTS
      CENT=(I-1)*CROS+0.5
C COMPUTE RANGE TO GROUND CELL UNIT
      RVEC=SQRT((TOP-A)**2+(CENT-B)**2+(SFC-ALT)**2)
C EVALUATE THETA, ZEN. ANT. ANGLE
      T=ARCOS(((TOP-A)*SINR*SINA-(CENT-B)*
     @SINR*COSA+(SFC-ALT)*COSR)/RVEC)
C EVALUATE PHE, ANTENNA AZIM. ANGLE
      XDP=(X-A)*COSA+(Y-B)*SINA
      YDP=(Y-B)*COSA-(X-A)*SINA
      P=ATAN(XDP/YDP)
C COMPUTE ACTUAL INCIDENCE ANGLE TO GND CELL UNIT
      TN=ARCOS(ALT/RVEC)
C    ''    UNIT AREA, RANGE SUM, RANGE COUNT
      RSUM=RSUM+RVEC
      RCNT=RCNT+1.0
C EVALUATE ANTENNA TEMPERATURES
      SM=SOILK*(1.0+DSMY*Y/2496.+DSMX*X/1650.)
      ROU=ROUK*(1.0+RUFY*Y/2496.+RUFX*X/1650.)
      CALL BRIGHT(SM,ILINE(I),NBND,TEMP,ROU,BTVSO,BTHSO)
      CALL BCORR(BTVSO,BTHSO,TN,BTV,BTH)
      TBV=BTV
      TBH=BTH
      BTH=BRTMP(TBH,TBV,P)
      BTV=BRTMP(TBV,TBH,P)
      SAVE=G(T,P)*COS(TN)*DA/RVEC**2
      XNV=XNV+BTV*SAVE
      XNH=XNH+BTH*SAVE
```

**ORIGINAL PAGE IS
OF POOR QUALITY**

```
      D=D+SAVE
   20 CONTINUE
   30 CONTINUE
      RAVG=SNGL(RSUM/RCNT)*S
      DO 36 LL=1,6
   36 CLASUM(LL)=CLASUM(LL)/RCNT
C  COMPUTE AND PRINT BRIGHTNESS VALUES
      BRITV(II)=XNV/D
      BRITH(II)=XNH/D
      WRITE(6,4)J,SALT,RAVG,BRITV(II),BRITH(II),A,BY(II),CLASUM
      WRITE(9,400)J,SALT,RAVG,BRITV(II),BRITH(II),A,BY(II),CLASUM
C
   10 CONTINUE
  110 WRITE(6,7)
      ENDFILE9
      GO TO 200
    2 FORMAT('1','SATELLITE ATTITUDE & CHARACTERISTICS'/'    AZIMUTH(HEAD
     DING)',3X,F4.0,'DEG',15X,'BACKGROUND TEMP',F5.0,'DEG'/'    BEAMWIDTH
     U',10X,F4.0,'DEG',16X,'SCENE BOUNDARY LIMITS:'/'    INCIDENT ANGLE',
     H5X,F4.0,'DEG',16X,'DOWNRANGE',7X,I4/'                    ',9X,
     @20X,'CROSSRANGE',6X,I4/'                    ',27X,
     ,'SATELLITE ALTITUDE ',F4.0,'KILOMETERS',/,
     11X,/' TARGET COORDINATES',11X,'SCENE INTEGRATION STEPS',10X,'NADIR
     R DISPLACEMENT STEPS'/'    INITIAL X     ',F7.1,  8X,'DOWNRANGE STEP',
     ,4X,F3.1,12X,'DOWNRANGE STEP    ',F5.3/'    INITIAL Y'
     ,,4X,F7.1,  8X,'CROSSRANGE STEP    ',F3.1,12X,'CROSSRANGE STEP   ',
     ,F3.1/'    INITIAL Z',4X,
     ,F7.1,  8X,'ELEVATION STEP     ',F3.1,12X,'ELEVATION STEP    ',F3.1)
    3 FORMAT('OSURFACE RANGE ',F6.1,5X,' NADIR COORDINATES (',F7.1,',',
     @F7.1,')',5X,'SOIL MOIST. CONST. ',F6.1,5X,'ROUGHNESS CONST. ',F6.2)
    4 FORMAT(1H ,I5,7X,F4.0,8X,F9.2,10X,F8.2,4X,F8.2,  7X,2F8.2,1X,
     @6(F6.2,1X))
    5 FORMAT('ORNG STEP',2X,'ALTITUDE(KM)',4X,'RANGE(KM)',6X,
     @'BRIGHTNESS VER/HOR (DEG K)',  7X,'BEAM COORD(X,Y)',10X,
     @'AVG CLASS PERCENTS')
    7 FORMAT(1H ,'END OF SCENE',//)
    8 FORMAT(4F5.0,2I5,2F6.1)
    9 FORMAT('OSTEP SIZE=',I2,5X,'BAND IDENT. ',I3,5X,'RESOLUTION=',F5.1)
   12 FORMAT('0','XU=',F9.2,2X,'YU=',F9.2,2X,'XL=',F9.2,2X,'YL=',F9.2,
     ,2X,'ANTENNA SPOT SIZE',F7.2,' BY',F7.2)
  210 FORMAT(4F4.0,2I4,F4.0,3(F7.1,2F3.1),65X)
  211 FORMAT(4F6.1,F6.2,2I3,F5.1,6F7.2,49X)
  300 FORMAT(64(39A2))
  400 FORMAT(I5,6(F8.2,2X),6F6.2,31X)
      END
      SUBROUTINE INPUT(A,B,I,D,C,H,T)
      REAL I
      INTEGER D,C
      READ(5,10,END=20)A,B,I,H,T,D,C
   10 FORMAT(5F5.0,2I5)
```

ORIGINAL PAGE IS
OF POOR QUALITY

```
      RETURN
   20 ENDFILE9
      STOP
      END
      FUNCTION TAN(X)
      TAN=SIN(X)/COS(X)
      RETURN
      END
      FUNCTION G(T,P)
      COMMON/GAN/BWID,XPI,IF
      X=((XPI-T)*XPI)/(BWID/2.)
      IF(X.EQ.0.) GO TO 7
      G=ABS((SIN(X)/X)**IF)
    5 RETURN
    7 G=1.0
      GO TO 5
      END
      SUBROUTINE ISKIP(IR,K)
      INTEGER*2 ILINE(2496),IMOIST(2496)
      COMMON/DAT/ILINE,IMOIST
      KM=K-1
    5 IF(IR.EQ.KM)GO TO 7
C     READ(7,20)IMOIST
      READ(8,20,END=30)ILINE
   20 FORMAT(64(39A2))
      IR=IR+1
      GO TO 5
    7 RETURN
   30 WRITE(6,35)IR,K
   35 FORMAT(' IR= ',I6,10X,'K= ',I6)
      ENDFILE9
      STOP
      END
      SUBROUTINE IBACK(IR,K)
      INTEGER*2 ILINE(2496),IMOIST(2496)
      COMMON/DAT/ILINE,IMOIST
      KM=K-1
    5 IF(IR.EQ.KM)GO TO 7
C     BACKSPACE 7
      BACKSPACE 8
      IR=IR-1
      GO TO 5
    7 RETURN
      END
```

ORIGINAL PAGE IS
OF POOR QUALITY

```
      SUBROUTINE BRIGHT(SM,ICW,NB,TP,ROU,BTV50,BTH50)
      INTEGER*2 ICW
      COMMON/ROUGH/RH,RV
      COMMON/CLAS/CLASUM(6)
      REAL W(8)
      DATA W(1),W(2), W(3), W(4), W(5), W(6), W(7), W(8)
     @/     0.0,18.75,31.25,43.75,56.25,68.75,81.25,93.75/
C
C UNPACK ICW TO GET % AREA CODES FOR OPEN WATER(I1),BARE SOIL(I2),
C   URBAN(I3), MIXED SOIL AND VEGETATION(I4), AND VEGETATION(I5)
      I5=ICW/4096
      ICW=ICW-I5*4096
      I4=ICW/512
      ICW=ICW-I4*512
      I3=ICW/64
      ICW=ICW-I3*64
      I2=ICW/8
      I1=ICW-I2*8
C
C ZERO BRIGHTNESS TEMPS FROM LAST CALL(IF ANY)
      BTVW=0.0
      BTHW=0.0
      BTVB=0.0
      BTHB=0.0
      BTVU=0.0
      BTHU=0.0
      BTVM=0.0
      BTHM=0.0
      BTVV=0.0
      BTHV=0.0
      BTVF=0.0
      BTHF=0.0
C
C CALL SUBROUTINES IF CODE WORDS I1...I5 ARE NOT =0
      IF(I1.NE.0)CALL WATER(NB,TP,BTVW,BTHW)
      IF(I2.NE.0)CALL BARE(NB,TP,SM,ROU,BTVB,BTHB)
      IF(I3.NE.0)CALL URBAN(TP,BTVU,BTHU)
      IF(I4.NE.0)CALL MIX(NB,TP,SM,ROU,BTVM,BTHM)
      IF(I5.NE.0)CALL VEG(NB,TP,SM,BTVV,BTHV)
C
C DETERMINE IF SUBROUTINE FOREST NEEDS TO BE CALLED
      SUM=W(I1+1)+W(I2+1)+W(I3+1)+W(I4+1)+W(I5+1)
      WFOR=100.-SUM
      IF(WFOR.LT.0.)WFOR=0.0
C SUM % OF EACH CLASS IN EACH UNIT CELL
      CLASUM(1)=W(I1+1)+CLASUM(1)
      CLASUM(2)=W(I2+1)+CLASUM(2)
      CLASUM(3)=W(I3+1)+CLASUM(3)
      CLASUM(4)=W(I4+1)+CLASUM(4)
      CLASUM(5)=W(I5+1)+CLASUM(5)
```

ORIGINAL PAGE IS
OF POOR QUALITY

```
      CLASUM(6)=WFOR+CLASUM(6)
      IF(WFOR.GT.5.)CALL FOREST(TP,BTVF,BTHF)
C
C CALCULATE COMPOSITE BRIGHTNESS TEMPERATURES
      SUMBTV=W(I1+1)*BTVW+W(I2+1)*BTVB+W(I3+1)*BTVU+W(I4+1)*BTVM
     @+W(I5+1)*BTVV+WFOR*BTVF
      SUMBTH=W(I1+1)*BTHW+W(I2+1)*BTHB+W(I3+1)*BTHU+W(I4+1)*BTHM
     @+W(I5+1)*BTHV+WFOR*BTHF
      BTV50=SUMBTV/100.
      BTH50=SUMBTH/100.
      RETURN
      END
```

ORIGINAL PAGE IS
OF POOR QUALITY

```
      SUBROUTINE WATER(NB,TP,BTVW,BTHW)
C CORRECT WATER TEMP(TWC(DEG C)--TWK(DEG K))
      TWC=(TP-25.)*0.25+25.
      TWK=TWC+273.15
C
C ROUTE ACCDNG TO BAND#, NB
      GO TO(100,200,300),NB
C
C CALCULATION FOR L-BAND
  100 EH50=0.256+TWC*0.000467
      EV50=0.505+TWC*0.000767
      SKYT=6.0
      GO TO 400
C
C C-BAND
  200 EH50=0.265
      EV50=0.522
      SKYT=8.0
      GO TO 400
C
C X-BAND
  300 EH50=0.288-TWC*0.0003
      EV50=0.557-TWC*0.0005
      SKYT=10.0
C
C COMPLETE CALCULATIONS
  400 BTVW=EV50*TWK+(1.-EV50)*SKYT
      BTHW=EH50*TWK+(1.-EH50)*SKYT
      RETURN
      END
```

ORIGINAL PAGE IS
OF POOR QUALITY

```
      SUBROUTINE URBAN(TP,BTVU,BTHU)
C CALCULATION FOR ALL BANDS
      TSK=TP+273.15
      BTVU=TSK*0.96
      BTHU=TSK*0.86
      RETURN
      END
```

ORIGINAL PAGE IS
OF POOR QUALITY

```
      SUBROUTINE WATER(NB,TP,BTVW,BTHW)
C CORRECT WATER TEMP(TWC(DEG C)--TWK(DEG K))
      TWC=(TP-25.)*0.25+25.
      TWK=TWC+273.15
C
C ROUTE ACCDNG TO BAND#, NB
      GO TO(100,200,300),NB
C
C CALCULATION FOR L-BAND
  100 EH50=0.256+TWC*0.000467
      EV50=0.505+TWC*0.000767
      SKYT=6.0
      GO TO 400
C
C C-BAND
  200 EH50=0.265
      EV50=0.522
      SKYT=8.0
      GO TO 400
C
C X-BAND
  300 EH50=0.288-TWC*0.0003
      EV50=0.557-TWC*0.0005
      SKYT=10.0
C
C COMPLETE CALCULATIONS
  400 BTVW=EV50*TWK+(1.-EV50)*SKYT
      BTHW=EH50*TWK+(1.-EH50)*SKYT
      RETURN
      END
```

ORIGINAL PAGE IS
OF POOR QUALITY

```
      SUBROUTINE BARE(NB,TP,SM,ROU,BTVB,BTHB)
      COMMON/ROUGH/RH,RV
C
C ROUTE ACCDNG TO BAND#, NB
      GO TO(100,200,300),NB
C
C L-BAND ALGORITHM
  100 TGK=250.15-0.26*SM+TP
      IF(SM.GT.38.)TGK=TP+240.15
      IF(SM.GT.12.)GO TO 101
      EH50=0.9-0.00917*SM
      EV50=0.98-0.0025*SM
      GO TO 500
  101 EH50=0.96-0.0139*SM
      EV50=1.047-0.00808*SM
      GO TO 500
C
C C-BAND
  200 TGK=260.15-0.53*SM+TP
      IF(SM.GT.38.)TGK=TP+240.15
      IF(SM.GT.12.)GO TO 201
      EH50=0.86-0.00833*SM
      EV50=0.97-0.0025*SM
      GO TO 500
  201 EH50=0.92-0.0135*SM
      EVH50=1.04-0.00846*SM
      GO TO 500
C
C X-BAND
  300 TGK=273.15+TP-0.87*SM
      IF(SM.GT.38.)TGK=TP+240.15
      IF(SM.GT.12.)GO TO 301
      EH50=0.91-0.00917*SM
      EV50=0.99-0.0025*SM
      GO TO 500
  301 EH50=0.96-0.0135*SM
      EV50=1.05-0.0077*SM
C
C COMPLETE CALCULATIONS
  500 RH=1.-EH50
      RV=1.-EV50
      RFAC=EXP(-ROU*0.4132)
      RH=RH*RFAC
      RV=RV*RFAC
      EH50=1.-RH
      EV50=1.-RV
      BTHB=EH50*TGK
      BTVB=EV50*TGK
      RETURN
      END
```

ORIGINAL PAGE IS
OF POOR QUALITY

```
SUBROUTINE MIX(NB,TP,SM,ROU,BTVM,BTHM)
COMMON/ROUGH/RH,RV
CALL BARE(NB,TP,SM,ROU,BTVB,BTHB)
CALL VEG(NB,TP,SM,BTVV,BTHV)
BTVM=(BTVV+BTVB)*0.5
BTHM=(BTHV+BTHB)*0.5
RETURN
END
```

ORIGINAL PAGE IS
OF POOR QUALITY

```
      SUBROUTINE VEG(NB,TP,SM,BTVV,BTHV)
      COMMON/ROUGH/RH,RV
C
C ADJUST CANOPY TEMP, TVC
      TVC=(TP-25.)*0.25+25.
      TVK=TVC+273.15
C
C CALL BARE FOR BASIC EMISSION DATA
      CALL BARE(NB,TVC,SM,0.0,BTVB,BTHB)
C
C COMPUTE VEGETATION CORRECTION FACTOR ACCDNG TO SOIL MOISTURE
      VFAC=0.8-0.00395*SM
C
C APPLY VEGETATION CORRECTION FACTOR
      XRH=RH*VFAC
      XRV=RV*VFAC
      SOLTMP=BTVB/(1.-RV)
      BTVV=(1.-XRV)*SOLTMP
      BTHV=(1.-XRH)*SOLTMP
C
C RETURN IF L-BAND
      IF(NB.EQ.1)RETURN
C
C X-BAND CALCULATION(CONSTANT EMISSIVITY FOR CANOPY)
      TV=TVK*0.95
      TH=TVK*0.92
C
C BRANCH IF C-BAND
      IF(NB.EQ.2)GO TO 200
      BTVV=TV
      BTHV=TH
      RETURN
  200 BTVV=(BTVV+TV)*0.5
      BTHV=(BTHV+TH)*0.5
      RETURN
      END
```

ORIGINAL PAGE IS
OF POOR QUALITY

```
SUBROUTINE FOREST(TP,BTVF,BTHF)
CALL VEG(3,TP,0.0,BTVF,BTHF)
RETURN
END
```

```
FUNCTION BRTMP(TA,TB,P)
BRTMP=TA*COS(P)**2+TB*SIN(P)**2
RETURN
END
```

```
      SUBROUTINE BCORR(EVSO,EHSO,ANGLE,BTV,BTH)
      REAL FH(81),FV(81)
      DATA      FV( 1),  FV( 2),  FV( 3),  FV( 4),  FV( 5),  FV( 6)
     @/        .539745, .539915, .540428, .541283, .542481, .544022/
      DATA      FV( 7),  FV( 8),  FV( 9),  FV(10),  FV(11),  FV(12)
     @/        .545907, .548136, .550713, .553637, .556910, .560535/
      DATA      FV(13),  FV(14),  FV(15),  FV(16),  FV(17),  FV(18)
     @/        .564511, .568844, .573533, .578682, .583993, .589768/
      DATA      FV(19),  FV(20),  FV(21),  FV(22),  FV(23),  FV(24)
     @/        .595911, .602424, .609311, .616574, .624216, .632241/
      DATA      FV(25),  FV(26),  FV(27),  FV(28),  FV(29),  FV(30)
     @/        .640652, .649453, .658646, .668234, .678221, .688610/
      DATA      FV(31),  FV(32),  FV(33),  FV(34),  FV(35),  FV(36)
     @/        .699404, .710604, .722215, .734237, .746672, .759522/
      DATA      FV(37),  FV(38),  FV(39),  FV(40),  FV(41),  FV(42)
     @/        .772787, .786467, .800562, .815070, .829987, .845311/
      DATA      FV(43),  FV(44),  FV(45),  FV(46),  FV(47),  FV(48)
     @/        .861037, .877156, .893661, .910541, .927783, .945371/
      DATA      FV(49),  FV(50),  FV(51),  FV(52),  FV(53),  FV(54)
     @/        .963285, .981504, 1.      , 1.018742, 1.037694, 1.056812/
      DATA      FV(55),  FV(56),  FV(57),  FV(58)
     @/       1.076046, 1.095339, 1.114622, 1.133818/
      DATA      FV(59),   FV(60),   FV(61),   FV(62),   FV(63)
     @/       1.152837, 1.171573, 1.189907, 1.207700, 1.224790/
      DATA      FV(64),   FV(65),   FV(66),   FV(67),   FV(68)
     @/       1.240991, 1.256089, 1.269835, 1.281941, 1.292072/
      DATA      FV(69),   FV(70),   FV(71),   FV(72),   FV(73)
     @/       1.299842, 1.304801, 1.306423, 1.304097, 1.297109/
      DATA      FV(74),   FV(75),   FV(76),   FV(77),   FV(78)
     @/       1.284619, 1.265646, 1.239028, 1.203400, 1.157136/
      DATA      FV(79),   FV(80),   FV(81)
     @/       1.098311, 1.024620, 0.933305/
      DATA      FH( 1),  FH( 2),  FH( 3),  FH( 4),  FH( 5),  FH( 6)
     @/        .539745, .539574, .539061, .538206, .537007, .535463/
      DATA      FH( 7),  FH( 8),  FH( 9),  FH(10),  FH(11),  FH(12)
     @/        .533572, .531333, .528742, .525796, .522494, .518829/
      DATA      FH(13),  FH(14),  FH(15),  FH(16),  FH(17),  FH(18)
     @/        .514799, .510399, .505623, .500466, .494922, .488986/
      DATA      FH(19),  FH(20),  FH(21),  FH(22),  FH(23),  FH(24)
     @/        .482649, .475906, .468747, .461165, .453150, .444695/
      DATA      FH(25),  FH(26),  FH(27),  FH(28),  FH(29),  FH(30)
     @/        .435788, .426421, .416581, .406258, .395440, .384113/
      DATA      FH(31),  FH(32),  FH(33),  FH(34),  FH(35),  FH(36)
     @/        .372266, .359884, .346953, .333459, .319385, .304715/
      DATA      FH(37),  FH(38),  FH(39),  FH(40),  FH(41),  FH(42)
     @/        .289434, .273522, .256961, .239734, .221819, .203198/
      DATA      FH(43),  FH(44),  FH(45),  FH(46),  FH(47),  FH(48)
     @/        .183846, .163745, .142870, .121198, .098705, .075365/
      DATA      FH(49),  FH(50),  FH(51),  FH(52),  FH(53),  FH(54)
     @/        .051152, .026040, .000000, -.026996, -.054978, -.083974/
```

PRECEDING PAGE BLANK NOT FILMED

```
SUBROUTINE CALT(RESL,ALTO)
COMMON/GAN/BWID,XPI,IF
COMMON/ORIEN/ROLL,AZIM,ALT,A,B
XJ=TAN((ROLL+BWID/2.)/57.3)-TAN((ROLL-BWID/2.)/57.3)
XM=TAN((BWID/2.)/57.3)/COS(ROLL/57.3)
ALTO=RESL/SQRT(2.*XJ*XM)
RETURN
END
```